SIGNALLING AND FUNCTION OF THE SMALL

RHO GTPASE RHOJ IN ENDOTHELIAL CELLS

by

KATARZYNA LESZCZYNSKA

A Thesis submitted to The University of Birmingham for the degree of

DOCTOR OF PHILOSOPHY

School of Immunity and Infection

College of Medical and Dental Sciences

The University of Birmingham

January 2011

UNIVERSITY OF BIRMINGHAM

University of Birmingham Research Archive

e-theses repository

ABSTRACT

RhoJ is an endothelial expressed Rho GTPase, and its knock-down impairs endothelial cell (EC) migration and tubulogenesis, increases stress fibre (SF) and focal adhesion (FA) numbers. This work aimed to determine the intracellular localisation of RhoJ, identify its binding partners, test how it is activated and further explore its function in ECs.

Endogenous RhoJ localised to FAs and overexpression of its active mutant (daRhoJ) promoted EC migration, and diminished FA and SF numbers. In addition to FAs, overexpressed RhoJ localised also to endosomes and RhoJ knock-down slightly delayed transferrin recycling. Vascular endothelial growth factor (VEGF), fibroblast growth factor 2 (FGF-2) and thrombin activated RhoJ in ECs. PAK-interacting exchange factor β (βPIX) and G protein-coupled receptor kinase-interacting target 1 (GIT1), which promote FA disassembly, were identified as RhoJ-binding partners. RhoJ co-localised with these proteins in ECs, and βPIX knock-down and to a lesser extent GIT1 knock-down reduced RhoJ localisation to FAs. Overexpression of daRhoJ increased the amount of GIT1 and βPIX in FAs, and increased the total amount of the βPIX protein in ECs.

In conclusion, RhoJ localises to FAs, promotes EC migration, regulates FA and SF numbers, interacts with βPIX and GIT1 and is activated by pro-angiogenic factors.

ACKNOWLEDGEMENTS

Firstly and foremost, I would like to express my sincere gratitude to my supervisor, Dr Victoria Heath. Thank you for all your friendship, support, advice, love to the science and invaluable experience that you shared with me. Huge thanks for your patience in convincing me that the glass is half full and not half empty. It was a great honour to be your student.

I would like to thank to my second supervisor, Prof. Roy Bicknell. I extremely appreciate all your help, guidance and support given to me during these studies. It was a great pleasure and a privilege to work in your team. Huge thanks go also to all the members of The Molecular Angiogenesis Group, both present and past. Thank you for the great time we spent together in the lab and for lots of joy during the lunch-time cross-word sessions. I extremely enjoyed working with all of you. Thank you to Sarah, Ana and Roman for the English support during this thesis writing.

Sincere thanks goes to all the members of Prof. John Heath's, Dr Neil Hotchin's, Dr Mike Tomlinson's and Dr Josh Rappoport's groups from the School of Biosciences. I truly enjoyed our common lab meetings, thank you for all your help and advice. Particularly, I would like to acknowledge Prof. John Heath for offering the collaboration on the mass spec project. This extremely raised the value of the results that I achieved during these studies and helped to take my work forward. My special thank you goes also to Dr Neil Hotchin for his invaluable advices.

I also thank to my parents, for their love and support. Huge thanks to Paula and Piotr for their friendship and time that we spent together. And finally, I would like to thank to my husband, Mirek, for his presence, support and endless optimism. I dedicate this thesis to you.

TABLE OF CONTENTS

LIST OF FIGURES

LIST OF TABLES

ABBREVIATIONS

aa – amino acids
Amp - ampicillin
Arp2/3 – a seven subunit complex comprising actin-related proteins 2 and 3
BSA – bovine serum albumin
CC – coiled-coil region
Chloramph – chloramphenicol
CRIB domain – Cdc42/Rac1-interacting binding domain
da – dominant active
DH – Dbl homology domain
DMEM – Dulbecco's Modified Eagle's Medium
dn – dominant negative
E. coli – Escherichia coli
EC(s) – endothelial cell(s)
ECM – extracellular matrix
EE/ES – early/sorting endosomes
ERK1/2 – extracellular signal-regulated kinase 1/2
FACS – fluorescence activated cell sorting
F-actin – filamentous actin
FAH – focal adhesion targeting homology domain
FAK – focal adhesion kinase
FA(s) – focal adhesion(s)
FCS – fetal calf serum
FGF-2 – fibroblast growth factor 2; also called basic FGF (bFGF)
FITC – fluorescein-5-isothiocyanate
G-actin – globular actin
GAP(s) – GTPase activating protein(s)
GDI(s) – guanine nucleotide dissociation inhibitor(s)
GDP – guanosine-5'-biphosphate
GEF(s) – guanine nucleotide exchange factor(s)
GIT1– G protein-coupled receptor kinase-interacting target 1
GPCR(s) – G protein-coupled receptor(s)
GST – glutathione-*S*-transferase
GTP – guanosine-5'-triphosphate
H – hour
HBS – HEPES-buffered saline
HEK 293T(s) - human embryonic kidney 293T cell(s)
HMEC-1 – human microvascular endothelial cell line-1
HRP – horseradish peroxidase
HUVEC(s) – human umbilical vein endothelial cell(s)
IF – immunofluorescence
IRSp53 – insulin receptor tyrosine kinase substrate p53
Kan – kanamycin
LB broth/agar– Luria Bertani broth/agar
LIMK – LIM motif containing protein kinase
MBP – maltose binding protein

mDia – mammalian Diaphanous formin
MLC – myosin light chain
MLCK – myosin light chain kinase
MLCP – myosin light chain phosphatase
MMP – matrix-metalloproteinase
MRCK, A or B – myotonic dystrophy kinase-related Cdc42-binding kinase A or B
NM II – non-muscle myosin II
N-WASP – neural-Wiskott-Aldrich syndrome protein
PAK – p21-activated kinase
PBS – phosphate-buffered saline
PCR – polymerase chain reaction
PH – pleckstrin homology domain
PIX, α or β – PAK-interacting exchange factor α or β
PI3K – phosphatidylinositol 3-kinase
pMLC – phosphorylated myosin light chain
ROCK – Rho-associated coiled coil kinase
RTK(s) – receptor tyrosine kinase(s)
SDS-PAGE – sodium dodecyl sulphate - polyacrylamide gel electrophoresis
SF(s) – stress fibre(s)
SHD – yeast Spa2 homology domain
SH3 – Src homology 3 domain
TBS – tris-buffered saline
TBST – tris-buffered saline tween
Tf – transferrin
TNF-α – tumor necrosis factor-α
VEGF – vascular endothelial growth factor
VEGFR – vascular endothelial growth factor receptor
WASP – Wiskott-Aldrich syndrome protein
WAVE – Wiskott-Aldrich syndrome protein-family verprolin homologous protein
WB – western blotting
wt – wild type
w/v – weight per volume
v/v – volume per volume
Y2H – yeast-two-hybrid

1. INTRODUCTION

1.1. Endothelial cells in angiogenesis

Endothelial cells (ECs) line the inner wall of blood and lymphatic vessels. Both circulation systems are important for homeostasis in the healthy organism as they mediate an exchange of gases, liquids and nutrients to the adjacent tissues as well as transportation of various cells within the organism (Adams and Alitalo 2007). Disruption of vascular or lymphatic systems leads to severe pathologies such as tissue ischemia or oedema (Carmeliet 2003; Alitalo, Tammela et al. 2005). The initial formation of blood vessels is called vasculogenesis and occurs in developing embryo when endothelial progenitor cells assemble into so called blood islands which then develop into vascular plexus (Flamme, Frolich et al. 1997; Patan 2004). In the later stages of development, new blood vessels are formed from the pre-existing vasculature and this process is called angiogenesis. Angiogenesis takes place not only during development but also in conditions such as wound healing or the female menstrual cycle. Neovascularisation also contributes to the pathogenesis of many diseases such as psoriasis, diabetic retinopathy, rheumatoid arthritis, heart diseases and cancer (Carmeliet 2003; Milkiewicz, Ispanovic et al. 2006; Adams and Alitalo 2007).

As indicated in the Fig. 1.1, angiogenesis is a multi-step process (Adams and Alitalo 2007). Firstly, blood vessels are stimulated with pro-angiogenic factors and become more permeable. This induces ECs to secrete matrix metalloproteinases, which then degrade the surrounding basement membrane. Some cells from the endothelial wall start to migrate toward the gradient of angiogenic stimuli. The column of cells extends as they migrate and proliferate. Subsequently, a sprouting tube merges with another already established or newly forming vessel and a lumen is formed. Eventually the vessel maturates and is stabilised by the recruitment of pericytes. Then a newly formed and fully functional capillary can supply nutrients to the adjacent tissue (Carmeliet 2003; Jain 2003). During vessel formation ECs
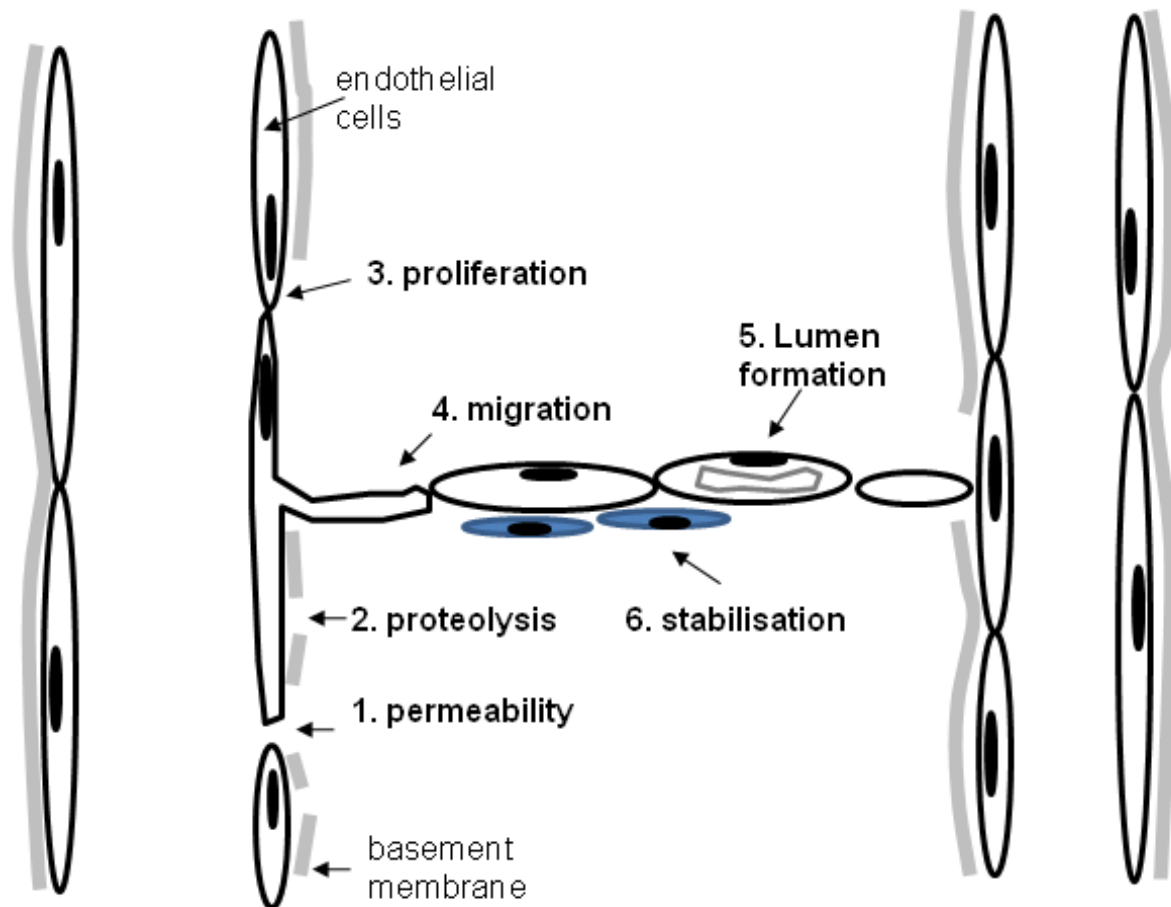
Fig. 1.1 Stages of angiogenesis.
Blood vessels are permeabilised by stimulation with pro-angiogenic factors (1) and endothelial cells (ECs) activate matrix metalloproteinases to degrade the basement membrane (2). Then ECs proliferate (3) and migrate (4) towards the gradient of stimuli and after joining with another vessel the lumen forms (5). Finally blood vessels are stabilised by recruitment of other cells such as pericytes (6).

which are at the front of a migrating sprout are called tip cells, and the ones that follow behind are called stalk cells (Carmeliet, De Smet et al. 2009; De Smet, Segura et al. 2009; Jakobsson, Franco et al. 2010). The gene expression in tip and stalk cells is different, resulting in the differences in phenotypes of these cells (Hellstrom, Phng et al. 2007b; Del Toro, Prahst et al. 2010). Tip cells are highly motile and invasive, while stalk cells have increased proliferation (Hellstrom, Phng et al. 2007a; Hellstrom, Phng et al. 2007b).

Various molecules or mechanical forces can induce the formation of blood vessels (Adams and Alitalo 2007). These include growth factors, cytokines, components of extracellular matrix (ECM), hypoxia, blood flow and shear stress. Vascular endothelial growth factor (VEGF) A is one of the most potent pro-angiogenic stimuli and it belongs to the larger family of proteins which comprises VEGFA, -B, -C, -D, -E and placental growth factors (PlGF1 and 2) (Gerhardt, Golding et al. 2003; Olsson, Dimberg et al. 2006). VEGF ligands induce various signalling pathways by binding to their cognate vascular endothelial growth factor receptors (VEGFR) 1-3, which belong to a larger family of receptor tyrosine kinases (RTKs). VEGFR2 (also known as KDR or FLK1) is the most active mediator of the angiogenic signal, and upon VEGFA binding undergoes autophosphorylation and then activates other associated proteins. VEGFR1 (also known as FLT1) has a higher affinity to VEGFA, but a weak tyrosine-kinase activity. When expressed in a soluble, catalytically inactive form it can trap VEGF and decrease the angiogenic signal. VEGFR3 (also known as FLT4) acts mainly as a receptor in lymphangiogenesis (Olsson, Dimberg et al. 2006). Different splice variants of VEGFA exist and can control various processes in angiogenesis. VEGFA165 has a heparan sulphate binding region and mediates a polarised extension of the tip-cell filopodia, while a shorter form of this growth factor, VEGFA121, does not bind heparan sulphate and is not able to promote EC branching; rather it acts to activate cell proliferation. Other molecules important in

development of blood vessels include basic fibroblast growth factor (bFGF, also known as FGF-2), platelet derived growth factors (PDGF), integrins, SLITs/ROBO4, angiopoietins and many other proteins (Adams and Alitalo 2007).

1.2. Rho GTPase family

1.2.1. Structure of Rho GTPases

Rho GTPases belong to the large superfamily of Ras-like small G proteins and comprise eight subgroups: RhoA-like group one (RhoA, RhoB, RhoC), Rac1-like group two (Rac1, Rac2, Rac3, RhoG), Cdc42-like group three (Cdc42, TC10/RhoQ, TCL/RhoJ), group four (Wrch1/RhoU, Chp/Wrch2/RhoV), Rnd-like group five (Rnd1/Rho6, Rnd2/RhoN, Rnd3/RhoE), group six (RhoD, Rif/RhoF), RhoBTB-like group seven (RhoBTB1, RhoBTB2/DBC2) and RhoH/TTF (Boureux, Vignal et al. 2007; Heasman and Ridley 2008). Fig. 1.2 illustrates the relationship between these family members.

The structure of Rho GTPases is highly conserved and the presence of the Rho-specific insert domain distinguishes them from other small G proteins (Madaule and Axel 1985; Jaffe and Hall 2005). Fig. 1.3 shows the protein sequence alignments of the Cdc42-like subfamily members obtained with the ClustalW 2.0.8 program (Chenna, Sugawara et al. 2003) and also the conserved domains of Rho GTPases. All Rho GTPases contain the effector domain and some possess a so-called CAAX box (C- cysteine, A- aliphatic amino acid, X- any amino acid) on the c-terminal tail. The CAAX box is a potential substrate for geranyl-geranyl- or farnesyltransferases (Foster, Hu et al. 1996; Liang, Ko et al. 2002). These enzymes catalyse a lipidation of the CAAX box, which facilitates protein anchoring in the membrane. A hypervariable region is situated upstream of the CAAX box and in some Rho GTPases this contains a polybasic sequence. The polybasic sequence varies in the number and order of
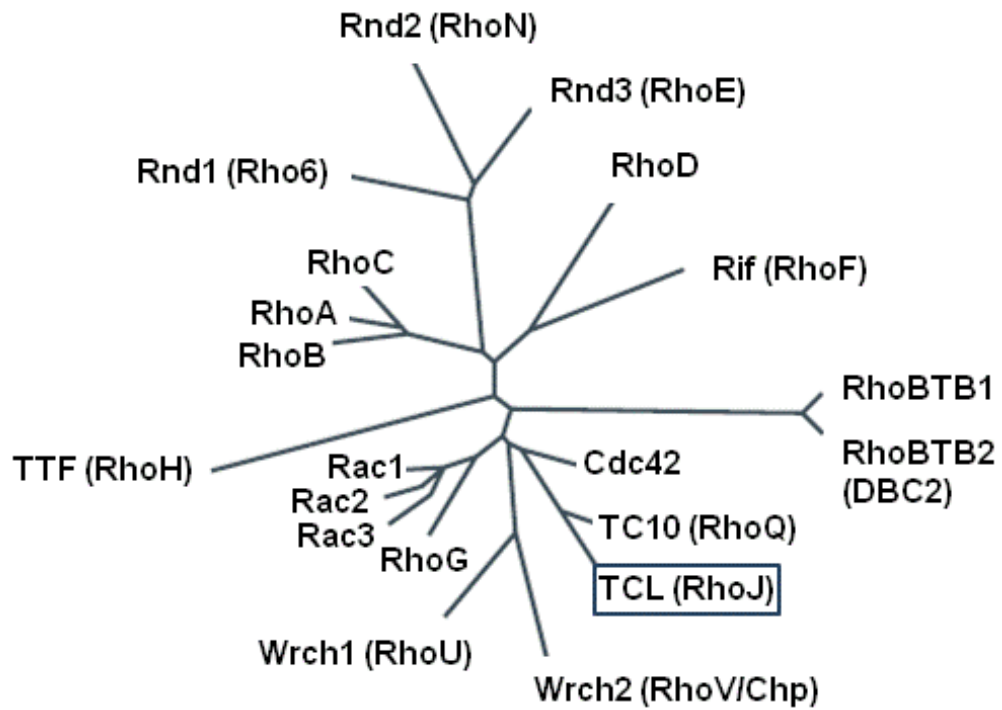
Fig. 1.2 RhoJ is a member of Rho GTPase family.
The family comprises the RhoA-like, Rac1-like, Cdc42-like, Wrch, Rnd-like, RhoBTB-like, RhoD/Rif and TTF subgroups. An unrooted phylogenetic tree of the human small Rho GTPases. Alternative names are given in brackets. The figure was adapted from Chardin (2006).

A, ClustalW 2.0.8 alignment of RhoJ, TC10 and Cdc42 showing similarities in their amino acid (aa) sequences. Similarity in amino acid substitutions is encoded by "*" for identical aa, ":" for conserved aa substitutions, "." for semi-conserved aa substitutions according to Chenna et al. (2003). **B**, Regions of Rho GTPases marked by colour-coded frames are described in the legend box. The corresponding aa sequences of these regions are marked for the Cdc42-like subfamily members as shown in **A**. Organisation of domains was drawn on the basis of those shown in reviews by Vega and Ridley (2008) and Johnson (1999).

Fig. 1.3 Domain organisation of Rho GTPases.

7

lysines and arginines and can determine the localisation of particular Rho GTPases to different cell compartments (Jack, Madine et al. 2008).

1.2.2. Regulation of Rho GTPase activation cycle

The characteristic feature of many Rho GTPases is their ability to bind the guanine nucleotides, namely guanosine-5'-triphosphate or guanosine-5'-biphosphate (GTP or GDP, respectively) (Nobes and Hall 1994). Rho GTPases act as molecular switches: binding of GTP or GDP determines the conformation of the so-called Switch I and Switch II regions (Fig. 1.4), and this regulates their interactions with various downstream proteins (Nobes and Hall 1994; Paduch, Jelen et al. 2001). When inactive (GDP-bound), some Rho GTPases can be stabilised by guanine nucleotide dissociation inhibitors (GDIs) (Olofsson 1999). Upon cell activation, the GDI is released and GDP exchanged into GTP by guanine nucleotide exchange factors (GEFs) (Cherfils and Chardin 1999). The active Rho GTPases are then able to bind to effector proteins and propagate signals in the cell (Bishop and Hall 2000). Inactivation of Rho GTPases occurs when they interact with GTPase activating proteins (GAPs). These promote the intrinsic hydrolytic activity of Rho GTPases to hydrolyse GTP to GDP (Moon and Zheng 2003). Fig. 1.5 summarises the activation cycle of typical Rho GTPases such as RhoA-like, Rac-like, Cdc42-like, RhoF and RhoD. Other Rho GTPases including RhoBTB-like, Rnd-like, Wrch1, Wrch2 and TTF are atypical since their activity is regulated in ways other than GDP/GTP exchange (Aspenstrom, Ruusala et al. 2007).

1.2.2.1.   GEFs

Rho GTPases can be activated by various stimuli such as hormones, cytokines, growth factors, mechanical forces, interactions with neighbouring cells and ECM (Kjoller and Hall 1999). These signals lead to the activation of GEFs, which then "turn on" Rho GTPases, by mediating an exchange of GDP to GTP and therefore inducing conformational changes

8
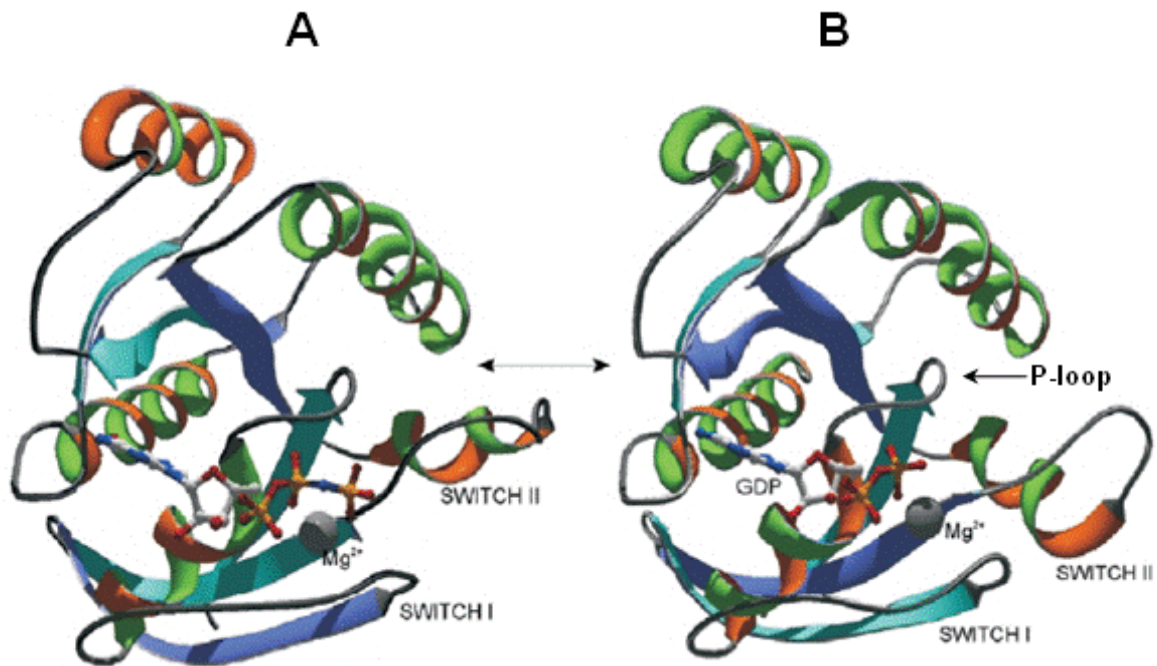
Fig. 1.4 Conformational changes of Ras as a result of binding with GTP or GDP.
Conformational changes caused by nucleotide binding are similar in different small G proteins (Paduch et al. 2001), and here are demonstrated in Ras GTPase. Both nucleotides (GTP in **A** or GDP in **B**) are locked within the protein in the presence of a magnesium ion. The presence of a GDP or GTP nucleotide determines the conformation of the Switch I and II regions of small G proteins and enables their interaction with other proteins. Adapted from Paduch *et al.* (2001).
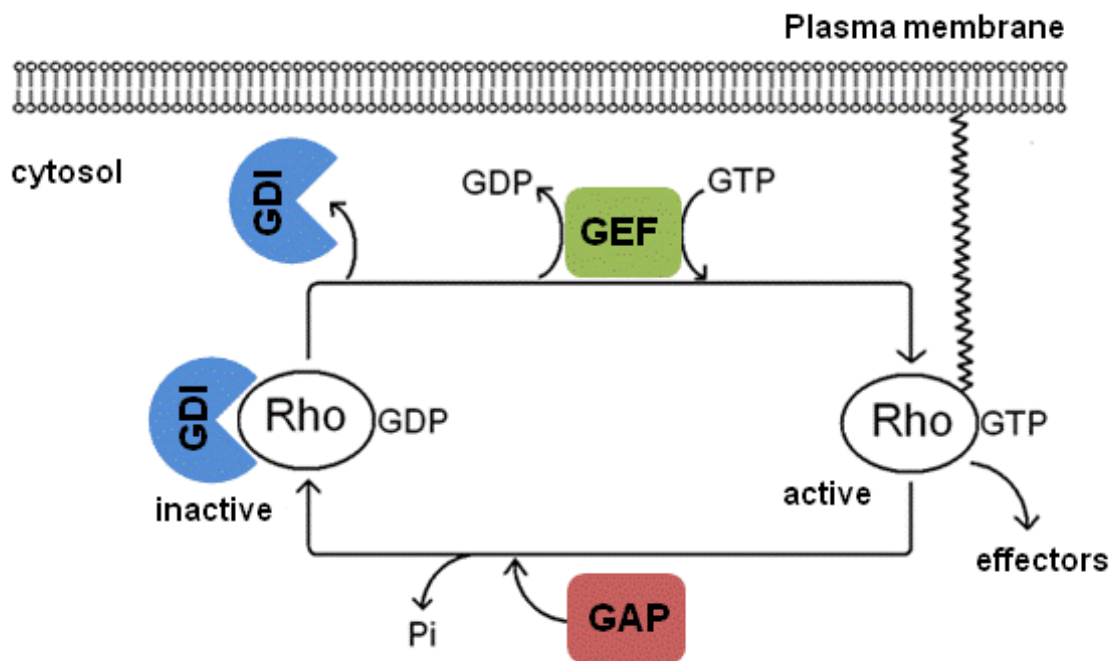
Fig. 1.5 Mode of activation of typical Rho GTPases.
Typical Rho GTPases cycle between active GTP-bound and inactive GDP-bound forms. These transitions are regulated by three families of proteins: guanine nucleotide exchange factors (GEFs) which mediate GDP to GTP exchange; GTPase activating proteins (GAPs) which promote the enzymatic activity of Rho proteins leading to hydrolysis of GTP to GDP; guanine nucleotide dissociation inhibitors (GDIs) which stabilise some Rho GTPases in their inactive form.

(Paduch, Jelen et al. 2001). The GDP-GTP exchange occurs in several stages (Cherfils and Chardin 1999). Firstly, the GEF binds with a low-affinity to the GDP-Rho GTPase complex and this leads to the dissociation of GDP. The GEF then stabilises a nucleotide-free Rho GTPase, by forming a high affinity complex, which is then dissociated by GTP. Magnesium ions coordinate binding of the guanine nucleotides to the Rho GTPases. The regions in small G proteins responsible for binding to a guanine nucleotide and magnesium ion include the p-loop and two regions called Switch I and Switch II. The p-loop mediates the interaction with GDP while the Switch regions coordinate the binding of the γ-phosphate group of GTP. Thus GEFs interact with p-loop to cause a dissociation of GDP and then their binding to small G proteins is stabilised by switch I and II regions (Cherfils and Chardin 1999).

Most GEFs have several domains; these may be involved in their dimerisation, their binding to membranes or other proteins in addition to the region required for activation of small G proteins (Cherfils and Chardin 1999; Schmidt and Hall 2002; Rossman, Der et al. 2005; Garcia-Mata and Burridge 2007). The catalytic GEF-domains include the Dbl-homology domain (DH) very often followed by the pleckstrin homology domain (PH). The latter one enhances the main GEF activity of the DH domain (Liu, Wang et al. 1998; Rossman and Campbell 2000), but also it can act as a membrane targeting domain (Chen, Corbalan-Garcia et al. 1997; Michiels, Stam et al. 1997; Stam, Sander et al. 1997; Snyder, Rossman et al. 2001). Some GEFs need to undergo additional modifications (such as phosphorylation) to become catalytically active. The GEF βPIX contains a T1 inhibitory insert located after the PH domain; this insert requires phosphorylation by Src for full GEF activity of βPIX (Feng, Albeck et al. 2002; Baird, Feng et al. 2005). Another group of GEF-activity domains includes Dock homology regions. These GEFs are called Dock180-related or CZH after the "CDM and Zizimin homology" (Cote and Vuori 2002; Meller, Merlot et al. 2005). In general, more than

70 GEFs had been found in the human genome, which can activate about 20 Rho GTPases. Some of the best studied ones include Vav (1-3), Sos, Tiam1, Dock1, Larg and Trio (Rossman, Der et al. 2005). It was found that one GEF can serve as an activator for several Rho GTPases, while one Rho GTPase can be triggered by multiple GEFs. This may lead to crosstalk between different Rho proteins (Garcia-Mata and Burridge 2007).

1.2.2.2. GAPs

RhoGAPs are negative regulators of Rho GTPase activity. They bind to activated Rho proteins and induce their enzymatic activity which mediates hydrolysis of GTP to GDP (Lamarche and Hall 1994; Moon and Zheng 2003). More precisely, RhoGAPs interact with p-loop, Switch I and Switch II regions of Rho GTPases that hold GTP. This leads to the conformational change in a small G protein's structure and induction of their hydrolytic activity (Li, Zhang et al. 1997; Nassar, Hoffman et al. 1998). Analysis of human genome revealed the existence of around 80 RhoGAPs, which is again several fold more than the number of Rho GTPases. It has been suggested that expression of some GAPs is tissue specific. As an example, p73RhoGAP is expressed in the blood vessels where it regulates angiogenesis (Su, Hahn et al. 2004), while the brain-specific GAP Grit (GTPase regulator interacting with TrkA) regulates neuritogenesis (Nakamura, Komiya et al. 2002).

As with GEFs, the activity of some RhoGAPs may be regulated by modifications such as phosphorylation or lipidation (Moon and Zheng 2003). As an example, the activity of p190RhoGAP is increased after its phosphorylation by Src (Hu and Settleman 1997; Roof, Haskell et al. 1998). On the other hand, the Rac-specific GAP chimaerin is regulated by a phospholipid modification (Moon and Zheng 2003). Due to their multi-domain structure, many GAPs can also serve as scaffold proteins, which mediate the cross-talk between various signalling pathways (Tcherkezian and Lamarche-Vane 2007).

1.2.2.3. GDIs

GDIs stabilise Rho proteins in a GDP-bound form and often cause their translocation from the membrane to cytosol (Olofsson 1999). Thus GDIs sequester inactive Rho GTPases in a soluble fraction which then can be switched back on upon the stimulation with an appropriate signal. Another role of GDIs is to deliver and withdraw Rho GTPases from their site of action, which is often located at membranes (Dransart, Olofsson et al. 2005). While numbers of RhoGAPs and RhoGEFs are rather large, only three RhoGDIs have been characterised (Fukumoto, Kaibuchi et al. 1990; Leonard, Hart et al. 1992; Lelias, Adra et al. 1993; Zalcman, Closson et al. 1996; Adra, Iyengar et al. 1998; Gorvel, Chang et al. 1998; Brunet, Morin et al. 2002).

1.2.3. General functions of Rho GTPases

Rho GTPases were originally characterised as regulators of actin dynamics. The three most studied ones RhoA, Rac1 and Cdc42 were found to have a major role in formation of stress fibres (SFs), lamellipodia and filopodia, respectively (Nobes and Hall 1995). SFs are comprised of actin and myosin bundles, which generate the tension and contraction in the cell while lamellipodia and filopodia are sheet-like and finger-like protrusions (respectively) generated in spreading or migrating cells (Ridley, Schwartz et al. 2003). Since the first Rho GTPase RhoA was identified in 1985 (Madaule and Axel 1985), there had been a great interest in discovering other family members. Numerous studies revealed that Rho GTPases control cellular processes such as cell migration, proliferation, cytoskeleton rearrangements, vesicle transport, phagocytosis, cell division, gene expression, cell-cell and cell-matrix adhesion (Jaffe and Hall 2005; Heasman and Ridley 2008). Many of these discoveries were based on studies using dominant active or dominant negative mutant forms of Rho GTPases created by single amino acid changes. The most typical mutants include GTP-bound active

(G12V or Q61L in Rac1), nucleotide-free inactive (G15A in Rac1) or GDP-bound inactive (T17N in Rac1) forms based on their analogy to known Ras mutations (Garcia-Mata, Wennerberg et al. 2006), with T to N mutations being mostly nucleotide-free in cells. Moreover, the availability of knock-out mice for several Rho GTPases provided further information about their function (Heasman and Ridley 2008). The paragraphs below list some of the main functions of various Rho GTPases. A detailed description of the role of Rho GTPases in cytoskeletal reorganisation and focal adhesion (FA) turnover is included in the section 1.3.3.

All members of RhoA-like subfamily activate acto-myosin contractility, induce SF and FA formation, regulate cytokinesis, gene transcription and cell migration (Wheeler and Ridley 2004). RhoB is involved in endocytic trafficking of growth factor receptors such as epidermal growth factor receptor (EGFR) and platelet derived growth factor receptor (PDGFR-β) (Gampel, Parker et al. 1999; Huang, Duhadaway et al. 2007). Global RhoB and RhoC knock-out mice were created, which implicated distinct roles for these two Rho GTPases (Heasman and Ridley 2008). RhoB was shown to regulate EC survival during vascular development (Adini, Rabinovitz et al. 2003). Mice lacking RhoB disclosed increased susceptibility to skin cancer (Liu, Rane et al. 2001). In many tumours RhoB expression was reduced and this GTPase was proposed to be a tumor suppressor since its overexpression inhibited cell growth, survival, invasion and metastasis (Huang and Prendergast 2006). In contrast, mice lacking RhoC had inhibited tumour cell motility and metastasis (Hakem, Sanchez-Sweatman et al. 2005). Numerous studies showed promotion of cancer cell invasion and metastasis by RhoC (Clark, Golub et al. 2000; Simpson, Dugan et al. 2004; Wu, Wu et al. 2004; Yao, Dashner et al. 2006; Liu, Zhang et al. 2007).

Rac1-like GTPases are known to regulate lamellipodia and focal complexes formation, membrane ruffling, cell migration, cell growth, cell survival, transcription, phagocytosis and endocytosis (Wennerberg and Der 2004; Heasman and Ridley 2008; Palamidessi, Frittoli et al. 2008; Bosco, Mulloy et al. 2009). Global knockout of Rac1 was embryonic lethal (Sugihara, Nakatsuji et al. 1998), while generation of various tissue specific Rac1 deletions in mice indicated its importance in many processes. These include neutrophil chemotaxis (Glogauer, Marchal et al. 2003), B-cell development (Walmsley, Ooi et al. 2003), hematopoietic stem/progenitor cell engraftment in the bone marrow (Gu, Filippi et al. 2003), hair follicle formation (Benitah, Frye et al. 2005; Chrostek, Wu et al. 2006), NADPH oxidase activity (Satoh, Ogita et al. 2006) regulation of Schwann cell biology (Benninger, Thurnherr et al. 2007; Nodari, Zambroni et al. 2007), lamellipodia formation and proliferation in mouse embryonic fibroblasts (Vidali, Chen et al. 2006), brain development and axon guidance (Chen, Liao et al. 2007) and vascular development (Tan, Palmby et al. 2008). Rac2, Rac3 and RhoG global knockouts resulted in viable mice but they had abnormalities in neutrophil functioning, behaviour, and lymphocyte responsiveness to antigen, respectively (Vincent, Jeanteur et al. 1992; Roberts, Kim et al. 1999; Vigorito, Bell et al. 2004; Cho, Zhang et al. 2005; Corbetta, Gualdoni et al. 2005).

Cdc42-like GTPases include Cdc42, TC10 and RhoJ (Heasman and Ridley 2008) and are involved in the actin reorganisation and formation of filopodia (Johnson 1999; Wennerberg and Der 2004). Cdc42-null mice die during embryonic developments, with defects in the primary ectoderm formation (Chen, Ma et al. 2000). Cell-type specific Cdc42 knock-out mouse models showed the importance of this GTPase in hematopoietic stem cell quiescence (Yang, Wang et al. 2007), fate determination of apical neural progenitor cells (Cappello, Attardo et al. 2006), cell polarity (Chen, Liao et al. 2006), axonogenesis (Garvalov, Flynn et

al. 2007), Schwann cell biology (Benninger, Thurnherr et al. 2007) and hepatocellular carcinogenesis (van Hengel, D'Hooge et al. 2008).

TC10 was implicated in the regulation of the insulin-induced glucose transporter trafficking (Ridley 2006), control of myofibril organisation (Coisy-Quivy, Touzet et al. 2009), adipocyte differentiation (JeBailey, Rudich et al. 2004) and also in gene transcription and NIH3T3 fibroblast cell transformation (Murphy, Solski et al. 1999). The role of RhoJ is described in detail in section 1.2.6.

RhoD and Rif GTPases are involved in actin cytoskeleton rearrangements. RhoD regulates actin-dependent transport of early endosomes and promotes FA and SF disassembly (Murphy, Saffrich et al. 1996; Murphy, Saffrich et al. 2001). Rif GTPase regulates the formation of filopodia and increase of SFs (Ellis and Mellor 2000; Aspenstrom, Fransson et al. 2004).

Rnd-like proteins are atypical Rho GTPases, which exist permanently in a GTP-bound form and their activity is regulated by expression levels, localisation and phosphorylation (Chardin 2006). Rnd1 and Rnd3 have opposite effects to RhoA as they reduce SFs and cause cell rounding (Guasch, Scambler et al. 1998; Nobes, Lauritzen et al. 1998). This was suggested to occur via activation of p190RhoGAP, which would lead to inactivation of RhoA (Wennerberg, Forget et al. 2003) or by direct binding and inactivation of Rho-associated coiled coil kinase I (ROCK I), a known effector of Rho-like proteins (Riento, Guasch et al. 2003). Rnd proteins were implicated in the function of neurons by regulating the actin cytoskeleton, axon guidance, neurite outgrowth and cytokinesis (Chardin 2006). Rnd3 was additionally shown to have a role in cancer progression (Vega and Ridley 2008). Other atypical Rho GTPases Wrch1 and Wrch2 induce filopodia formation (Aronheim, Broder et al. 1998; Tao, Pennica et al. 2001). In HeLaS3 cells Wrch-1 localised to FAs and its knock-down

with siRNA resulted in increased numbers of FAs and impaired cell migration (Chuang, Valster et al. 2007). In another study, activated Wrch-1 was shown to disrupt epithelial cell tight junctions and epithelial morphogenesis (Brady, Alan et al. 2009). On the other hand, Wrch-2, overexpression in T-cells caused inhibition of cell migration and triggered Pak1 ubiquitination and degradation (Weisz Hubsman, Volinsky et al. 2007). This Rho GTPase was also found to promote cell transformation (Chenette, Mitin et al. 2006). RhoBTB2 and RhoBTB1 were proposed as tumour suppressor genes (Wilkins, Ping et al. 2004; Berthold, Schenkova et al. 2008). RhoH, another atypical Rho GTPase, was found to inhibit Rac1, RhoA and Cdc42 signalling in T cells (Li, Bu et al. 2002). The global knock-out of RhoH gene in mice showed the importance of this Rho GTPase in T-cell differentiation and T-cell receptor signalling (Gu, Chae et al. 2006; Dorn, Kuhn et al. 2007).

1.2.4. Main effectors of Rho GTPases

Although members of Rho GTPase family are quite homologous in their structure (Wennerberg and Der 2004), the selectivity in their binding of different effector proteins is remarkable (Bishop and Hall 2000). Rho GTPases can interact with a whole range of structurally different proteins; these include various scaffold proteins, serine/threonine kinases, tyrosine kinases, lipid kinases, lipases and oxidases (Jaffe and Hall 2005). Through binding to effector proteins Rho GTPases regulate different cellular processes such as actin polymerisation, generation of actomyosin contractility, cell migration, FA turnover, cell polarity, cell-cell interactions, cell-cycle progression, enzymatic activities, vesicular trafficking, microtubule dynamics and gene expression (Bishop and Hall 2000; Etienne-Manneville and Hall 2002; Schwartz 2004; Jaffe and Hall 2005; Ridley 2006; Heasman and Ridley 2008; Spiering and Hodgson 2011). Examples of interactions between Rho proteins and their effectors that regulate these processes are depicted in the Fig. 1.6.

Some effector proteins contain conserved domains that are recognised selectively by activated Rho GTPases. The Cdc42/Rac-interacting binding (CRIB) domain, which is present in proteins such as Wiskott–Aldrich syndrome protein (WASP) or p21-activated kinases (PAKs), can be recognised by activated Rac1, Rac2, Cdc42, TC10 and RhoJ (Sander, van Delft et al. 1998; Benard, Bohl et al. 1999; Vignal, De Toledo et al. 2000; Haddad, Zugaza et al. 2001; Benard and Bokoch 2002; Chiang, Hou et al. 2002; Tong, Liss et al. 2007). The RhoA-binding domain (RBD) from rhotekin can interact with activated RhoA, RhoB and RhoC (Ren, Kiosses et al. 1999; Ren and Schwartz 2000; Arthur, Ellerbroek et al. 2002; Gampel and Mellor 2002; Bellovin, Simpson et al. 2006).
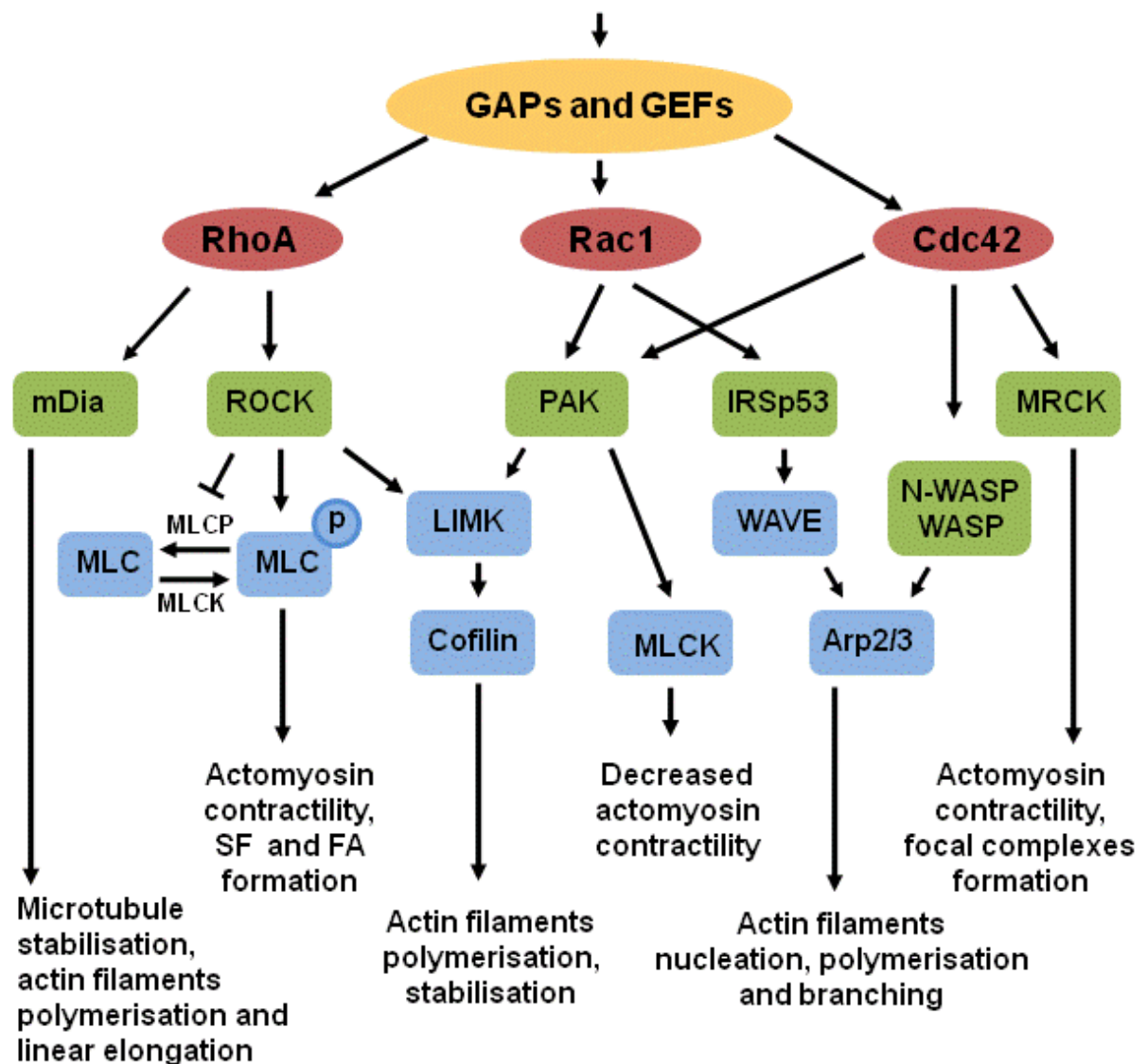
Fig. 1.6 Main effectors of Rho GTPases.
Rho GTPases regulate many cellular processes including cytoskeletal rearrangements, cell migration, vesicular trafficking, focal adhesion dynamics, cell-cycle progression, cell polarity or gene expression (Jaffe and Hall 2005). The scheme shows some main effectors of Rho GTPases which play a crucial role in the regulation of cytoskeletal dynamics. The green boxes indicate direct effectors of Rho GTPases. Abbreviations: mDia, mammalian Diaphanous formin; ROCK, Rho-associated coiled coil kinase; PAK, p21-activated kinase; IRSp53, insulin receptor tyrosine kinase substrate p53; MRCK, myotonic dystrophy kinase-related Cdc42-binding kinase; MLC, myosin light chain; p, phosphorylated; LIMK, LIM motif containing protein kinase; MLCK, myosin light chain kinase; MLCP, myosin light chain phosphatase; WASP, Wiskott-Aldrich syndrome protein; N-WASP, neuronal-Wiskott-Aldrich syndrome protein; WAVE, Wiskott-Aldrich syndrome protein-family verprolin homologous protein; Arp2/3, a seven subunit complex comprising actin-related proteins 2 and 3.

Regulation of effector proteins by Rho GTPases may vary. Some effectors are folded in an auto-inhibitory form which is relieved upon binding to small GTPase (Bishop and Hall 2000). This is exampled by group I of PAKs (PAK1-3). These kinases contain the CRIB domain, which partially overlaps with an auto-inhibitory domain (AID). The latter binds to and inhibits a kinase domain present at the C-terminus of PAK. Binding of activated Rho GTPase to the CRIB domain destabilises the AID domain. This leads to the release of a C-terminal kinase domain, subsequent autophosphorylation of PAK and its full activation (Zhao, Manser et al. 1998; Lei, Lu et al. 2000). Alternatively, Rho GTPases may activate their target proteins by bringing them to specific complexes or locations in the cell (Jaffe and Hall 2005).

1.2.5. Role of Rho GTPases in angiogenesis

1.2.5.1.   Rho GTPases in vascular permeability

ECs that line blood vessels are inter-connected by adherens and tight junctions (Bazzoni and Dejana 2004). These connections are disrupted when angiogenic stimuli such as VEGF or thrombin permeabilise an EC wall resulting in the formation of intercellular gaps (Mehta and Malik 2006). It is well known that RhoA, Rac1 and Cdc42 can regulate the EC permeability (Beckers, van Hinsbergh et al. 2010; Spindler, Schlegel et al. 2010). Stimulation by thrombin activates the RhoA-ROCK signalling cascade which leads to myosin light chain (MLC) phosphorylation, increased cell contractility and permeability of endothelial wall. Activation of RhoA is likely to be mediated by p115RhoGEF (Holinstat, Mehta et al. 2003), GEFH1 (Birukova, Adyshev et al. 2006) and inhibition of RhoGDI (Mehta, Rahman et al. 2001). On the other hand, RhoA mediated permeability can be antagonised by Rac1 and Cdc42. These GTPases activate PAK leading to the stabilisation of junctional complexes including cadherin/catenin/actin and integrity of cell-cell contacts (Waschke, Baumgartner et al. 2004; Seebach, Madler et al. 2005; Waschke, Burger et al. 2006). Moreover, activation of focal

adhesion kinase (FAK) can lead to the phosphorylation of p190RhoGAP, which inhibits RhoA activity and eventually restores the integrity of EC barrier (Holinstat, Knezevic et al. 2006). Thus different Rho GTPases can both inhibit or promote a vascular permeability and this appears to be regulated temporarily, depending on the signal that leads to their activation or inhibition (Beckers, van Hinsbergh et al. 2010; Spindler, Schlegel et al. 2010).

1.2.5.2. Rho GTPases in ECM remodelling

ECs which are selected to initiate sprouting, need to change their morphology and become highly motile and invasive (Adams and Alitalo 2007). These cells are required to activate secreted or cell surface anchored proteases to degrade surrounding endothelial basement membranes and invade adjacent tissues. An important matrix-metalloproteinase (MMP) expressed in ECs is MMP-9 (Qian, Wang et al. 1997). Some studies showed that overexpression of dominant active RhoA in ECs up-regulated the transcription of MMP-9 and promoted cell invasion into a 3D matrix-protein gel (Abecassis, Olofsson et al. 2003). In this case MMP-9 colocalised with RhoA at the forefront of advancing lamellipodia in migrating ECs. Other studies showed that RhoA and Cdc42 were differently regulating some other matrix metalloproteinases (Ispanovic, Serio et al. 2008). Expression of dominant active Cdc42 increased the localisation of a membrane type 1 (MT1)-MMP to the cell surface and activated MMP-2 in ECs. A similar effect was seen upon inhibition of ROCK, an effector of RhoA. Moreover, expression of dominant active Cdc42 or dominant negative RhoA increased EC sprouting in a 3D collagen matrix and inhibition of Cdc42 was sufficient to reduce VEGF-dependent activation of MMP-2 (Ispanovic, Serio et al. 2008). Thus Rho GTPases are important in the regulation of expression and activity of MMPs and thereby in remodelling of ECM.

1.2.5.3.   Rho GTPases in endothelial cell migration

After successful degradation of the basement membrane, a sprouting endothelial tip cell migrates into surrounding tissue (Adams and Alitalo 2007). As described in detail in section 1.3, the turnover of both the actin cytoskeleton and FAs facilitates cell migration (Nobes and Hall 1995; Raftopoulou and Hall 2004; Parsons, Horwitz et al. 2010). In ECs similar events occur and these are accompanied by spatio-temporal activation of Rho GTPases (Cascone, Giraudo et al. 2003; Fryer and Field 2005). Activated by pro-migratory stimuli, RhoA and Rac1 translocate from the cytosol to the SF-associated perinuclear region and F-actin at leading edge, respectively. There they regulate actin polymerisation, actomyosin contraction and FA turnover (Bryan and D'Amore 2007). Multiple studies suggested that disruption of Rho GTPases-mediated signalling in ECs inhibits cytoskeleton rearrangements and results in impaired cell migration (Okamoto, Yatomi et al. 2000; Paik, Chae et al. 2001; Fryer and Field 2005; Lee and Kay 2006; Bryan, Dennstedt et al. 2010; Del Valle-Perez, Martinez et al. 2010; Enciso, Konecny et al. 2010; Liebl, Weitensteiner et al. 2010). During the sprouting of ECs the levels of phosphorylated MLC (pMLC) are being reduced and Rac1 activity is induced (Mavria, Vercoulen et al. 2006; Abraham, Yeo et al. 2009). Regulation of PAK activity, which acts downstream of Rac1 and Cdc42, was shown to be critical in the regulation of EC migration (Kiosses, Daniels et al. 1999). Kiosses and colleagues showed that overexpression of dominant active or dominant negative PAK mutants significantly decreased EC migration. Another group showed that Rac1 was essential for the matrix-induced morphological changes of EC and promoted their migration acting through PAK (Connolly, Simpson et al. 2002). Garret and colleagues showed that in VEGF-induced EC migration Rac1 was activated by its GEF Vav2 (Garrett, Van Buul et al. 2007). This signalling pathway was also dependent on the activation of Src (Gavard and Gutkind 2006). Many other studies exist which demonstrate the

importance of Rho GTPases in EC migration, however a description of all of these is beyond the scope of this introduction.

1.2.5.4. Rho GTPases and endothelial cell proliferation

Proliferation of ECs contributes to angiogenesis and enables the extension of newly sprouting capillaries. Different signalling pathways are involved in this process (Bryan and D'Amore 2007). VEGFR2-dependent activation of PLCγ leads to the induction of extracellular signal-regulated kinase 1/2 (ERK1/2) signalling and subsequent proliferation of ECs (Pages, Milanini et al. 2000; Takahashi, Yamaguchi et al. 2001). Moreover the VEGF-induced activation of phosphatidylinositol 3-kinase (PI3K) leads to the activation of its downstream target, the serine/threonine kinase AKT/PKB, which promotes EC proliferation and survival (Fujio and Walsh 1999; Dayanir, Meyer et al. 2001). Some studies showed that Rho GTPases also promote EC proliferation by regulation of cell-cycle progression (Bryan and D'Amore 2007). Stimulation of human umbilical vein endothelial cells (HUVECs) by estradiol, a hormone that acts via estrogen receptors, induced the RhoA/ROCK signalling cascade which led to the increased expression of cell-cycle related proteins and enhanced EC migration and proliferation (Oviedo, Sobrino et al. 2010). In some other studies Rac induced the expression of tumor endothelial marker 5, which in turn mediated contact inhibition of proliferation in ECs (Vallon, Rohde et al. 2010).

1.2.5.5. Rho GTPases in stabilisation and survival of newly formed capillaries

When a sprouting column of ECs joins with another vessel the lumen is formed to enable the blood flow. This process appears to be complex and is not fully understood yet. The existing data suggested a mechanism dependent on interaction of ECs with components of the ECM (Adams and Alitalo 2007). This involves integrin-mediated signalling, which leads to the

activation of Rac and Cdc42. These GTPases are then involved in the vacuole formation and coalescence (Davis, Koh et al. 2007). It was shown that in growing inter-segmental vessels in zebrafish the lumen forms firstly by intracellular and then inter-cellular fusion or large vacuoles, which are positive for Cdc42 (Kamei, Saunders et al. 2006). Some other studies tested lumen formation in 3 dimensional matrices by ECs treated with Clostridium difficle toxin B or C3 transferase (Bayless and Davis 2002). The former toxin inhibits RhoA, Rac1 and Cdc42 GTPases, while the latter one blocks RhoA, RhoB and RhoC. It was found that C3 transferase did not inhibit the lumen formation as opposed to toxin B treatment. Thus it was concluded that Cdc42 and Rac1, but not RhoA play a major role in the lumen formation (Bayless and Davis 2002). It was proposed that downstream effectors of Rac and Cdc42 such as Pak and WASP are likely to mediate this process (Bryan and D'Amore 2007).

To stabilise newly forming vasculature, the regulation of EC survival is very important (Adams and Alitalo 2007). The blood flow in vessels stabilises connections between cells while the supply of oxygen lowers the local expression of VEGFA, resulting in reduction of EC proliferation. Then the ECM is formed and other cells such as pericytes are recruited to cover the vessel (Jain 2003; Adams and Alitalo 2007). Rho GTPases were shown to play a role in EC survival. Inhibition of RhoA but not Rac1 or Cdc42 induced apoptosis in HUVECs (Hippenstiel, Schmeck et al. 2002; Li, Liu et al. 2002). Moreover, apoptosis in the newly forming retinal vasculature was observed in RhoB knock-out mice (Adini, Rabinovitz et al. 2003). Pharmacological depletion of RhoB or its dominant negative mutant resulted in apoptosis in ECs and reduced EC tube sprouting. This was thought to be due to the elimination of Akt from the nucleus and its degradation (Adini, Rabinovitz et al. 2003). On the contrary, other studies showed that a dominant negative RhoA or pharmacological inhibition of ROCK decreased tumor necrosis factor-α (TNF-α)-induced apoptosis of bovine

ECs (Petrache, Crow et al. 2003), which may suggest that Rho-mediated survival/apoptosis might be cell type dependent.

1.2.6. RhoJ

RhoJ is a member of the Cdc42-like subfamily of Rho GTPases, and it is also called TCL or TC10-like due to its highest similarity to other small Rho GTPase TC10 (Vignal, De Toledo et al. 2000). RhoJ is encoded by five exons, which span over 85 kilo bases on human chromosome 14. Vignal *et al.* showed that RhoJ very rapidly exchanges GDP into GTP and when activated, it binds to the CRIB domain of PAK and WASP (Vignal, De Toledo et al. 2000). In addition, Aspenstrom *et al.* performed a yeast-two-hybrid (Y2H) study in which they showed that the dominant active RhoJ mutant interacted with known effectors of Cdc42 such as WASP, neural WASP (N-WASP), Cdc42-interacting protein 4 (CIP4), partitioning defective 6 (Par6), p50RhoGAP, PAK1B and PAK4 (Aspenstrom, Fransson et al. 2004). However there is a lack of data showing the physiological relevance of these interactions in mammalian cells.

Ectopically expressed RhoJ localised to the dorsal cell membrane and was associated with large intra-cytoplasmic vesicles in REF-52 fibroblasts (Vignal, De Toledo et al. 2000). In these cells, an active mutant of RhoJ caused the production of large and dynamic F-actin ruffles on the dorsal membrane. This phenotype was blocked by dominant negative Rac1 and Cdc42 mutants, suggesting that these three GTPases may share similar GEFs. In another study, constitutively active RhoJ caused the formation of lamellipodia and FA-like assemblies at the cell periphery of porcine aortic ECs stably expressing the human platelet-derived growth factor β-receptor (Aspenstrom, Fransson et al. 2004). Moreover, Billottet and colleagues showed that an overexpressed active mutant of RhoJ induced the formation of podosomes in ECs (Billottet, Rottiers et al. 2008). Podosomes are another type of cellular

adhesions formed by a central actin core surrounded by a ring of integrins and other proteins; they play a role in highly motile, invasive cells (Albiges-Rizo, Destaing et al. 2009).

Some other studies indicated a role for RhoJ in early endocytosis of the transferrin (Tf) receptor (de Toledo, Senic-Matuglia et al. 2003). De Toledo *et al.* showed localisation of ectopically expressed myc-tagged RhoJ to the plasma membrane and early/sorting endosomes (EE/ES) in HeLa cells. The knock-down of RhoJ with siRNA perturbed Tf release while the overexpression of constitutively active RhoJ (daRhoJ) promoted the accumulation of Tf in the EE/ES. In addition daRhoJ blocked the movement of Tf to perinuclear recycling endosomes resulting in Tf recycling to the plasma membrane directly from the EE/ES (de Toledo, Senic-Matuglia et al. 2003).

Several studies have suggested a role for RhoJ both in adipocytes and adipogenesis. The mouse ortholog of RhoJ (called in this study TC10β), when transfected into 3T3-L1 adipocytes was activated by insulin stimulation (Chiang, Hou et al. 2002). This activation was CAP/Cbl/CrkII/C3G pathway dependent. Another group demonstrated increased RhoJ (TC10β-long) expression in 3T3-L1 cells induced to differentiate into adipocytes (Nishizuka, Arimoto et al. 2003). This differentiation was inhibited upon antisense mediated knock-down of RhoJ. Moreover, the constitutive expression of RhoJ in NIH-3T3 fibroblasts, which do not spontaneously differentiate into adipocytes, caused the accumulation of oil droplets and adipogenic markers (Nishizuka, Arimoto et al. 2003). Subsequent studies by this group revealed that RhoJ regulated the differentiation of mouse adipocytes by controlling mitotic clonal expansion (MCE) and this regulatory effect was closely linked to the expression of C/EBPβ and C/EBPδ genes (Kawaji, Nishizuka et al. 2010).

1.2.6.1. RhoJ in endothelial cells

Work performed by members of our laboratory showed that RhoJ is a Rho GTPase that may play a special role in the vasculature. Herbert *et al.* initially found that in publicly available human expression libraries RhoJ was present only in EC libraries (Herbert, Stekel et al. 2008). This bioinformatic prediction was supported by examining RNA expression using reverse transcription and quantitative polymerase chain reaction (qPCR), where among several cell types tested (fibroblasts, hepatocytes, lymphocytes, keratinocytes, endothelial and epithelial cells) RhoJ was present only in the cDNA of ECs (Herbert, Stekel et al. 2008). More recently, *in situ* hybridisation studies in both developing mouse embryo at embryonic day 9.5 (when the angiogenesis occurs) and in human tissue sections showed that RhoJ gene was expressed in the blood vessels (Kaur, Leszczynska et al. 2011). More specifically, RhoJ expression was detected in the blood vessels of the heart, adrenal gland, lymph node, muscle, pancreas, placenta, liver, lung, bladder cancer, bone cancer and ovarian cancer but not in the vessels of testis, brain, kidney, stomach, colon or rectal cancer. The presence of RhoJ in human smooth muscle cells and pericytes was also detected (both RNA and protein) but at a very low level when compared to ECs (Kaur, Leszczynska et al. 2011).

Since RhoJ was expressed in endothelium, a series of experiments aimed to determine its function in this tissue (Kaur, Leszczynska et al. 2011). Firstly, silencing of RhoJ using siRNA significantly decreased the migration of ECs. This was demonstrated in chemotaxis and chemokinesis assays. In the former RhoJ knock-down significantly impaired a movement of cells towards serum and FGF-2. In the latter silencing of RhoJ slowed down the migration of cells in a scratch wound assay. Another set of experiments tested the effect of silencing RhoJ on tubulogenesis *in vitro*. When plated on Matrigel, which is a solubilised basement membrane extract, ECs were induced to form a two dimensional network of tubes and RhoJ

knock-down significantly inhibited this process. Similarly, silencing of RhoJ significantly impaired tubulogenesis by ECs co-cultured on a monolayer of fibroblasts. In this assay human dermal fibroblasts (HDFs) grown to a monolayer produce their own ECM and secrete VEGF. These conditions, together with the exogenously added FGF-2 provide an appropriate environment for ECs to form tubules with lumens, which are highly reminiscent of those present *in vivo* (Bishop, Bell et al. 1999).

Sukhbir Kaur in our laboratory also showed that lowering RhoJ expression significantly increased a number of FAs and SFs in HUVECs. This effect was most prominent in migrating ECs such as those present at the edge of a wounded monolayer. Interestingly, RhoJ knock-down did not affect FAs and SFs in ECs situated within the monolayer, suggesting that RhoJ plays a particular role in regulating these structures in motile cells. Moreover, a general increase in EC contractility was observed in the absence of RhoJ. This was detected by increased MLC phosphorylation and increased contraction of the type I collagen (Kaur, Leszczynska et al. 2011).

Subsequently, Sukhbir Kaur showed that the pharmacological inhibition of ROCK with Y27632 or direct inhibition of MLC phosphorylation with blebbistatin reversed the migrating and tube forming defects of RhoJ-knocked-down cells Thus, it was concluded the RhoJ plays important role in the regulation of motility, actomyosin contractility and FA turnover in ECs.

1.3.   Actin cytoskeleton and focal adhesions in cells

1.3.1. Actin cytoskeleton

The actin cytoskeleton is a dynamic scaffold, which determines the shape and mediates motility of cells (Lee and Dominguez 2010). The actin filaments (filamentous actin, F-actin) are formed from monomeric units of globular actin (G-actin), and formation of filaments

requires energy from hydrolysis of ATP to ADP. On the growing end of the actin filament (the barbed end) ATP-bound G-actin monomers are added while in the actin disassembling end (the pointed end) ADP-bound actin monomers dissociate, and this process is called actin filament treadmilling (Lee and Dominguez 2010). Various proteins can bind to actin and mediate the nucleation, elongation, branching, crosslinking or disassembly of its filaments. Formins can nucleate and elongate linear actin filaments, while the Arp2/3 complex (a seven-subunit complex comprising actin-related proteins 2 and 3) is a regulator of filament branching (Campellone and Welch 2010). Cofilin/ADF can lead to the dissociation of actin filaments into globular monomers (Bamburg 1999). Actin filaments are crosslinked by various proteins including α-actinin and non-muscle myosin II (NM II) (Vicente-Manzanares, Ma et al. 2009). NM II is a dimer which comprises two identical units connected via their α-helical coiled-coil rod domains. Each of the two NM II units contains a globular head domain with Mg^{2+}-ATPase activity, regulatory and essential myosin light chains (MLC). NM II can act with and connect actin filaments and this is known as actomyosin. Upon phosphorylation of the regulatory MLC, NM II moves the antiparallel actin filaments and causes actomyosin contraction (Vicente-Manzanares, Ma et al. 2009). Bundles of actomyosin filaments can assemble into thicker structures, SFs, which provide tension and contraction in the cells (Amano, Chihara et al. 1997; Hotulainen and Lappalainen 2006; Pellegrin and Mellor 2007). The alignment of actin filaments varies in different cellular regions. In the lamellipodium of migrating cells actin filaments are highly branched, while in the following lamellum they are organised as parallel bundles (Pollard and Borisy 2003; Nicholson-Dykstra, Higgs et al. 2005). Some actin filaments are linked to the ECM via FAs (Lauffenburger and Horwitz 1996; Webb, Parsons et al. 2002). Fig. 1.7 shows a typical organisation of cytoskeletal filaments and FAs in the migrating cell.

1.3.2. Focal adhesions

FAs are dynamic, multiprotein complexes which connect the actin cytoskeleton with the ECM and therefore allow cells to attach to the underlying surface (Dubash, Menold et al. 2009). In the lamellipodium small nascent adhesions are being formed, some of which assemble and disassemble quickly. Other adhesions maturate and gradually "move" to the rear while the cell is shifting its body forward (Fig. 1.7). Eventually the rear FAs disassemble as the cell migrates (Webb, Parsons et al. 2002; Parsons, Horwitz et al. 2010).

The components of FAs vary but the most common ones include: integrins, talin, vinculin, α-actinin, paxillin, FAK, Src, Arp2/3 (Parsons, Horwitz et al. 2010). The Fig. 1.8 shows a connection between actomyosin filaments and the typical proteins which form FAs. Integrins are crucial elements of FAs as they link the cell directly with the ECM and mediate bidirectional signalling between the cell and its environment (Dubash, Menold et al. 2009; Shattil, Kim et al. 2010). In so called "inside-out" signalling various proteins can activate integrins by binding to the β-integrin tails inside the cell. This leads to conformational changes of integrins and increases their affinity for extracellular ligands. Using this signalling, cells can modulate their ability to bind and remodel the ECM. On the other hand, extracellular ligands can bind to integrins and signal to the cell via integrin activation in a so-called "outside-in" way. This induces conformational changes in integrins and their clustering. As a result integrins transmit the signal into the cell and induce processes such as cell proliferation, cytoskeletal rearrangements or gene expression (Shattil, Kim et al. 2010).

There are two models describing FAs assembly (Parsons, Horwitz et al. 2010). The first suggests that integrins bind to the components of ECM such as collagen or fibronectin. This leads to the activation of their cytoplasmic tails and results in their clustering. The cytoplasmic tail of β-integrins recruits initially talin followed by other FA proteins which
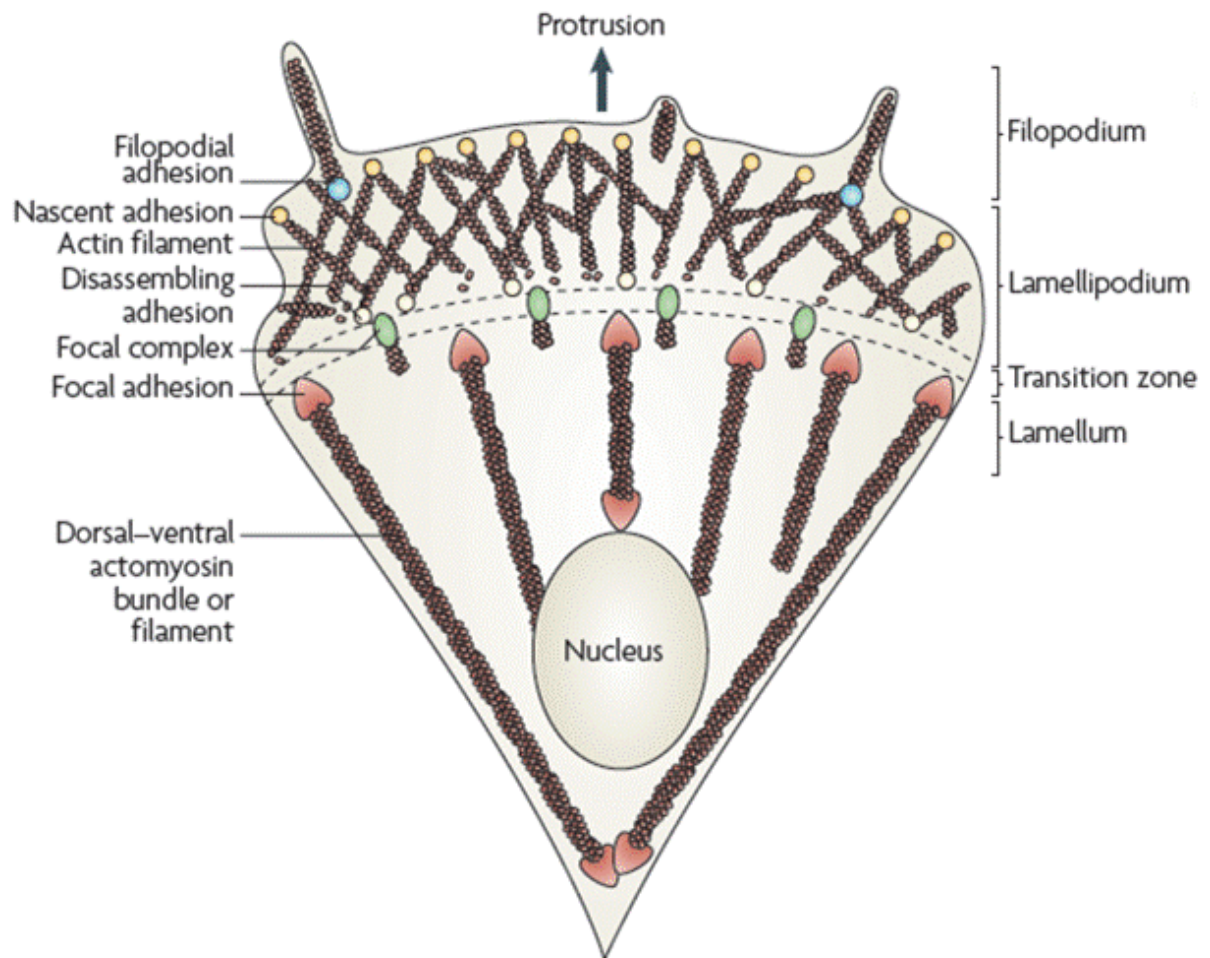
Fig. 1.7 Regulation of the actomysoin cytoskeleton and focal adhesions during cell migration.
During migration cells polarise and extend protrusions such as spike-like filopodia and sheet-like lamellipodia towards the pro-migratory factors. These protrusions comprise actin filaments and are stabilised by nascent focal adhesions, which connect the actin filaments to the extracellular matrix. Attached to the underlying surface, cells use the actomyosin contractility to move forwards and subsequently focal adhesions at the rear are disassembled. Thus a constant turnover of focal adhesions and actomyosin cytoskeleton occurs during cell migration. The picture was adapted from Parsons et al. (2010).
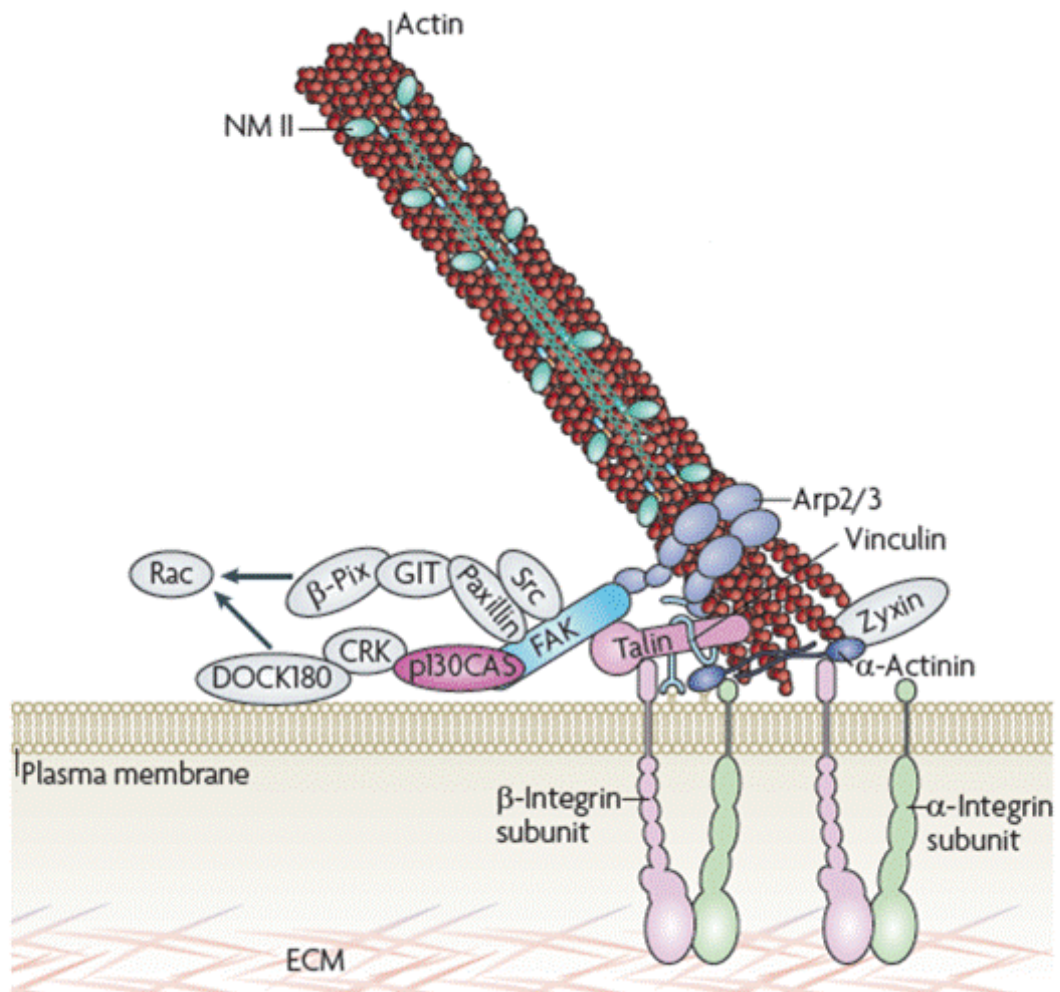
Fig. 1.8 Main components of focal adhesions and their connection to the actomyosin filaments.
The scheme shows typical proteins which are recruited to focal adhesion complexes. Firstly, integrins bind to the components of extracellular matrix (ECM) such as collagen or fibronectin and this leads to the activation of cytoplasmic tails of integrins which then recruit talin, vinculin and other proteins to form an adhesion complex. NM II, non-muscle myosin II. The picture was adapted from Vicente‑Manzanares et al. (2010).

form an adhesion complex, and this complex eventually joins with the actin filaments. Another model suggests that proteins such as vinculin or pFAK bind firstly to the Arp2/3 complex associated with actin filaments. Then subsequent binding of this complex to integrins stabilises formation of a FA (Parsons, Horwitz et al. 2010). Some proteins when recruited to FAs become activated by phosphorylation (e.g. paxillin or FAK) (Tomar and Schlaepfer 2009) and this determines the recruitment of other proteins. On the other hand, some components of FAs need mechanical tension to be applied to enable their activation. For example, talin binds to integrins in an autoinhibitory form. Then its tail connects to actin filaments and the actomyosin contraction generates a tension which causes conformational changes in talin and reveals its binding site for vinculin (del Rio, Perez-Jimenez et al. 2009). This again leads to the recruitment of other proteins and FA maturation (Humphries, Wang et al. 2007).

It is not completely understood how FAs are disassembled. Clearly, dispersion of FAs is required for rearrangement of F-actin (Parsons, Horwitz et al. 2010). Some studies showed that FAK and Src kinases are very important for FAs disassembly as loss of these proteins significantly deacreases a disassembly rate in cells (Ilic, Furuta et al. 1995; Webb, Donais et al. 2004). Similarly the activity of mitogen-activated protein kinases is important for this process as overexpression of dominant negative mutant of MEK impaires FA disassembly (Sieg, Hauck et al. 1999; Webb, Donais et al. 2004). Other studies showed that calpain, which is a calcium dependent protease, cleaves talin and cytoplasmic tail of $\beta 3$ integrin leading to a FA disassembly (Franco and Huttenlocher 2005). In addition, phosphorylation of some FA components may lead to disassembly of these structures. Some data suggested that phosphorylation of paxillin and its interaction with the PAK/PIX/GIT1 complex promotes FAs turnover (described in details in the section 1.5) (Zhao, Manser et al. 2000; Nayal, Webb

et al. 2006). FA disassembly also largely depends on the dynamics of microtubules and related endocytic recycling of FA components. As an example, after FA disassembly integrins are transported through the endocytic pathway from the rear of the cell to its front (Ezratty, Partridge et al. 2005; Caswell, Vadrevu et al. 2009).

1.3.3. Actomyosin contractility and focal adhesion turnover – involvement of Rho GTPases

The dynamics of FA and actin cytoskeleton turnover are interdependent (Parsons, Horwitz et al. 2010). When cells move forward some actin protrusions grow in the front while other retract in the rear and this is accompanied by assembly and disassembly of FAs (Raftopoulou and Hall 2004). These processes are highly dependent on the activity of Rho GTPases (Fig. 1.6) (Nobes and Hall 1995; Pollard and Borisy 2003; Machacek, Hodgson et al. 2009). Firstly, Cdc42 and Rac1 induce their downstream effectors such as WASP and WASP-family verprolin homologue (WAVE), respectively (Raftopoulou and Hall 2004). These proteins activate the Arp2/3 complex, which initiates the branching and nucleation of actin filaments (Nicholson-Dykstra, Higgs et al. 2005). Rac1 and Cdc42 also stabilise actin filaments by activating PAK. This kinase phosphorylates LIM kinase which then inactivates cofilin – a protein that disassembles actin filaments (Yang, Higuchi et al. 1998; Wang, Eddy et al. 2007). As a result, the actin filaments extend and are stabilised. RhoA, on the other hand, activates the formin mammalian Diaphanous (mDia) at the front of the cell to perform a linear elongation of actin filaments (Kurokawa and Matsuda 2005; Pertz, Hodgson et al. 2006; Chesarone, DuPage et al. 2010). Moreover RhoA activates ROCK, which then leads to the phosphorylation of MLC. This generates tension forces which enable retraction of the rear of cell body during migration (Vicente-Manzanares, Koach et al. 2008). As the actin nucleation proceeds, the FAs are being assembled in the front and simultaneous actomyosin retraction in

the rear is accompanied by disassembly of the rear FAs (Raftopoulou and Hall 2004). Thus it is important during cell migration that the balance between constant turnover of the actin cytoskeleton and FAs is preserved, and for example excessive formation of SFs and FAs induced by RhoA signalling may inhibit cell migration (Raftopoulou and Hall 2004; Parsons, Horwitz et al. 2010).

Interestingly, RhoGAPs and RhoGEFs are very often recruited to FAs where they spatio-temporally control the activation of certain Rho GTPases. Rac1 can activate p190RhoGAP, which then inactivates RhoA leading to a decrease of cellular tension and a more continuous extension of protrusions (Arthur and Burridge 2001; Nimnual, Taylor et al. 2003). Some other evidence suggests that RhoA may lead to the inactivation of Rac1 via the GAP ARHGAP22 (Katsumi, Milanini et al. 2002; Sanz-Moreno, Gadea et al. 2008), thus suggesting that these GTPases can reciprocally regulate their activity and influence dynamics of actomyosin contraction and FA turnover.

1.3.4. Focal adhesions and stress fibres in endothelial cells in vivo

Although FAs and SFs form most prominently in many cells grown on plastic tissue culture dishes, the formation of similar structures may be observed in some cell types *in vivo,* including smooth muscle cells, myofibroblasts or endothelial cells (Dubash, Menold et al. 2009). *In vitro* studies allowed to establish that the size and quantity of FAs in cells largely depend on the elasticity and stiffnes of a substratum, to which these cells are attached (Dubash, Menold et al. 2009). In quiescent ECs that line blood vessels, FAs are thought to play a role in connecting the endothelial wall and basement membrane, while formation of SFs and contractility induced by RhoA signalling leads to increased cell permeability (Bogatcheva and Verin 2008). Some studies suggest that EC migration which happens during

vascular remodelling and angiogenesis is likely to be accompanied by turnover of FAs and cytoskeletal rearrangements (Li, Huang et al. 2005).

1.4.   Endocytosis

Endocytosis is a process in which the extracellular or membrane-bound material is transported to the intracellular compartments. This serves to mediate nutrient uptake, drug delivery, signalling, cell migration, adhesion, polarity, growth, differentiation, mitosis or pathogen entry. It also regulates the availabilty of various receptors and other membrane-bound signalling proteins on the cell surface (Doherty and McMahon 2009; Grant and Donaldson 2009; Sorkin and von Zastrow 2009). During endocytosis portions of the plasma membrane are being engulfed into the cell body in the form of vesicles. Various transmembrane proteins with bound ligands and extracellular liquid are internalised with these vesicles and join early endosomes (EE). Cargo delivered to EE is subsequently transported to sorting endosomes (ES), from where different cargos are trafficked to different cellular destinations. Internalised material can be passed to recycling endosomes and back to the plasma membrane, or alternatively, it can be sent to late endosomes and eventually to lysosomes for degradation (Doherty and McMahon 2009). Some endosomes may be associated with microtubules which regulate their trafficking (Grant and Donaldson 2009). The pH of the lumen in different endosomes varies from mildly acidic in EE/ES to more acidic in late endosomes and lysosomes. Upon these pH changes some internalised receptors release their cargo and recycle back to the plasma membrane or are directed into a degradative pathway (Sorkin and von Zastrow 2009). Endosomes and lysosomes also take part in trafficking of macromolecules biosynthesised by the cell (Luzio, Rous et al. 2000; Gould and Lippincott-Schwartz 2009).

Different types of endocytosis have been described including phagocytosis, macropinocytosis, and caveaole or clathrin-mediated endocytosis; endocytosis may also be classified as clathrin-

dependent or clathrin-independent (Doherty and McMahon 2009). Phagocytosis mediates the internalisation of larger material such as cell debris or microorganisms (Greenberg and Grinstein 2002), while macropinocytosis is the uptake of extracellular liquid and solutes (Falcone, Cocucci et al. 2006). Caveolae are small vesicles regulated by proteins called caveolins and their membranes are enriched in cholesterol and glycosphingolipids (Parton and Simons 2007). Another type of membrane budding is controlled by clathrin (Higgins and McMahon 2002). Clathrin is a protein which covers inner portions of the plasma membrane called clathrin-coated pits. When these pits are internalised into the cell body, vesicles are being formed which are coated with clathrin on their cytoplasmic side. With the assistance of other proteins, such as dynein or adaptin, clathrin mediates budding of the vesicle and also takes part in the selection of a cargo to be internalised. Shortly after internalisation, the clathrin coat is discarded and the vesicle fuses with EEs. Clathrin-coated pits are involved in the internalisation of various receptors together with their ligands such as low density lipoprotein, Tf, antibodies or growth factors (Ungewickell and Hinrichsen 2007).

One of the most well-defined pathways in endocytosis is the trafficking of Tf receptor. Tf is a glycoprotein which delivers iron ions to the cells. Tf receptors present on the cell surface can bind, internalise and deliver the Tf-iron complex into endosomes, where low pH causes a dissociation of the iron ion. Subsequently, Tf can be recycled back by its receptor to the plasma membrane and released in order to bind more iron ions (Macedo and de Sousa 2008). Endocytosis also mediates the internalisation of many other receptors (Sorkin and von Zastrow 2009). In ECs, VEGFR2 traffics between the plasma membrane and endosomes and a proportion of this protein is sent to lysosomes for degradation (Scott and Mellor 2009). This trafficking may regulate the surface levels of VEGFR2 and therefore the sensitivity of ECs to VEGF signalling.

Many studies have shown the importance of Rho GTPases in various types of endocytosis and other intracellular vesicular trafficking (Ellis and Mellor 2000; Ridley 2001; Qualmann and Mellor 2003; Symons and Rusk 2003). Rac1-dependent recruitment of PAK to membrane ruffles and pinocytic vesicles can stimulate pinocytosis (Dharmawardhane, Schurmann et al. 2000). Insulin-stimulated activation of TC10 increases glucose uptake by recruitment of GLUT4 transporter to the plasma membrane (Chiang, Baumann et al. 2001). RhoD and RhoJ were shown to regulate the early endocytosis pathway (Murphy, Saffrich et al. 2001; de Toledo, Senic-Matuglia et al. 2003; Gasman, Kalaidzidis et al. 2003), while RhoB is involved in the regulation of receptor trafficking from EE to late endosomes (Gampel, Parker et al. 1999; Huang, Duhadaway et al. 2007). Cdc42 and its effector N-WASP were shown to control the transport of proteins from Golgi to endoplasmic reticulum (Luna, Matas et al. 2002), while RhoG was found to play a role in lysosomal dynamics (Vignal, Blangy et al. 2001). The activity of Rac1 and RhoA may affect the clathrin-dependent and -independent internalisation of various receptors (Lamaze, Chuang et al. 1996; Lamaze, Dujeancourt et al. 2001).

1.5.   The GIT/PIX complex

1.5.1. Domain organisation of PIX proteins

The family of PIX proteins (discovered as PAK-interacting exchange factors) comprises αPIX (Cool-2) and βPIX (Cool-1), which are encoded by *ARHGEF6* and *ARHGEF7* genes, respectively (Bagrodia, Taylor et al. 1998; Manser, Loo et al. 1998). These PIX proteins are homologous in multiple domains as described in Fig. 1.9. αPIX contains an additional N-terminal calponin homology (CH) domain, which is absent in most splice variants of βPIX and determines an interaction of αPIX with the FA protein β-parvin/affixin. βPIX on the other hand contains a ZB domain at the C-terminus, which can bind with the PDZ motif in proteins

such as scribble and shank (Park, Na et al. 2003; Audebert, Navarro et al. 2004). Both PIX proteins contain a Src homology 3 (SH3) domain and thus are able bind to proline-rich sequences such as those present in PAK, c-Cbl ubiquitin ligase and Rac1 (Bagrodia, Taylor et al. 1998; Manser, Loo et al. 1998; Flanders, Feng et al. 2003; ten Klooster, Jaffer et al. 2006). The DH and PH domains regulate the GEF activity, which is inhibited by T1 insert present in βPIX forms only (Feng, Albeck et al. 2002). The GEF activity of βPIX can be restored upon Y442 phosphorylation by Src (Feng, Baird et al. 2006). The common domains of αPIX and most βPIX splice variants include a proline-rich (PR) region which determines interactions with POPX1 and POPX2 phosphatases (Koh, Tan et al. 2002); a GIT-binding domain (GBD) (Bagrodia, Bailey et al. 1999; Turner, Brown et al. 1999; Zhao, Manser et al. 2000), and a coiled-coil (CC) motif responsible for homo- and heterodimerisation (Kim, Lee et al. 2001; Koh, Manser et al. 2001). SH3, PH and DH domains additionally mediate an interaction with the protease Calpain 4 (Rosenberger, Gal et al. 2005).

1.5.1. Domain organisation of GIT proteins

GITs were discovered as G protein-coupled receptor (GPCR) kinase-interacting targets binding to β2-adrenergic receptors (Premont, Claing et al. 1998; Claing, Perry et al. 2000). The family comprises GIT1 and GIT2. GIT1 and/or GIT2 are also known as CAT (Cool-associated tyrosine phosphorylated protein), PKL (paxillin-kinase linker) and p95-APP (ArfGAP-putative, PIX-interacting, paxillin-interacting protein) (Bagrodia, Bailey et al. 1999; Turner, Brown et al. 1999; Di Cesare, Paris et al. 2000). GIT proteins contain multiple domains (Fig. 1.9). These include: an N-terminal GAP domain which specifically binds Arf GTPases (Vitale, Patton et al. 2000); the ankyrin repeats responsible for intramolecular folding of GIT1 and its targeting to endosomes (Di Cesare, Paris et al. 2000; Paris, Za et al. 2002; Totaro, Paris et al. 2007); a Spa2 homology domain (SHD)
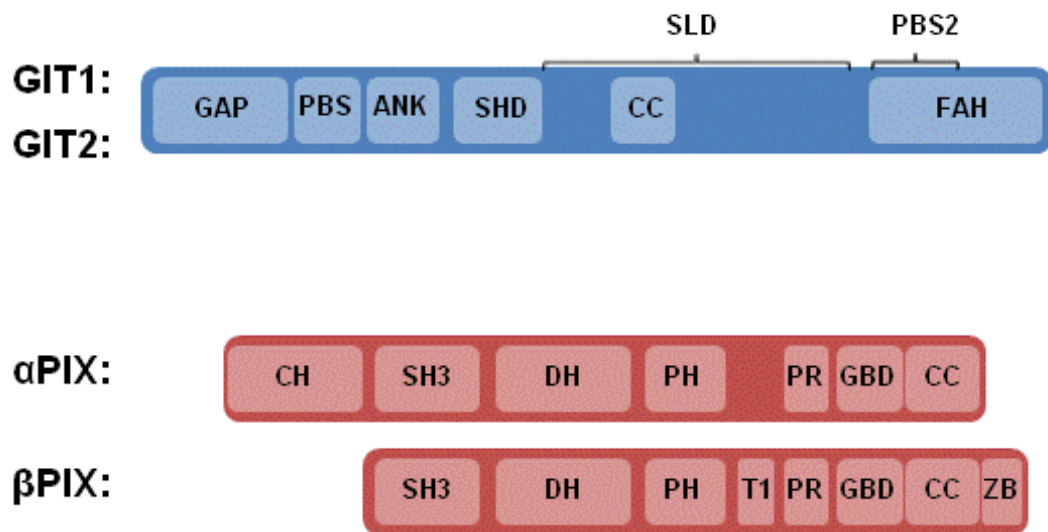
Fig. 1.9 Domain organisation of GIT and PIX proteins.
GIT and PIX proteins have multiple domains, which are responsible for interactions with various proteins. The figure illustrates domain organisation of GIT1, the predominant form of GIT2 (long), αPIX and predominant form of βPIX. Abbreviations: GAP, GTPase-activating protein domain; PBS, paxillin binding sequence; ANK, ankyrin repeats; SHD, yeast Spa2 homology domain; CC, coiled-coil region; FAH, focal adhesion targeting homology domain; SLD, synaptic localisation signal; CH, calponin homology domain; SH3, Src homology 3 domain; DH, Dbl homology domain; PH, pleckstrin homology domain; T1, GEF inhibitory T1 insert; PR, proline-rich region; GBD, GIT-binding domain; ZB, PDZ domain binding motif.

involved in interactions with PIX, FAK, MEK, Piccolo and PLCγ (Kim, Ko et al. 2003; Premont, Perry et al. 2004; Yin, Haendeler et al. 2004; Zhao and Manser 2005; Jones and Katan 2007); a coiled-coil region, which together with the SHD domain mediates homo- and heterodimerisation of GIT (Paris, Longhi et al. 2003); and a focal adhesion targeting homology domain (FAH) which binds to paxillin (Turner, Brown et al. 1999; Zhao, Manser et al. 2000). The middle region of GIT1 including the CC motif spans a synaptic localisation domain responsible for its targeting to dendritic protrusions (Zhang, Webb et al. 2003). In addition, stimulation with thrombin, epidermal growth factor or angiotensin II can lead to the phosphorylation of GIT1 and this is normally mediated by Src and FAK kinases (Bagrodia, Bailey et al. 1999; Kawachi, Fujikawa et al. 2001; Haendeler, Yin et al. 2003; van Nieuw Amerongen, Natarajan et al. 2004; Yin, Haendeler et al. 2004; Webb, Mayhew et al. 2006; Wang, Taba et al. 2009). A protein tyrosine phosphatase PTPζ was shown to dephosphorylate GIT1 (Kawachi, Fujikawa et al. 2001).

1.5.2. Functions of PIX and GIT

Both PIX proteins have a GEF activity towards Rac1 and Cdc42 *in vitro*, with αPIX being a stronger GEF than βPIX (Bagrodia, Taylor et al. 1998; Manser, Loo et al. 1998; Koh, Manser et al. 2001; Feng, Albeck et al. 2002; ten Klooster, Jaffer et al. 2006). The GEF activity of αPIX towards particular Rho GTPases may be regulated by dimerisation. Feng and colleagues showed that monomeric αPIX was a GEF for both Rac1 and Cdc42 while as a dimer αPIX activated only Rac1 (Feng, Baird et al. 2004). Usually GEFs bind inactive small GTPases and mediate their activation (Cherfils and Chardin 1999). Interestingly, studies by Baird *et al.* showed that activated Rho GTPases can also bind to αPIX (Baird, Feng et al. 2005). They demonstrated that active Cdc42 bound to the αPIX dimer and induced its GEF activity

towards Rac1. In addition they found that activated Rac1 also bound to αPIX but this reduced its Rac-specific GEF activity thus providing a negative feedback loop.

PIX and GIT proteins form tight complexes, which may be homo- or heterodimers (Bagrodia, Bailey et al. 1999; Zhao, Manser et al. 2000). A model was proposed in which these complexes form larger assemblies as they were found as large aggregates in cells (Paris, Longhi et al. 2003; Premont, Perry et al. 2004; Hoefen and Berk 2006). GIT and PIX have multiple domains and their complexes often serve as scaffolds to bring into close proximity various proteins (Hoefen and Berk 2006; Frank and Hansen 2008). The C-terminus of GIT1 binds to paxillin, which is associated with FAs usually via binding to FAK (Turner, Brown et al. 1999). Then PIX, which is bound to GIT, concomitantly associates with PAK and drives its recruitment to FAs (Manser, Loo et al. 1998; Zhao, Manser et al. 2000). Thus the FAK/paxillin/GIT/PIX/PAK complex localises to FA where its particular components play specific functions. PIX as a GEF can activate Rho GTPases Rac1 and Cdc42, which in turn activate PAK inducing membrane ruffling and cytoskeletal reorganisation (Manser, Loo et al. 1998; Obermeier, Ahmed et al. 1998). Some studies suggested that GIT can also bind directly to PAK to induce its autophosphorylation and activation (Loo, Ng et al. 2004), however there is greater evidence to suggest that PAK is recruited to this complex via direct interaction with the SH3 domain of PIX. The whole complex may play a role in FA turnover (Zhao, Manser et al. 2000). Moreover, Zhao *et al.* proposed that GIT may occur in an autoinhibited form and its interaction with PIX unmasks its C-terminal domain thus enabling its binding to paxillin. Interaction of GIT with paxillin initiates phosphorylation of paxillin which promotes its dissociation from FAs and hence their disassembly (Zhao, Manser et al. 2000). More recent studies showed that FA disassembly can be regulated by phosphorylation of βPIX (Feng, Baird et al. 2010). Feng and colleagues demonstrated that Src can phosphorylate βPIX on the

tyrosine 442 which causes dissociation of βPIX from GIT1. This in turn increases interaction between GIT1 and paxillin and facilitates FA disassembly. Consistently, inhibition of the phosphorylation of βPIX restores its interaction with GIT1 and promotes FA formation (Feng, Baird et al. 2010).

In addition to FAs, the GIT/PIX complex can also localise to the plasma membrane and intracellular vesicles (Di Cesare, Paris et al. 2000; Matafora, Paris et al. 2001; Manabe, Kovalenko et al. 2002; Rosenberger and Kutsche 2006; Frank and Hansen 2008). Trafficking to these distinct compartments is likely to be dependent on Arf GTPases, which regulate a transport between the plasma membrane and endosomes (Nie, Hirsch et al. 2003). GIT proteins are GAPs for Arf GTPases and can strongly bind to them (Premont, Claing et al. 1998; Vitale, Patton et al. 2000). It was proposed that after the FA disassembly components of the paxillin/GIT/PIX/PAK complex can cycle to endosomes or other intracellular vesicles and from there they can move back to the leading edge of the cell to join with nascent FAs (Di Cesare, Paris et al. 2000; Matafora, Paris et al. 2001; Manabe, Kovalenko et al. 2002; Rosenberger and Kutsche 2006).

Some other studies suggested that PIX proteins can localise to FAs via other mechanisms. Filipenko *et al.* showed that αPIX can be recruited to FAs via the β-parvin/integrins-linked kinase complex and regulate cell spreading via activation of Rac1 and Cdc42 (Filipenko, Attwell et al. 2005). Moreover, αPIX can also interact with calpain 4. This calcium-dependent protease may cleave some components of FA such as α-actinin and spectrin leading to FA disassembly (Glading, Lauffenburger et al. 2002; Rosenberger, Gal et al. 2005; Rosenberger and Kutsche 2006).

GIT1 and βPIX also play a role at the cell periphery where they regulate directional cell migration (Frank and Hansen 2008). GIT1 acting as a GAP reduces active levels of Arf GTPases which leads to the inhibition of prolonged Rac1 activity and prevents random formation of lamellipodia (West, Zhang et al. 2001; Nishiya, Kiosses et al. 2005). In addition, during directional cell migration the actin cytoskeleton is rearranged and Golgi apparatus is relocated to the front of the nuclei, which is controlled by activation of Cdc42 (Osmani, Vitale et al. 2006). To enable this, scribble binds and targets βPIX to the leading edge of migrating cells where βPIX activates Cdc42. This induces the reorientation of the Golgi apparatus and perturbation of the PIX/scribble interaction blocks the reorientation of Golgi apparatus and thus disrupts directional cell migration (Audebert, Navarro et al. 2004; Osmani, Vitale et al. 2006; Dow, Kauffman et al. 2007). Scribble is also important for a polarised distribution of the PAK/PIX complex to the front of motile cells and for activation of Rac1 during chemoattractant-induced directional cell migration (Nola, Sebbagh et al. 2008). GIT may also play a role in forming connections between neurons since it localises to pre- and postsynaptic regions where it regulates formation of synapses formed along dendrites (Kim, Ko et al. 2003; Ko, Kim et al. 2003; Zhang, Webb et al. 2003).

1.5.3. The GIT/PIX complex in endothelial cells

Some studies indicated a role for GIT and PIX proteins in ECs. Shikata and colleagues showed that GIT1 and GIT2 were involved in the regulation of FA turnover in ECs. In the sphingosine-1 phosphate or thrombin stimulated ECs GIT1 promoted FA disassembly while GIT2 redistributed paxillin from the cytoplasmic pool to the nascent FAs (Shikata, Birukov et al. 2003a; Shikata, Birukov et al. 2003b). In other studies GIT1 was shown to regulate EC permeability, where stimulation of ECs with thrombin increased localisation of GIT1 to FAs. This process was mediated by activation of RhoA/ROCK pathway and inhibition of GIT1 in

HUVECs increased thrombin induced cell rounding, contraction and FA formation (van Nieuw Amerongen, Natarajan et al. 2004). Using microarray technology Slevin *et al.* showed up-regulation of GIT1 in ECs isolated from the places of arterial carotid plaques where increased haemorrhages and tissue ulceration occurs (Slevin, Elasbali et al. 2006). In other studies the integrity of the PAK/PIX/GIT1 complex was necessary for the activation of ERK1/2 in induction of vascular permeability by lipopolysaccharide (Stockton, Reutershan et al. 2007). A global knock-out of GIT1 gene in mice led to 60 % perinatal mortality and this phenotype was caused by the severe impairment of lung development significantly reducing the numbers of pulmonary blood vessels and increasing alveolar spaces (Pang, Hoefen et al. 2009). This study also showed that GIT1 regulated pulmonary vascular development by mediation of VEGF-induced PLCγ and ERK1/2 activation. Another study showed that GIT1 was involved in the regulation of VEGF-induced EC migration and podosome formation (Wang, Taba et al. 2009).

1.6.   Aim of the study

Our group has shown that RhoJ is expressed predominantly in ECs and lowering of its expression by siRNA impairs EC migration, tube formation, proliferation but also increases actomyosin contractility and the number of FAs (Kaur, Leszczynska et al. 2011). However, little was known about signals and proteins which regulate the function of RhoJ in ECs. Therefore these PhD studies aimed to explore the role of RhoJ in ECs by studying its intracellular localisation and function, determining its binding partners, and testing its activation by pro-angiogenic stimuli.

1. Determine the localisation of endogenous RhoJ.

One of the goals of these PhD studies was to examine the localisation of RhoJ in ECs and then further explore its function (chapter 3). It was important to establish the intracellular localisation of endogenous RhoJ, since overexpression of some proteins may drive their aberrant localisation. A polyclonal rabbit RhoJ antibody was made, purified and validated for immunofluorescence, which enabled a comparison of localisation of endogenous and overexpressed RhoJ in ECs.

2. Characterise the role of daRhoJ in ECs.

In order to further examine the function of RhoJ in ECs, the daRhoJ mutant was stably overexpressed in HUVECs and its role in cell migration, and regulation of the number of SFs and FAs was tested (chapter 3).

3. Explore the role of RhoJ in endocytosis in ECs.

Another group had shown that RhoJ played a role in the early endocytosis pathway in HeLa cells (de Toledo, Senic-Matuglia et al. 2003), thus some experiments were performed to test this function of RhoJ in HUVECs (chapter 3).

4. Determine RhoJ binding partners.

Another goal of these studies was to determine RhoJ-binding partners in ECs (chapter 4). An approach was taken, which involved a pull-down of RhoJ-binding proteins from cellular lysates using constitutively active or inactive mutants of RhoJ fused with glutathione-*S*-transferase (GST). The pulled-down RhoJ-binding candidates were then identified by mass spectrometry and the most interesting hits, such as these involved in cell migration, CRIB domain-containing proteins, GAPs or GEFs were further tested for direct interactions with RhoJ in a Y2H assay. Mass spectrometry indicated that RhoJ pulled-down the GIT1/βPIX complex and the Y2H experiment proved direct interaction between RhoJ and GIT1. Both RhoJ and the GIT1/βPIX complex were implicated in the regulation of cell motility and FA dynamics, thus further experiments aimed to examine the interaction of RhoJ with this complex in ECs. Firstly, the co-localisation of RhoJ with GIT1 and βPIX proteins was verified. Then siRNA knock-downs of RhoJ, GIT1 and βPIX were performed to test the interdependence of these proteins on their localisation to FAs. In addition, the role of a dominant active RhoJ mutant in the localisation of GIT1 and βPIX proteins in ECs was determined.

5. Identify fators which activate RhoJ.

Another series of experiments aimed to test RhoJ activation by pro-angiogenic stimuli (chapter 5). Firstly, an assay was optimised to detect active RhoJ in ECs and it was subsequently used to measure the levels of active RhoJ in ECs treated with VEGFA, FGF-2 and thrombin.

2. MATERIALS AND METHODS

2.1.   Reagents and equipment

Reagents and chemicals used in methods were purchased from Sigma-Aldrich (Gillingham, UK), unless otherwise stated.

Centrifuges used with different speed ranges were as follows:

- Biofuge Pico Heraeus centrifuge for 1.5 ml microfuge tubes with up to 16060 x g (Kendro Laboratory Products GmbH, Langenselbold, Germany);

- Hettich Mikro 22R refrigerated centrifuge for 1.5 ml microfuge tubes with up to 21910 x g (Andreas Hettich GmbH, Tuttlingen, Germany),

- Biofuge Primo Heraeus centrifuge for up to 50 ml tubes with up to 2576 x g (Thermo Electron Corporation, Waltham, USA),

- Avanti^{TM} J-20XP refrigerated centrifuge for up to 500 ml bottles with up to 26000 x g, JLA-10.5 or JA-25.5 rotors used (Beckman Coulter, Brea, CA, USA).

The names and suppliers of other equipment are stated throughout the method sections.

2.2.   Common buffers

Common buffers and their contents are listed in Table 2.1. These were used in various methods described in the subsequent sections.

Tab. 2.1 Common buffers.

Buffer name	Contents
Rho-assay lysis buffer	1 % (v/v) Igepal 1 % (w/v) N-octyl-β-D-glucopyranoside 25 mM HEPES pH 7.5 30 mM $MgCl_2$ [a] 150 mM NaCl [a]
Nucleotide-loading lysis buffer	1 % (v/v) Igepal 1 % (w/v) N-octyl-β-D-glucopyranoside 25 mM HEPES pH 7.5 10 mM $MgCl_2$ [a] 150 mM NaCl [a]
E. coli **lysis buffer**	50 mM Tris-HCl, pH 7.5 [a] 50 mM NaCl [a] 5 mM $MgCl_2$ [a] 1 mM dithiothreitol (DTT, added fresh) 1 mM phenylmethylsulfonyl fluoride (PMSF, dissolved in methanol and added fresh)
E. coli **washing buffer**	50 mM Tris-HCl, pH 7.5 [a] 50 mM NaCl [a] 5 mM $MgCl_2$ [a]
PBS (Phosphate-Buffered Saline) [a]	137 mM NaCl 2.7 mM KCl 10 mM Na_2HPO_4 1.76 mM KH_2PO_4 pH 7.4
PBST (PBS Tween)	PBS [a] as above 0.1 % (v/v) Tween-20
TBS (Tris-Buffered Saline)	20 mM Tris-Cl, pH 7.5 [a] 150 mM NaCl [a]
TBST (TBS Tween)	TBS as above 0.1 % (v/v) Tween-20
High salt TBST	20 mM Tris-Cl, pH 7.5 [a] 650 mM NaCl [a] 0.1 % (v/v) Tween-20
HBS (HEPES-Buffered Saline)	20 mM HEPES, pH 7.5 150 mM NaCl [a]

48

TAE buffer [a]	40 mM Tris-base 18 mM glacial acetic acid 1 mM EDTA [a]
6x sample loading buffer	30 % (v/v) glycerol [a] 0.25 % (w/v) bromophenol blue 0.25 % (w/v) xylene cyanol FF
2x SDS-PAGE sample-loading buffer	100 mM Tris-Cl, pH 6.8 20% (v/v) β-mercaptoethanol 4% (w/v) SDS 0.2% (w/v) bromophenol blue 20% (v/v) glycerol [a]
SDS-PAGE running buffer	25 mM Tris-base [b] 250 mM glycine [b] 0.1 % (w/v) SDS
Transfer buffer	6 mM Tris-base [b] 47.6 mM glycine [b] 20 % (v/v) methanol [b], pH 8.3
Coomassie staining buffer	40 % (v/v) methanol [b] 10 % (v/v) acetic acid 0.2 g Coomassie Briliant Blue dye
Coomassie de-staining buffer	10 % (v/v) acetic acid 12.5 % (v/v) isopropanol

[a] reagents purchased from Cancer Research UK (CRUK) Central Services (Clare Hall, UK);
[b] reagents purchased from Fisher Scientific (Loughborough, UK)

2.3. Antibodies

Tab. 2.2 Primary antibodies.
Abbreviations: mAb, monoclonal antibody; polycl., polyclonal; aa, amino acids; WB, western blotting; IF, immunofluorescence; FACS, fluorescence activated cell sorting.

Antibody	Clone number, isotype	Immunogen	Working concentration μg/ml	Supplier
Mouse mAb anti-human **RhoJ**	ab57584, IgG1	Full-length human RhoJ	1 μg/ml (WB)	Abcam, Cambridge, UK
Mouse mAb anti-human **Cdc42**	44, IgG1	1-191 aa of human Cdc42	1 μg/ml (WB)	BD Biosciences, Oxford, UK
Mouse mAb anti-human **RhoA**	26C4, IgG1	120-150 aa of human RhoA	0.4 μg/ml (WB)	Santa Cruz Biotechnology, Santa Cruz, USA
Mouse mAb anti-human **Rac1**	23A8, IgG2b	Full-length human Rac1	1 μg/ml (WB)	Millipore, Livingstone, UK
Mouse mAb anti-**HA**	12CA5, IgG2b	HA epitope	0.8 μg/ml (WB), 1.6 μg/ml (IF)	CRUK Central Services
Mouse mAb anti-**myc**	9E10, IgG1	408-432 aa of human c-myc	1 μg/ml (WB), 10 μg/ml (IF)	CRUK Central Services
Rabbit mAb anti-**myc**	71D10, IgG	410-419 aa of human c-myc	1:500 (IF), stock conc. not known	Cell Signalling Technology, Danvers, USA
Mouse mAb anti-**flag**	M2, IgG	Flag epitope	2.25 μg/ml (WB)	Sigma-Aldrich
Mouse mAb anti-human **EEA1**	14, IgG1	3-281 aa of human EEA1	1.25 μg/ml (IF)	BD Biosciences
Rabbit polycl. anti-human **Rab 5A**	Code s-19	C-terminal region of human Rab 5A	1.33 μg/ml (IF)	Santa Cruz Biotechnology
Rabbit polycl. anti-human **Rab11**	Code 71-5300	C-terminal region of human Rab11a	10 μg/ml (IF)	Invitrogen, Paisley, UK

Mouse mAb anti-human **Lamp1**	H4A3, IgG1	Human Lamp1	0.4 µg/ml (IF)	Abcam
Rabbit polycl. anti-mouse or human **β-Pix**	Code 07-1450	GST fusion of SH3 domain of βPIX	1 µg/ml (WB), 10 µg/ml (IF)	Millipore
Mouse mAb anti-rat **GIT1**, recognises human GIT1	13, IgG2a	C-terminal 664-770 aa of rat GIT1	1.25 µg/ml (WB)	BD Biosciences
Rabbit polycl. anti-human **GIT1**	Code H-170	471-640 aa of human GIT1	2 µg/ml (IF)	Santa Cruz Biotechnology
Mouse mAb anti-chicken **talin**, recogn. human talin	8D4, IgG1	Talin purified from chicken gizzard	1:200 (stock as ascites fluid)	Sigma-Aldrich
Mouse mAb anti-human **vinculin**	hVIN-1, IgG1	Human vinculin from uterus	20 µg/ml (IF)	Sigma-Aldrich
Mouse mAb anti-human **pFAK (Y397)**	14, IgG1	Human FAK (pY397) Peptide	1.25 µg/ml (IF)	BD Biosciences
Goat polycl. anti-human **VEGFR2**	AF357	Human VEGFR2 extracellular domain	2 µg/ml (FACS)	R&D Systems, Minneapolis, USA
Mouse mAb anti-chicken **tubulin,** recognises human tubulin	DM1A, IgG1	Chick brain α-tubulin	0.1 µg/ml (WB)	Sigma-Aldrich

Tab. 2.3 Secondary antibodies.
Abbreviations: HRP, horseradish peroxidise; FITC, fluorescein-5-isothiocyanate; WB, western blotting; IF, immunofluorescence; FACS, fluorescence activated cell sorting

Antibody against	Conjugation	Host species	Working concentration	Supplier
Mouse IgG	HRP	Goat	1 µg/ml (WB)	Dako, Ely, UK
Rabbit IgG	HRP	Donkey	0.056 µg/ml (WB)	GE Healthcare, Chalfont St Giles, UK
Goat IgG	FITC	Donkey	15 µg/ml (FACS)	Stratech Scientific, Newmarket, UK
Mouse IgG	Alexa488	Goat	4 µg/ml (IF)	Invitrogen
Mouse IgG	Alexa546	Goat	4 µg/ml (IF)	Invitrogen
Rabbit IgG	Alexa488	Donkey	4 µg/ml (IF)	Invitrogen
Rabbit IgG	Alexa546	Goat	4 µg/ml (IF)	Invitrogen

2.4. DNA oligonucleotides

Tab. 2.4 DNA oligonucleotides used for cloning, sequencing or mutagenesis.
All DNA primers were purchased from Eurogentec (Southampton, UK) and were designed to amplify sequences of human genes, unless otherwise stated. For the sequencing primers in the brackets are given the spans of bases in the open reading frame of indicated genes. Abbreviations: fw, forward; rv, reverse; aa, amino acids; seq, sequencing.

Primer	Primer sequence (5'-3')	Primer application
SH01	tagtagggatccatgaactgcaaagagggaactg	Fw RhoJ, cloning
VH05	cacgtttggtggtggcgacc	Fw pGEX, seq.
VH266	tagtagaagcttgaattctcagataattgaacagcagctgtg	Rv RhoJ, cloning
VH274	tagtagaagctttcagctgtgaccctcagaacagcg	Rv RhoJ (-CAAX), cloning
VH292	ccggagctgcatgtgtcagagg	Rv pGEX, seq.
KB1	cagcaggcaggttttcgccacggcgccgtcccccaccaccac	Fw G33A RhoJ, mutagenesis
KB2	gtggtggtgggggacggcgccgtggcgaaaacctgcctgctg	Rv G33A RhoJ, mutagenesis
KB3	tagtagggatccaactgcaaagagggaactg	Fw RhoJ (-ATG), cloning
KB4	cgccaccatggaacaaaaactcatctcagaagaggatctgg	Fw Kozak-myc, cloning
KB5	gatcccagatcctcttctgagatgagttttttgttccatggtggcggtac	Rv Kozak-myc, cloning
KB6	tagtaggaattcatgaactgcaaagagggaactg	Fw RhoJ, cloning
KB7	tagtagggatcctcagctgtgaccctcagaacagcgttt	Rv RhoJ (-CAAX), cloning
KB12	tagtagggatccttatgtcaaataacggcttagacgtc	Fw CRIB, cloning
KB13	tagtaggaattctcagatctcctcatcagacatttctgg	Rv CRIB, cloning
KB14	tagtagggatccttatgtctggagaagtgcgtttgaggcagttg	Fw MRCKA, cloning
KB15	tagtagctcgagtcacgggtcccagctcccgcggtcagtgct	Rv MRCKA, cloning
KB16	tagtagggatccttatgctcaagtgcatcccgctgtggcgc	Fw scribble, cloning
KB18	tagtaggaattcctaggagggcacagggcccaggccacggcg	Rv scribble, cloning
KB19	tagtaggaattcttatgaatccagaagaacaaatcgtgaca	Fw αPIX, cloning

KB20	tagtagctcgagttatggaagaattgaggtcttgctact	Rv αPIX, cloning
KB23	tagtaggaattcttatgtcccgaaaggggccgcgagcggaggtg	Fw GIT1, cloning
KB24	tagtaggaattctcactgcttcttctctcgggtggtgatggt	Rv GIT1, cloning
KB26	tagtagctcgaggaatgtccgccgcagacgaggttgacgggctg	Fw IQGAP1, cloning
KB27	tagtagctcgagttacttcccgtagaacttttttgttgagaag	Rv IQGAP1, cloning
KB28	gagtagtaacaaaggtcaaagaca	Fw pGBT9, insert seq.
KB29	gagtcactttaaaatttgtatacac	Rv pGBT9, insert seq.
KB30	aataccactacaatggatgatgta	Fw pACT2, insert seq.
KB34	gcaaatttgaagatagattgcc	Fw MRCKA, seq. (500-521)
KB35	catcgaattttgatgtagatgatg	Fw MRCKA, seq. (1103-1126)
KB36	cgcacactgtcagaggaaactgg	Fw MRCKA, seq. (1701-1723)
KB37	ctgacgagtgaacttgataagc	Fw MRCKA, seq. (2235-2356)
KB38	ctggatcaatttgaaactgtagac	Fw MRCKA, seq. (2890-2913)
KB39	gctagcagacactgagaatgag	Fw MRCKA, seq. (3504-3525)
KB40	ctaagatacccccttgaatggag	Fw MRCKA, seq. (4102-4123)
KB41	caagattcaactttaagcagac	Fw αPIX, seq. (500-521)
KB42	cattttaacaacaaacctcagc	Fw αPIX, seq. (1101-1122)
KB43	gcaccacacctctgcacgtggc	Fw GIT1, seq. (500-521)
KB44	gagcctgagcagccccacagac	Fw GIT1, seq. (1101-1122)
KB45	gcgtccctgtcatttctggtcaagc	Fw scribble, seq. (502-526)
KB46	ccgcctgcagagtctgccgttcg	Fw scribble, seq. (1104-1126)
KB47	ccacggtgcatttcgcagaggacg	Fw scribble, seq. (1700-1726)
KB48	gccctgcggcccgggctggagtc	Fw scribble, seq. (2300-2322)
KB49	ccgctgctgttgccaccaccagc	Fw scribble, seq.(2897-2919)
KB50	gcctgacgcacggcgaggcggtg	Fw scribble, seq. (3500-3522)

KB51	gaggatgcccctgcccagccccccc	Fw scribble, seq. (4000-4023)
KB52	cctcagattcaagacctatatgg	Fw IQGAP1, seq. (496-518)
KB53	ctgcagtctggagtggatgctgc	Fw IQGAP1, seq. (1111-1133)
KB54	gaaatccaggatgagtcagctgtg	Fw IQGAP1, seq. (1777-1800)
KB55	ggcatatcaagatcggttagct	Fw IQGAP1, seq. (2379-2400)
KB56	ccaccaagttcatggactctgtaatc	Fw IQGAP1, seq. (2993-3018)
KB57	gttgctcctgatgcctttgacatc	Fw IQGAP1, seq. (3601-3624)
KB58	ggagagaccttgactgaaatcc	Fw IQGAP1, seq. (4201-4222)
KB63	gtttttcagtatctacgattc	Rv pACT2, insert seq.
KB64	tagtaggaattcctatagattggtctcatcccaagcagg	Rv rat βPIX, cloning
KB67	tagtaggaattcttatgactgataacgccaacagccaactg	Fw rat βPIX, cloning
KB68	accgctcatcctgggactggcaga	Rv rat βPIX, seq. (1000-1023)
KB69	ttttggcagcagcttttcatggt	Rv rat βPIX, seq. (1501-1524)
KB71	tagtagaagctttgatgaactgcaaagagggaactgac	Fw RhoJ, cloning
KB72	tagtagggatccgccaccatggtgagcaagggc	Fw Kozak-GFP, cloning
KB73	gggattggggggtacagtgcaggg	Fw pWPXL, seq. (3361-3384)
KB77	tagtaggaattctcagtctgtggggctgctcaggctctt	Rv GIT1$_{\ldots\text{-}378aa}$, cloning
KB80	cccatggcgccaggcgggagcaca	Fw GIT1, seq. (1501-1524)
KB81	tagtagggatcctttctcggcaaaagtgcatgtctcag	Fw GIT1$_{255aa\text{-}\ldots}$, cloning
KB82	tagtaggaattctcaggcactgcgctctgtcaccagagt	Rv GIT1$_{\ldots\text{-}320aa}$, cloning

2.5.   Plasmids

DNA constructs were generated according to cloning or mutagenesis procedures, as described in 2.9.1 or 2.9.2, respectively. These are listed in Table 2.5. The DNA constructs provided by other scientists and used for transfections or as templates for cloning are listed in Table 2.6.

Tab. 2.5 Cloned DNA constructs.
The amplified inserts contain sequences of human genes, unless otherwise stated.

Construct	Cloning details
pGEX-4T2-wtRhoJ (lacking CAAX box)	wtRhoJ-CAAX was amplified with the SH01 & VH274 primers (BamHI-blunt insert digest) and cloned into the BamHI-SmaI restriction sites of pGEX-4T2.
pGEX-4T2-daRhoJ (Q79L) (lacking CAAX box)	daRhoJ-CAAX was amplified with the SH01 & VH274 primers (BamHI-blunt insert digest) and cloned into the BamHI-SmaI restriction sites of pGEX-4T2.
pGEX-4T2-dnRhoJ (T35N) (lacking CAAX box)	dnRhoJ-CAAX was amplified with the SH01 & VH274 primers (BamHI-blunt insert digest) and cloned into the BamHI-SmaI restriction sites of pGEX-4T2.
pGEX-4T2-dnRhoJ (G33A) (lacking CAAX box)	Created by mutagenesis of pGEX-4T2-wtRhoJ-CAAX construct with primers KB1 & KB2.
pMAL-2CE-wtRhoJ (lacking CAAX box)	wtRhoJ-CAAX was amplified with the SH01 & VH274 primers and cloned into the BamHI-HindIII restriction sites of pMAL-2CE.
pEF6A-myc-wtRhoJ	Kozak-myc sequence was generated by annealing of KB4 & KB5 primers and digested with KpnI-BamHI. wtRhoJ (-ATG) was amplified with the KB3 & VH266 and digested with BamHI-EcoRI. Kozak-myc and wtRhoJ inserts were cloned into the KpnI-EcoRI restriction sites of pEF6A.
pWPXL-GFP-wtRhoJ	wtRhoJ was amplified with the KB71 & VH266 primers and cloned into the HindIII-EcoRI restriction sites of pEGFP-C1. GFP-wtRhoJ insert was then amplified from pEGFP-C1-wtRhoJ with the KB72 & VH266 primers and cloned into the BamHI-EcoRI restrictions sites of pWPXL, replacing the existing EGFP insert.
pWPXL-GFP-daRhoJ (Q79L)	daRhoJ was amplified with the KB71 & VH266 primers and cloned into the HindIII-EcoRI restriction sites of pEGFP-C1. GFP-daRhoJ insert was then amplified from pEGFP-C1-daRhoJ with the KB72 & VH266 primers and cloned into the BamHI-EcoRI restrictions sites of pWPXL, replacing the existing EGFP insert.

pGBT9-wtRhoJ (lacking CAAX box)	wtRhoJ-CAAX was amplified with the KB6 & KB7 primers and cloned into the EcoRI-BamHI restriction sites of pGBT9.
pGBT9-daRhoJ (Q79L) (lacking CAAX box)	daRhoJ-CAAX was amplified with the KB6 & KB7 primers and cloned into the EcoRI-BamHI restriction sites of pGBT9.
pGBT9-dnRhoJ (T35N) (lacking CAAX box)	dnRhoJ-CAAX was amplified with the KB6 & KB7 primers and cloned into the EcoRI-BamHI restriction sites of pGBT9.
pACT2-CRIB (1-252 aa of rat PAK1 which encompasses the CRIB domain)	The CRIB domain was amplified with the KB12 & KB13 primers and cloned into the BamHI-EcoRI restriction sites of pACT2.
pACT2-MRCKA	MRCKA was amplified with the KB14 & KB15 primers and cloned into the BamHI-XhoI restriction sites of pACT2.
pACT2-GIT1	GIT1 was amplified with the KB23 & KB24 primers and cloned into the EcoRI restriction site of pACT2.
pACT2-GIT1$_{255-378aa}$	GIT1$_{255-378aa}$ was amplified with the KB81 & KB77 primers and cloned into the BamHI-EcoRI restriction sites of pACT2.
pACT2-GIT1$_{255-320aa}$	GIT1$_{255-320aa}$ was amplified with the KB81 & KB82 primers and cloned into the BamHI-EcoRI restriction sites of pACT2.
pACT2-αPIX	αPIX was amplified with the KB19 & KB20 primers and cloned into the EcoRI-XhoI restriction sites of pACT2.
pACT2-βPIX (rat)	βPIX was amplified with the KB67 & KB64 primers and cloned into the EcoRI restriction site of pACT2
pACT2-IQGAP1	IQGAP1 was amplified with the KB26 & KB27 primers and cloned into the XhoI restriction site of pACT2.
pACT2-scribble	Scribble was amplified with the KB16 & KB18 primers and cloned into the BamHI-EcoRI restriction sites of pACT2.

Tab. 2.6 Other plasmids.
The plasmids listed in the table contain sequences of human genes, unless otherwise stated.

Plasmid	Kindly provided by
pEF6A-HA-wtRhoJ, pEF6A-HA-daRhoJ(Q79L), pEF6A-HA-dnRhoJ(T35N), pEF6A-flag-wtRhoJ, pEF6A-flag-daRhoJ(Q79L), pEF6A-flag-dnRhoJ(T35N), pEF6A	Dr Victoria Heath University of Birmingham, UK (unpublished)
pGBT9, pACT2	Dr Victoria Heath (Heath, Shaw et al. 2004)
pEGFPC2-wtRhoJ	Dr Phillipe Fort CNRS, Montpellier, France (Vignal, De Toledo et al. 2000)
pRK5-HA-wtRac1, pRK5-flag-wtCdc42, pRK5-myc-daRhoA (G14V)	Prof L.Machesky University of Birmingham, UK (unpublished)
pEF-flag-MRCKA-isob-FL	Prof Chris J. Marshall The Institute of Cancer Research, London, UK (unpublished)
pCDEF3-flag-β-Pix (rat) pEGFP-N1-wt-β-Pix (rat)	Prof Arthur Weiss UCSF, USA (Phee, Abraham et al. 2005)
pMT2SH-HA-α-Pix	Dr Georg Rosenberger University Hospital, Hamburg-Eppendorf, Germany (Rosenberger, Gal et al. 2005)
pEGFP-GIT1	Dr Alan Horwitz University of Virginia, USA (Manabe, Kovalenko et al. 2002)
pEGFP-C1-scribble	Dr Michael Sebbagh CRCM, Marseille, France (Audebert, Navarro et al. 2004)
pEF-BOS-mycIQGAP	Prof. John Heath University of Birmingham, UK (unpublished)
Lentiviral plasmids: pWPXL, pWPI, psPAX2, pMD2G	Addgene, Didier Trono Lab http://www.addgene.org

2.6.   siRNA duplexes

Tab. 2.7 siRNA duplexes.
All designed siRNA duplexes contain dTdT overhang modifications on sense and antisense strands. The base pair numbers of isoforms 1 of βPIX or GIT1 genes that are targeted by corresponding duplexes are indicated. However, both βPIX- or GIT1-specific duplexes listed here target all isoforms of βPIX or GIT1 genes, respectively. All siRNA duplexes were purchased from Eurogentec.

siRNA duplex name	Targeted gene	Duplex sense strand (5'-3')	Gene base pairs targeted by duplex
RhoJ-siRNA1	Human RhoJ	ccacuguguuugaccacuau	155-174
RhoJ-siRNA2	Human RhoJ	agaaaccucucacuuacgag	455- 474
βPIX-siRNA1	Human βPIX	ggaagaagaugcucagauu	1587-1605 (in isoform 1)
βPIX-siRNA2	Human βPIX	agagacacauggaggauua	728-746 (in isoform 1)
GIT1-siRNA1	Human GIT1	ccaagaacauucaggaacu	1985-2003 (in isoform 1)
GIT1-siRNA2	Human GIT1	cgagcugcuuguaguguau	549-567 (in isoform 1)
Ctrl-siRNA	Non-silencing control	Sequence not disclosed by Eurogentec; (Cat No: OR-0030-Neg05)	Non-specific to known sequences of human genes

2.7. Mammalian cell culture

2.7.1. Mammalian cells and media

HUVECs were isolated from umbilical veins obtained from Birmingham Women's Health Care NHS Trust; cords were donated with informed consent. HUVECs were grown in M199 medium (CRUK Central Services or Sigma-Aldrich) supplemented with either bovine brain extract (prepared as in (Maciag, Cerundolo et al. 1979)) or with large vessel endothelial growth supplements (TCS CellWorks, Buckingham, UK). This medium contained also 90 µg/ml of heparin, 10 % (v/v) fetal calf serum (FCS) (PAA Cell Culture Co, Ontario, USA), 4 mM L-glutamine (CRUK Central Services or Sigma-Aldrich), and if required antibiotics gentamicin/amphotericin B (TCS CellWorks) and/or penicillin/streptomycin (Invitrogen). This medium is referred to as HUVECs medium. The isolation of HUVECs and preparation of bovine brain extract was performed by Mr James Beesley (Molecular Angiogenesis Group, University of Birmingham). HUVECs were cultured in medium containing antibiotics unless the siRNA-mediated knock-down of genes was performed (as in section 2.16). The immortalised human microvascular endothelial cell line-1 (HMEC-1) (Ades, Candal et al. 1992) was maintained in the same conditions as HUVECs. Human embryonic kidney 293T cells (HEK 293Ts) were grown in Dulbecco's Modified Eagle's Medium (DMEM) (Sigma-Aldrich) supplemented with 10 % (v/v) FCS (PAA Cell Culture Co), 4 mM L-glutamine (CRUK Central Services or Sigma-Aldrich) and pen/strep antibiotics (Invitrogen).

All mammalian cells were grown in sterile plastic culture dishes (Falcon, Becton Dickinson Labware, Franklin Lakes, USA) and incubated in a humidified atmosphere with 5 % CO_2 supply at 37 °C (Sanyo CO_2 incubator, Sanyo Electric CO, Japan). For culturing HUVECs and HMEC-1, plastic dishes were coated additionally with gelatin, prior to use. This was performed by covering dishes with 0.1 % (w/v) gelatin (dissolved in PBS and filtered) and

incubating for 20 min at 37 °C. After this time, gelatin solution was removed and cells were seeded in culture medium. Media for culturing cells were filtered through sterile 0.22 µm pore filters (Millipore) before use. PBS (CRUK Central Services or Sigma-Aldrich) for washing cells was sterilised by autoclaving prior to use.

Growth and conditions of mammalian cells in culture were routinely monitored using Leica DM IL microscope (Leica Microsystems, Houston, USA).

2.7.2. Passaging cells

Cells were split at a ratio of 1:3 once a week (HUVECs and HMEC-1) or at a ratio of 1:10 twice a week (HEK 293Ts). A confluent monolayer of cells (in a 10 cm-diameter culture dish) was washed with 10 ml of PBS, covered with 2.5 ml of trypsin-EDTA solution (CRUK Central Services or Sigma-Aldrich) and incubated for 5 min at 37 °C. Afterwards cells were collected from a plate with 10 ml of PBS and 10 ml of complete medium. It was important to add medium as it contains FCS, which inhibits the enzymatic activity of trypsin. Cells were then centrifuged for 5 min (195 x g, room temperature), resuspended in fresh complete medium and plated in a volume of 10 ml per one 10 cm-diameter dish.

2.7.3. Counting cells

When specified numbers of cells were required in particular experiments, the cells were counted before plating. After trypsinisation (section 2.7.2) cells were resuspended in fresh complete medium. 5 µl of cell suspension was then mixed with 5 µl of trypan blue to identify dead cells and cells were counted using the haemocytometer counting chamber (Neubauer, Paul Marienfeld GmbH & CO, Germany) according to manufacturer's instructions.

2.7.4. Freezing and storing cells

After trypsinisation (section 2.7.2) cells were resuspended in freezing medium containing 10 % (v/v) dimethyl sulfoxide and 90 % (v/v) FCS (PAA Cell Culture Co). The cell suspension was then frozen in the Mr. Frosty freezing container (Nalgene™, Thermo Fisher Scientific, Rochester, USA) for 24 h at -80 °C and subsequently transferred to the liquid nitrogen stores.

2.8. Bacteria strains, media and antibiotics

The chemically competent *Escherichia coli* (*E. coli*) strains DH5α, BL21(DE3) pLys S or XL1-Blue Supercompetent Cells (Stratagene, La Jolla, USA) were used for transformations with various plasmids. All bacteria were cultured in Luria Bertani (LB) broth or LB agar (both from CRUK Central Services or Fisher Scientific) with addition of appropriate antibiotics. Final concentrations of antibiotics were used as follows: 0.1 mg/ml ampicillin (Amp), 0.02 mg/ml chloramphenicol (Chloramph) and 0.03 mg/ml kanamycin (Kan). Bacteria were grown on LB agar at 37 °C (CellStar incubator, Borolabs Ltd, Basingstoke, UK) and when in liquid LB medium bacteria were grown in the orbital shaking incubator (Sanyo/Gallenkamp, Loughborough, UK) at 30-37 °C.

2.9. Manipulation of DNA material

2.9.1. Cloning

The cloning process was performed as summarised in Fig. 2.1 and particular steps are described in the next sections. Reagents, enzymes and their compatible buffers used in cloning were purchased from New England Biolabs (NEB) (Herts, UK), unless otherwise stated.

```
           ┌──────────────┐                    ┌─────────────────────────┐
           │    Vector    │                    │  Insert generated by PCR │
           └──────────────┘                    └─────────────────────────┘
                  │                                       │
                  ▼                                       ▼
           ┌──────────────┐                    ┌─────────────────────────┐
           │ Restriction  │                    │ PCR quick DNA purification│
           │    digest    │                    └─────────────────────────┘
           └──────────────┘                                │
                  │                                       ▼
                  ▼                             ┌──────────────┐
           ┌──────────────────┐                 │ Restriction  │
           │ DNA gel          │                 │    digest    │
           │ purification     │                 └──────────────┘
           └──────────────────┘                          │
                  │                                       ▼
                  │                             ┌──────────────────┐
                  │                             │ DNA gel          │
                  │                             │ purification     │
                  │                             └──────────────────┘
                  ▼                                       │
           ┌──────────────────────────────────────┐      │
           │   Ligation of plasmid and insert      │◄─────┘
           └──────────────────────────────────────┘
                                │
                                ▼
                        ┌───────────────┐
                        │ Transformation │
                        └───────────────┘
                          │           ╲
                          ▼            ╲
   ┌────────────────────────────────┐   ┌────────────────────┐
   │ Construct DNA mini-preparation │◄──│ Colony-PCR screen  │
   └────────────────────────────────┘   └────────────────────┘
                   │
                   ▼
          ┌──────────────────────────┐
          │ Restriction digest screen│
          └──────────────────────────┘
                   │
                   ▼
              ┌──────────────┐
              │  Sequencing  │
              └──────────────┘
```
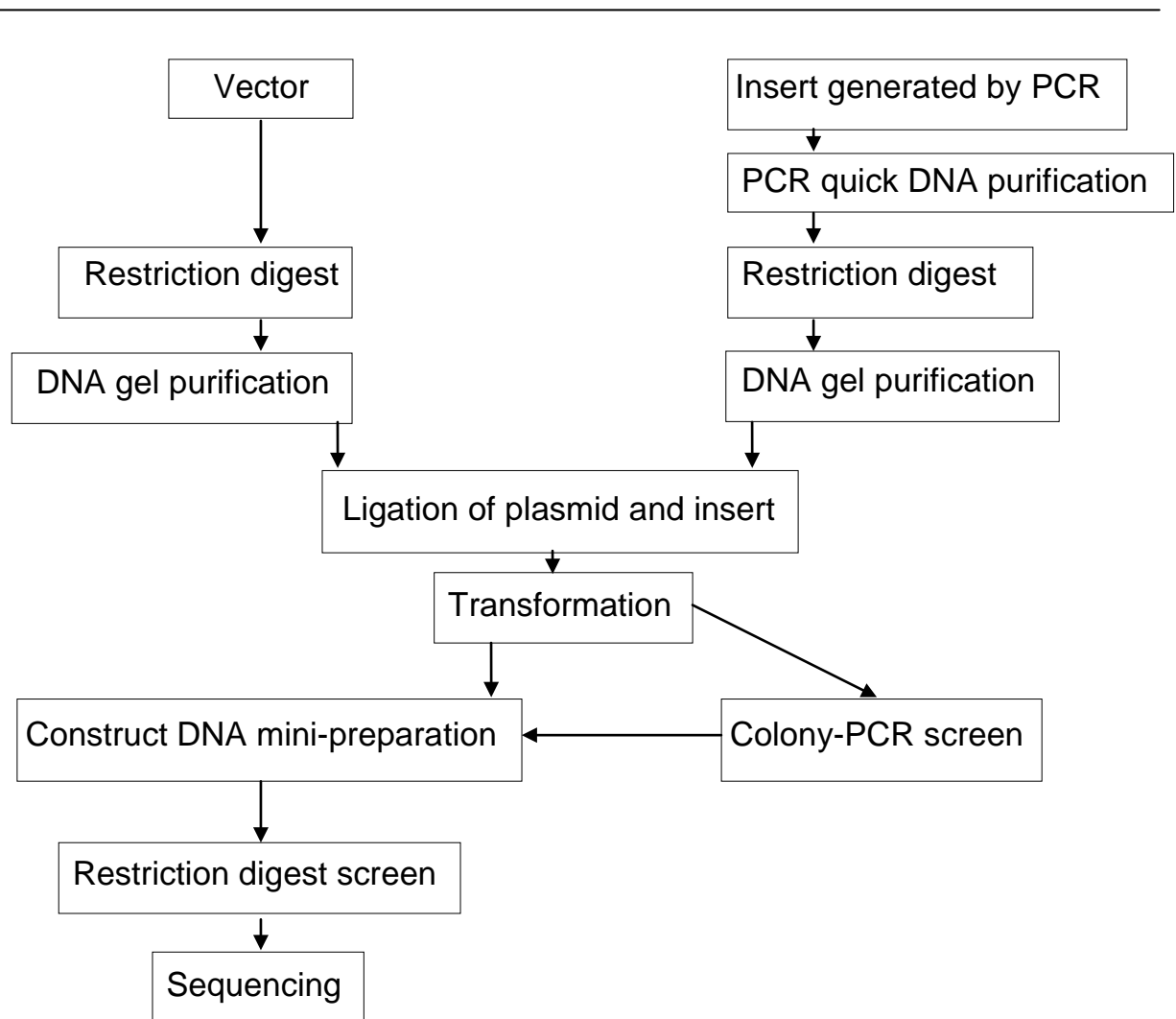
Fig. 2.1 Cloning process.
The DNA sequence of interest (insert) was amplified with forward and reverse primers which contained specific restriction sites. The insert and vector were then digested with restriction enzymes, resolved by agarose gel electrophoresis and purified. The insert was then ligated into specific sites of vector created earlier by restriction digest. The vector-insert construct was subsequently introduced into bacteria by transformation and bacteria were grown on selective LB agar medium. Colonies positive for cloned construct were then identified by PCR screening or diagnostic digest. Plasmids were isolated from positive colonies and were finally sequenced to verify the absence of mutations.

2.9.1.1. Production and purification of plasmids

Large scale preparation of plasmids was performed from bacterial cultures using the GenElute^{TM} Plasmid Maxiprep Kit or Qiagen Plasmid Maxi Kit (Qiagen, Crawley, UK) according to the manufacturer's protocols. For small-scale plasmid preparations DNA was isolated using the GeneJET^{TM} Plasmid Miniprep Kit (Fermentas, York, UK). Final DNA concentration was measured with the NanoDrop ND-1000 Spectrophotometer (Labtech, Ringmer, UK).

2.9.1.2. Amplification of insert by PCR

Inserts were prepared by polymerase chain reaction (PCR) using a high fidelity polymerase as follows. 100 μl reaction mixes were prepared by adding: 74 μl of water, 20 μl of 5x Phusion HF Buffer, 2 μl of 10 mM deoxyribonucleotide triphosphate (dNTP) mix (Bioline, London, UK), 1 μl of each 100 μM primer (Eurogentec) and 1 μl of Phusion^{TM} High-Fidelity DNA Polymerase (Finnzymes, Espoo, Finland). Finally 500 ng of template DNA was added. The PCR reaction involved an initial denaturation (98 ºC, 30 s), then 24 cycles of denaturation (98 ºC, 10 s), annealing (55 ºC, 30 s) and elongation (72 ºC, 1 min/kb of amplicon). A final DNA elongation step of 72 ºC for 10 min was included.

2.9.1.3. PCR quick DNA purification

Inserts generated by PCR reaction were purified with QIAquick Purification Kit (Qiagen) to remove nucleotides and salts prior to restriction digest.

2.9.1.4. Digestion of DNA with restriction enzymes

Large scale preparative restriction digests of insert and vector DNA for cloning were performed as follows. Purified PCR product (from a 100 μl reaction) or 5 μg of plasmid were incubated in 50 μl of digestion solution containing: 5 μl of 10x NEBuffer compatible with the

appropriate restriction enzymes, 5 μl of 10x bovine serum albumin (BSA) (if necessary), 2.5 μl of each restriction enzyme (20000 U/ml) and water. Digestion was carried out for 2 h in the temperature required for each enzyme. Restriction digests for diagnostic purposes only were scaled down appropriately to 10 μl volumes.

2.9.1.5. DNA gel electrophoresis

DNA agarose-gel electrophoresis was performed using equipment for horizontal electrophoresis (Jencons Scientific Ltd, a VWR Division, East Grinstead, UK). Gels were prepared by dissolving 0.8 – 1.5 % (w/v) agarose (VWR International, Lutterworth, UK or Sigma-Aldrich) in TAE buffer (CRUK Central Services) and stained with SYBR Safe (Invitrogen). Gels were visualised and imaged using Gene Genius Bio Imaging System (Syngene, Cambridge, UK).

2.9.1.6. DNA gel purification

DNA bands were cut from the gel and DNA was extracted using QIAEX II Agarose Gel Extraction Kit (Qiagen) or GeneJET™ Gel Extraction Kit (Fermentas) according to the manufacturer's instructions.

2.9.1.7. DNA ligations

Inserts were ligated with appropriate plasmids using T4 Ligase as follows. 2 μl of 400000 U/ml T4 Ligase enzyme and 2 μl of T4 Ligase Buffer were added to the 16 μl of insert:vector mixture prepared in a ratio of 3:1. Ligations were performed at room temperature for 1 h.

2.9.1.8. Heat-shock transformation of bacteria

Chemically competent *E. coli* (20-50 μl) were mixed with 5 μl of ligation mix or 50-500 pg of plasmid and incubated on ice for 30 min. Afterwards, bacteria were heat shocked at 42 ºC for 90 s and incubated on ice for further 2 min. The transformation mix was diluted into 250 μl of

pre-warmed antibiotic-free LB-broth and allowed to recover for 1 h in an orbital shaker incubator at 37 ºC. Subsequently bacteria were plated on LB-agar plates (containing appropriate antibiotics) for overnight incubation at 37 ºC.

2.9.1.9. Colony- PCR screen

Colony PCR was used to screen for successful ligation of vector and insert. A 20 µl PCR reaction was prepared per colony screened by adding: 16 µl of water, 0.4 µl of 10 mM dNTPs (Bioline), 2 µl of 10x NH4 buffer (Bioline), 1 µl of 50 mM MgCl$_2$ (Bioline), 0.2 µl of each 100 µM primer (Eurogentec), 0.2 µl of Taq polymerase (Bioline) and bacterial colony sample. Prior to mixing with the PCR mix, a replica plate was set up containing samples of each colony screened. The PCR reaction was performed as follows: initial denaturation (94 ºC, 2 min), then 30 cycles of denaturation (94 ºC, 30 s), annealing (55 ºC, 30 s) and elongation (72 ºC, 1 min/ 1kb of amplicon). A final DNA elongation step of 72 ºC for 5 min was included. PCR products were visualised by DNA gel electrophoresis. Colonies which gave positive results were used for small or large scale plasmid preparations as described above.

2.9.1.10. Sequencing and storing of plasmids

All constructed plasmids were verified by sequencing by the Functional Genomics and Proteomics Laboratory (School of Biosciences, University of Birmingham, UK). All constructs were stored as glycerol stocks at -80 ºC. These were prepared by mixing the saturated bacterial cultures with an equal volume of 30 % (v/v) glycerol (CRUK Central Services).

2.9.2. Site-directed mutagenesis

The nucleotide free dominant negative RhoJ mutant was created using the QuickChange® II Site-Directed Mutagenesis Kit (Stratagene) according to the manufacturer's method. Briefly,

a PCR reaction with pGEX-4T2-wtRhoJ plasmid as a template and primers (KB1 and KB2) was performed. These primers encoded a single amino acid change (G33A) and additionally contained single nucleotide changes, which created a restriction site for NarI, a RhoJ-non-cutting enzyme, without affecting the amino acid sequence. The PCR reaction mixture was then treated with DpnI, which digested methylated parental plasmid. Then 1 µl of DpnI-treated solution was transformed into 50 µl of XL1-Blue Supercompetent Cells by heat-shock (30 min on ice, then 45 sec at 42 ℃ and back on ice for 2 min). Subsequently cells were recovered by incubation in 250 µl of pre-warmed antibiotic-free LB medium and plated on LB-agar plate containing Amp. Colonies were screened by colony PCR followed by restriction digest with NarI. Successful mutagenesis was confirmed by DNA sequencing.

2.10. Analysis of proteins

2.10.1. Protein production and purification

Plasmids encoding fusion proteins were transformed into chemically competent BL21(DE3) pLys S *E. coli* strain by heat shock (method 2.9.1.8) and plated on LB-agar plates containing appropriate antibiotics (Amp or Kan with Chloramph). Colonies were inoculated in LB-broth (Amp or Kan and Chloramph), incubated over night at 37 ℃ with shaking and then diluted 100-fold into LB-broth (Amp or Kan and Chloramph). Then bacteria were cultured at 30 ℃ until they reached the mid-log phase growth, when they were induced with 0.3 mM iso-propyl-β-D-thiogalactopyranoside (IPTG) (Melford Laboratories, Suffolk, UK) for 2.5 h. After induction, bacteria were centrifuged (10 min, 4435 x g, 4 ℃), washed with *E. coli* washing buffer and centrifuged again. Bacterial pellets were frozen at -80 ℃ prior to lysis. Subsequently, bacteria were thawed on ice, lysed with ice-cold *E. coli* lysis buffer (2 ml of lysis buffer per bacterial pellet from 100 ml of culture) and ultra-sonicated for 3 min (Ultrasonicator Vibra CellTM, Sonics & Materials, Newtown, USA). For purification of

67

proteins other than RhoJ fusions, Triton-X-100 (Sigma-aldrich) was added to a final concentration of 1% (v/v) and bacterial lysates were left on ice for 30 min. After sonication and optional incubation with Triton-X-100, lysates were clarified by centrifugation (10 min, 21910 x g, 4 ℃), the supernatant collected and mixed with an equal volume of glycerol (CRUK Central Services) to give a final concentration of 50% (v/v). Protein lysates were stored at -20 ℃.

Fusion proteins were purified from bacterial lysates by pull-down with appropriate beads. Glutathione-agarose beads were used to pull-down/purify proteins fused to GST and amylose beads (NEB) were used to pull-down/purify proteins fused to maltose binding protein (MBP). Firstly the amount of fusion protein in bacterial lysate was assessed as follows. Different volumes of bacterial lysate (e.g. 25, 50, 100 and 200 µl) were diluted with *E. coli* lysis buffer up to 1 ml and incubated with 12.5 µl of packed beads for 45-60 min at 4 ℃ on a rotating wheel. The beads were then washed 3 times with *E. coli* lysis buffer and finally resuspended in equal volume of 2x SDS sample-loading buffer. These samples along with 1, 5 and 10 µg of BSA samples were loaded on a polyacrylamide gel and subjected to sodium dodecyl sulphate – polyacrylamide gel electrophoresis (SDS-PAGE) (as described in section 2.10.4). The proteins were then stained in gel by Coomassie dye (as described in section 2.10.4) and the amount of pulled-down fusion proteins was determined by comparison to BSA markers.

In order to purify approximately 5-15 µg of fusion protein from bacterial lysate 12.5 µl of packed glutathione-agarose or amylose beads were used. Fusion proteins on beads were then used for various assays or alternatively beads with proteins were resuspended in equal volume of 2x SDS sample-loading buffer and analysed by SDS-PAGE/western blotting (sections 2.10.4-2.10.5).

MBP-wtRhoJ-CAAX protein used as antigen for production of polyclonal RhoJ antibodies in rabbits was produced as above and purified from bacterial lysate using amylose beads. To elute MBP-wtRhoJ-CAAX from amylose beads 10 mM maltose (made in 20 mM Tris-Cl pH 7.5, 200 mM NaCl, 1mM EDTA, 10 mM 2-mercaptomethanol) was used and the concentration of the fusion protein was assesd with the Bio-Rad assay (as in section 2.10.3).

2.10.2.   Preparation of mammalian cell lysates

Unless specified otherwise, the procedure described in this section was used to obtain mammalian cellular lysates. Confluent plates (10 cm diameter) of HUVECs, HMEC-1 or HEK 293Ts were washed with PBS and lysed on plates by adding 200 µl (for HUVECs and HMEC-1) or 1 ml (for HEK 293Ts) of Rho-assay lysis buffer (supplemented with protease inhibitor cocktail, 2 mM NaVO$_3$ and 10 mM NaF). Cells were scraped quickly with a cell scraper (Fisher Scientific) and transferred into 1.5 ml microfuge tubes. The cells were lysed for 10 min on ice and centrifuged for another 10 min (21910 x g, 4 ℃). The supernatant was used directly in different assays or stored at -80 ℃ in 10 % (v/v) glycerol. Alternatively, for further SDS-PAGE (section 2.10.4) mammalian cell lysates were mixed with equal volumes of 2x SDS sample-loading buffer.

2.10.3.   Protein quantification

The amount of proteins present in mammalian cellular lysates was measured using Bio-Rad DC Protein Assay (Bio-Rad Laboratories, Hemel Hempstead, UK) according to the manufacturer's instructions. This was performed in a 96-well plate (C96 Maxisorp, Thermo Fisher Scientific). Briefly, 5 µl of lysate was mixed in well with 25 µl of Bio-Rad mixture (made by combining of 20 µl reagent S with 1 ml reagent A) and with 200 µl reagent B. In parallel, samples containing known amount of BSA (0, 2, 4, 8, 1.6 mg/ml) were mixed with the same Bio-Rad reagents in separate wells. After 15 min incubation at room temperature the

colour in protein samples had developed and absorbance was measured at 750 nm wavelength using Versamax microplate reader spectrophotometer (Molecular Devices). Based on the absorbance values obtained for known BSA concentrations the protein standard curve was created using Microsoft Excel Software and the concentration of proteins in lysate samples was determined. When possible, the protein samples were measured in triplicate to obtain more accurate values.

2.10.4. SDS-PAGE

Protein samples (mixed previously with 2x SDS sample-loading buffer) were boiled for 5 min, collected by centrifugation for 10 s and loaded on a polyacrylamide gel. Polyacrylamide gels were prepared according to Sambrook and Russel (Sambrook and Russel 2001). The polyacrylamide used to make these gels (Protogel) was from National Diagnostics (Hessle Hull, UK) and contained 30 % w/v Acrylamide : 0.8 % (w/v) Bis-Acrylamide in a proportion of 5:1. SDS-PAGE was carried-out using the X cell II™ Mini cell and X cell sure lock™ system (Invitrogen). Electrophoresis was performed in SDS-PAGE running buffer at 100 V until the dye front had reached the resolving buffer at which point the voltage was increased to 160 V. When electrophoresis was finished the gel was stained with Coomassie dye. This was performed by immersing gel in Coomassie staining buffer and rocking for at least 1 h at room temperature. The gel was then de-stained at room temperature using Coomassie de-staining buffer. Alternatively, after SDS-PAGE the gel with proteins was subjected to western blotting (2.10.5).

2.10.5. Western blotting

The Immobilon-P polyvinylidene fluoride (PVDF) membrane with 0.45 μm pores (Millipore) was activated by pre-wetting in methanol for 30 s and then placed in transfer buffer. The polyacrylamide gel with protein samples (after SDS-PAGE), blotting paper and blotting pads

were also soaked in transfer buffer for 10 min prior to assembling the transfer apparatus in the X cell II™ Mini cell, X cell II™ Blot Module and X cell sure lock™ (Invitrogen). Wet transfer was performed at 30 V for 1-2 h at 4 °C. Proteins transferred onto the membrane were stained with Ponceau S dye to check for successful transfer. The membrane was then blocked with 5 % dried milk (prepared in TBST buffer) for 1 h at room temperature. Subsequently, the membrane was incubated overnight with an appropriate primary antibody (diluted in solution containing 3 % (w/v) BSA, 3 mM NaN$_3$ and TBST) at 4 °C. The membrane was then washed for 30 min in TBST with 6 buffer changes and placed in secondary antibody conjugated with horseradish peroxidase (HRP). After 1 h of incubation at room temperature, the membrane was washed for 30 min as above and developed with ECL Western Blotting Detection Reagents (GE Healthcare) for 1 minute. Finally, results were visualised on Hyperfilm ECL (GE Healthcare) which was exposed to the membrane for different times. When required, densitometry of protein bands on western blotting films was performed using ImageJ software which measured the mean grey values of protein bands.

Primary and secondary antibodies used in western blotting (and their working concentrations) are listed in Tables 2.2 and 2.3, respectively (section 2.3).

2.10.6.   Comparing the protein levels of endogenous Rho GTPases in HUVECs

A comparison of endogenous protein levels of RhoJ, Cdc42 and Rac1 in HUVECs was performed by western blotting. This is described below using the example of comparing RhoJ with Cdc42.

Firstly, HEK 293Ts were transfected with plasmids to express flag-tagged versions of RhoJ and Cdc42 proteins (calcium-phosphate transfection method, section 2.14.1) and their lysates

were prepared (section 2.10.2). These and HUVEC lysates were subjected to SDS-PAGE (2.10.4) and western blotting (2.10.5) with flag-, RhoJ- and Cdc42-specific antibodies (3 membrane replicates were made with a separate membrane for each antibody). The western blotting protocol was followed as described in section 2.10.5 until the step when the ECL reagents were added. Here, the membranes were incubated with the Supersignal detection reagent (Pierce, Thermo Fisher Scientific, Cramlington, UK) instead of the incubation with ECL Western Blotting Detection Reagents. After 1 min of incubation, membranes were scanned with the GeneGnome HR scanner (Syngene), which measures the real time chemiluminescent signal.

The intensity values of flag-RhoJ bands obtained with RhoJ- or flag-specific antibodies were compared with the intensity values of flag-Cdc42 bands obtained with Cdc42- or flag-specific antibodies. Using the flag-RhoJ and flag-Cdc42 protein, and the flag-specific antibody allowed the calculation of the relative efficacies of the RhoJ and Cdc42-specific antibodies and so enabled relative expression levels of RhoJ and Cdc42 in HUVECs to be determined. The formulas shown in boxes below were used in these calculations (abbreviations: WB, western blotting; α, anti).

$$\frac{\text{RhoJ}}{\text{in HUVECs}} = \frac{\text{WB: α-RhoJ (HUVECs)} \times \text{WB: α-flag (flag-RhoJ)}}{\text{WB: α-RhoJ (flag-RhoJ)}} \qquad \frac{\text{Cdc42}}{\text{in HUVECs}} = \frac{\text{WB: α-Cdc42 (HUVECs)} \times \text{WB: α-flag (flag-Cdc42)}}{\text{WB: α-Cdc42 (flag-Cdc42)}}$$

A similar approach was used to compare relative expression levels of RhoJ and Rac1 in HUVECs using the HA tag and the HA-specific antibody as a common reference.

2.11. Pull-down and identification of RhoJ-binding partners

2.11.1. Pull-down of RhoJ-binding partners from cellular lysates

Dominant active RhoJ (daRhoJ, Q79L) and dominant negative RhoJ (dnRhoJ, G33A) fusions of GST proteins were bound to glutathione agarose beads and used to pull-down potential RhoJ-binding proteins from cellular lysates.

Before lysis, HUVECs, HEK 293Ts and HMEC-1 were washed in ice-cold HBS, scraped in 0.5 ml of ice-cold HBS per plate and collected. Cells were then collected by centrifugation (1 min, 2000 x g, 4 °C) and lysed in Rho-assay lysis buffer (supplemented with protease inhibitor cocktail, 2 mM $NaVO_3$ and 10 mM NaF). 100 µl of lysis buffer per pellet from one 10 cm-diameter dish of HUVECs and 200 µl of lysis buffer per pellet from one 10 cm-diameter dish of HEK 293Ts or HMEC-1 were used. Then for each pull-down condition the amount of cellular lysates was used as follows: 10 x 100 µl of HUVECs lysate, 7 x 200 µl of HMEC-1 lysate and 3.3 x 200 µl of HEK 293Ts lysate. Lysates were firstly precleared with 10 µg of GST bound to 25 µl of packed glutathione-agarose beads by rotation on wheel for 10 min at 4 °C. The beads were then washed 3 times in 1 ml of Rho-assay lysis buffer (supplemented with protease inhibitor cocktail, 2 mM $NaVO_3$ and 10 mM NaF) and washes were pooled with the precleared lysate. Next, the precleared lysates were incubated with glutathione-agarose beads loaded with 10 µg of GST, GST-daRhoJ or GST-dnRhoJ for 1 h at 4 °C on a rotating wheel. Then the beads were washed 5 times with 1 ml Rho-assay lysis buffer (supplemented with protease inhibitor cocktail, 2 mM $NaVO_3$ and 10 mM NaF) and mixed with 40 µl of 2x SDS sample loading buffer. Samples were then subjected to SDS-PAGE (2.10.4) and mass spectrometry analysis (2.11.2-2.11.3) or western blotting (2.10.5).

2.11.2.   Preparation of samples for mass spectrometry

In preparation for mass spectrometry sequencing most of the steps (when possible) were carried out in a sterile hood to avoid contamination of the samples.

Pull-down samples obtained in section 2.11.1 were run in SDS-PAGE as follows. Samples were loaded on gradient gels (4-12 % gradient NuPAGE® Novex® Bis-Tris Mini gels, Invitrogen) and electrophoresis was carried-out for 50 min at 200 V (constant) using NuPAGE® MOPS SDS Running Buffer (Invitrogen). Proteins in gels were visualised with ProtoBlue Safe colloidal Coomassie reagent (National Diagnostics) according to the manufacturer's instructions and gels were placed on a clean glass plate. The gel fragments containing protein bands, which were present in the GST-daRhoJ or GST-dnRhoJ pull-down lanes, and which did not have corresponding bands in the GST pull-down lane, were excised with a sterile scalpel blade and placed in 1.5 ml microfuge tubes. These tubes were washed with 0.1 % (w/v) formic acid / 50 % (v/v) acetonitrile solution prior to use. Gel slices in tubes were then washed twice with 100 µl of 50 % (v/v) acetonitrile / 50 mM ammonium bicarbonate solution for 45 min at 37 ℃ (with agitation) and subsequently were dried in a speed vacuum. The dried gel slices were then covered with 50 µl of 50 mM DTT (made in 10 % (v/v) acetonitrile / 50 mM ammonium bicarbonate solution) and incubated at 56 ℃ for 1 h. Subsequently, the supernatant was discarded and gel slices were covered with 50 µl of 100 mM iodoacetamide (made in 10 % (v/v) acetonitrile / 50 mM ammonium bicarbonate solution) for 30 min incubation at room temperature in the dark. This solution was then removed and the gel slices were washed 3 times with 100 µl of 10 % (v/v) acetonitrile / 40 mM ammonium bicarbonate solution for 15 min, and dried down in a speed vacuum. Afterwards, samples were covered in 1.5 x gel volume of 12.5 µg/ml sequencing grade modified trypsin (Promega, Southampton, UK) diluted in 10 % (v/v) acetonitrile / 40 mM

ammonium bicarbonate and incubated for 1 h at room temperature. Then 20 μl more of 10 % (w/v) acetonitrile / 40 mM ammonium bicarbonate was added and samples were incubated overnight at 37 ℃. The next day the supernatant was collected, 30 μl of 3 % (w/v) formic acid was added to the gel samples and incubated for 1 h at 37 ℃. Then this supernatant was pooled with the previous one. This procedure was repeated with another 30 μl of 3 % (w/v) formic acid and again the supernatant was pooled with the previous ones. The collected solutions (approximately 70 – 90 μl) containing digested proteins were stored in -80 ℃ until their analysis by mass spectrometry.

2.11.3. Mass spectrometry

The samples prepared in section 2.11.2 were then used in liquid chromatography and mass spectrometry (LC-MS), which was performed by Dr Cleidi Zampronio in collaboration with Prof. John Heath (School of Biosciences, University of Birmingham, Functional Genomics and Proteomics Unit). The LC-MS procedure was described by Dr Cleidi Zampronio and permission was given to copy the method description in this thesis:

"Samples were injected using online Micro AS autosampler and Surveyor MS pump (Thermo Fisher Scientific, Germany). A 75 μm (internal diameter) Integrafrit (New Objective, USA) C8 resolving column (length 10 cm) was used and peptides were separated using a binary solvent system consisting of (A) water (J.T.Baker, Holland) and 0.1% formic acid and (B) acetonitrile (J.T.Baker, Holland) and 0.1% formic acid. A linear 40 min gradient increasing the composition of (B) from 5% to 40% was used. The Triversa Nanospray source (Advion Biosciences, NY) was used to spray the peptide eluted in a flow rate of approximately 300 nL min^{-1} into the mass spectrometer. The nanoelectrospray voltage was typically +1.7 kV.

A 7-T LTQ FT mass spectrometer (Thermo Fisher Scientific, Germany) was used to perform a data-dependent scanning. Data acquisition was controlled by Xcalibur 2.0 software. The mass spectrometer alternated between a full FT-MS scan (m/z 380 – 2000) and subsequent Collision-Induced Dissociation (CID) MS/MS scans of the three most abundant ions. Survey scans were acquired in the ICR cell with a resolution of 100 000 at m/z 400. Precursor ions were isolated and subjected to CID in the linear ion trap, which the product ion was acquired with a resolution of 25 000 at m/z 400. Collision activation for the experiment was performed in the linear trap using helium gas at collision energy normalised to precursor m/z of 35% and q_{excite} = 0.25. The width of the precursor isolation window was m/z 2 and only multiply charged precursor ions were selected for MS/MS."

Identification of proteins encompassing detected peptide sequences was performed by Dr Cleidi Zampronio who used the TurboSEQUEST search algorithm (Eng, McCormack et al. 1994).

2.12.   Yeast-two-hybrid

2.12.1.   Yeast strain and media

For Y2H experiments the PJ69-4A yeast strain was used (genotype: MATa, trp1-901, leu2-3,112, ura3-52, his3-200, gal4Δ, gal80Δ, GAL2-ADE2, LYS2::GAL1-HIS3, met2::GAL7-lacZ).

For routine yeast growth, yeast-peptone-dextrose (YPD) full medium was used, which contained 1 % (w/v) bacto-yeast extract, 2 % (w/v) bacto-peptone, 2 % (w/v) dextrose, 2 % (w/v) bacto-agar (required for solid medium only) and 0.01 % (w/v) tryptophan (trp).

For selective yeast growth, special synthetic complete dextrose (SCD) medium was used that contained 0.67 % (w/v) yeast nitrogen base without amino acids, 2 % (w/v) dextrose, 2 % (w/v) bacto-agar (required for solid medium only) and 0.14 % (w/v) yeast synthetic drop-out media supplement lacking histidine (his), leucine (leu), uracil (ura) and trp. When necessary, SCD medium was supplemented with 100 mg/L trp, 50 mg/L leu, 40 mg/L his or 20 mg/L ura.

Most of stock solutions for making Y2H media were autoclaved prior to use except of trp, which was sterilised by filtering through 0.22 µm-pore filters (Millipore). All Y2H procedures, such as preparing media, transforming and plating yeast were carried out using aseptic technique.

2.12.2.   Yeast-two-hybrid method

Y2H analyses were used to test the interactions of RhoJ with its candidate binding proteins identified earlier by mass spectrometry (section 2.11). Wild type RhoJ (wt) as well as its dominant active (da, Q79L) and dominant negative (dn, T35N) mutants were fused with the DNA binding domain (DBD) of Gal4p (pGBT9 constructs, selected on SCD media lacking trp) and RhoJ-binding candidate proteins were fused with the activation domain (AD) of Gal4p (pACT2, selected on media lacking leu). These constructs were sequentially transformed into the PJ69-4A yeast strain which contains Gal1 promoter-*HIS3* reporter gene (as described in section 2.12.3). Interaction of RhoJ with the candidate proteins was then tested in a spot assay. For this purpose, yeast colonies with both pGBT9 and pACT2 constructs were grown in SCD medium (lacking leu and trp) and diluted to optical density (OD) at 600 nm of 0.5. A five five-fold dilution series of yeast were prepared and spotted onto SCD agar plates lacking leu and trp (SCD-leu-trp) and onto SCD agar plates lacking leu, trp and his (SCD-leu-trp-his). The plates were then incubated at 30 ºC for 3-5 days. Growth of

yeast on SCD-leu-trp-his indicated an interaction of RhoJ with candidate protein tested. To eliminate false positive interactions, plates with SCD-leu-trp-his were additionally supplemented with 3 mM 3-Amino-1,2,4-triazole (3AT). 3AT competitively inhibits imidazoleglycerol-phosphate dehydratase, which participates in the production of histidine (Bartel, Chien et al. 1993).

2.12.3.   Yeast transformation

Yeast transformation was performed according to the lithium acetate / single stranded carrier DNA / polyethylene glycol method (Gietz and Woods 2002) with some changes. Briefly, yeast grown overnight in YPD or SCD media as appropriate, were diluted to optical density (OD) at 600 nm of 0.25 and grown for another two generations up to OD_{600} of 0.5-1. Then $2x10^8$ yeast (yeast solution with OD_{600} of 1 contains approximately $2x10^7$ yeast/ml) were centrifuged (2 min, 5000 x g, room temp.), washed with 1 ml of sterile water and centrifuged again as above. The yeast pellet was resuspended with transformation reagents in the following order: 240 µl of 50 % (w/v) polyethylene glycol (PEG, molecular weight of 3350 g), 36 µl of 1 M lithium acetate, 10 µl of 10 mg/ml single-stranded-carried DNA from salmon sperm (previously boiled for 5 min and chilled on ice, Invitrogen) and 34 µl of plasmid DNA diluted with water (0.1 to 1 µg of DNA). Yeast resuspended in these transformation reagents were incubated with agitation for 30 min at 30 ºC and heat shocked at 42 ºC for 15 min. Then yeast were centrifuged (1 min, 5000 x g, room temp.), washed with 1 ml of water, centrifuged again (2 min, 5000 x g, room temp.) and plated onto appropriate SCD medium-agar plates. Plates with transformed yeast were incubated at 30 ºC for 3-5 days.

2.13. Development of RhoJ polyclonal antibodies

2.13.1. Production of polyclonal RhoJ antibodies in rabbits

To make polyclonal anti-RhoJ antibodies, recombinant RhoJ protein fused to MBP was produced and used as the immunogen. Firstly, pMAL-2CE plasmid containing wild type (wt) RhoJ without the region encoding the CAAX box (pMAL-2CE-wtRhoJ-CAAX) was transformed into BL21 (DE3) pLys S *E. coli*. MBP-wtRhoJ-CAAX protein was produced in these bacteria and purified according to the protocol described in section 2.10.1. Immunisation of 2 rabbits with purified MBP-wtRhoJ-CAAX was performed by Harlan Sera Lab (CRUK Central Services). Rabbits were given 6 injections as follows. The primary immunisation required 400 μg immunogen in complete Freund's adjuvant. The following 5 injections were given every two weeks thereafter and contained 100 μg of immunogen in incomplete Freund's adjuvant. The rabbits were terminally bled one week after the 6th injection.

2.13.2. Purification of polyclonal RhoJ antibodies from rabbit antiserum

Purification of RhoJ antiserum included removal of the MBP-specific antibodies by MBP-amylose beads, purifying RhoJ-specific antibodies by GST-wtRhoJ-CAAX bound to PVDF membrane, and elution of RhoJ-specific antibodies by low pH glycine.

A batch of RhoJ antibody was purified at a time from 3 mls of RhoJ antiserum divided into 6x 0.5 ml aliquots. Firstly, RhoJ antiserum was depleted of MBP-specific antibodies. For this purpose, 6 aliquots of 15 μg MBP protein purified from bacterial lysate and bound to 25 μl packed amylose beads (NEB) (as in section 2.10.1) were blocked in 3 % (w/v) BSA (diluted in TBST) for 1 h at 4 °C. Each aliquot of beads was then collected by centrifugation,

resuspended in 0.5 ml of MBP-RhoJ antiserum and incubated on a rotating wheel for 1 h at 4 °C. The beads were then collected by centrifugation, pre-cleared antiserum collected and beads were washed 4 times with 1 ml of TBST. These washes were pooled with precleared antiserum and the total volume of each precleared aliquot of RhoJ antiserum was then adjusted to 5 ml with TBST and supplemented with 3 mM NaN_3.

In the meantime, binding of the GST-wtRhoJ-CAAX protein to PVDF membrane was performed. Firstly, the GST-wtRhoJ-CAAX protein was produced and purified from bacteria as described in section 2.10.1. Then 10 μg of GST-wtRhoJ-CAAX was loaded in each well of 6 polyacrylamide gels (12%) and SDS-PAGE was carried out (as in section 2.10.4). Subsequently, proteins were transferred from gels to PVDF membranes as in the standard western blotting procedure (section 2.10.5). After the transfer, the membranes were stained with Ponceau S dye to visualise the GST-wtRhoJ-CAAX protein bands, which were then cut out as strips (one membrane strip containing the GST-wtRhoJ-CAAX bands was excised from each membrane). These strips were then blocked in 3 % (w/v) BSA (diluted in TBST) for 1 h at room temperature. Subsequently, each of the 6 membrane strips was placed in a separate 50 ml tube containing 5 ml of pre-cleared RhoJ antiserum/TBST/ NaN_3 solution and incubated overnight on a rotating wheel at 4 °C. The next day membrane strips were washed with ice-cold solutions of TBST (3 x 10 min), high salt TBST (1 x 10 min) and finally TBS (3 x 10 min). All 6 membrane strips were then placed in one fresh 50 ml tube and covered with 3 ml of ice-cold 100 mM glycine (pH 2.5). This caused the elution of antibody from the membranes and was carried out for 7 min by gentle tilting of the tube with strips (at 4 °C). Then glycine/RhoJ antibody solution was transferred into a fresh tube and neutralised immediately by adding 1 M Tris-Cl (pH 9.5) in 50 μl aliquots until the pH of antibody solution was approximately 7.0; usually 150-200 μl of Tris-Cl was enough to neutralise 3 ml

of antibody. In the meantime, the membranes were incubated with another 3 ml of 100 mM glycine (pH 2.5) for 5 min and the stripping/neutralisation of the antibody was repeated as above. Purified antibodies were stored at 4 °C supplemented with 3mM NaN_3 and 4 % (w/v) BSA.

The quality of the purified antiserum was then tested in western blotting (as in section 2.10.5) and in immunofluorescence (as in section 2.18). The purified RhoJ antiserum was used as a primary antibody in western blotting (diluted 1:25) or in immunofluorescence (diluted 1:3).

2.14. Plasmid transfections of mammalian cells

2.14.1. Calcium-phosphate transfection of HEK 293Ts

3×10^6 cells were plated in sterile culture dishes (10 cm diameter) and the next day the transfection was performed as follows. 5 µg of DNA plasmid was mixed with 450 µl distilled water and 63 µl 2M calcium chloride ($CaCl_2x6H_2O$) in a 5 ml tube. Then 500 µl of 2x HBS-based buffer (containing 1.6 % (w/v) NaCl, 0.074 % (w/v) KCl, 0.027 % (w/v) $Na_2HPO_4x2H_2O$, 0.2 % (w/v) dextrose, 1.0 % (w/v) HEPES; pH adjusted to 7.05 and sterilised by passing through a 0.22 µm-pore filter) was added dropwise with shaking and allowed to precipitate for 15 min. The media of the plated HEK 293Ts was replaced with the fresh media and transfection mixture was added. Cells were then incubated in a humidified atmosphere with 5% CO_2 at 37 °C and the next day transfection medium was replaced with fresh medium. 24 hours later cells were used in various assays.

2.14.2. TransPass D2 transfection of HUVECs

10^6 of HUVECs were seeded on gelatin-coated plates (10 cm diameter) and the next day transfection was performed as follows. 4 µg of plasmid was mixed with 12 µl of TransPass D2 reagent (NEB) in 1 ml of OptiMEM medium (Invitrogen) and incubated for 20 min at

room temperature. In the meantime, cells were washed with 10 ml OptiMEM and covered with 3 ml of OptiMEM. The transfection mix was added and cells were incubated for 2 hours in a humidified atmosphere with 5% CO_2 at 37 °C. After this time the transfection mixture was replaced with 10 ml HUVEC complete medium without antibiotics and cells were used in assays 24 h after transfection. For immunofluorescence staining, cells were seeded on gelatin-coated glass coverslips (13 mm diameter) placed in a 24-well culture plate and the transfection reaction was scaled down appropriately.

2.15. Lentivirus infections of HUVECs

2.15.1. Production of lentivirus

Lentivirus was produced in HEK 293Ts. 2.5×10^6 cells were plated in sterile culture dishes (10 cm diameter) and the next day calcium-phosphate transfection was performed similarly as in section 2.14.1. 20 µg transfer vector (pWPXL-wtRhoJ, pWPXL-daRhoJ(Q79L) or pWPI), 15 µg packaging vector (psPAX2) and 6 µg envelope vector (pMD2G) were used per plate. After addition of the transfection mix cells were incubated in a humidified atmosphere with 5% CO_2 at 37 °C for 8 hours when the transfection mixture was removed and 5 ml of fresh medium was added. After 48 hours of incubation, the medium with virus was collected, centrifuged for 5 min at 1100 rpm, cleared through 0.45 µm-pore syringe filters (Corning Incorporated, Germany) and stored at -80 °C. Lentivirus was frozen/thawed only once before infection.

2.15.2. Infection of HUVECs

10^6 HUVECs were seeded on gelatin-coated culture dishes (10 cm diameter) and the next day HUVEC medium was replaced with 7.5 ml of lentivirus supernatant supplemented with 8 µg/ml polybrene, bovine brain extract and 90 µg/ml heparin. 24 h after infection the lentivirus

supernatant was replaced with fresh complete HUVEC medium and cells were left to grow for another 2 days. Then GFP-positive cells were sorted by FACS (MoFlo Cytomation fluorescence activated cell sorter). Lentivirus infection according to this procedure yielded typically in 90 % of GFP-expressing and 40-60 % of GFP-wtRhoJ or GFP-daRhoJ-expressing HUVECs.

2.16. Knock-down of genes using siRNA

10^6 HUVECs were seeded on gelatin-coated culture dishes (10 cm diameter) and the next day transfection was performed with 10-25 nM siRNA duplexes and 0.3 % (v/v) lipofectamine^{TM} RNAiMAX (Invitrogen). All siRNA duplexes used are listed in Table 2.7 (section 2.6). Per transfection of a 10 cm HUVEC plate, duplex (or water for mock transfection) was diluted with OptiMEM in one tube to give a final volume of 680 µl, and 12 µl of RNAiMAX lipofectamine^{TM} was diluted with 108 µl of OptiMEM medium in another tube. Both solutions were mixed gently and incubated for 10 min at room temperature. The mixtures were then combined, mixed gently and incubated for another 10 min at room temperature. In the meantime, cells were washed twice with PBS and 3200 µl of OptiMEM medium was added per plate. Then the transfection mixture was added, the plates were gently tilted for mixing and incubated for 4 h at 37 ℃. Afterwards the transfection mix was replaced with complete HUVEC medium (without antibiotics) and 48 h after transfection cells were used in various assays.

2.17. Endocytosis assays

2.17.1. Trafficking of transferrin receptor in HUVECs

The up-take and release of fluorescently labelled Tf was tested in HUVECs with siRNA-silenced RhoJ. 24 h after the siRNA RhoJ knock-down (10 nM siRNA duplexes used, section

2.16), 10^5 HUVECs were seeded on gelatin-coated wells of a 12-well plate and incubated overnight in complete HUVEC medium. Afterwards, cells were incubated first in starving medium (M199, 4 mM L-glutamine) for 1 h and then for another hour in complete HUVEC medium containing 5 µg/ml Alexa-488 labelled Tf (Invitrogen). Subsequently, cells were washed with PBS and complete HUVEC medium with 50 µg/ml of unlabelled Tf was added and cells were incubated at 37 °C for different time periods (0-30 min). Cells were then washed quickly with PBS, covered with 0.75 ml trypsin-EDTA and incubated for 2 min at 37 °C. Then 0.25 ml of 4 % (w/v) paraformaldehyde (PFA, prepared in PBS) was added and cells were immediately transferred into FACS tubes. Fixation with PFA was performed for 15 min at room temperature in the dark. The amount of fluorescently labelled Tf in HUVECs was measured with FACS-Becton Dickson FACSCalibur cell sorter (Becton and Dickson, USA) in FL-1. At least 10^3 cells were counted in each condition and the geometric mean fluorescence levels were determined. To plot the results of the Tf uptake, the mean for each condition (with or without RhoJ knock-down) from 3 experiments was depicted as bar chart with standard errors. To present the results of Tf release firstly the geometric mean of cell fluorescence before the incubation with unlabelled Tf (0 min release) was averaged from 3 experiments and considered as 100 %. The subsequent time points for Tf release (5, 15, 30 min) were then plotted as a percentage in relation to 100 %.

2.17.2.   Testing the surface levels of VEGFR2 in HUVECs

The amount of VEGFR2 present at the cell surface was tested in HUVECs with siRNA-silenced RhoJ. 24 h after the siRNA RhoJ knock-down (25 nM siRNA duplexes used, section 2.16), 10^5 HUVECs were seeded on gelatin-coated wells of a 12-well plate and incubated overnight in complete HUVEC medium. Cells were then treated in three different ways. In the first condition cells were starved for 1 h in HUVECs starving medium (M199, 4 mM L-

glutamine). In the second condition cells were starved for 1 h in HUVEC starving medium and then stimulated for 30 min by 10 ng/ml VEGF-A (PeproTech, Rocky Hill, USA), which was diluted in HUVEC starving medium. In the third condition cells were left in complete HUVEC medium without any treatment. After applying these conditions cells were washed with PBS and 0.75 ml of non-enzymatic cell dissociation solution was added to each well and incubated for 5 min at 37 °C. Cells in this solution were then transferred into 1.5 ml microfuge tubes containing 0.25 ml of 4 % (w/v) PFA (prepared in PBS) and incubated for 15 min at room temperature. Cells were then centrifuged (195 x g, 5 min, room temperature), the supernatant removed and blocking performed for 30 min in 4 % (w/v) BSA (prepared in PBS). Cells were then centrifuged as above and incubated with 2 µg/ml goat anti-VEGFR2 antibody (diluted in blocking buffer) for 1 h. This was followed by 2 washes with PBS and 30 min incubation with 15 µg/ml anti-goat FITC-conjugated secondary antibody diluted in blocking buffer. Cells were then washed twice and diluted in PBS. Subsequently FACS analysis was performed using FACS-Becton Dickson FACSCalibur cell sorter. At least 10^3 cells were counted for each condition and the geometric mean fluorescence levels were determined. The results were shown in a form of bar chart with standard errors, containing means for each condition from 3 experiments.

2.18.   Immunofluorescence

For immunofluorescence, cells were grown on glass coverslips (13 mm diameter, VWR International). Prior to use, coverslips were immersed in 1 M HCl for 10 min, then washed 5 times with sterile distilled water and stored in 70 % ethanol (Fisher Scientific). Before each experiment, coverslips were placed in wells of a 24-well culture plate and were washed 5 times with sterile distilled water in a sterile hood to remove residual ethanol. Coverslips were then coated with gelatin or with Matrigel (BD Biosciences, Oxford, UK). For gelatin coating,

coverslips were covered with 0.1 % (w/v) gelatin and left for 20 min at 37 °C. After this time gelatin solution was removed. For Matrigel coating, an aliquot of Matrigel was firstly thawed on ice at 4 °C for several hours. 100 % (v/v) Matrigel was then spread on coverslips with a pipette tip and its excess was immediately aspirated leaving only a very thin coating. Coverslips were then allowed to dry out prior to seeding HUVECs. For analysis of sparse cells, HUVECs were seeded at the concentration of 2×10^4 cells/well at least 4 h prior to fixation. To obtain a confluent monolayer of cells, HUVECs were seeded at the concentration of 7.5×10^4 cells/well the day before fixation. A general staining procedure (except endogenous RhoJ staining, please see below) was carried out as follows at room temperature. HUVECs were gently washed with PBS and fixed in 4 % (w/v) PFA (in PBS) for 15 min. The cells were then washed once in PBS and permeabilised with 0.1 % (v/v) Triton-X-100 (in PBS) for 4 min. Afterwards cells were washed again with PBS and left in blocking buffer (3% (w/v) BSA, 10% (v/v) FCS, 0.1% (v/v) tween-20, 0.01% (w/v) NaN_3 in PBS) for 30-60 min. The cells were then incubated with a primary antibody diluted in blocking buffer for 1 h and then were washed 3 times with PBS. Subsequently a secondary antibody diluted in blocking buffer was added and after 30-60 min of incubation cells were washed 3 times with PBS and once with distilled water. Antibodies and their concentrations used are described in Tables 2.2 and 2.3 (section 2.3). Coverslips with cells were then mounted on slides (Menzel-Glaser GmbH, Braunschweig, Germany) using 6 µl ProLong Gold Antifade reagent with DAPI (Invitrogen) per one coverslip. The mounting reagent was warmed up for 30 min at room temperature prior to use.

In order to immunostain endogenous RhoJ with the polyclonal rabbit RhoJ antibody (developed and purified in section 2.13), cells were fixed and permeabilised with ice-cold 100 % methanol for 5 min. This was followed by one wash in PBS and 1 hour blocking in 4 %

(w/v) BSA at room temperature. Subsequently cells were incubated with RhoJ antibody diluted in 4 % (w/v) BSA for 2 hours and this was followed by 2 x 5 min washes in PBST. Incubation with a secondary antibody diluted in 4 % BSA was carried out for 45 min and was followed by 3 x 5 min washes in PBST and one wash in distilled water. Cells were then mounted as described in the general procedure above.

Images of immunofluorescently stained cells were acquired using the Axiovert 100M confocal microscope and LSM 510 software (Zeiss). LSM Image Browser software (Zeiss) was used to export images, which were then cropped in Microsoft Office Power Point program.

2.19. Testing the functions of endothelial cells expressing dominant active RhoJ

HUVECs were infected with lentivirus to express GFP or GFP-daRhoJ (section 2.12.2) and were FACS-sorted for GFP-positive cells. Cells were then expanded in complete HUVECs medium supplemented with pen/strep antibiotics and were used in the assays described below.

2.19.1. Scratch wound assay

3.6×10^5 HUVECs expressing either GFP or GFP-daRhoJ were seeded on gelatin-coated wells of a 6-well plate in complete medium and left at 37 °C. The next day scratches were made with 200 µl sterile pipette tips, cells were then washed twice with PBS and fresh medium supplemented with 2.5 µg/ml mitomycin C was added. Pen marks perpendicular to the scratches were made and pictures were taken in the same scratch places at 0, 4, 8 and 12 hours using USB 2.0 2M Xli camera connected to the Leica DM IL microscope (Leica, Milton Keynes, UK). The wound areas were measured with ImageJ software. To compare the speed of a wound closure between GFP and GFP-daRhoJ expressing cells, the wound areas

measured at different time-points were compared to the wound areas at 0 hours. Wound sizes at 0 hours were considered as 100 %, thus plotted graphs were representing the % of remaining wound areas.

2.19.2. Analysis of focal adhesions and stress fibres

To analyse the number of FAs and SFs in migrating HUVECs a scratch wound assay was performed on cells cultured on coverlips. 7.5×10^4 HUVECs expressing either GFP or GFP-daRhoJ were plated on gelatin-coated coverslips in a 24-well plate. 24 h later the monolayers of cells were scratched with 10 µl sterile pipette tip, washed twice with PBS and covered with fresh complete medium supplemented with 2.5 µg/ml mitomycin C. Cells were allowed to migrate for 2-4 h before the opposite edges of wounds started to merge. Then coverslips were washed gently with PBS, cells were fixed with 4 % PFA and stained according to the procedure described in section 2.18. A vinculin-specific antibody was used to visualise FAs and actin was stained with 50 µg/ml phalloidin-TRITC (Invitrogen). Images of cells within a monolayer and at the edge of a monolayer were acquired using the Axiovert 100M confocal microscope and LSM 510 software (Zeiss). FAs were counted manually using the cell counter plug-in tool of ImageJ. The mean fluorescent intensity of F-actin per cell was determined from acquired images using the LSM 510 software.

2.19.3. Organotypic tube forming assay

HUVECs stably expressing GFP or GFP-daRhoJ were sent to Dr Georgia Mavria's Laboratory (Leeds Institute of Molecular Medicine, St James's University Hospital, Leeds, UK), where Margherita Scarcia and Sabu Abraham used them to perform an organotypic angiogenesis assay. The permission was given to present the data in this thesis (Fig. 3.10 B and C). The results of this experiment were also published in Kaur *et al.* (2011)*, where the full experimental procedure is included.

2.20.   Examining the localisation of RhoJ, GIT1 and βPIX to focal adhesions

RhoJ, GIT1 and βPIX were knocked-down in HUVECs using 25 nM siRNA duplexes as described in section 2.16. 48 hours after siRNA transfection cells were sparsely plated on gelatin-coated coverslips and left for 4 hours to adhere. The cells were then fixed and stained with RhoJ-, GIT1- or βPIX-specific antibodies as described in section 2.18. These cells were also counter-stained with vinculin-specific antibody to visualise FAs. The cell images were acquired using the Axiovert 100M confocal microscope and LSM 510 software (Zeiss) and FAs in each cell were counted manually using the cell counter plug-in tool of ImageJ. The total number of FAs per cell was determined by counting vinculin-positive FA-like regions. The number of RhoJ, GIT1 or βPIX-positive FAs was then determined and presented as a percentage of total FAs per cell.

2.21.   RhoJ activation assay

2.21.1.   Optimisation of RhoJ-GTP pull-down

2.21.1.1. Preparation of cellular lysate for GTP/GDP loading on Rho GTPases

Confluent monolayers of HUVECs or HMEC-1 (in 10 cm plates) were washed with PBS, covered with 2 ml of non-enzymatic cell dissociation solution and incubated at 37 ℃ for 10 min. Afterwards cells were collected in two washes of 10 ml PBS and centrifuged (5 min, 195 x g, room temperature). The pellet of cells from one plate was then lysed in 180 μl of nucleotide-loading lysis buffer (supplemented with protease inhibitor cocktail, 2 mM $NaVO_3$ and 10 mM NaF) for 10 min on ice. Subsequently the lysate was centrifuged for 10 min (21910 x g, 4 ℃), the supernatant collected and mixed with 20 μl of glycerol to make its final

concentration 10 % (v/v). Lysates were stored at -80 ℃. The lysates of HEK 293Ts ectopically expressing wt-, da- or dnRhoJ were prepared in a similar way with only difference in the amount of lysis buffer used, which was 5 times higher than that used for lysis of HUVECs or HMEC-1.

2.21.1.2. Preparation of GST-CRIB beads

In order to pull-down active RhoJ, Cdc42 or Rac1 from cellular lysates the CRIB domains of PAK (1-254 amino acids of rat PAK1) or WASP (228-268 amino acids of human WASP) proteins fused with GST were produced and loaded on glutathione-agarose beads as described in section 2.10.1. For each pull-down condition 5 μg of GST-CRIB was bound to 12.5 μl of packed glutathione-agarose beads, which were then washed 3 x with 1 ml nucleotide-loading lysis buffer (supplemented with protease inhibitor cocktail, 2 mM $NaVO_3$ and 10 mM NaF) and finally diluted with this buffer to give a 50 % slurry. The beads were then left on ice ready for pull-down.

2.21.1.3. GTP/GDP loading on Rho GTPases and pull-down

200 μl of HUVECs or HMEC-1 lysate (made from one confluent plate) was used to perform one nucleotide-loading condition. When the HEK 293Ts lysate was used for nucleotide loading, the original lysate (prepared as in section 2.21.1.1) was diluted 10 times to give a final volume of 200 μl. Initially this experiment was carried out according to the protocol adapted from commercially available "Rac1/Cdc42 Activation Assay Kit" (Upstate Cell Signalling Solutions, 17-441, Temecula, USA). However, since the loading of nucleotides on RhoJ was not successful, the method was slightly changed, according to the protocol used by Erasmus and Braga, which measured active Cdc42 and Rac1 (Erasmus and Braga 2006). Briefly, 200 μl of cellular lysate was mixed with EDTA (final concentration 10 mM) and GTPγS (a stable analogue of GTP) or GDP (final concentration of nucleotides 1 mM). After

incubation for 10 min at room temperature, $MgCl_2$ was increased to a final concentration of 30 mM, and then these samples were mixed with GST-CRIB fusion protein bound earlier to glutathione-agarose beads. The pull-down was performed for 45 min at 4 ℃ on a rotating wheel. After the pull-down the beads were washed 3 times with 1 ml of Rho-assay lysis buffer (supplemented with protease inhibitor cocktail, 2 mM $NaVO_3$ and 10 mM NaF) and resuspended in 30 µl of 2x SDS sample-loading buffer. Pull-down and lysate samples were then subjected to the SDS-PAGE (2.10.4) and western blotting (2.10.5) with RhoJ-, Cdc42- or Rac1-specific antibodies.

2.21.2. Measuring RhoJ activation after VEGFA, FGF-2 and thrombin stimulation

The day before treatment 10^6 HUVECs were seeded on gelatin-coated 10 cm plates in HUVEC medium. Prior to the treatment with various stimuli, cells were washed with PBS and rested for 1 h in starving medium (M199, 4 mM L-glutamine). Subsequently the starving medium was replaced with 5 ml of stimuli (diluted in fresh starving medium) and cells were incubated for 1, 15, 30 and 60 min. The concentration of stimuli used was as follows: 10 ng/ml VEGFA (Peprotech), 10 ng/ml FGF-2 (kindly provided by Prof. John Heath, School of Biosciences, University of Birmingham, UK) or 2.5 U/ml thrombin. FGF-2 stimulus was supplemented with 10 µg/ml heparin. After treatment medium was quickly removed, the plates were placed on ice and 200 µl of 2x Rho-assay lysis buffer (supplemented with 2x protease inhibitor cocktail, 4 mM $NaVO_3$ and 20 mM NaF) was added. One plate of cells was lysed straight after 1 h of resting without treatment and was considered as 0 min. Cells were scraped in lysis buffer, collected in 1.5 ml eppendorf tubes and incubated on ice for 10 min. The lysates were then clarified by centrifugation (5 min, 21910 x g, 4 ℃). 20 µl of each lysate sample was mixed with equal amount of 2x SDS sample-loading buffer and the rest was

mixed with GST-CRIB bound to glutathione-agarose beads (CRIB domain of PAK was used, prepared as in section 2.21.1.2). Samples were placed on the rotating wheel and pull-down was performed for 45 min at 4 ℃. Then beads were washed 3 times with Rho-assay lysis buffer (supplemented with protease inhibitor cocktail, 2 mM $NaVO_3$ and 10 mM NaF) and resuspended in 30 μl of 2x SDS sample-loading buffer. Samples were finally subjected to SDS-PAGE and western blotting with RhoJ- or Cdc42-specific antibodies (as in sections 2.10.4 and 2.10.5).

2.22.   Statistical analyses

Results were plotted as the mean of at least 3 experiments with standard errors (except of Fig. 3.1). Where possible, the statistical significance of results was analysed using the GraphPad Prism 4.03 software and was denoted as follows: *** for $p<0.001$, ** for $0.001<p<0.01$, * for $0.01<p<0.05$ and ns for non-significant. The Wilcoxon signed-rank test was used to analyse significance of RhoJ and Cdc42 activation by VEGF. The Mann Witney test was used to analyse statistical difference in the amount of FAs and in the fluorescent intensity of F-actin staining in pairs of GFP and GFP-daRhoJ-expressing cells.

2.23.   Preparation of figures

Calculations were performed and graphs were plotted using the Microsoft Office Excel software. Graphs with data displayed as a box and whisker plot were created using the GraphPad Prism 4.03 software. Some pictures were rotated and cropped using GIMP 2.4.5 GNU Image Manipulation Program before they were inserted into Microsoft Office Power Point program. All graphs and pictures were finally assembled into figures and edited using the Microsoft Office Power Point program.

3. INTRACELLULAR LOCALISATION AND FUNCTION OF RHOJ IN ENDOTHELIAL CELLS

3.1. Intra-cellular localisation, expression and known functions of RhoJ

RhoJ is a member of the Cdc42-like sub-family that belongs to the larger family of small Rho GTPases and is also called TCL or TC10-like due to its high similarity to TC10 GTPase (Vignal, De Toledo et al. 2000). Many Rho GTPases, including RhoJ, cycle between an active GTP-bound and an inactive GDP-bound state. Once activated, these proteins act as molecular switches that regulate a variety of cellular processes, such as cytoskeletal reorganisation, cell migration, endocytosis and cell proliferation (Hall 1998; Jaffe and Hall 2005).

In initial studies ectopically expressed tagged RhoJ localised to the dorsal cell membrane and was associated with large intra-cytoplasmic vesicles in REF-52 fibroblasts (Vignal, De Toledo et al. 2000). In these cells, an active mutant of RhoJ caused the production of dynamic F-actin ruffles on the dorsal membrane. This phenotype was blocked by dominant negative Rac1 and Cdc42 mutants, which suggested that these three GTPases may share similar GEFs. In another study, constitutively active RhoJ caused the formation of lamellipodia and FA-like assemblies at the cell periphery of porcine aortic ECs stably expressing the human platelet-derived growth factor β-receptor (Aspenstrom, Fransson et al. 2004). Lamellipodia are sheet-like protrusions extended by migrating cells (Small, Stradal et al. 2002), while FAs are dynamic, multiprotein complexes, which connect the intracellular cytoskeleton with the ECM (Dubash, Menold et al. 2009).

Some other studies showed that RhoJ played a role in endocytosis and localised to the plasma membrane and intracellular vesicles in HeLa cells (de Toledo et al. 2003). These studies revealed that RhoJ mostly localised to the EE/ES and played a role in the clathrin-dependent endocytosis, since its knock-down by siRNA perturbed the Tf release by HeLa cells.

Overexpression of the constitutively active RhoJ promoted an accumulation of Tf in the EE/ES and blocked its movement to the perinuclear recycling endosomes, resulting in Tf recycling to the plasma membrane straight from the EE/ES (de Toledo et al. 2003).

More recent work performed by members of our laboratory revealed that RhoJ is predominantly expressed in ECs (Herbert, Stekel et al. 2008; Kaur, Leszczynska et al. 2011). These cells are very important in the maintenance of the healthy state of the whole organism as they line the inner wall of blood and lymphatic vessels (Adams and Alitalo 2007). ECs are also crucial in the process of angiogenesis, when new blood vessels sprout from the pre-existing vasculature, and many Rho GTPases play an important role in this process (Bryan and D'Amore 2007). Initially, using a bioinformatic method, RhoJ was found to be present only in endothelial expression libraries but not in those from other cell types (Herbert, Stekel et al. 2008). This finding was supported by discovering high mRNA levels of RhoJ in ECs but not in some non-EC types tested (Herbert, Stekel et al. 2008). More recently, *in situ* hybridisation studies in both the developing mouse embryo at embryonic day 9.5 (when angiogenesis occurs) and in various human tissue sections have shown that the RhoJ gene was expressed in the blood vessels (Kaur, Leszczynska et al. 2011). The presence of RhoJ in human smooth muscle cells and pericytes was also detected (both RNA and protein) but appeared to be very low in comparison to ECs (Kaur, Leszczynska et al. 2011).

Since RhoJ was endogenously expressed in endothelium, a series of experiments were performed to determine its function in this tissue (Kaur, Leszczynska et al. 2011). Firstly, a set of experiments tested the role of RhoJ in tubulogenesis *in vitro*. ECs may be induced to form a 2-dimensional network of tubes when cultured on Matrigel, which is a solubilised basement extract (Passaniti, Taylor et al. 1992). ECs will also form a 3-dimensional network of tubes with lumens when cultured on a monolayer of fibroblasts and in the presence of pro-

angiogenic growth factors VEGF and FGF-2 (Bishop, Bell et al. 1999). Knock-down of RhoJ impaired tubule formation in both of these systems.

One of the important steps in angiogenesis is EC migration (Carmeliet 2003). This strongly depends on a constant turnover of the actomyosin cytoskeleton and FAs (Raftopoulou and Hall 2004). Kaur *et al.* discovered that silencing of RhoJ using siRNA significantly decreased EC migration. This was tested in chemotaxis and chemokinesis assays. In the former RhoJ knock-down significantly impaired the movement of cells towards the serum and FGF-2. In the latter silencing of RhoJ slowed down the migration of cells in a scratch wound assay. Subsequently, Sukhbir Kaur showed that RhoJ knock-down increased numbers of FAs and SFs in migrating ECs. These cells also had increased levels of pMLC and were able to strongly contract the type I collagen gel. Importantly, indirect inhibition of MLC phosphorylation by adding a pharmacological inhibitor of ROCK (Y27632), or its direct inhibition by blebbistatin, improved the migration of RhoJ-silenced cells and also decreased the contractility in these cells. Thus, findings by Kaur *et al.* showed that RhoJ plays an important role in EC migration, proliferation and *in vitro* tubulogenesis as well as in modulating actomyosin contractility and FA numbers in ECs (Kaur, Leszczynska et al. 2011).

The work described in this chapter aimed to determine the endogenous localisation of RhoJ in ECs and to further investigate its function in these cells. Firstly, the protein levels of RhoJ and other crucial Rho GTPases were compared in ECs. Secondly, a polyclonal rabbit RhoJ antibody was made, validated and used to study the localisation of endogenous RhoJ in ECs. In addition, the localisation of overexpressed RhoJ in these cells was determined. Thirdly, a dominant active mutant of RhoJ was used to verify the role of RhoJ in EC migration, tubule formation and its influence on FAs and SFs in these cells. Fourthly, the potential role of RhoJ in endocytosis in ECs was investigated.

3.2. Comparison of RhoJ, Cdc42 and Rac1 proteins in HUVECs

RhoJ is a Rho GTPase that is expressed in ECs, where it regulates processes such as cell migration and proliferation (Kaur, Leszczynska et al. 2011). However, it is well established that other Rho GTPases are expressed abundantly in ECs and are very important for their proper functioning (Bryan and D'Amore 2007). Therefore it was important to compare the levels of RhoJ protein with some of the other key Rho GTPases expressed in ECs.

The relative quantitation of RhoJ and Cdc42 proteins in HUVECs was performed by western blotting. Firstly, HEK 293Ts were transfected with plasmids to express flag-tagged versions of these proteins and their lysates were prepared. These and HUVECs lysates were used in western blotting with flag, RhoJ and Cdc42 specific antibodies (Fig. 3.1 A). The intensity values of flag-RhoJ bands obtained with RhoJ- or flag-specific antibodies were compared with the intensity values of flag-Cdc42 bands obtained with Cdc42- or flag-specific antibodies. This allowed the calculation of relative efficacies of RhoJ and Cdc42-specific antibodies and so enabled relative expression levels of RhoJ and Cdc42 in HUVECs to be determined. The chemiluminescence intensity of specific bands was acquired using GeneGnome HR scanner, which measures the real time chemiluminescent signal.

A similar approach was used to compare relative expression levels of RhoJ and Rac1 in HUVECs using the HA tag and the HA-specific antibody as a common reference. It was found that HUVECs contain 3.5 times more Rac1 and 11 times more Cdc42 than RhoJ proteins respectively (Fig. 3.1 B).
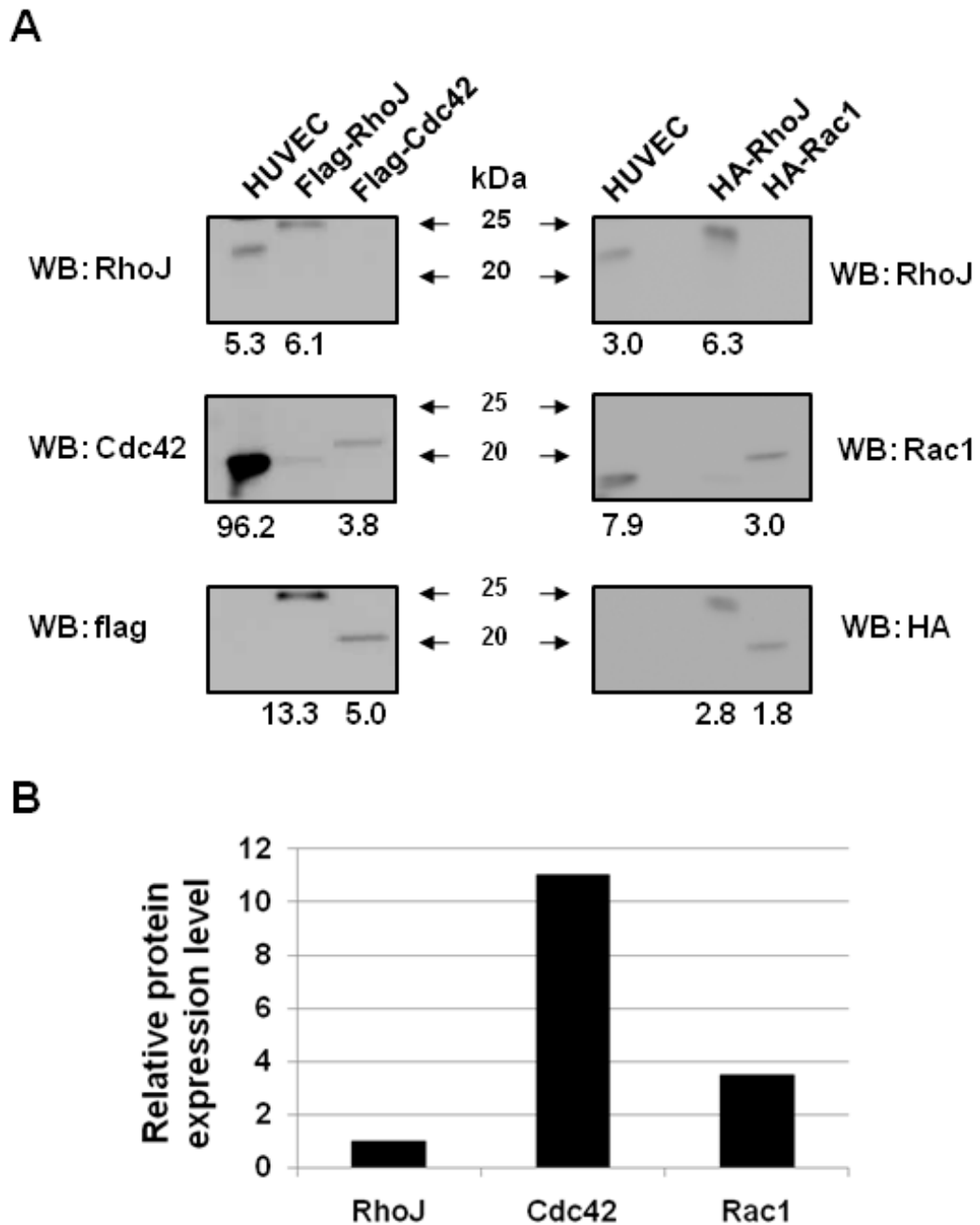
Fig. 3.1 Quantitation of RhoJ, Cdc42 and Rac1 protein levels in HUVEC.
A, HEK 293Ts were transfected with plasmids encoding flag-RhoJ, flag-Cdc42, HA-RhoJ and HA-Rac1 and lysates were prepared. These and HUVEC lysates were compared in western blotting with indicated antibodies and chemiluminescent intensities of particular bands (stated under each lane) were measured using GeneGnome HR scanner. **B**, the bar chart shows calculated relative RhoJ, Cdc42 and Rac1 protein levels in HUVECs.

3.3. Production and purification of RhoJ polyclonal antibodies

Initial experiments showed that the commercially available mouse monoclonal RhoJ antibody (Ab57584 from Abcam) was suitable for western blotting but did not detect RhoJ by immunofluorescence. To enable the localisation of endogenous RhoJ there was a need to generate alternative RhoJ-specific antibodies and these were developed in rabbits.

To create reagents for production and purification of RhoJ antibodies, recombinant RhoJ proteins were made as the c-terminal fusions with GST or MBP proteins. Both constructs were designed to have the last five amino acids of RhoJ missing (-CCSII, known as CCAAX box). The CCAAX box undergoes posttranslational lipidation and anchors proteins in cellular membranes. It was removed to avoid potential difficulties in protein production and purification from bacteria.

MBP-RhoJ recombinant fusion protein was used to immunise two rabbits as described in the methods and materials. Antiserum from the terminal bleed was firstly depleted of MBP-specific antibodies and then RhoJ-specific antibodies were affinity purified with GST-RhoJ protein attached to the PVDF membranes.

3.3.1. Testing the specificity of RhoJ antibodies in western blotting

The quality of the purified antibody was firstly assessed by western blotting (Fig. 3.2). Since the antibody was raised using the full-length RhoJ protein (-CCAAX box), it was crucial to check that it would not recognise other Rho GTPases that share some sequence homology with RhoJ. To test this HEK 293Ts were transfected with plasmids to express epitope tagged RhoJ, RhoA, Cdc42 and Rac1. Lysates were prepared and used in western blotting to test the specificity of the RhoJ mouse monoclonal antibody (Abcam) and the purified RhoJ rabbit
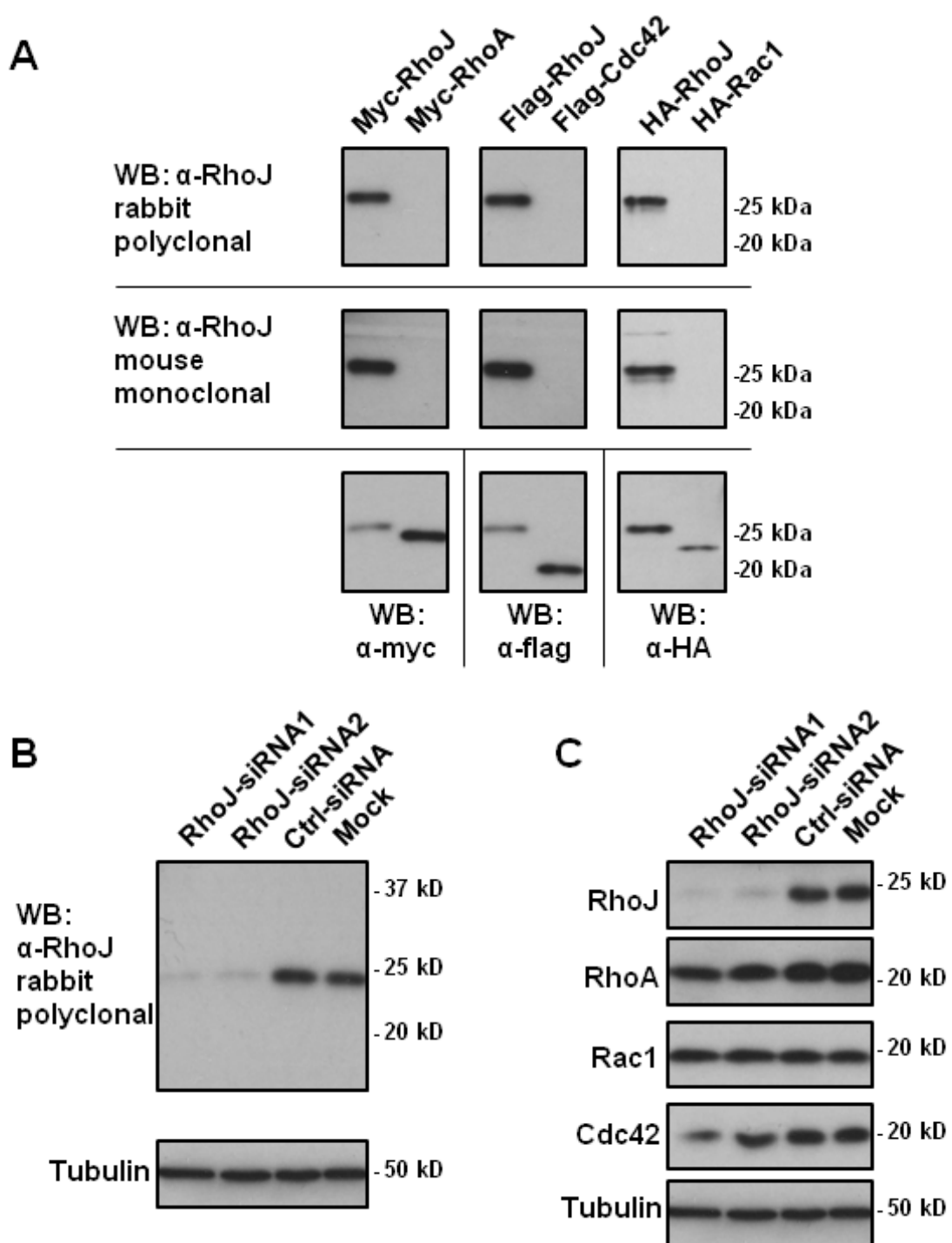
Fig. 3.2 Testing the specificity of RhoJ antibodies and siRNA duplexes.
A, HEK 293Ts were transfected with plasmids encoding epitope tagged RhoJ, RhoA, Cdc42 and Rac1; lysates were prepared and subjected to SDS-PAGE and western blotting with antibodies as indicated. Neither of the RhoJ antibodies detected RhoA, Cdc42 or Rac1. **B** and **C,** HUVECs were transfected with 25 nM RhoJ-siRNA1, RhoJ-siRNA2 and Ctrl-siRNA duplexes or were mock transfected. 48 h later cells were lysed and the protein amount adjusted to be equal between the samples. **B**, Western blot showing the specificity of the purified anti-RhoJ polyclonal antibody that detects a single RhoJ band. **C**, Western blot (representative of 3 experiments) showing that RhoJ siRNA knock-down does not affect the levels of RhoA, Rac1 and Cdc42 proteins in HUVECs.

polyclonal antisera (Fig. 3.2 A). Both the commercially available RhoJ mouse monoclonal antibody and the purified RhoJ rabbit polyclonal antisera recognised only RhoJ protein. The other Rho GTPases tested were not detected by any of the RhoJ antibodies.

In order to further validate the specificity of the purified polyclonal RhoJ antibody, it was tested in western blotting on lysates from cells that had RhoJ silenced with siRNA. HUVECs were transfected with two different RhoJ-specific siRNAs (RhoJ-siRNA1 and RhoJ-siRNA2), control non-specific siRNA (Ctrl-siRNA) or were mock transfected (no siRNA). The Ctrl-siRNA has no homology to known human sequences. Lysates from these cells were used in western blotting with the purified polyclonal RhoJ antibody. Only one band was detected of the correct size (~25 kDa) and this was absent in the lanes containing lysates from the RhoJ knocked-down cells (Fig. 3.2 B). Western blotting showed that RhoJ silencing had no effect on the levels of RhoA, Rac1 and Cdc42 proteins (Fig. 3.2 C), thus demonstrating the specificity of the siRNA duplexes for RhoJ. This also showed that there was no up-regulation of these Rho GTPases to compensate for the loss of RhoJ.

3.3.2. Testing the purified polyclonal rabbit RhoJ antibody for immunofluorescence

The purified polyclonal RhoJ antibody was tested to determine if it would detect RhoJ protein by immunofluorescence (Fig. 3.3). HEK 293Ts transfected with myc-RhoJ encoding plasmids were fixed and co-stained with purified anti-RhoJ polyclonal antisera, anti-myc antibody and DAPI reagent to mark nuclei. RhoJ- and myc-specific antibodies gave a similar staining pattern in myc-RhoJ transfected cells, while in the mock transfected cells only a weak background signal was detected (Fig. 3.3 A). The expression of myc-RhoJ in HEK 293Ts was confirmed by western blotting with the RhoJ-specific monoclonal antibody (Abcam) (Fig. 3.3 C).
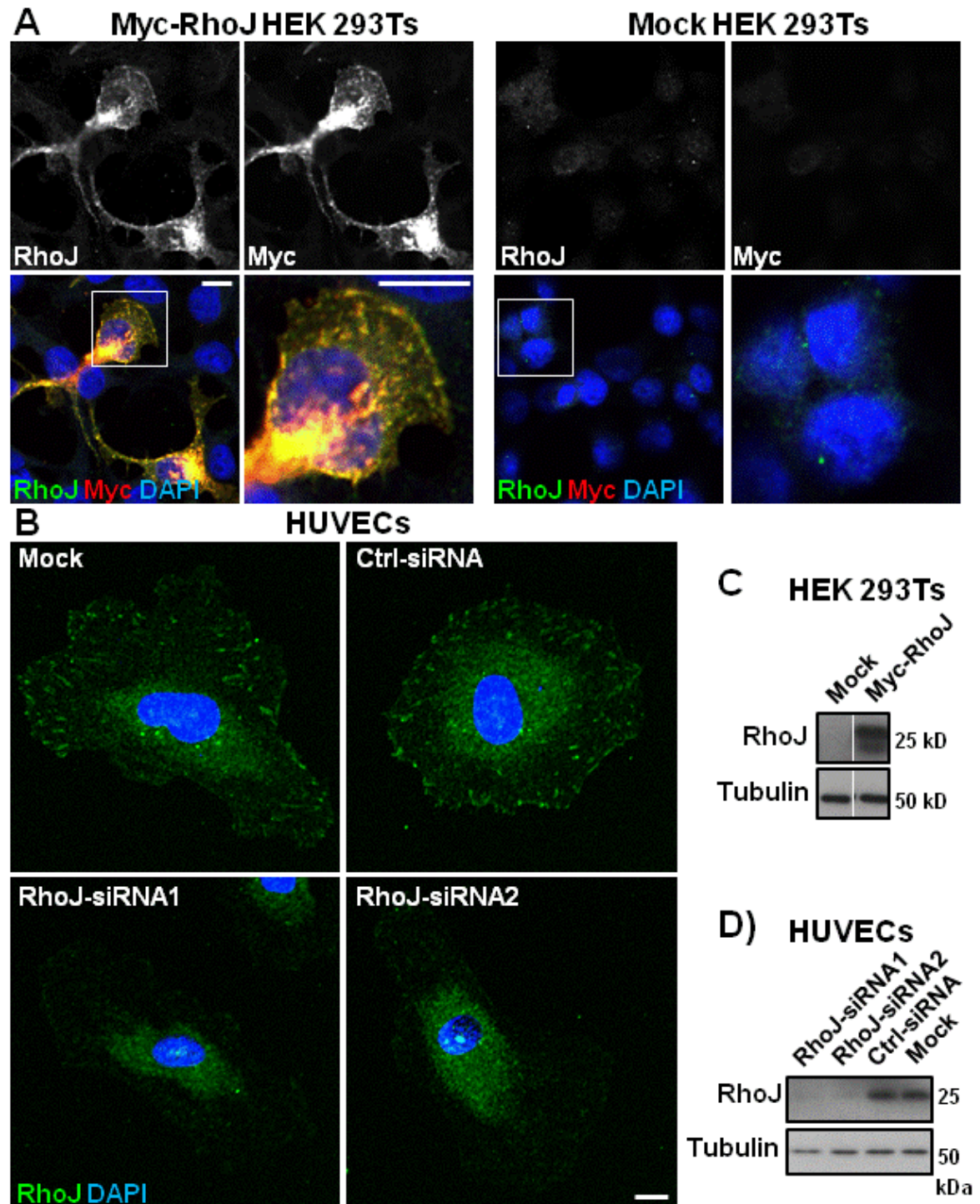
Fig. 3.3 Testing the purified polyclonal RhoJ antibody in immunofluorescence.
A, HEK 293Ts were transfected with myc-RhoJ encoding plasmids or were mock transfected. 48 h later cells were fixed and co-stained with myc and purified polyclonal RhoJ antibodies. Regions marked in the white boxes are expanded to give a more detailed view of the staining. **B**, HUVECs were transfected with 10 nM RhoJ-siRNA1, RhoJ-siRNA2 and Ctrl-siRNA duplexes or were mock transfected. 48 h later cells were fixed and stained with the purified polyclonal RhoJ antibody. RhoJ knock-down significantly reduced the peripheral punctate staining pattern. DAPI was used to visualise nuclei. All scale bars: 10 µm. Western blots showing the expression of myc-RhoJ (**C**) or RhoJ knock-down (**D**).

The purified polyclonal RhoJ antibody also detected endogenous RhoJ in HUVECs (Fig. 3.3 B). These cells were transfected with RhoJ-specific siRNAs (RhoJ-siRNA1 and RhoJ-siRNA2), control non-specific siRNA (Ctrl-siRNA) or were mock transfected (no siRNA). Staining with the polyclonal RhoJ antibody gave a peripheral punctate pattern that was significantly reduced in the RhoJ siRNA silenced cells. The RhoJ staining pattern was clearer when cells were fixed using the ice-cold methanol (Fig. 3.3 B) in comparison to 4% paraformaldehyde fixed cells (data not shown). The efficiency of RhoJ knock-down in stained cells was tested by western blotting with the RhoJ-specific monoclonal antibody (Abcam) (Fig. 3.3 D).

These experiments validate the specificity of the RhoJ monoclonal and polyclonal antibodies. In all further experiments the RhoJ monoclonal antibody from Abcam will be used for western blotting and the purified rabbit RhoJ polyclonal antibody will be used for immunofluorescent staining.

3.4. Localisation of endogenous RhoJ to FAs

In order to determine endogenous localisation of RhoJ in ECs, HUVECs were stained with the purified polyclonal RhoJ antisera. These initial experiments showed punctate, peripheral localisation of RhoJ reminiscent of FAs (Fig. 3.3 B), which are dynamic multiprotein complexes that via integrins connect the intracellular cytoskeleton with the ECM (Dubash, Menold et al. 2009).

To more precisely test this hypothesis, RhoJ co-localisation with FA markers was verified by immunofluorescence. This was done in HUVECs cultured on gelatin or Matrigel substrates. In standard HUVECs culturing conditions gelatin is used to facilitate the adhesion of cells to the plate. Matrigel, on the other hand, is a richer substrate for ECs as it contains collagen,

Fig. 3.4 RhoJ localises to focal adhesions, co-localising with vinculin, talin and pFAK in HUVECs cultured on gelatin-coated coverslips.
HUVECs were seeded on glass coverslips that were previously coated with gelatin. After 24 h cells were fixed with ice-cold methanol, blocked in BSA and co-stained with the indicated antibodies. DAPI was used to visualise nuclei. Regions marked in the white boxes are expanded in the bottom panel. RhoJ co-localised with vinculin (**A**), talin (**B**) and pFAK (**C**) as indicated with arrows. Scale bars: 10 μm.
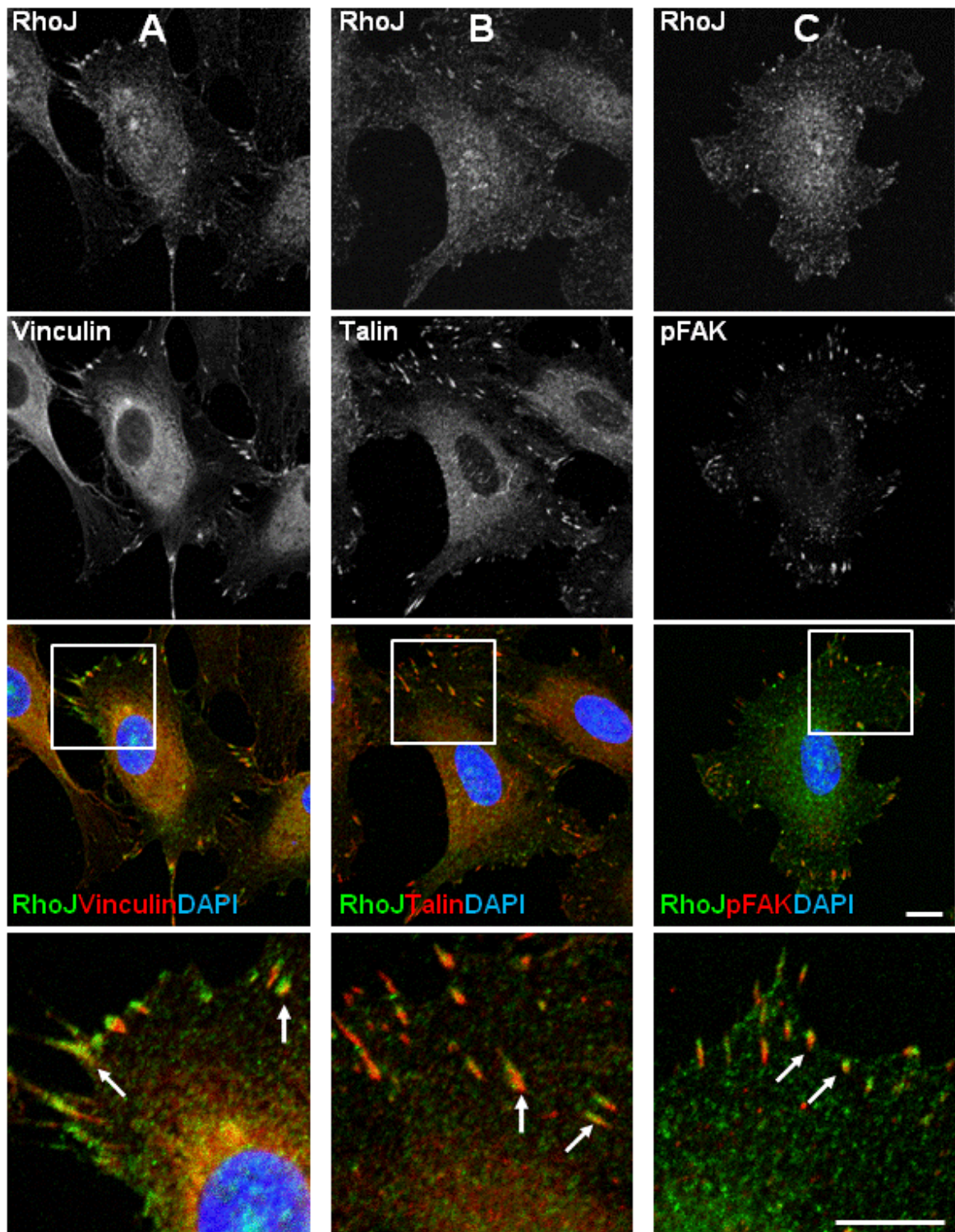
Fig. 3.5 RhoJ localises to focal adhesions, co-localising with vinculin, talin and pFAK in HUVECs cultured on Matrigel-coated coverslips.
HUVECs were seeded on glass coverslips that were previously coated with a thin layer of Matrigel. After 24 h cells were fixed with ice-cold methanol, blocked in BSA and co-stained with the indicated antibodies. DAPI was used to stain nuclei. Regions marked in the white boxes are expanded in the bottom panel. RhoJ co-localised with vinculin (**A**), talin (**B**) and pFAK (**C**) as indicated with arrows. Scale bars: 10 μm.
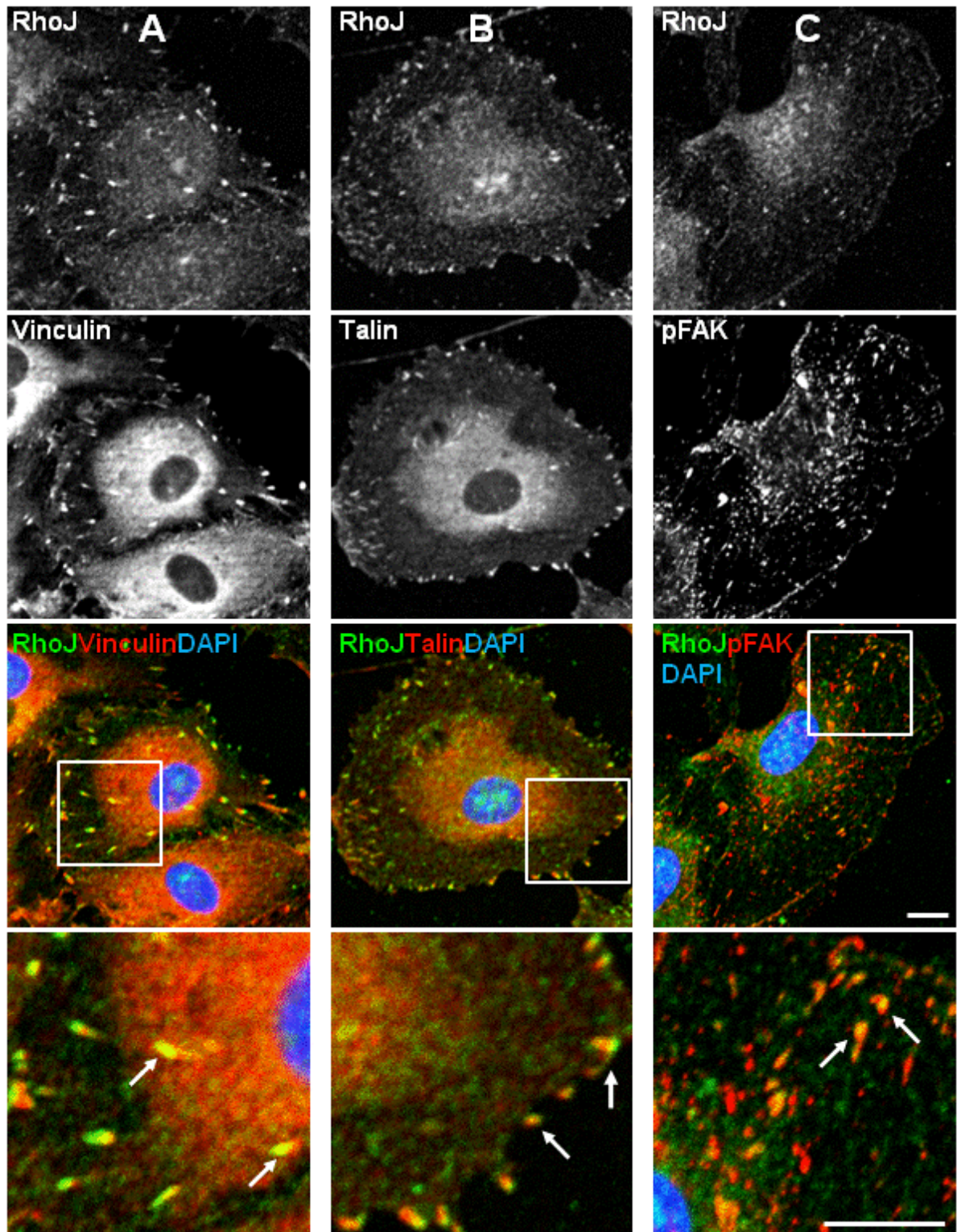
laminin, growth factors and other components such as these present in a basement membrane, which surrounds blood vessels, and this substrate induces tubule formation by ECs (Kubota, Kleinman et al. 1988; Passaniti, Taylor et al. 1992).

HUVECs plated on these substrates were co-stained with antibodies specific to RhoJ and to the FA proteins vinculin, talin and phosphorylated FAK (pFAK). RhoJ co-localised with all of these FA markers in cells cultured on both substrates (Fig. 3.4 and 3.5). Very often this co-localisation was adjacent but not completely overlapping. This suggests that RhoJ, although present in these same FAs, might localise in different regions of the FA. The presence of Matrigel did not increase the localisation of RhoJ to FAs.

3.5. Localisation of overexpressed RhoJ to vesicles and FAs

The localisation of endogenous RhoJ in HUVECs to FAs was contradictory to that reported in HeLa cells, where ectopically expressed myc-RhoJ was found in the early endosomal compartment (de Toledo et al. 2003). Therefore to verify the localisation of overexpressed RhoJ, HUVECs were transiently transfected with GFP-RhoJ and myc-RhoJ encoding plasmids. Cells were then fixed and stained with a myc-specific antibody (for myc-RhoJ expressing cells) and antibodies against the early/sorting endosomal markers EEA1 and Rab5, the recycling endosomal marker Rab11 and the lysosomal marker Lamp1. The expression efficiency was very low with only a few cells highly overexpressing tagged RhoJ. In these cells both GFP-RhoJ (Fig. 3.6) and myc-RhoJ (Fig. 3.7) clearly localised to the early/sorting endosomes positive for EEA1 but not for Rab5, there was localisation of a small amount of RhoJ to the Rab11 positive recycling endosomes. In addition RhoJ was clearly present in the lysosomes stained for Lamp1.

Fig. 3.6 Overexpressed GFP-RhoJ localises to endosomes and lysosomes in HUVECs.
HUVECs were cultured on gelatin-coated glass coverslips and 24 h later were transfected with GFP-RhoJ encoding plasmids using the TransPass D2 transfection reagent. 48 h later cells were fixed with PFA and immunofluorescent staining was performed with the indicated antibodies. DAPI was used to stain nuclei. Regions marked in the white boxes are expanded in the bottom panel. GFP-RhoJ clearly co-localised with the early/endosomal marker EEA1 (**A**) but not with the Rab5 (**B**). Some co-localisation was observed with the recycling endosomal marker Rab11 (**C**) and with the lysosomal marker Lamp1 (**D**). Scale bars: 10 μm.
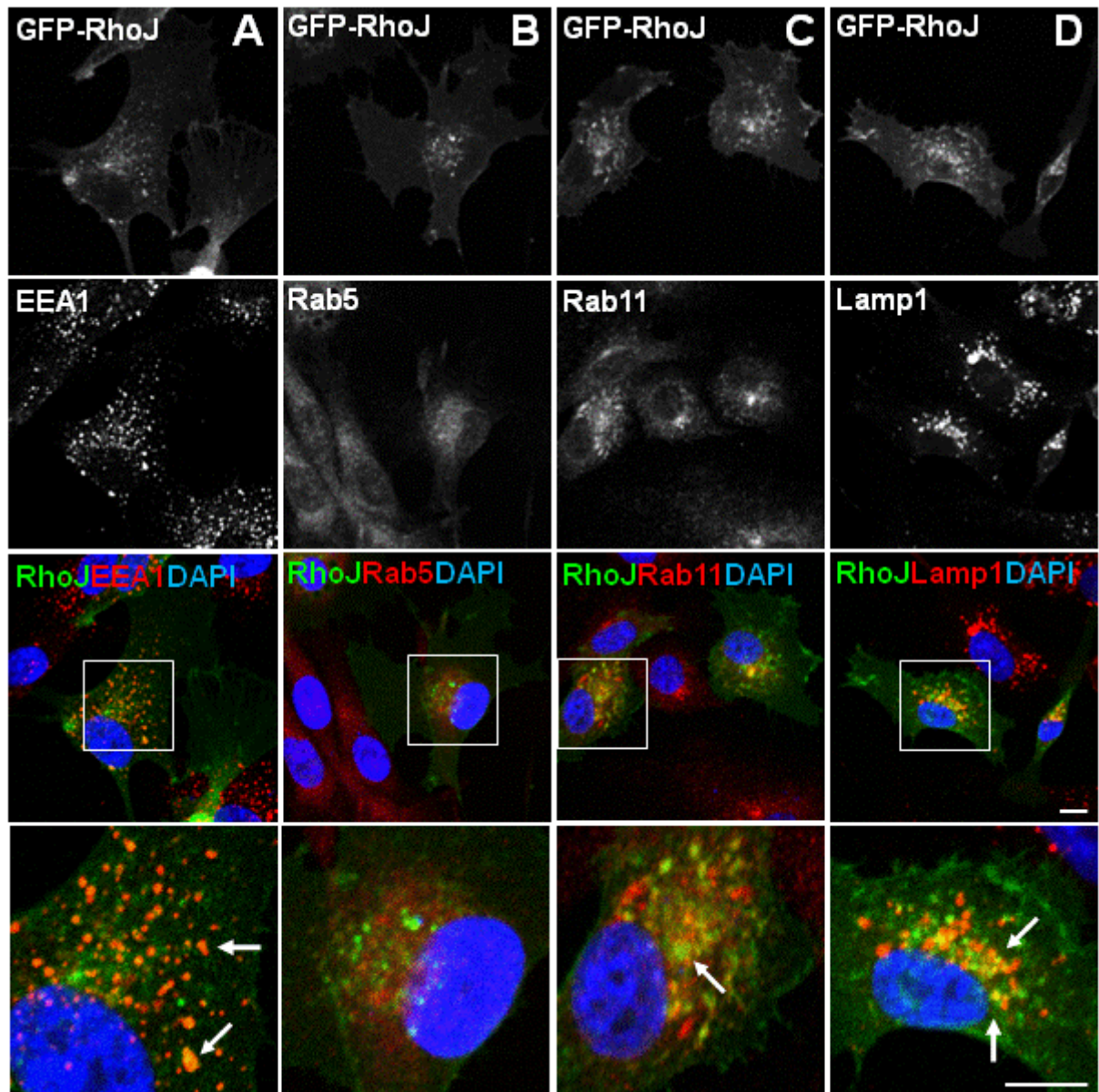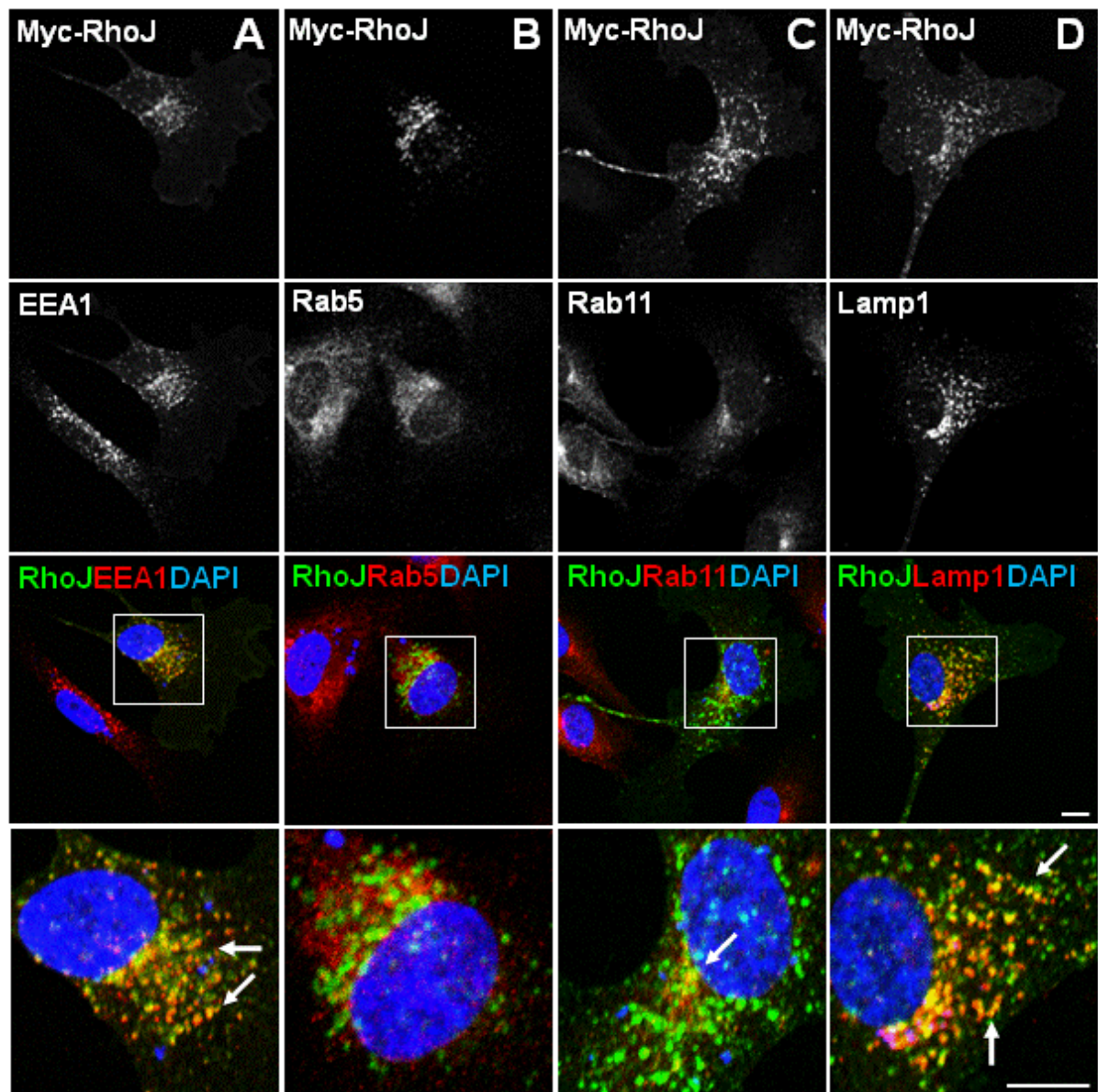
Fig. 3.7 Overexpressed myc-RhoJ localises to endosomes and lysosomes in HUVECs.
HUVECs were cultured on gelatin-coated glass coverslips and 24 h later were transfected with myc-RhoJ encoding plasmids using the TransPass D2 transfection reagent. 48 h later cells were fixed with PFA and immunostaining was performed with the indicated antibodies. DAPI was used to stain nuclei. Regions marked in the white boxes are expanded in the bottom panel. Myc-RhoJ clearly co-localised with the early/endosomal marker EEA1 (**A**) but not with the Rab5 (**B**). Some co-localisation was observed with the recycling endosomal marker Rab11 (**C**) and with the lysosomal marker Lamp1 (**D**). Scale bars: 10 µm.

However, this transient HUVECs transfection resulted in only a few cells expressing very high levels of tagged RhoJ. Thus an alternative approach was used to introduce tagged wild type and active mutant RhoJ into a higher proportion of cells. HUVECs were transduced with the lentivirus to express GFP-wtRhoJ (wild type RhoJ), GFP-daRhoJ (Q79L dominant active RhoJ mutant), GFP-dnRhoJ (T35N dominant negative RhoJ mutant) or GFP proteins. GFP-positive cells were then purified by flow cytometry.

The lentivirus infection efficiency reached approximately 90 % for GFP control cells and 40-60 % for GFP-wtRhoJ and GFP-daRhoJ expressing cells. No protein expression was observed in HUVECs infected with GFP-dnRhoJ lentivirus. It is possible that the dominant negative RhoJ mutant sequesters GEFs essential for other related Rho GTPases resulting in the down-regulation of many crucial signalling pathways and cell lethality. The expression of proteins in GFP-positive sorted cells was confirmed by western blotting (Fig. 3.8). Confocal microscopy showed that in these cells both GFP-wtRhoJ and GFP-daRhoJ localised to the plasma membrane in addition to FAs which positively stained for vinculin (marked by white arrows, Fig. 3.9). GFP-RhoJ was also observed in the intracellular vesicles (marked by yellow arrows, Fig. 3.9).

These results suggest that endogenous RhoJ localises mainly to FAs in HUVECs, and when overexpressed it also localises to intracellular vesicles.

3.6. Testing the role of dominant active RhoJ in endothelial cell motility

Studies performed by other members in our laboratory showed that silencing of RhoJ with siRNA significantly impaired EC migration, proliferation and tube formation. It was shown that this motility defect was accompanied by increased FA numbers and cell contractility
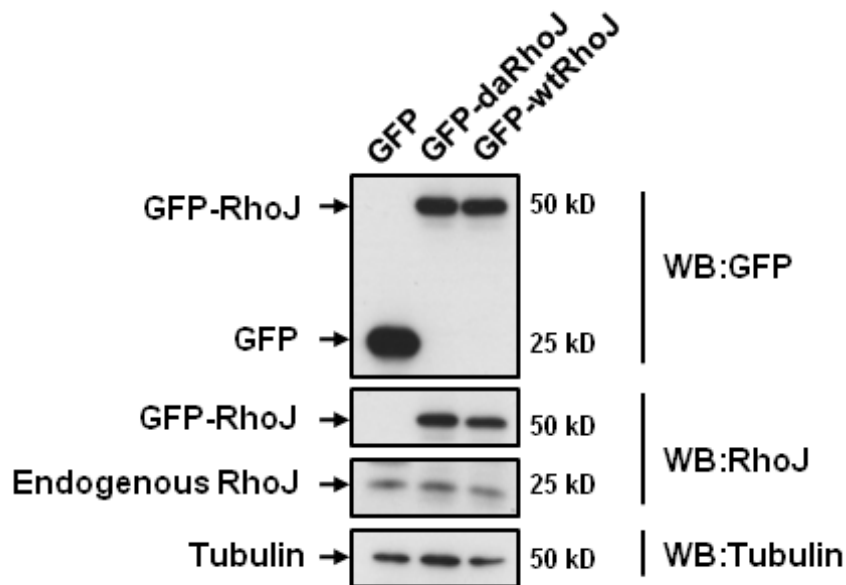
Fig. 3.8 Stable expression of GFP-wtRhoJ and GFP-daRhoJ in HUVECs.
HUVECs were infected with lentivirus to express GFP, GFP-wtRhoJ or GFP-daRhoJ proteins. GFP-positive cells were sorted using flow cytometry. Subsequently lysates were prepared from the same number of cells for each infection. Western blotting was performed with GFP, RhoJ and tubulin-specific antibodies as indicated.
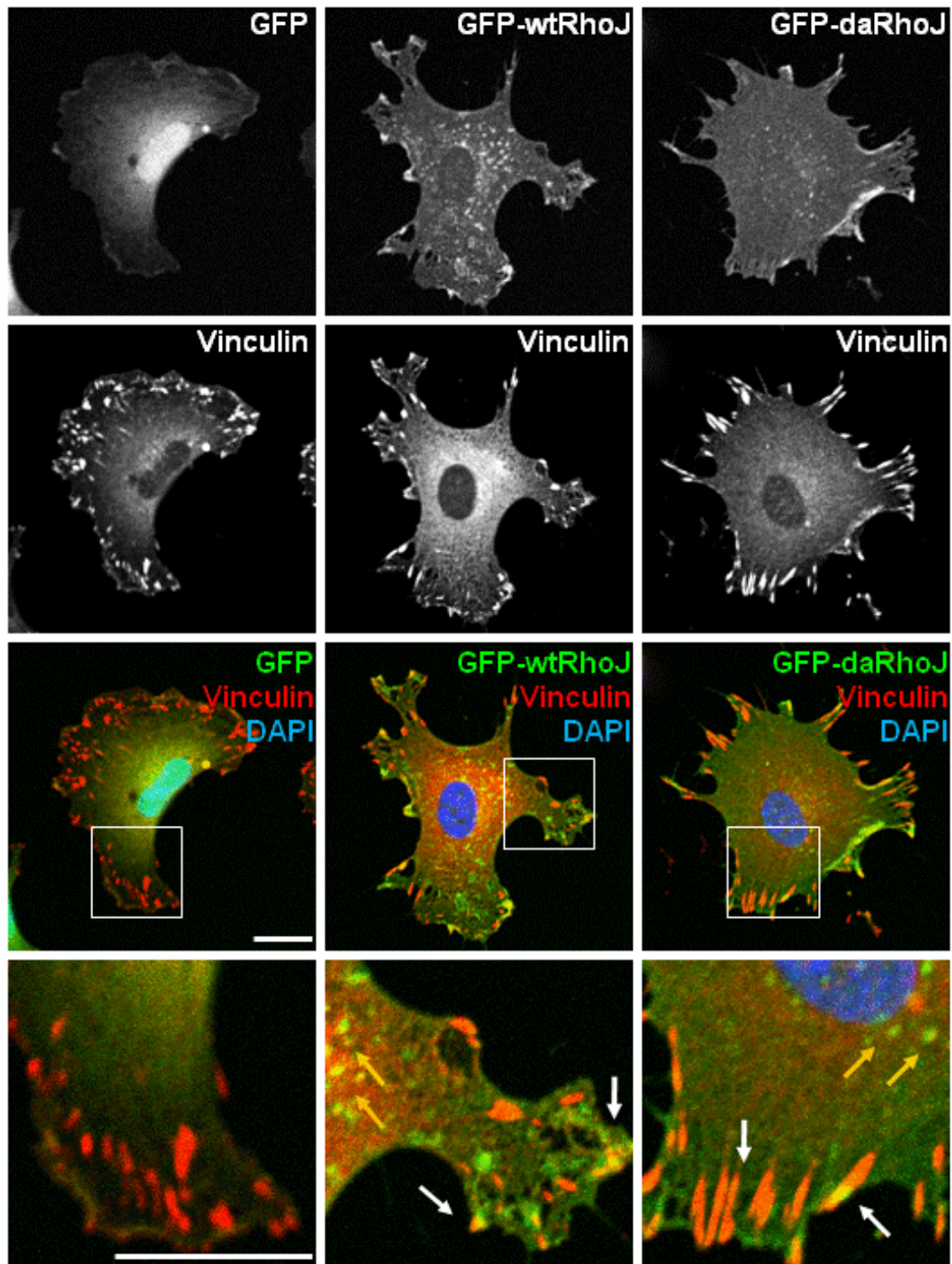
Fig. 3.9 Lentivirally transduced GFP-RhoJ localises to vesicles and focal adhesions in HUVECs. HUVECs were transduced with lentivirus to stably express GFP, GFP-wtRhoJ or GFP-daRhoJ, and were sorted for GFP-positive cells using flow cytometry. Cells were then cultured on gelatin-coated coverslips and immunofluorescent staining was performed with the vinculin-specific antibody. DAPI was used to visualise nuclei. Regions marked in the white boxes are expanded in the bottom panel. Both GFP-wtRhoJ and GFP-daRhoJ localised to the membrane, focal adhesions (white arrows) and intracellular vesicles (yellow arrows). Scale bars: 10 µm.

(Kaur, Leszczynska et al. 2011). Since RhoJ function had only been probed by determining the effect of silencing RhoJ, it was important to establish the effect of expressing a dominant active mutant form of RhoJ in various cell motility and tube formation assays. In order to do this, HUVECs were transduced with lentivirus to stably express GFP or GFP-daRhoJ, and GFP-positive cells were sorted by flow cytometry. These cells were expanded by passaging and tested in various assays described in the subsequent sections. The expression of GFP and GFP-daRhoJ in the flow cytometry-sorted HUVECs was confirmed by western blotting (Fig. 3.8). It was determined that these cells were expressing approximately 15-20 times more GFP-daRhoJ than endogenous RhoJ.

3.6.1. Dominant active RhoJ promotes endothelial cell tube branching

It was noticed that all HUVECs donors stably expressing GFP-daRhoJ had a different morphology from GFP-expressing cells when cultured in standard gelatin-coated petri dishes. Unlike the GFP control cells, HUVECs with GFP-daRhoJ very often had an arched elongated shape with numerous protrusions (indicated by arrows in Fig. 3.10 A).

In order to verify the potential role of active RhoJ in the tubule formation, these cells were used in an organotypic angiogenesis assay. This was performed in collaboration with Margherita Scarcia and Sabu Abraham in Dr Georgia Mavria's Laboratory (Leeds Institute of Molecular Medicine, St James's University Hospital, Leeds, UK; permission given to present the data). In this assay they seeded HUVECs on a monolayer of human dermal fibroblasts, which produce ECM and secrete VEGF. These conditions and exogenously added FGF-2 stimulate ECs to form tubules with lumens that are highly reminiscent of the *in vivo* microvasculature (Bishop, Bell et al. 1999; Donovan, Brown et al. 2001). After 5 days of co-culture assay cells were stained with the CD31-specific antibody to visualise HUVECs (Fig. 3.10 B). More tubules were formed by GFP-daRhoJ-expressing HUVECs in comparison to
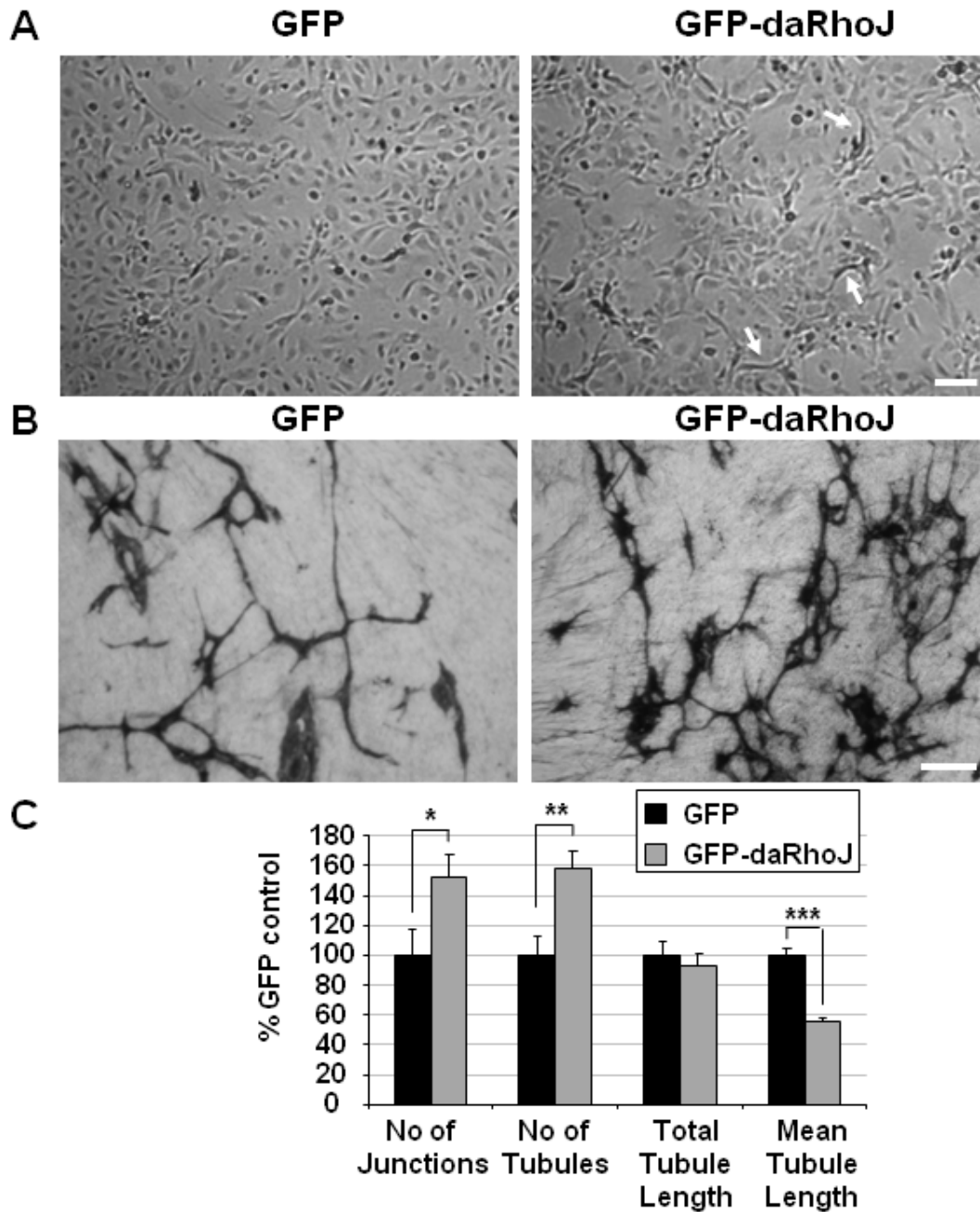
Fig. 3.10 Dominant active RhoJ changes HUVECs morphology and promotes endothelial tube branching.
HUVECs were transduced with lentivirus to express either GFP or GFP-daRhoJ and were sorted for GFP-positive cells by flow cytometry. **A**, The GFP-daRhoJ expressing HUVECs had a distinct morphology with arched elongated protrusive shapes (indicated with arrows) as compared to GFP control cells. **B**, GFP and GFP-daRhoJ cells were used by Margherita Scarcia and Sabu Abraham in co-culture assay with human dermal fibroblasts (permission given to re-print the data). After 5 days of co-culture endothelial tubules were visualised by staining with CD31-specific antibody. Numbers of junctions, tubules, total and mean tubule lengths were quantified using the Angiosys software (**C**). Statistically significant differences between GFP and GFP-daRhoJ containing tubes were determined with the Mann Whitney test (*** for $p < 0.001$; ** for $0.001 < p < 0.01$ and * for $0.01 < p < 0.05$.) All scale bars: 100 µm.

GFP-expressing cells. In addition, GFP-daRhoJ-containig tubes were shorter and had more branches (Fig. 3.10C). This result supports the hypothesis that active RhoJ may play a role in promoting tubule formation.

3.6.2. Dominant active RhoJ increases cell migration

In order to test the role of RhoJ in cell migration, a scratch wound assay was performed. Monolayers of HUVECs expressing either GFP or GFP-daRhoJ were scratched with a pipette tip and then incubated in complete HUVEC medium to allow the wound closure. During this incubation mitomycin C was added, which inhibits cell proliferation. Therefore in such conditions wound closure rates are affected by cell motility alone. It was found that HUVECs expressing GFP-daRhoJ migrated faster to close the wound in comparison to GFP control cells (Fig. 3.11). Combining data from three different HUVECs isolates did not give a statistically significant increase in the speed of wound closure by GFP-daRhoJ expressing cells compared to the GFP control cells. However GFP-daRhoJ expressing cells migrated consistently faster than GFP expressing cells in at least 3 different HUVECs isolates. The presence of a dominant active form of RhoJ induced an opposite phenotype to that seen in cells where RhoJ was silenced with siRNA (Kaur, Leszczynska et al. 2011). Both data indicate that RhoJ plays important role in the regulation of EC migration.

3.6.3. Dominant active RhoJ decreases the numbers of FAs and SFs in migrating cells

Experiments performed by Sukhbir Kaur in our laboratory showed that RhoJ-siRNA silencing caused an increase in the number of FAs and SFs (Kaur, Leszczynska et al. 2011). This was observed in sparsely plated cells or in cells that were at the edge of a migrating monolayer but not in cells that were within a monolayer. This suggested that RhoJ was affecting FAs and
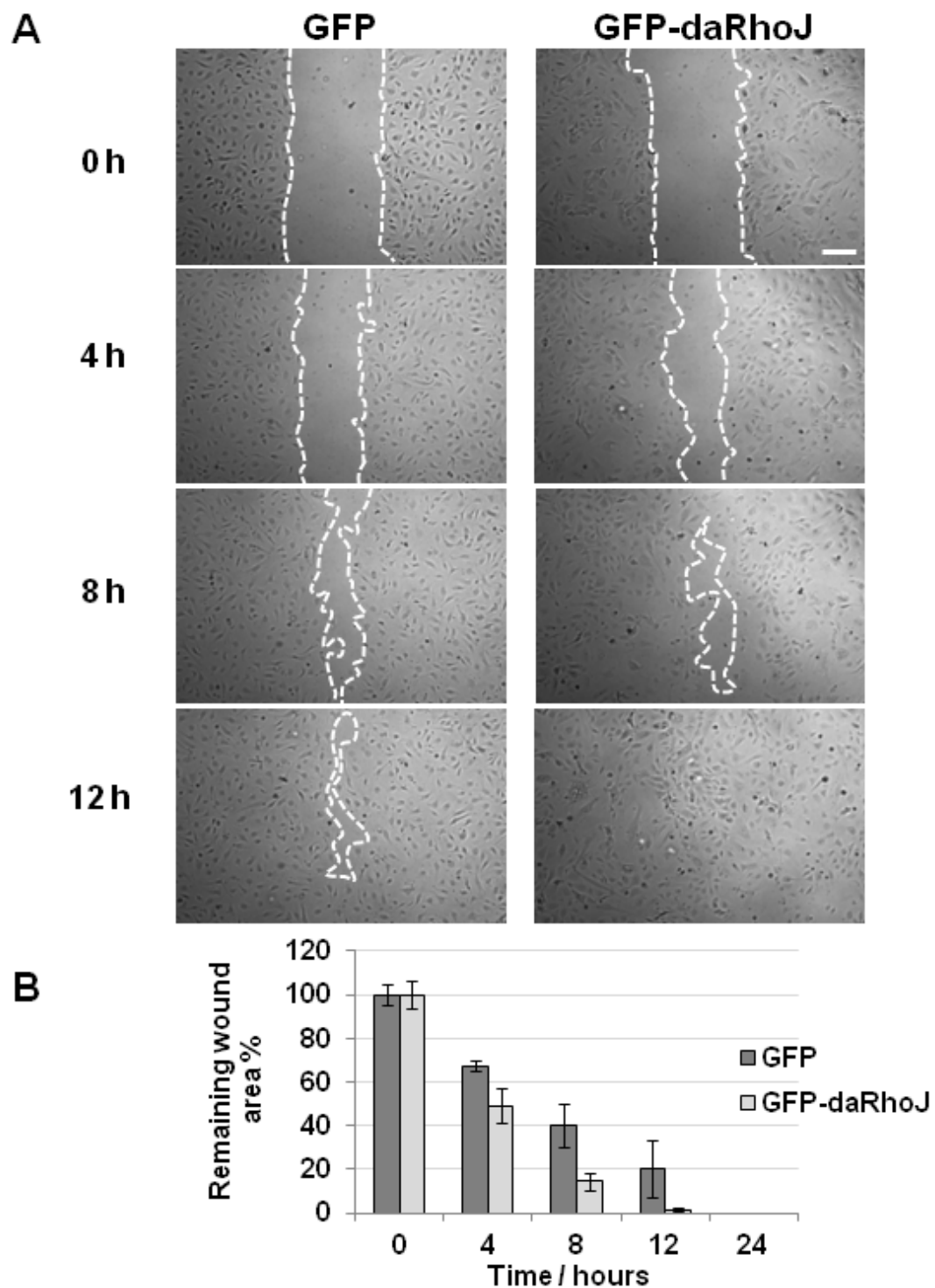
Fig. 3.11 Dominant active RhoJ promotes HUVECs migration in the scratch wound assay.
HUVECs were transduced with lentivirus to express either GFP or GFP-daRhoJ and were sorted for GFP-positive cells by flow cytometry. Cells were then grown to a monolayer, scratched with a pipette tip and the wound closure was monitored (**A**). The scale bar: 200 μm. **B**, Graph showing the quantitation of remaining wound area for different time points. The means from 3 different experiments and standard errors are plotted. Although the difference in the speed of a wound closure between the GFP and GFP-daRhoJ expressing cells is not statistically significant, accelerated wound closure as a result of GFP-daRhoJ expression was observed in 3 different HUVEC isolates.
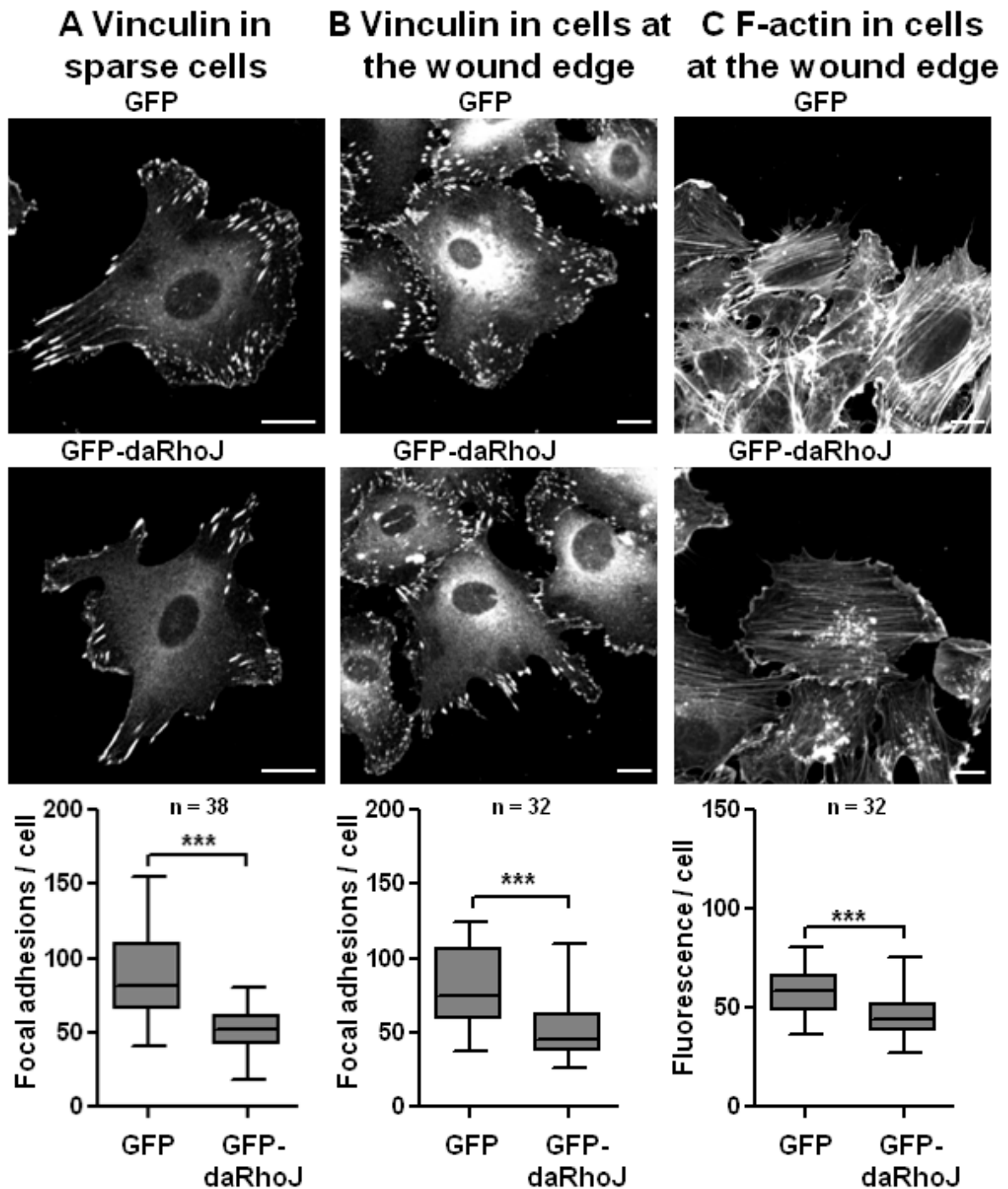
Fig. 3.12 Dominant active RhoJ decreases the numbers of focal adhesions and stress fibres in migrating endothelial cells.
HUVECs were transduced with lentivirus to express either GFP or GFP-daRhoJ and were sorted for GFP-positive cells by FACS. **A,** These were sparsely plated and 4 h later fixed and stained with vinculin-specific antibody. **B** and **C**, Monolayers of HUVECs expressing either GFP or GFP-daRhoJ were scratched with a pipette tip and cells were allowed to migrate. 2-3 h later cells were fixed and stained with vinculin-specific antibody (**B**) or with phalloidin (**C**). Focal adhesions were counted and actin fluorescence measured per cell in at least 32 cells from 3 experiments. The graphs show box and whisker plots indicating the maximum, minimum, 25th and 75th percentiles and median values (*** for $p < 0.001$, a Mann-Whitney test used). Scale bars: 20 µm.

SFs particularly in motile cells. Therefore the effect of dominant active RhoJ was tested in these same assays. Firstly, in sparsely plated HUVECs, GFP-daRhoJ significantly decreased the number of FAs (Fig. 3.12 A). SFs, stained for F-actin, were also decreased, but only in two HUVEC isolates out of three isolates tested (data not shown). Secondly, GFP-daRhoJ expressing cells, which were at the wound edge of a migrating monolayer, had decreased numbers of FAs (Fig. 3.12 B) and SFs (Fig. 3.12 C) in comparison to GFP-expressing cells. A difference in the FA numbers was not observed in HUVECs that were within a monolayer. In addition, there were no consistent differences in the intensity of the SF staining between different HUVECs isolates transduced with GFP or GFP-daRhoJ which were situated within a monolayer.

It was concluded that active RhoJ significantly reduced FAs and SFs in the migrating cells. This result, together with effect of silencing of RhoJ, suggests that this small Rho GTPase plays a crucial role in cell motility via the regulation of FA turnover and cell contractility.

3.7. The role of RhoJ in an endocytosis of transferrin receptor in endothelial cells

Previous studies indicated that ectopically expressed RhoJ localised to endosomes and played a role in an early endocytosis in HeLa cells, whereas silencing of RhoJ caused a delay in recycling of Tf receptor (de Toledo, Senic-Matuglia et al. 2003). We compared the levels of endogenous RhoJ proteins in HeLa cells and HUVECs and we were not able to detect it in HeLa cell lysates (Fig. 3.13 A). However other isolates of HeLa might express RhoJ. Since, we also showed that overexpressed RhoJ localised to intracellular vesicles including endosomes and lysosomes in HUVECs (Fig. 3.6, 3.7 and 3.9), it was important to test the
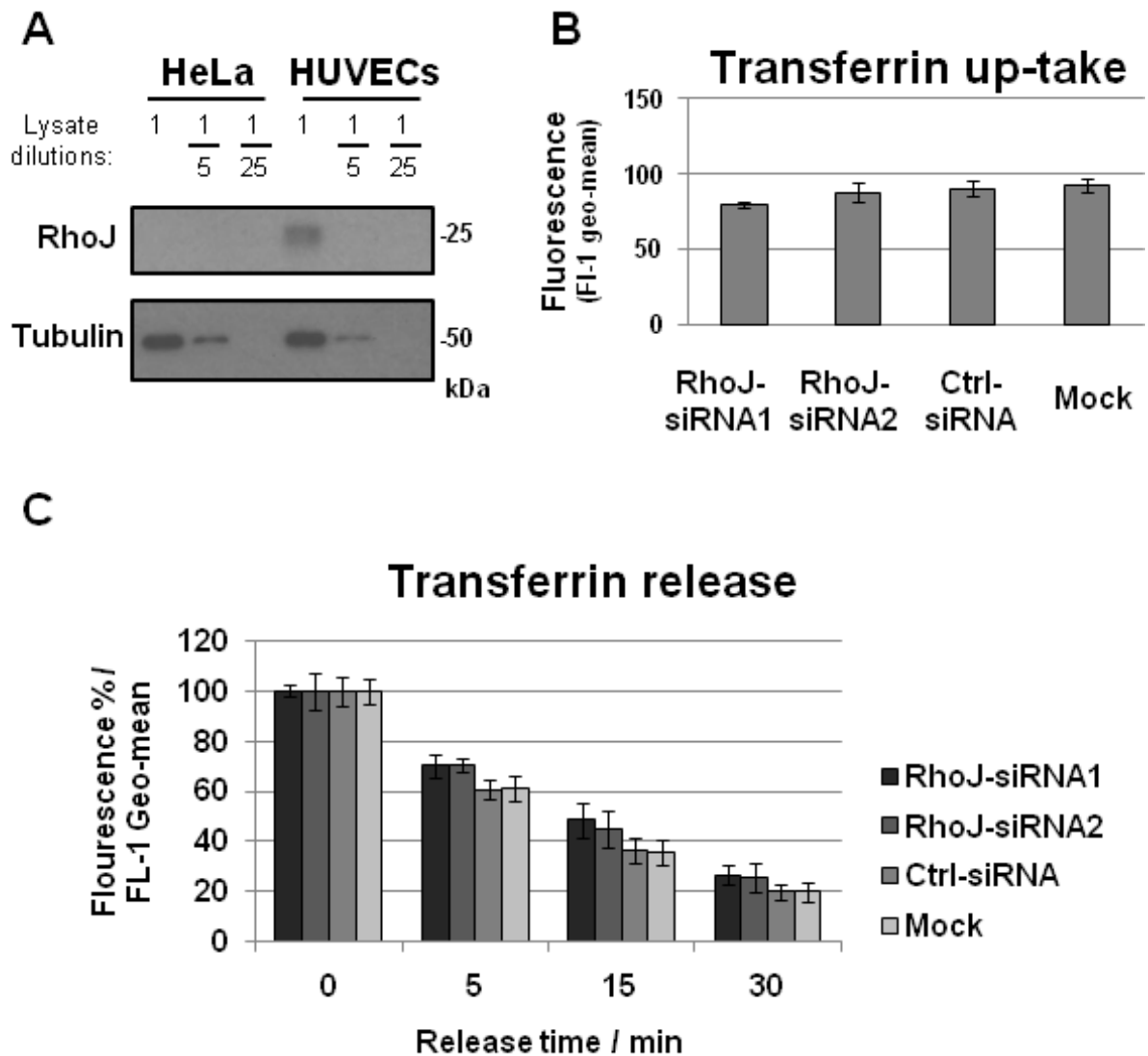
Fig. 3.13 RhoJ siRNA silencing delays Tf release in HUVECs.
A, Western blotting showing comparison of the RhoJ protein levels in HUVECs and HeLa lysates. **B** and **C**, HUVECs were transfected with 10 nM RhoJ-siRNA1, RhoJ-siRNA2 and Ctrl-siRNA duplexes or were mock transfected. 48 h later cells were depleted of endogenous Tf by serum starvation for 1 h and then were incubated with 5 µg/ml of Alexa 488-conjugated Tf for another hour (**B**). Cells were then washed and incubated with 50 µg/ml of un-labelled Tf for the indicated time periods (**C**). The plots represent the geometric mean fluorescence of the cells (analysed by FACS) which gives an indication of the Tf uptake (**B**), or that remaining in the cells (**C**). The 0 time point in **C** shows the mean cell fluorescence of the cells prior to incubation with unlabelled Tf. This was considered to be 100 % and subsequent time points are plotted as a percentage. Although not statistically significant, RhoJ siRNA silencing caused a slight but reproducible delay in the Tf release in 3 different HUVEC isolates.

effect of RhoJ silencing on the uptake and recycling of the Tf receptor in ECs, which express RhoJ abundantly. In order to measure an uptake of Tf, HUVECs with siRNA-silenced RhoJ as well as control cells were loaded with a fluorescently labelled Tf and then analysed by flow cytometry. Similarly to the study on HeLa cells (de Toledo, Senic-Matuglia et al. 2003), RhoJ knock-down did not affect the levels of Tf taken up in HUVECs (Fig. 3.13 B).

In the next step Tf release was measured. Medium with a fluorescently labelled Tf was removed from the cells and fresh media with an excess of un-labelled Tf was added. Cells were then incubated for different time periods and FACS analysis was performed to measure the amount of fluorescent Tf remaining in these cells. It was found that RhoJ silencing caused a slight but reproducible delay in the Tf release (Fig. 3.13 C). Although a statistically significant difference was not observed between RhoJ-knocked-down or RhoJ-expressing cells, the trend in the delay of Tf release caused by RhoJ knock-down was consistent for 3 different HUVEC isolates.

3.8. Testing an influence of RhoJ knock-down on the surface levels of VEGFR2 in HUVECs

VEGFR2 is a major receptor that responds to VEGFA, a very potent mediator of angiogenesis (Gerhardt, Golding et al. 2003; Olsson, Dimberg et al. 2006). VEGFR2 traffics between the plasma membrane, endosomes and degradative cellular compartments, and this is regulated by the presence of VEGFA ligand (Ewan, Jopling et al. 2006; Gampel, Moss et al. 2006). Since RhoJ loss had only a slight effect on the Tf release in HUVECs it was important to examine whether it plays a role in the trafficking of VEGFR2. This was tested by looking at VEGFR2 surface levels in the RhoJ siRNA-silenced cells.
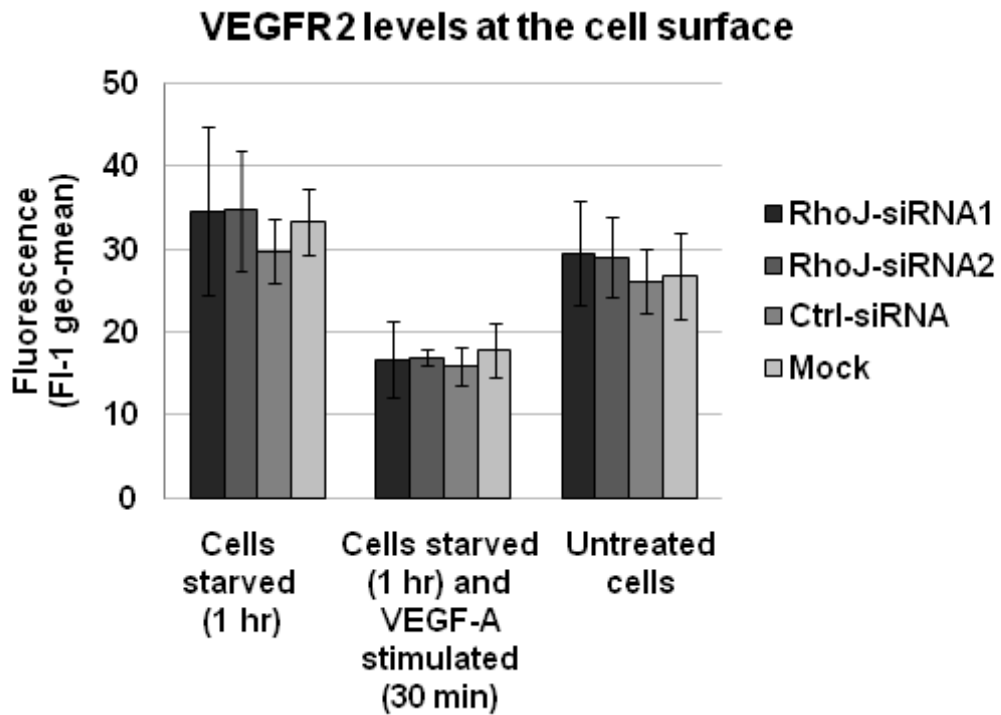
Fig. 3.14 RhoJ siRNA silencing does not affect the VEGFR2 surface distribution in HUVECs.
Cells were transfected with 25 nM RhoJ-siRNA1, RhoJ-siRNA2 and Ctrl-siRNA duplexes or were mock transfected. 48 h later HUVECs were serum starved and then VEGF-A (10 ng/ml) stimulated. One group of cells was not starved but was left untreated in complete medium, as indicated. Cells were then harvested with non-enzymatic dissociation solution and fixed with PFA. Since they were not permeabilised the immunofluorescent staining with VEGFR2-specific antibody detected only VEGFR2 present on the cell surface. FACS analysis showed that RhoJ siRNA silencing did not affect surface levels of VEGFR2. The graph shows the means and standard errors for combined 3 experiments.

HUVECs with RhoJ knock-down were tested for the presence of VEGFR2 at a cell surface by immunofluorescent staining with VEGFR2-specific antibody. This was done in cells that were fixed with PFA but not permeabilised with any detergent to prevent staining of intracellular VEGFR2. Since receptor trafficking is regulated by the availability of VEGA, cells treated in three different conditions were tested: starved cells, VEGF stimulated cells or cells left in complete HUVEC medium. FACS analyses did not reveal any significant differences in VEGFR2 levels between RhoJ-silenced and control cells under any of these conditions (Fig. 3.14). These studies did not include thorough analysis of co-localisation of VEGFR2 with particular endosomal markers in the presence or absence of RhoJ. Nonetheless it was concluded that RhoJ was not important in regulating the surface levels of VEGFR2.

3.9. Discussion

ECs are critical for the formation of new blood vessels, a process known as angiogenesis (Carmeliet 2003). Our group has shown that RhoJ, a small Rho GTPase, is expressed predominantly in ECs where it plays a critical role in many processes important during angiogenesis. These include the regulation of EC migration, tube formation, FA numbers and actomyosin contractility (Kaur, Leszczynska et al. 2011). All these findings were based on the observations of the effects of RhoJ siRNA silencing in HUVECs. Work described in this chapter was first to show the intracellular localisation of endogenous RhoJ in ECs. Overexpression of dominant active RhoJ promoted endothelial tube formation and migration, the converse to that seen with RhoJ knock-down, and thus reinforcing our conclusions about the role of RhoJ in endothelial motility and tubulogenesis. Additionally, the potential role of RhoJ in endocytosis in ECs was investigated.

The first group that characterised RhoJ (Vignal, De Toledo et al. 2000) showed in subsequent studies that ectopically expressed tagged RhoJ was present on the plasma membrane and

EE/ES in HeLa cells (de Toledo, Senic-Matuglia et al. 2003). Nonetheless, none of the published data so far have indicated the localisation of endogenous RhoJ. Thus knowing that this protein is abundantly expressed in ECs it was important to determine its intracellular localisation in these cells, as this would enable a better understanding of its function. Polyclonal RhoJ antibodies were made in rabbits, purified and validated for immunofluorescence. Using these antibodies, it was established that endogenous RhoJ localised to FAs in ECs as shown by co-localisation with vinculin, pFAK and talin. Since FAs play a critical role in the regulation of cell motility (Dubash, Menold et al. 2009; Parsons, Horwitz et al. 2010), this finding was consistent with the role our group have discovered for RhoJ in EC motility. In addition, when the localisation of overexpressed myc- and GFP-tagged RhoJ in ECs was tested, it was found that transient and high overexpression of tagged RhoJ in ECs drove its localisation not only to endosomes, as seen by de Toledo *et al.* in HeLa cells (de Toledo, Senic-Matuglia et al. 2003), but also to lysosomes. However, in ECs transduced with lentivirus to moderately and stably express GFP-tagged RhoJ (both wild type and dominant active mutant forms), its localisation was observed in intracellular vesicles as well as in FAs.

Previously, our laboratory showed that silencing of RhoJ with siRNA in HUVECs impaired cell motility and tubule formation and this was accompanied by an increase in the number of FAs and SFs in migrating cells (Kaur, Leszczynska et al. 2011). During migration cells polarise and extend protrusions such as spike-like filopodia and sheet-like lamellipodia towards the pro-migratory factors. These protrusions are built on the actin cytoskeleton and stabilised by nascent FAs, which connect the actin filaments with the ECM. Attached to the underlying surface, cells use the actomyosin contractility to move forwards and subsequently FAs at the rear are disassembled. Thus a constant turnover of FAs and actomyosin

cytoskeleton is very important in cell migration (Raftopoulou and Hall 2004; Parsons, Horwitz et al. 2010). Importantly, RhoJ knock-down increased the numbers of FAs and SFs only in sparsely plated cells or in these present at the edge of a migrating monolayer, but not within a monolayer. Thus this suggested that RhoJ played a role in highly motile cells, while in cells within a monolayer cell-cell contacts might have induced signalling pathways that compensated for the loss of RhoJ. To more thoroughly test the function of RhoJ in ECs, a constitutively active RhoJ mutant was used. As expected, active RhoJ increased the EC migration in a scratch wound assay. Its role was also profound in the formation of tubes by ECs, as observed by excessive sprouting by these cells. Finally, active RhoJ decreased the number of FAs and SFs in the migrating cells. Together, the effects of RhoJ knock-down and overexpression of its active form led to the conclusion that RhoJ is a critical player in the regulation of EC motility, as it controls the turnover of FAs and SFs in migrating cells.

Other Rho GTPases such as RhoA, Rac1 and Cdc42 are known to drive the formation of FAs and rearrange the cytoskeleton: Cdc42 induces peripheral focal complexes associated with filopodia, Rac1 drives formation of focal complexes in lamellipodia, and RhoA induces SF-associated FAs (Nobes and Hall 1995). RhoJ knock-down did not affect the expression levels of these Rho GTPases, which are also present in HUVECs (Fig. 3.2 C). Since RhoJ is expressed predominantly in ECs and its knock-down phenotype is not rescued by the presence of other Rho GTPases such as RhoA, Rac1 and Cdc42, it was concluded that RhoJ plays a distinct role in ECs.

De Toledo and colleagues demonstrated that ectopically expressed myc-RhoJ localised to EE/ES where it played a role in the early endocytosis of Tf receptor in HeLa cells (de Toledo, Senic-Matuglia et al. 2003). Work described in this chapter also showed that in ECs overexpressed RhoJ was partially localising to endosomes and other intracellular vesicles.

Therefore, it was important to examine the role of RhoJ in endocytosis of ECs and this was initially tested by investigating the trafficking of Tf. Whereas no difference was observed in the Tf uptake, the RhoJ knock-down caused a slight delay in the Tf release and this was consistent with the previous observation by de Toledo *et al.* (2003).

The major role of Tf is delivering iron ions to the cells and this process takes place in various tissues (Macedo and de Sousa 2008). Since RhoJ knock-down only slightly affected this endocytosis pathway common to many cell types, it was hypothesised that RhoJ may regulate trafficking of molecules which are more specific to ECs. VEGFR2, a key receptor in ECs which responds to the pro-migratory and pro-angiogenic factor, VEGF, is constantly endocytosed and recycled to the plasma membrane, and this is regulated via stimulation by its ligand (Ewan, Jopling et al. 2006; Gampel, Moss et al. 2006; Gerhardt 2008). Thus the role of RhoJ in distribution of this receptor to the plasma membrane was investigated but no change was observed in RhoJ-knocked-down ECs. Additionally, a single experiment was performed to investigate the endocytosis via scavenger receptors in HUVECs. This was done by measuring the uptake of acetylated low-density-lipoprotein fluorescently labelled with 1,1'-dioctadecyl-3,3,3'3'-tetramethyl-indocarbocyanine perchlorate (DiI-Ac-LDL). The uptake of this chemically modified lipoprotein is specific to ECs end macrophages and is mediated by the family of scavenger receptors (Voyta, Via et al. 1984; Adachi and Tsujimoto 2006). Again, RhoJ-siRNA silenced cells were able to normally uptake the DiI-Ac-LDL as analysed by FACS or fluorescent microscopy (data not shown). Given that RhoJ did not play a role in the VEGFR2 trafficking or uptake of DiI-Ac-LDL and the role of RhoJ in Tf recycling was not major, other endocytosis pathways would need to be investigated to explore the role of RhoJ present in the intracellular vesicles. Existing evidence shows that during FA turnover some components of FAs such as paxillin are endocytosed and then recycled to the new focal

complexes (Di Cesare, Paris et al. 2000; Matafora, Paris et al. 2001; Rosenberger and Kutsche 2006). Since it was shown here that active RhoJ decreased the number of FAs, it is possible that it might regulate the endocytosis of their components. However, future studies would be required to test this hypothesis.

In conclusion, work presented in this chapter was first to show the localisation of endogenous RhoJ to FAs. Overexpression of a dominant active RhoJ mutant in ECs showed that RhoJ promotes EC migration, tubulogenesis and decreases the numbers of FAs and SFs in migrating cells. This supported previous findings by Sukhbir Kaur where RhoJ knock-down caused opposite effects. Combining these data, the evidence suggests that RhoJ plays a critical role in EC biology as it regulates EC migration, tubulogenesis, FA turnover and actomyosin contractility, and therefore it might be an important player in angiogenesis.

4. IDENTIFICATION OF RHOJ BINDING PARTNERS

IN ENDOTHELIAL CELLS

4.1. RhoJ binding partners

RhoJ belongs to the Cdc42-like subfamily of Rho GTPases as structurally it is most similar to TC10 and Cdc42. Vignal *et al.* showed that active RhoJ, like active TC10 and Cdc42, interacts with the CRIB domain present in PAK and WASP; this was demonstrated by both GST-CRIB pull-down and Y2H assays (Vignal, De Toledo et al. 2000). This was also subsequently observed by Aspenstrom *et al.* who additionally demonstrated a weak interaction of active RhoJ with rhotekin (Aspenstrom, Fransson et al. 2004). This group also performed a Y2H study in which they tested interactions of the dominant active RhoJ mutant with known Cdc42 effectors; positive interactions were found for WASP, N-WASP, Cdc42-interacting protein 4 (CIP4), partitioning defective 6 (Par6), p50RhoGAP, PAK1B and PAK4 (Aspenstrom, Fransson et al. 2004). However, no further studies have been published that show the physiological relevance of these interactions in mammalian cells.

Chiang *et al.* identified and characterised TC10β and TC10βLong, which are the mouse orthologs of RhoJ. They found that TC10β when transfected into murine 3T3L1 adipocytes localised to lipid rafts and was activated by insulin stimulation, this was dependent on Cbl/CAP (Chiang, Hou et al. 2002). Cbl/CAP is a complex which regulates the glucose uptake by mobilisation of the glucose transporter GLUT4 from the intracellular storage sites to the cell surface. Upon insulin stimulation the Cbl/CAP complex becomes phosphorylated by the insulin receptor. Then Cbl/CAP translocates to lipid rafts via interaction with flotillin, and recruits CrkII along with C3G. C3G is a guanine nucleotide exchange factor that has been shown to activate human TC10 (Chiang, Baumann et al. 2001). The activation of TC10β by insulin was inhibited by a dominant negative mutant of CAP which does not localise to the lipid rafts, thus it was possible that TC10β activation was mediated by the C3G GEF recruited to lipid rafts by the Cbl/CAP/CrkII complex (Chiang, Hou et al. 2002).

Since it was established that RhoJ is expressed in ECs (Herbert, Stekel et al. 2008; Kaur, Leszczynska et al. 2011), one of the main aims of these PhD studies was to determine the binding partners of RhoJ in these cells. It was anticipated that the most likely candidates would be found among proteins containing a CRIB domain. Some of the known effectors of Cdc42 which contain the CRIB motif and were shown to play a role in ECs, include PAK, myotonic dystrophy kinase-related Cdc42-binding kinase (MRCK), WASP and N-WASP (Groeger and Nobes 2007; Galan Moya, Le Guelte et al. 2009; Sheldon, Andre et al. 2009; Kang, Wang et al. 2010). These proteins regulate processes such as cytoskeletal rearrangements, actin polymerisation, actomyosin contractility, FA dynamics (Bishop and Hall 2000). FAs are multiprotein dynamic complexes, which connect the intracellular cytoskeleton with the ECM. Their constant turnover along with protrusion and retraction of the actomyosin filaments are important in the cell migration (Parsons, Horwitz et al. 2010). RhoJ is likely to interact with the components of FAs as work described in the previous chapter established that RhoJ localises to FAs and when activated it decreases the number of FAs, SFs and promotes EC migration.

The PIX and GIT proteins form a complex which localises to FAs via the C-terminal domain of GIT1, which binds to paxillin (Bagrodia, Bailey et al. 1999; Turner, Brown et al. 1999). The interaction of GIT1 with paxillin was shown to promote FA disassembly and cell migration (Zhao, Manser et al. 2000; Feng, Baird et al. 2010). Moreover, PIX and GIT have multiple domains and can serve as scaffolds which interact with and bring together a number of proteins including PAK, Cdc42, Rac1, paxillin, pFAK (Frank and Hansen 2008). PIX serves as a GEF for Cdc42 and Rac1, and concomitantly it binds to their effector – PAK, which was shown to promote FA disassembly (Manser, Huang et al. 1997; Bagrodia, Taylor et al. 1998; Manser, Loo et al. 1998).

The aim of the work described in this chapter was to identify the proteins that interact with RhoJ in ECs, and thus help to elucidate the mechanism through which RhoJ functions. RhoJ-binding candidates were pulled-down from cellular lysates using GST-RhoJ fusion proteins and identified by mass spectrometry. The most interesting candidates such as those involved in cell migration, FA turnover, potential GAPs, GEFs or CRIB domain containing proteins were shortlisted and their interactions with RhoJ were tested in a Y2H assay. This experiment revealed that RhoJ interacted directly with GIT1 and MRCKA. Thus further studies focused on examining the interaction of RhoJ with the GIT1/βPIX complex in ECs. Firstly, immunofluorescence was used to verify the co-localisation of RhoJ with this complex. Secondly, the single components of the hypothetical βPIX/GIT1/RhoJ complex were knocked-down to test how their loss would affect the localisation of these proteins to FAs.

4.2. Pull-down of RhoJ binding partners and their identification by mass spectrometry

In order to look for GAPs, GEFs and other RhoJ-interacting proteins, pull-down assays were performed according to the method described by Garcia-Mata and colleagues (Garcia-Mata, Wennerberg et al. 2006). This used GST-daRhoJ (Q79L, GTP-bound) and GST-dnRhoJ (G33A, nucleotide-free) fusion proteins, which were loaded on glutathione-agarose beads and incubated with various cellular lysates (HUVECs, HMEC-1 or HEK 293Ts). The dominant active RhoJ mutant should bind GAPs and effector proteins and the dominant negative RhoJ mutant should sequester GEFs (Garcia-Mata, Wennerberg et al. 2006). Mixtures of protein samples from pull-down experiments were firstly resolved by SDS-PAGE and then visualised in gels by Coomassie staining (Fig. 4.1). Some of the interesting protein bands (as indicated in the Fig. 4.1) which appeared only in the GST-RhoJ but not in the GST control pull-downs
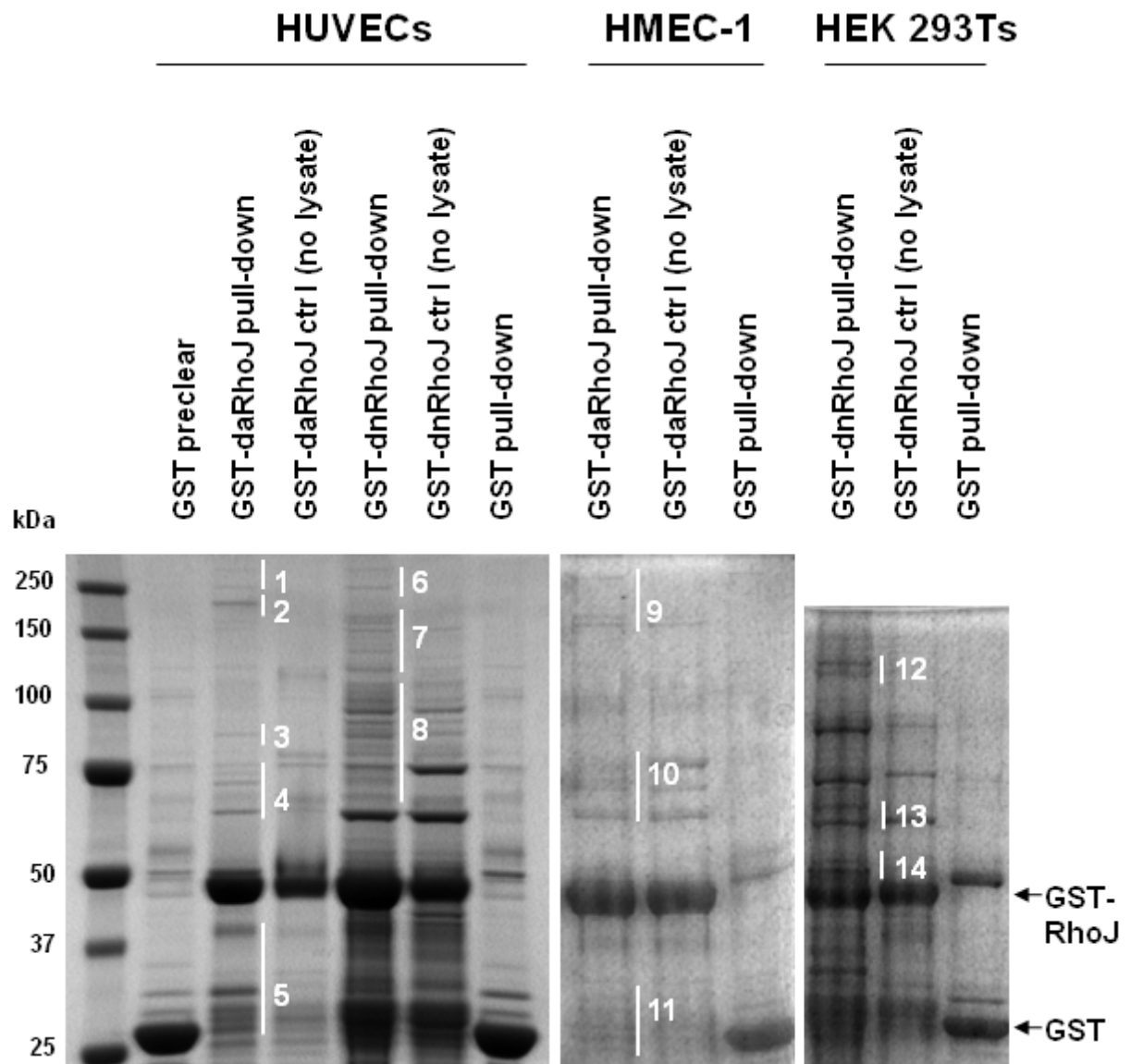
Fig. 4.1 Pull-down of GAPs, GEFs and effectors of RhoJ.
HUVECs, HMEC-1 and HEK 293Ts were grown in appropriate complete medium and lysed. Subsequently their lysates were firstly precleared with GST-glutathione agarose beads and then incubated with GST-daRhoJ, GST-dnRhoJ or GST control proteins bound to the glutathione agarose beads as indicated. After the pull-downs the beads were washed and resuspended in 2x SDS sample-loading buffer. Samples were subjected to SDS-PAGE and stained with the Coomassie dye. The protein bands that were visible in GST-RhoJ pull-down lanes (marked with the white numbers) but not in GST alone pull-down control lanes were excised, processed and analysed by mass spectrometry.

Tab. 4.1 Mass spectrometry results showing potential RhoJ-binding proteins.
The table indicates the gene symbol, name and the sample number that corresponds to the digested gel fragment as labelled in Fig. 4.1.

Gene symbol	Name	Sample No from MS

Potential GAPs or GEFs

Gene symbol	Name	Sample No from MS
ARHGEF6	Rac/Cdc42 guanine nucleotide exchange factor 6 (αPIX)	3
ARHGEF7	PAK-interacting exchange factor beta isoform b (βPIX)	3
IQGAP1	IQ motif containing GTPase activating protein 1	1, 2, 9, 7
GIT1	G protein-coupled receptor kinase-interacting target 1	3
GNL3	guanine nucleotide binding protein-like 3 isoform 1	10
GUF1	GUF1 GTPase homolog	4
G3BP1	Ras-GTPase-activating protein SH3-domain-binding protein	13
OBSCN	obscurin, cytoskeletal calmodulin and titin-interacting RhoGEF isoform a	14

CRIB-domain containing

Gene symbol	Name	Sample No from MS
CDC42BPA	CDC42-binding protein kinase alpha, also called myotonic dystrophy kinase-related cell division cycle 42-binding kinase alpha (MRCKA)	1, 2
CDC42BPB	CDC42-binding protein kinase beta, also called myotonic dystrophy kinase-related cell division cycle 42-binding kinase beta (MRCKB)	1, 2

Cytoskeletal-related proteins

Gene symbol	Name	Sample No from MS
FLNA	filamin A, alpha isoform 2	1,6,9
FLNB	filamin B, beta (actin binding protein 278)	6
CEP250	centrosomal protein 2 isoform 1	6,7,12,11
TUBA1B	tubulin, alpha, ubiquitous	14
TUBA1C	tubulin alpha 6	14
TUBA3D	tubulin, alpha 3d	14
TUBA4A	tubulin, alpha 4a	14
TUBAL3	tubulin, alpha-like 3	14
TUBB	tubulin, beta	14
TUBB2A	tubulin, beta 2	14
TUBB2C	tubulin, beta, 2	14
TUBB4	tubulin, beta 4	14
TUBB4Q	tubulin, beta polypeptide 4, member Q	14
TLN1	talin 1	9
SCRIB	scribble isoform b	13
MYO1B	myosin IB isoform 2	5, 8
MYO1C	myosin IC isoform c	7

MYO1D	myosin ID	7
MYH9	myosin, heavy polypeptide 9, non-muscle	1, 6
MYH11	smooth muscle myosin heavy chain 11 isoform SM1A	1, 6
MYH14	myosin, heavy chain 14 isoform 2	1, 6

Other miscellaneous hits

IKIP	IKK interacting protein isoform 1	5,8
THBS1	thrombospondin 1 precursor	7
TRAP1	TNF receptor-associated protein 1	3
CUL5	Vasopressin-activated calcium-mobilising receptor-1	11
TSGA10	testis specific, 10	2
SLC4A2	solute carrier family 4, anion exchanger, member 2 (erythrocyte membrane protein band 3-like 1)	4
EEF1A1	eukaryotic translation elongation factor 1 alpha 1	5
EEF1B2	eukaryotic translation elongation factor 1 beta 2	5
EEF1G	eukaryotic translation elongation factor 1 gamma	5
ZBTB37	zinc finger and BTB domain containing 37 isoform b	5
	various heat shock proteins	

lanes were digested with trypsin and analysed by mass spectrometry. Protein sequencing was performed by Dr Cleidiane Zampronio using liquid chromatography and mass spectrometry (LS-MS) (in collaboration with Prof. John Heath, School of Biosciences, University of Birmingham, Functional Genomics and Proteomics Unit). The results revealed many interesting candidates for RhoJ-binding proteins, which were grouped into the following categories: GAPs, GEFs, CRIB domain-containing proteins, cytoskeleton-related proteins and other miscellaneous hits (Tab. 4.1).

4.3. Confirmation of the interactions between RhoJ and pulled-down proteins

Having identified candidates for RhoJ-binding proteins (Tab. 4.1), the next step was to confirm these interactions by another method; here a Y2H assay was used. The most interesting RhoJ-binding candidates important in cell motility-related processes, potential GAPs, GEFs or CRIB domain containing proteins (shortlisted and briefly described in the Table 4.2) were cloned into the pACT2 vector to generate fusion proteins with the activating domain (AD) of the Gal4 transcription factor. The wild type RhoJ or its mutant versions (GTP-bound dominant active (Q79L) and GDP-bound dominant negative (T35N) forms) were cloned into the pGBT9 vector to generate fusion proteins with the DNA-binding domain (DBD) of the Gal4 transcription factor.

Various combinations of pGBT9 and pACT2 constructs were transformed into pJ69-4A yeast strain, which is auxotropic for histidine and contains the Gal1 promoter-*HIS3* reporter gene. The interaction of candidate proteins with RhoJ or its mutants should result in the expression of *HIS3* gene and allow yeast to grow on a histidine-free medium. Thus, yeast were spotted

Tab. 4.2 RhoJ-binding protein candidates tested in the Y2H assay.
The table shows the list of proteins tested for the interaction with RhoJ in the Y2H assay and indicates their known functions.

| Protein	Known functions	Key references
MRCKA	Contains CRIB domain; effector of Cdc42; mediates Cdc42-induced filopodia formation; phosphorylates MLC; regulates the nuclear repositioning during cell polarisation and migration; modulates the lamellar actomyosin retrograde flow during cell protrusion and migration.	(Gomes, Jani et al. 2005; Zhao and Manser 2005; Tan, Yong et al. 2008)
GIT1	GAP for Arf GTPases; trafficks between cytoplasmic complexes, FAs and cell periphery; participates in the internalisation of GPCRs; interacts with mitogen-activated protein kinases (MAPK) and phospholipase Cγ; interacts with PAK, PIX and paxillin in the regulation of FA turnover; participates in the formation of podosomes; required for pulmonary vascular development.	(Hoefen and Berk 2006; Frank and Hansen 2008; Pang, Hoefen et al. 2009; Wang, Taba et al. 2009)
αPIX	GEF for Rac1 and Cdc42, regulates the actin cytoskeleton and FA through the interactions with PAK, Rho GTPases, GIT, β-Parvin and calpain; forms homo- or heterodimers with βPIX.	(Rosenberger and Kutsche 2006; Frank and Hansen 2008)
βPIX	Displays a weak GEF activity towards Rac1 and Cdc42, forms homo- or heterodimers with αPIX; together with GIT1 and PAK localises to FA and plays a role in FA turnover and cell migration; regulates formation of podosomes; interacts with scribble and shank in the cell polarisation process.	(Rosenberger and Kutsche 2006; Frank and Hansen 2008)
IQGAP1	Involved in calcium/calmodulin signalling, MAPK signalling, regulation of the cytoskeleton, cell-cell contacts, cell adhesion and cell motility, EC proliferation; potential oncogene.	(Brown and Sacks 2006; Johnson, Sharma et al. 2009)
Scribble	Regulates cell polarity and proliferation, binds to βPIX and interacts with βPIX/PAK/GIT1 complex	(Iden and Collard 2008; Etienne-Manneville 2009)
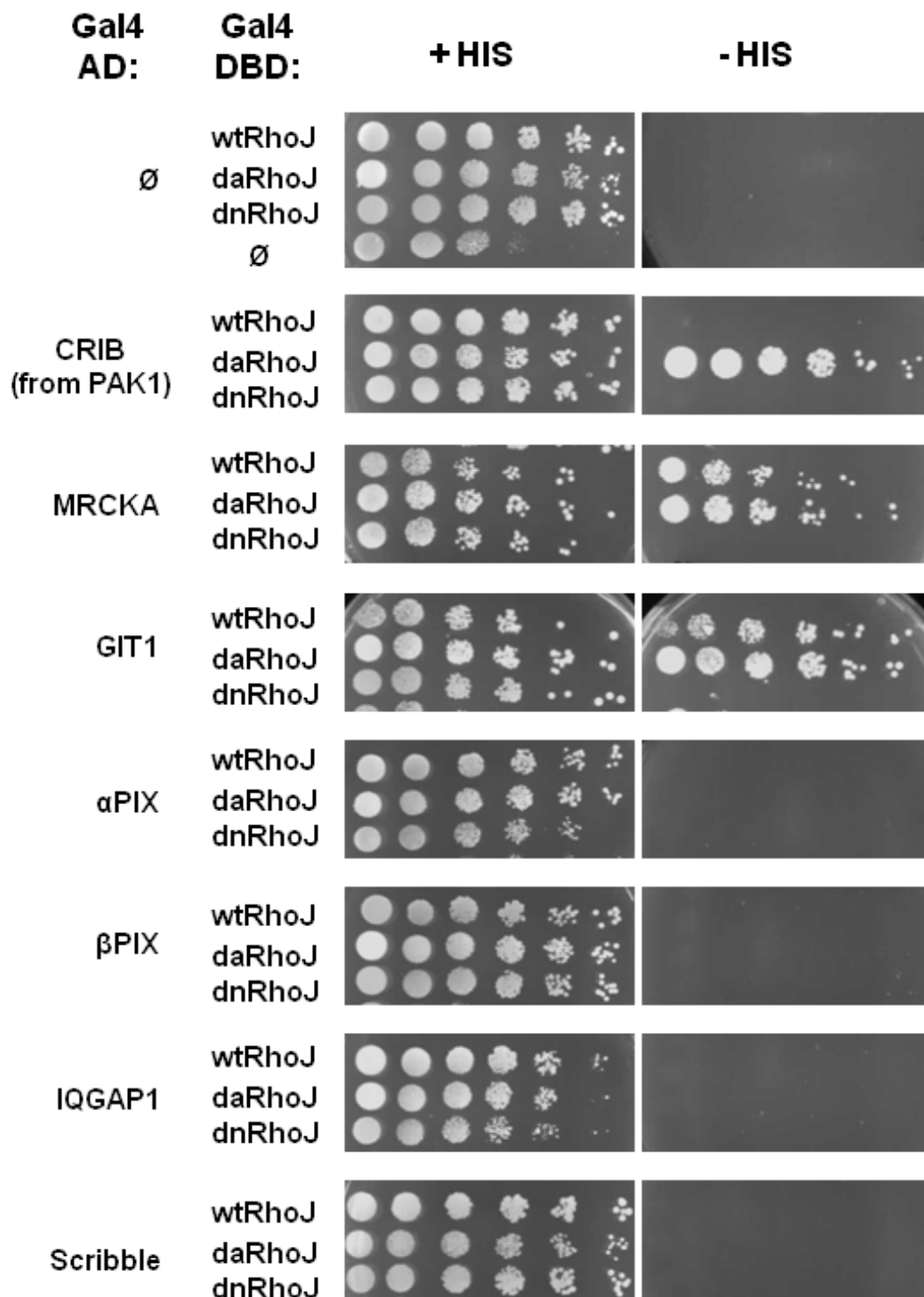
Fig. 4.2 Comparison of the interactions between RhoJ and candidate proteins.
A yeast strain (PJ69-4A) containing a Gal1 promoter - *HIS3* reporter gene was transformed with combinations of pGBT9 and pACT2 plasmids. pGBT9 plasmids encoded Gal4 DNA-binding domain (DBD) fusions of RhoJ (wild type, da or dn mutants) and pACT2 encoded Gal4 activation domain (AD) fusions of RhoJ-binding candidates as indicated. Five fivefold serial dilutions starting with an OD_{600} of 0.5 (left column) for each culture were prepared and spotted on to synthetic media either containing (+HIS) or lacking (-HIS) histidine. Yeast were grown for 3-5 days at 30 °C.

and grown as dilution series on a synthetic medium containing or lacking histidine. It was found that among all proteins tested, RhoJ (in its wild type or dominant active forms) interacted only with MRCKA and GIT1 (Fig. 4.2). A positive interaction between the dominant active RhoJ and the CRIB domain acted as a positive control for this assay (Vignal, De Toledo et al. 2000). Although α- and βPIX did not bind to RhoJ in the Y2H experiment, these proteins were clearly pulled-down by GST-daRhoJ from HUVEC lysate. PIX proteins strongly bind to GIT1 (Hoefen and Berk 2006) and possibly in the GST-daRhoJ pull-down they were precipitated via their binding to GIT1. Thus a potential interaction of RhoJ with PIX proteins in ECs, in particular βPIX, was considered in the subsequent experiments.

Due to the availability of GIT1- and βPIX-specific antibodies the pull-down and mass spectrometry results for these hits were verified by western blotting. GST and GST-daRhoJ pull-downs were repeated from HUVEC lysates and western blotting with anti-βPIX and anti-GIT1 antibodies was performed. The GIT1 and βPIX bands were detected in the GST-daRhoJ but not in the GST alone pull-down lanes (Fig. 4.3). This and Y2H results together suggested that RhoJ binds to the GIT1/βPIX complex via direct interaction with GIT1. Interestingly, the GIT1/βPIX complex plays a very important role in FA turnover (Rosenberger and Kutsche 2006) and in the previous chapter it was shown that RhoJ localises to FAs where it regulates the FA numbers. Thus subsequent experiments were focused on the closer characterisation of this RhoJ and GIT1/βPIX complex interaction and then on the verification of its physiological relevance in ECs. Due to the time limit of these PhD studies, no further characterisation of the interaction of RhoJ and MRCKA was performed.
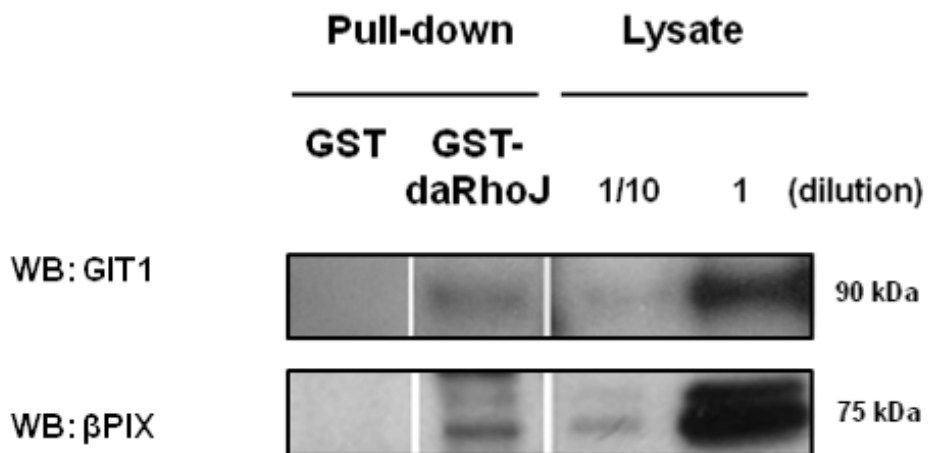
Fig. 4.3 Western blot confirming the pull-down of GIT1 and βPix with GST-daRhoJ.
HUVECs were grown in complete medium and lysed. Subsequently their lysates were firstly precleared with GST-glutathione agarose beads and then incubated with either GST-daRhoJ or GST control protein bound to the glutathione agarose beads, as indicated. After the pull-downs the beads were washed and resuspended in 2x SDS sample-loading buffer. Samples were subjected to SDS-PAGE and western blotting with anti-βPIX and anti-GIT1 antibodies.

4.4. Further investigation of RhoJ interactions with GIT1 and βPix proteins

4.4.1. Mapping the GIT1 domain that interacts with RhoJ

GIT1 contains several domains which mediate its binding to various proteins (described in the Fig. 4.4 A). In order to better understand the context of the RhoJ and GIT1 interaction, the domain of GIT1 which binds to RhoJ was determined. Francesca Edelmann in our laboratory made a series of C-terminal truncation mutants of GIT1 as shown in the Fig. 4.4 B. These were fused with the AD domain of GAL4, co-expressed with wild type or dominant active RhoJ fused to the DBD domain of GAL4 and screened using a Y2H assay as described above (Francesca Edelmann, unpublished data). Binding of GIT1 to dominant active RhoJ was lost upon truncation of the SHD domain, suggesting that this domain is necessary for RhoJ interaction.

In order to identify the exact region of SHD domain which interacts with RhoJ, further Y2H studies were undertaken. The SHD domain comprises two homology repeats (Premont, Perry et al. 2004). These and the whole SHD were cloned again to generate fusions with the AD domain of GAL4 and were tested for the interaction with RhoJ fused to the DBD of GAL4 (Fig. 4.4 C). No yeast growth was observed on the histidine-lacking selective medium which suggested that the SHD domain appeared to be critical but not sufficient for binding with RhoJ, providing this fusion was correctly expressed in the yeast. Possibly other domains of GIT1 are required to enable this interaction.
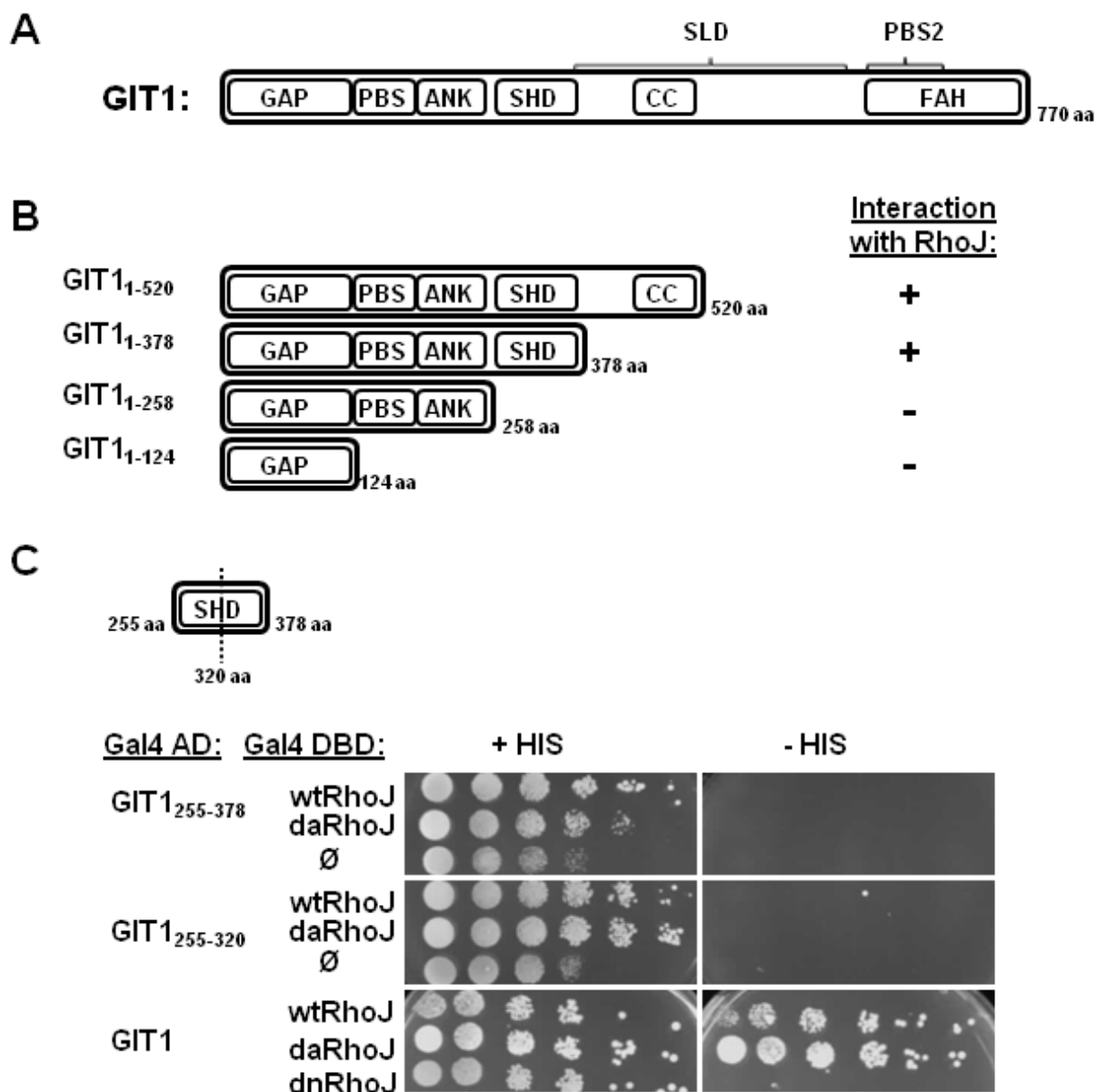
Fig. 4.4 Mapping of the GIT1 domain that interacts with RhoJ.
A, The scheme shows domains of GIT1. GAP, a GTPase activating domain for Arf GTPases; PBS, a minor interaction site with paxillin; ANK, ankyrin repeats, interact with C-terminus of GIT1 and are involved in its localisation to endosomes; SHD, yeast Spa2 homology domain, interacts with many proteins including MEK, αPIX, βPIX, FAK; CC, coiled-coil region with a leucine zipper motif, involved in homo- and heterodimerisation of GIT1; FAH, focal adhesion targeting homology domain, includes major paxillin binding site (PBS2); SLD, synaptic localisation domain, targets GIT1 to dendritic protrusions. Domains were described as reviewed by Frank and Hansen (2008). **B**, Truncation mutants of GIT1 cloned and tested for RhoJ interactions in Y2H system (Francesca Edelmann, unpublished data). **C**, Testing the SHD domain for interaction with RhoJ. A yeast strain (PJ69-4A) containing the Gal1 promoter - HIS3 reporter gene was transformed with combinations of plasmids to express Gal4 DBD fusions of RhoJ (wild type or its da mutant) and Gal4 AD fusions of GIT1 fragments. Five fivefold serial dilutions starting with an OD_{600} of 0.5 (left column) for each culture were prepared and spotted on to synthetic media either containing (+HIS) or lacking (-HIS) histidine. Yeast were grown for 3-5 days at 30 °C.

4.4.2. Testing co-localisation of RhoJ with βPix and GIT1 in HUVECs

If RhoJ interacts with the GIT1/βPIX complex in HUVECs, these proteins should co-localise in this cell type. Experiments in chapter 3 demonstrated that RhoJ localised to FA and it is well known that the GIT1/βPIX complex can localise to FAs (Zhao, Manser et al. 2000; Rosenberger and Kutsche 2006). Available antibodies suitable for immunostaining of RhoJ, βPIX and GIT1 were made in rabbits, thus it was not possible to use them for the co-localisation of endogenous proteins. Therefore GFP, GFP-wtRhoJ and GFP-daRhoJ expressing HUVECs were used and stained with βPIX and GIT1-specific antibodies separately (Fig. 4.5 and 4.6 respectively). It was found that both βPIX and GIT1 co-localised with RhoJ in the cell periphery in regions resembling FAs (as indicated with the yellow arrows). Moreover it was evident that there was more βPIX or GIT1 localising to these FAs when RhoJ was overexpressed in wild type or activated form (as indicated with the white arrows). Subsequently, western blotting was performed to determine the expression levels of βPIX, GIT1 and GFP-RhoJ (Fig. 4.7). Each HUVEC isolate overexpressing the activated RhoJ mutant contained more βPIX protein than the GFP-expressing controls. This suggested that active RhoJ may play a role in the stabilisation of βPIX protein or in the regulation of its expression levels.

4.4.3. Testing the interdependence in the localisation of RhoJ, βPIX and GIT1 to FAs

The next step was to assess if the loss of single components of the hypothetical βPIX/GIT1/RhoJ complex would affect the localisation of these proteins to FAs. Two different siRNA duplexes were designed to knock-down βPIX and GIT1 and they were tested in HUVECs at the 25 nM concentration. Firstly it was important to check that these duplexes
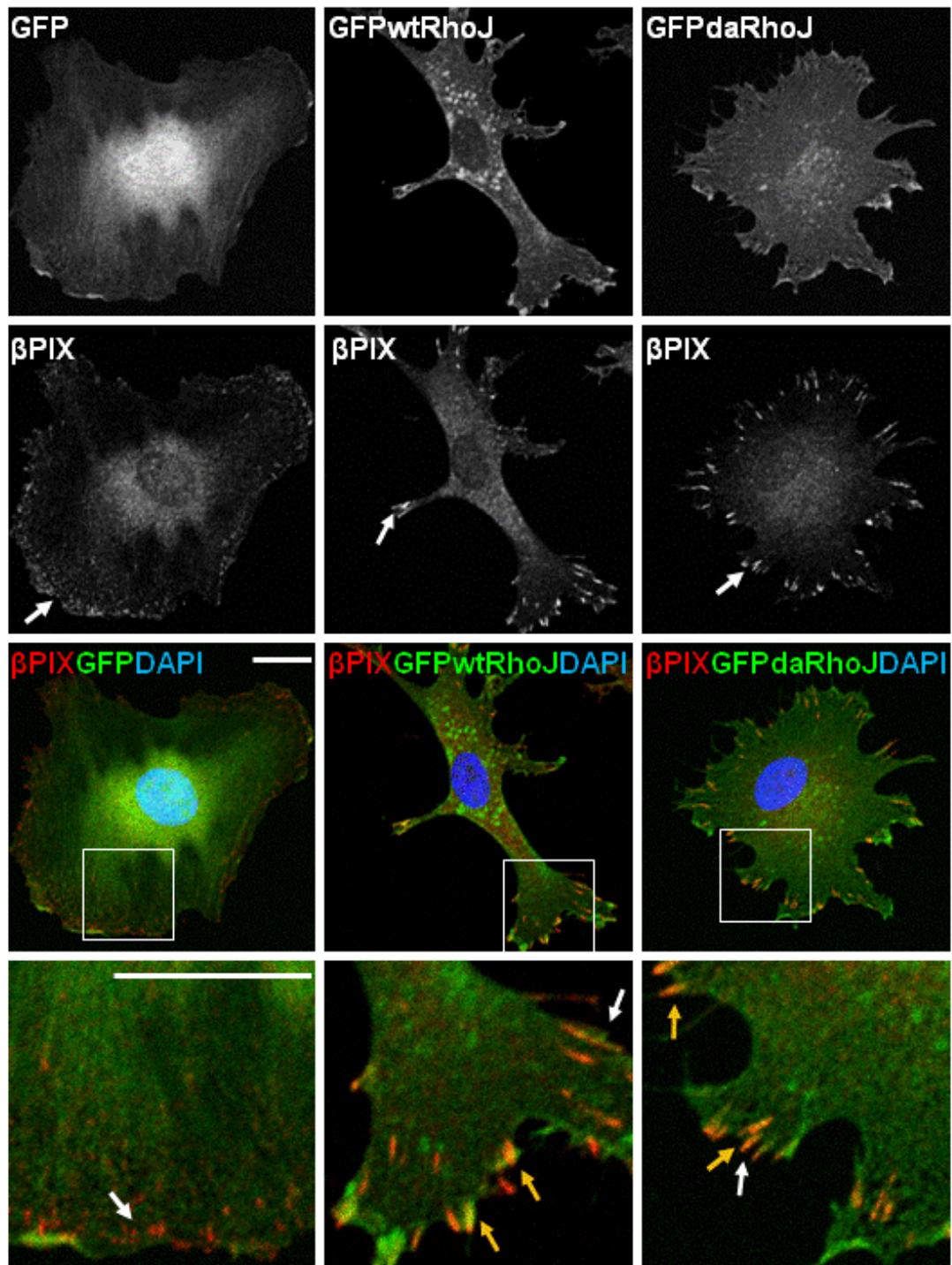
Fig. 4.5 GFP-RhoJ co-localises with βPix in HUVECs.
HUVECs were transduced with lentivirus to stably express GFP, GFP-wtRhoJ or GFP-daRhoJ, and were sorted for GFP-positive cells using flow cytometry. Cells were then cultured on gelatin-coated coverslips and immunofluorescent staining was performed with the βPIX-specific antibody. DAPI was used to stain nuclei. Regions marked in the white boxes are expanded in the bottom panel. Both GFP-wtRhoJ and GFP-daRhoJ co-localised with βPIX as indicated with the yellow arrows. Expression of GFP-wtRhoJ or GFP-daRhoJ increased βPIX levels in FAs compared with GFP controls, as indicated with the white arrows. Scale bars: 10 µm.
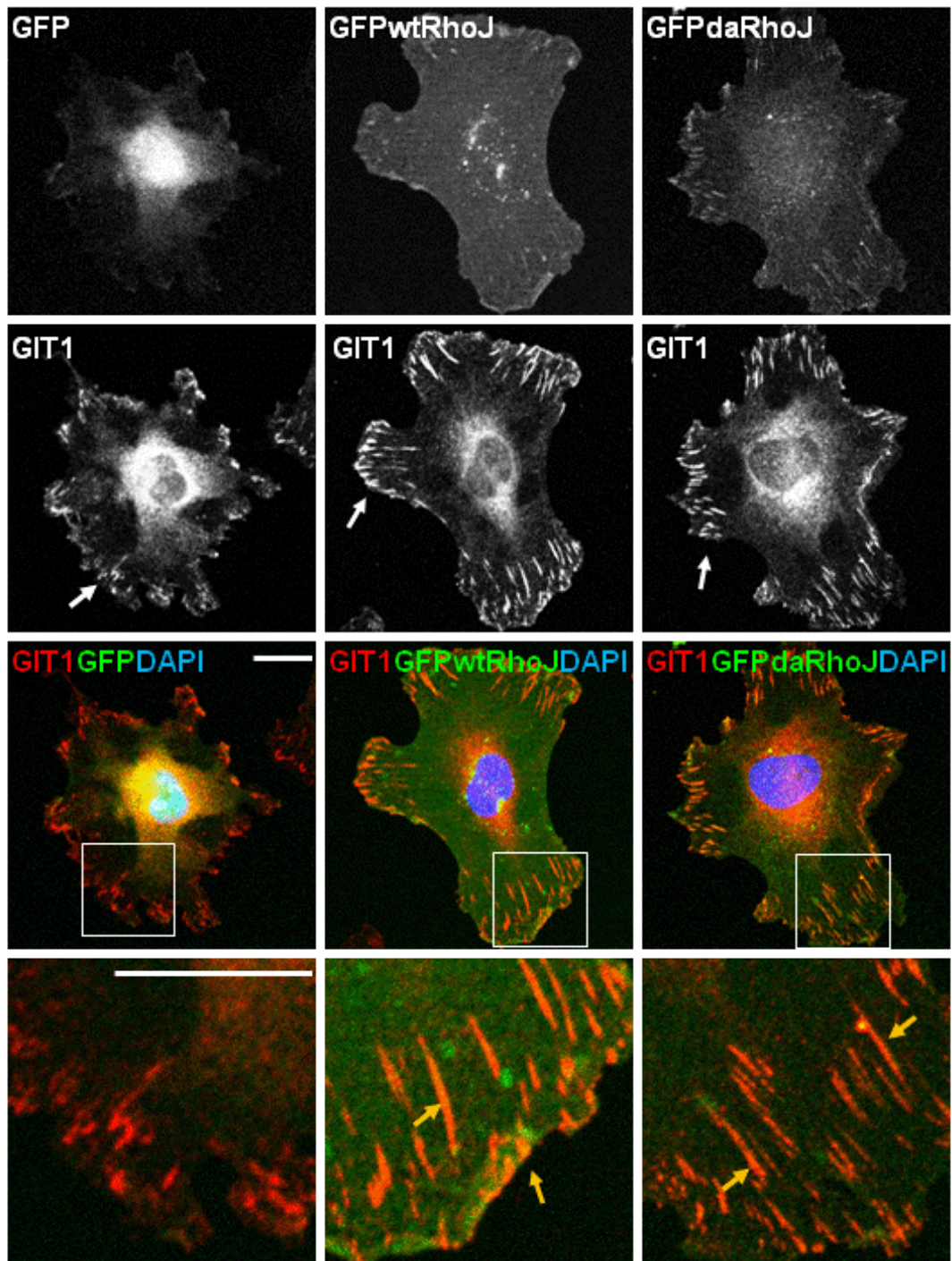
Fig. 4.6 GFP-RhoJ co-localises with GIT1 in HUVECs.
HUVECs were transduced with lentivirus to stably express GFP, GFP-wtRhoJ or GFP-daRhoJ, and were sorted for GFP-positive cells using flow cytometry. Cells were then cultured on gelatin-coated coverslips and immunofluorescent staining was performed with the GIT1-specific antibody. DAPI was used to stain nuclei. Regions marked in the white boxes are expanded in the bottom panel. Both GFP-wtRhoJ and GFP-daRhoJ co-localised with GIT1 as indicated with the yellow arrows. Expression of GFP-wtRhoJ or GFP-daRhoJ increased GIT1 levels in FAs compared with GFP controls, as indicated with the white arrows. Scale bars: 10 µm.
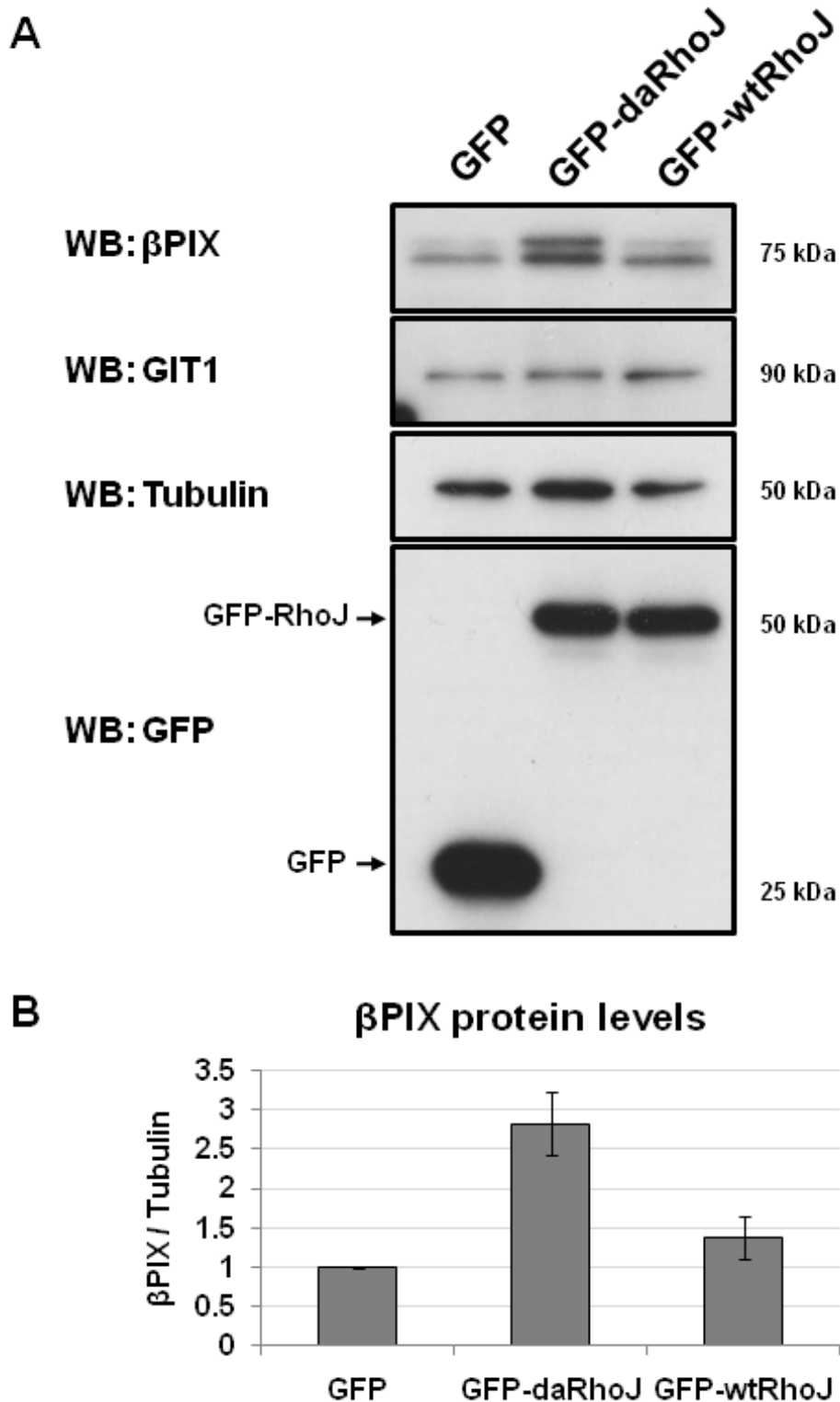
Fig. 4.7 Dominant active RhoJ increases the level of βPix protein.
A, HUVECs were infected with lentivirus to stably express GFP, GFP-wtRhoJ or GFP-daRhoJ proteins. GFP-positive cells were sorted using flow cytometry. Subsequently lysates were prepared from the same number of cells for each condition and these were subjected to western blotting with antibodies as indicated. **B**, Graph showing the densitometry of βPIX protein relative to tubulin, which was normalised to 1 for GFP control. The mean and standard errors were plotted for 3 HUVEC isolates expressing GFP or GFP-RhoJ.

do not induce the interferon response. Interferon is a cytokine which is induced during the viral infection with double-stranded RNA. Induced interferon leads to the activation of signalling cascade which up-regulates transcriptional activation of hundreds of interferon stimulated genes (Haque and Williams 1998) which in turn will affect EC behaviour. Thus a quantitative PCR was performed to test the expression of the interferon inducible genes 2',5'-oligoadenylate synthetase 1 (Clemens 2005) and IFN-Stimulated Gene of 20 kDa (Espert, Rey et al. 2004). No significant up-regulation of these genes was observed in the RhoJ-, βPIX- or GIT1-siRNA-silenced cells and it was assumed that these duplexes did not induce the interferon response at the concentration of duplexes tested (data not shown). Then the succesful knock-downs with these duplexes were examined by western blotting, as shown in the Fig. 4.8. Duplexes at this concentration of 25 nM were used in all subsequent experiments.

Firstly the localisation of RhoJ to FAs was examined (Fig. 4.9). HUVECs with siRNA-silenced RhoJ, βPIX and GIT1 (knock-down of each gene separately) were co-stained with vinculin- and RhoJ-specific antibodies (Fig. 4.9 A and B). Vinculin is one of the crucial components of FAs (Parsons, Horwitz et al. 2010) and its visualisation allowed monitoring of all FAs in each cell. All vinculin-positive FAs per cell were counted and the number of these that positively stained for RhoJ was quantified. βPIX knock-down significantly reduced the number of FAs positively staining for RhoJ from approximately 60 to 25 % (Fig. 4.9 C). This reduction was comparable to the decrease of βPIX in FAs after its knock-down (Fig. 4.10 C). GIT1 knock-down caused a more modest but still statistically significant decrease of RhoJ localisation to FAs. Moreover RhoJ knock-down caused an increase in total FAs, which was consistent with previous findings (Kaur *et al.* 2010).

The localisation of βPIX and GIT1 in FAs was assessed in a similar way. It was found that βPIX localisation to vinculin-positive FAs was slightly but significantly reduced in either
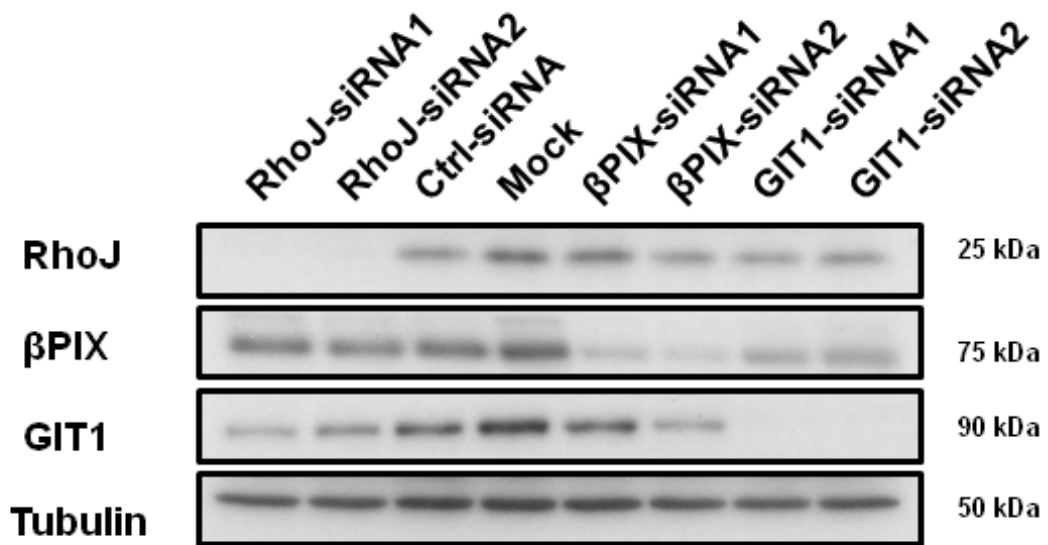
Fig. 4.8 Western blots showing siRNA knock-downs of βPIX, GIT1 and RhoJ.
HUVECs were transfected with 25 nM RhoJ-siRNA1, RhoJ-siRNA2, βPIX-siRNA1, βPIX-siRNA2, GIT1-siRNA1, GIT1-siRNA2 and Ctrl-siRNA duplexes or were mock transfected. 48 h later cells were lysed and lysates subjected to SDS-PAGE and western blotting with antibodies as indicated.

Fig. 4.9 The influence of βPIX- or GIT1-siRNA silencing on the localisation of RhoJ to focal adhesions.

A and **B**, HUVECs were transfected with 25 nM RhoJ-siRNA1, RhoJ-siRNA2, βPIX-siRNA1, βPIX-siRNA2, GIT1-siRNA1, GIT1-siRNA2 and Ctrl-siRNA duplexes or were mock transfected. 48 h later cells were plated on the gelatin-coated coverslips and allowed to spread for 4 h. Cells were then fixed and immunofluorescent staining was performed with antibodies specific to RhoJ and vinculin. Scale bars 10 µm. **C**, Graphs showing the numbers of total FAs positive for vinculin (**b**) and the percentage of vinculin staining FAs also positively staining for RhoJ (**a**). Counting of FAs was performed with ImageJ software in at least 22 cells from 3 different experiments. The box and whisker plots indicate the maximum, minimum, 25th and 75th percentiles and median values. The Mann Whitney test was used to calculate p values (*** for $p<0.001$; ** for $0.001<p<0.01$; * for $0.01<p<0.05$ and ns for non-significant).

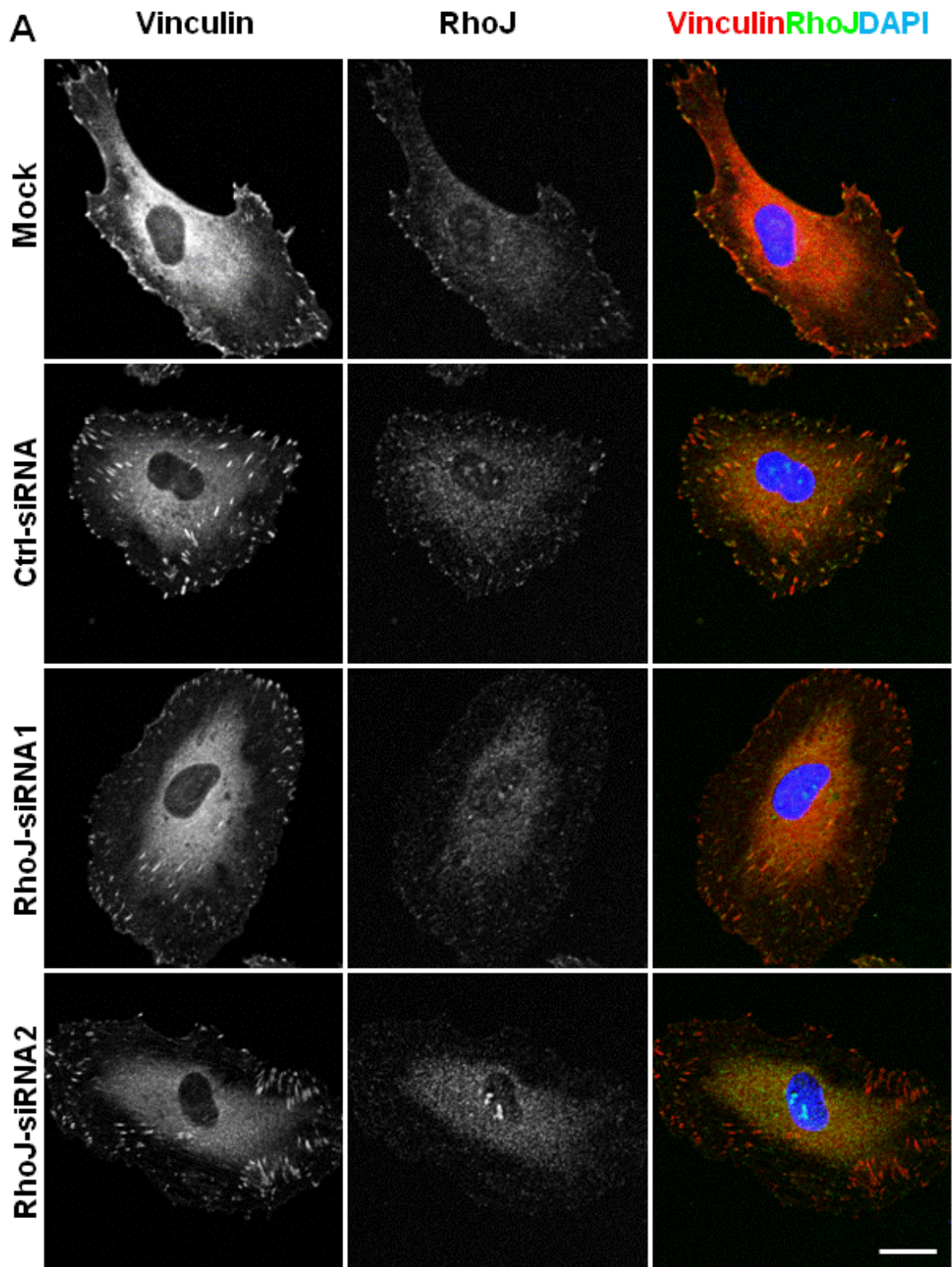The figure is presented on the next 3 pages.

Fig. 4.9 The influence of βPIX or GIT1 siRNA silencing on the localisation of RhoJ to focal adhesions.
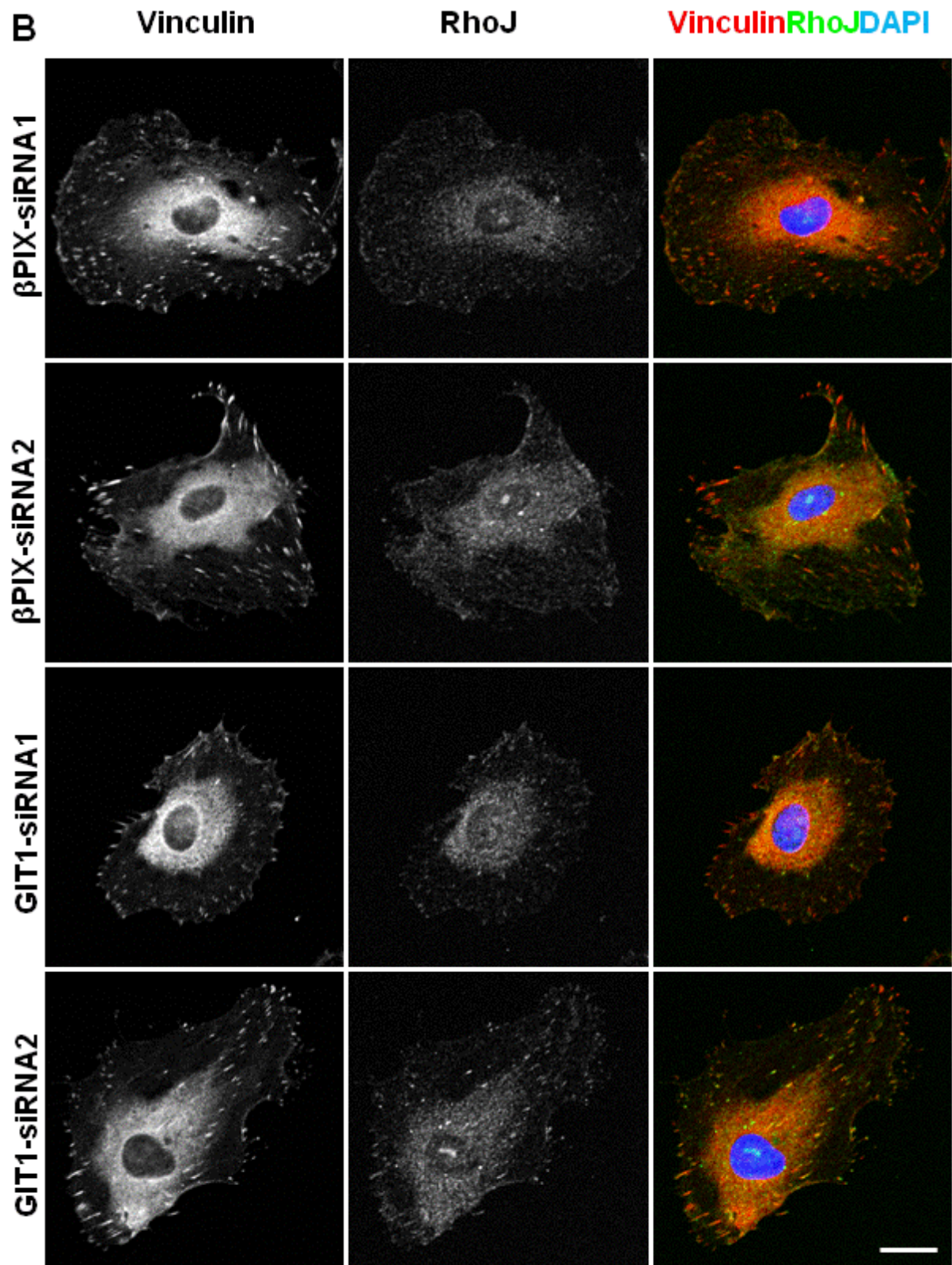
Fig. 4.9 The influence of βPIX or GIT1 siRNA silencing on the localisation of RhoJ to focal adhesions (continued).
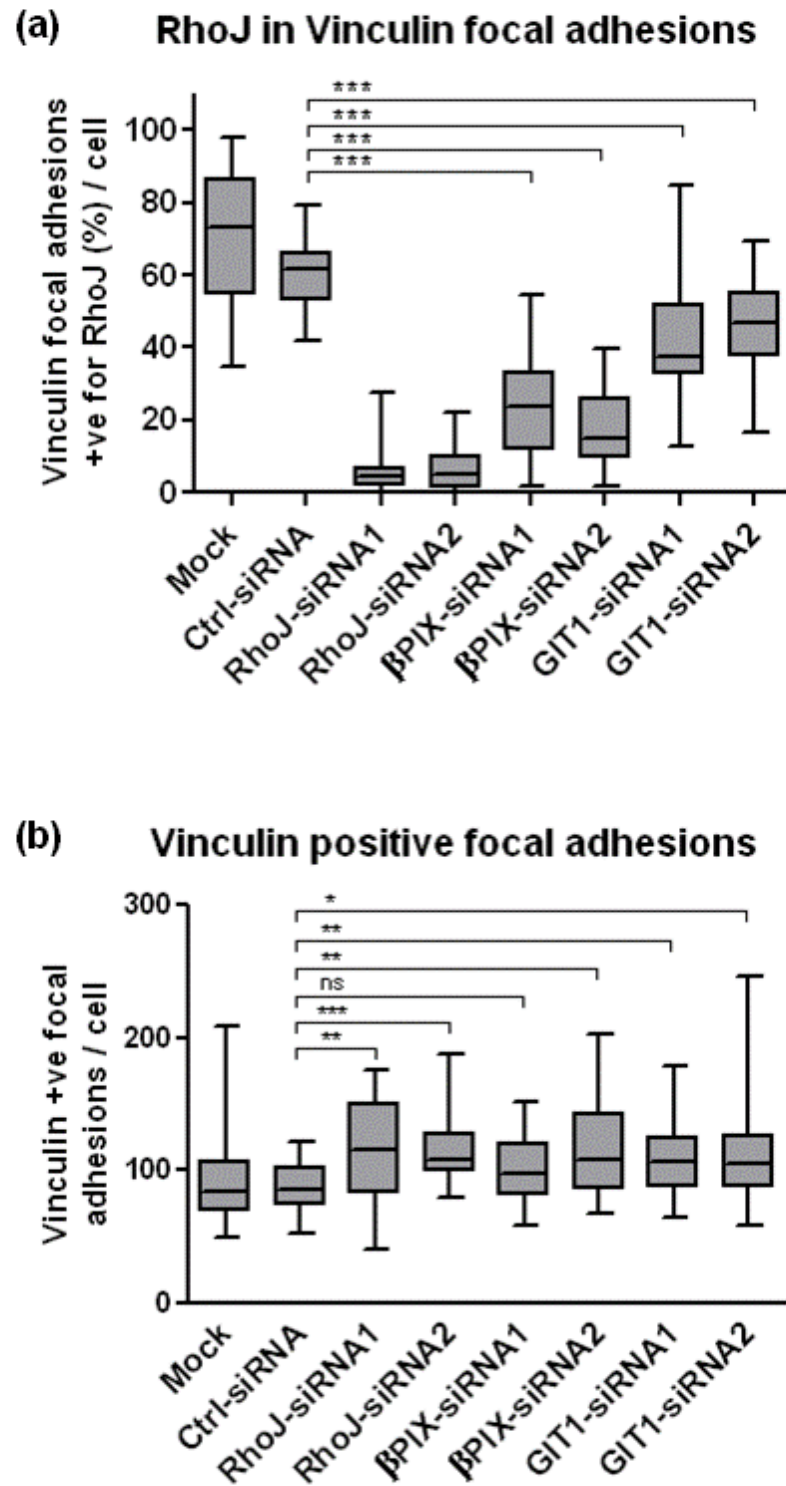
C

Fig. 4.9 The influence of βPIX or GIT1 siRNA silencing on the localisation of RhoJ to focal adhesions (continued).

Fig. 4.10 The influence of RhoJ- or GIT1-siRNA silencing on the localisation of βPIX to focal adhesions.
A and **B**, HUVECs were transfected with 25 nM RhoJ-siRNA1, RhoJ-siRNA2, βPIX-siRNA1, βPIX-siRNA2, GIT1-siRNA1, GIT1-siRNA2 and Ctrl-siRNA duplexes or were mock transfected. 48 h later cells were plated on the gelatin-coated coverslips and allowed to spread for 4 h. Cells were then fixed and immunofluorescent staining was performed with antibodies specific to βPIX and vinculin. Scale bars 10 µm. **C**, Graphs showing the numbers of total FAs positive for vinculin (**b**) and the percentage of vinculin staining FAs also positively staining for βPIX (**a**). Counting of FAs was performed with ImageJ software in at least 25 cells from 3 different experiments. The box and whisker plots indicate the maximum, minimum, 25th and 75th percentiles and median values. The Mann Whitney test was used to calculate p values (*** for $p<0.001$; ** for $0.001<p<0.01$; * for $0.01<p<0.05$ and ns for a non-significant).
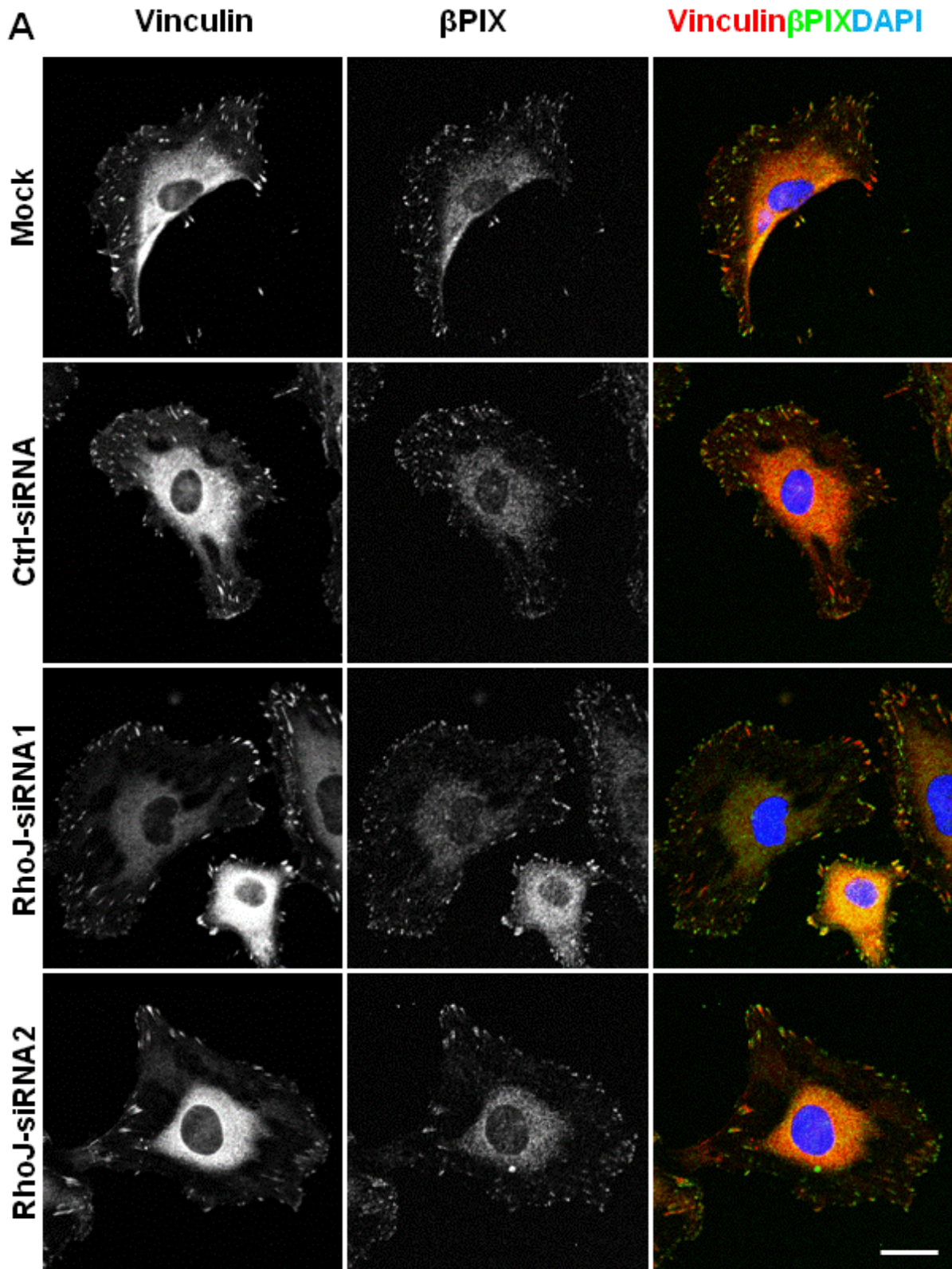The figure is presented on the next 3 pages.

Fig. 4.10 The influence of RhoJ or GIT1 siRNA silencing on the localisation of βPIX to focal adhesions.
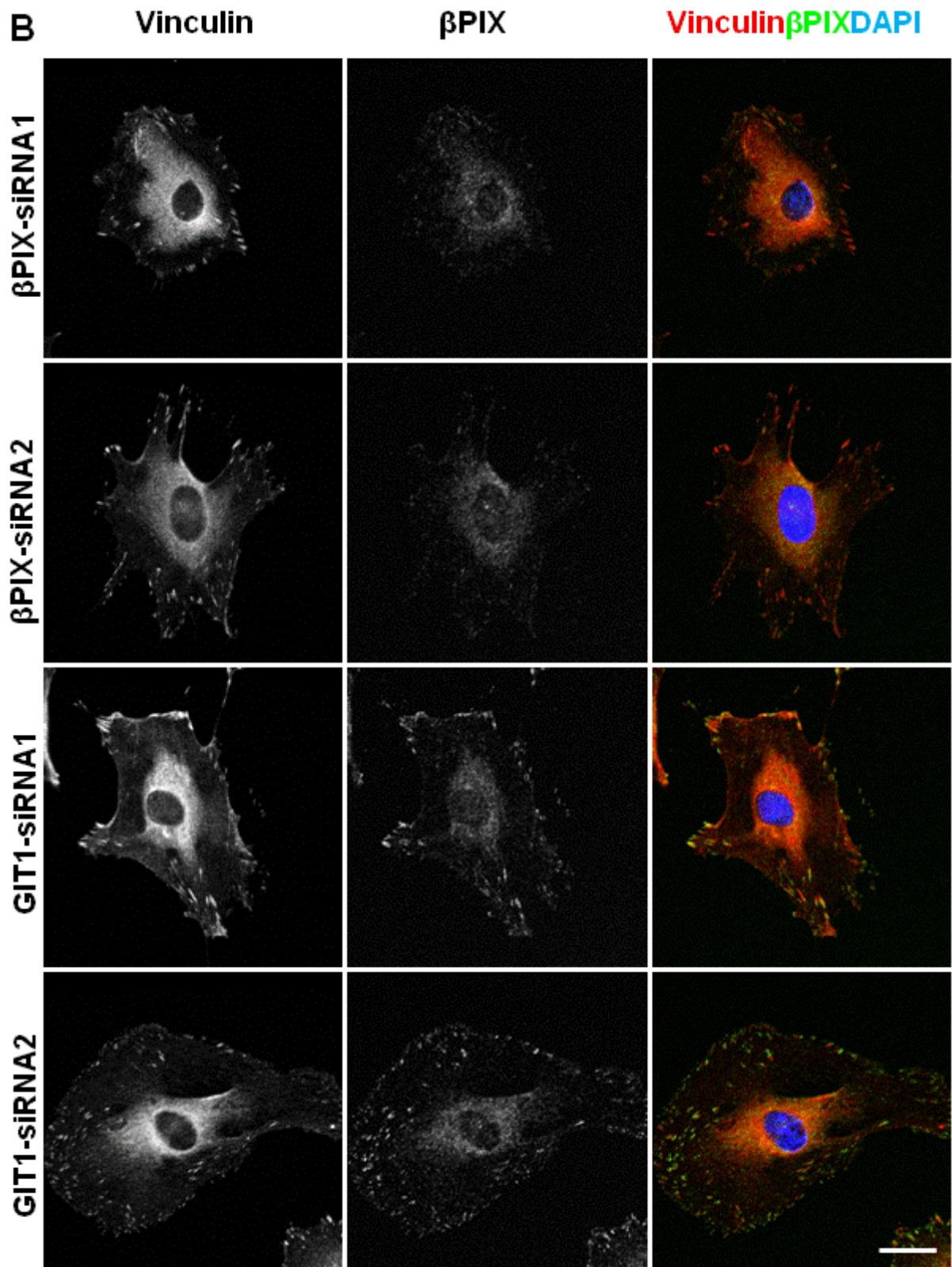
Fig. 4.10 The influence of RhoJ or GIT1 siRNA silencing on the localisation of βPIX to focal adhesions (continued).

C

Fig. 4.10 The influence of RhoJ or GIT1 siRNA silencing on the localisation of βPIX to focal adhesions (continued).

Fig. 4.11 The influence of RhoJ- or βPIX-siRNA silencing on the localisation of GIT1 to focal adhesions.

A and **B**, HUVECs were transfected with 25 nM RhoJ-siRNA1, RhoJ-siRNA2, βPIX-siRNA1, βPIX-siRNA2, GIT1-siRNA1, GIT1-siRNA2 and Ctrl-siRNA duplexes or were mock transfected. 48 h later cells were plated on the gelatin-coated coverslips and allowed to spread for 4 h. Cells were then fixed and immunofluorescent staining was performed with antibodies specific to GIT1 and vinculin. Scale bars 10 µm. **C**, Graphs showing the numbers of total FAs positive for vinculin (**b**) and the percentage of vinculin staining FAs also positively staining for GIT1 (**a**). Counting of FAs was performed with ImageJ software in at least 17 (for GIT1 knock-down) and at least 23 (all other conditions) cells from 3 different experiments. The box and whisker plots indicate the maximum, minimum, 25th and 75th percentiles and median values. The Mann Whitney test was used to calculate p values (*** for $p<0.001$; ** for $0.001<p<0.01$; * for $0.01<p<0.05$ and ns for a non-significant).

The figure is presented on the next 3 pages.

Fig. 4.11 The influence of RhoJ or βPIX siRNA silencing on the localisation of GIT1 to focal adhesions.
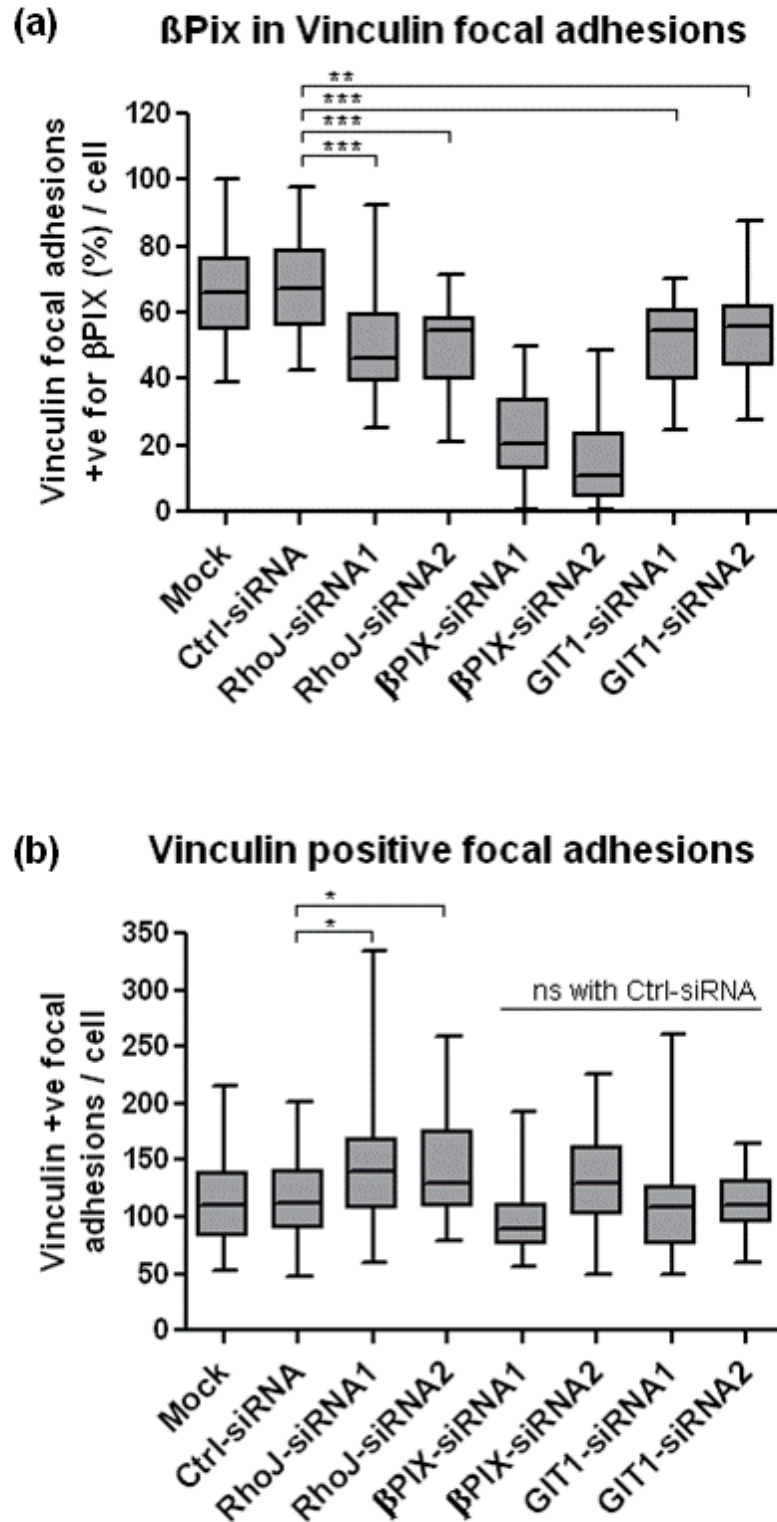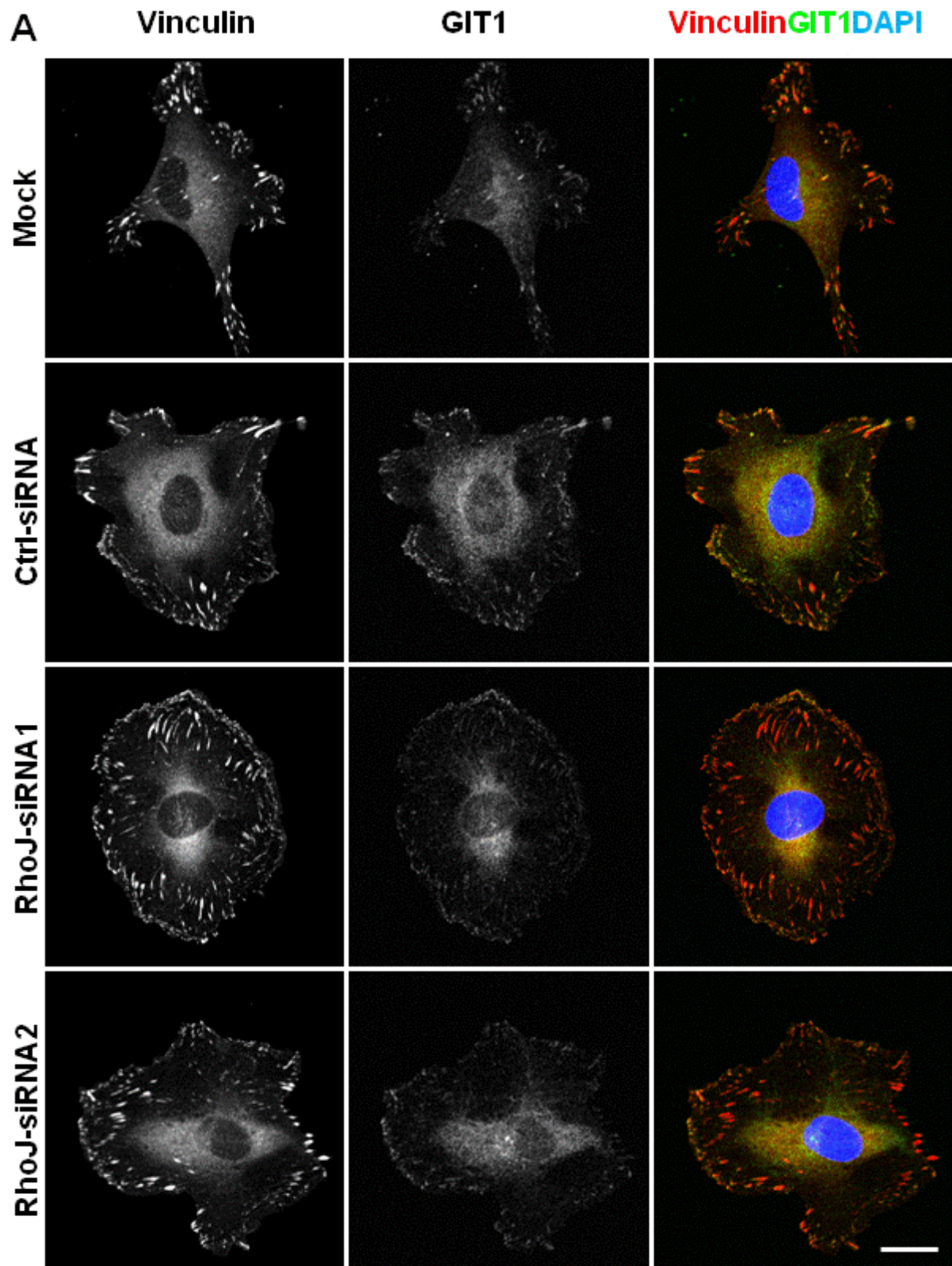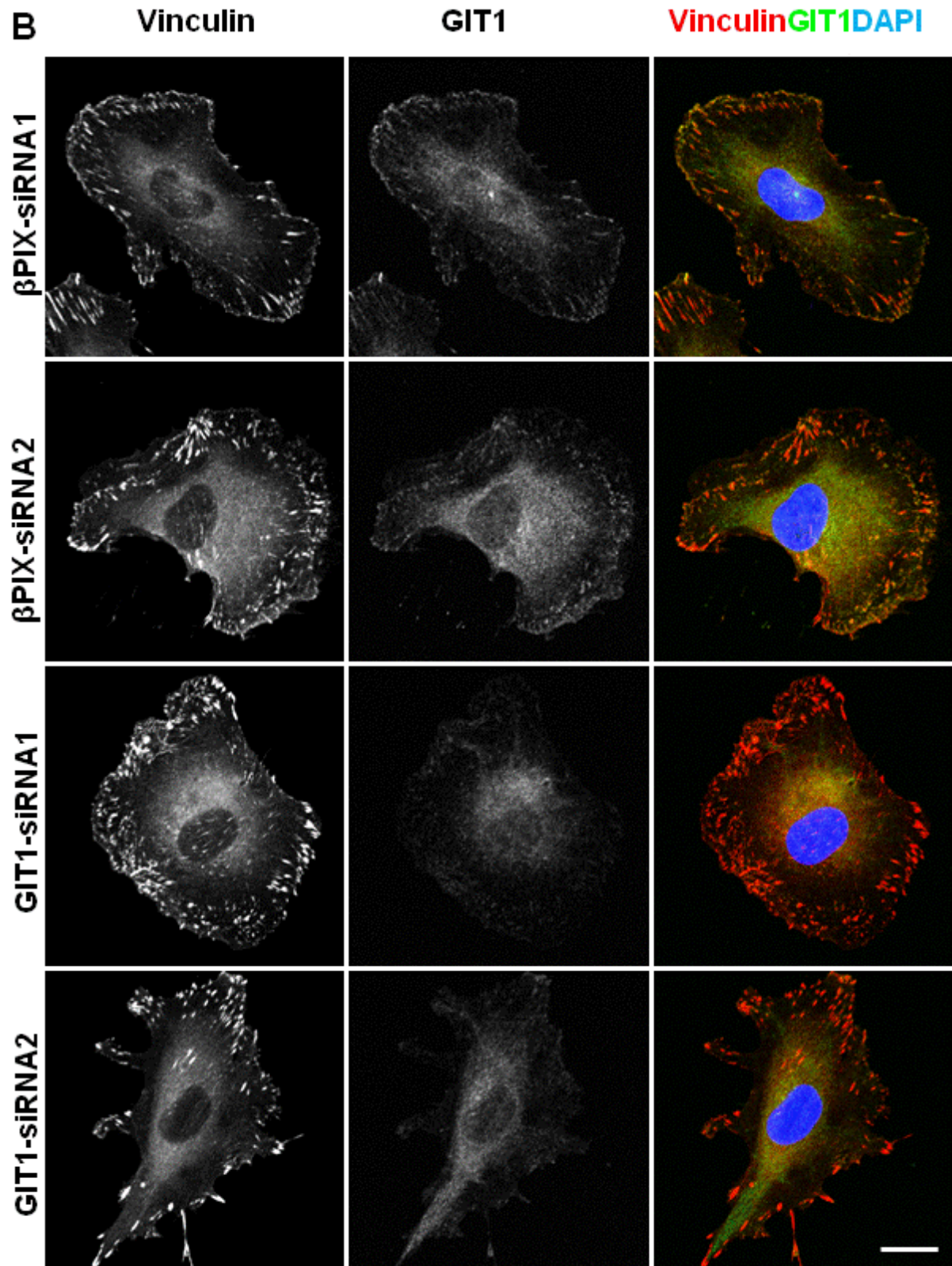
Fig. 4.11 The influence of RhoJ or βPIX siRNA silencing on the localisation of GIT1 to focal adhesions (continued).

C
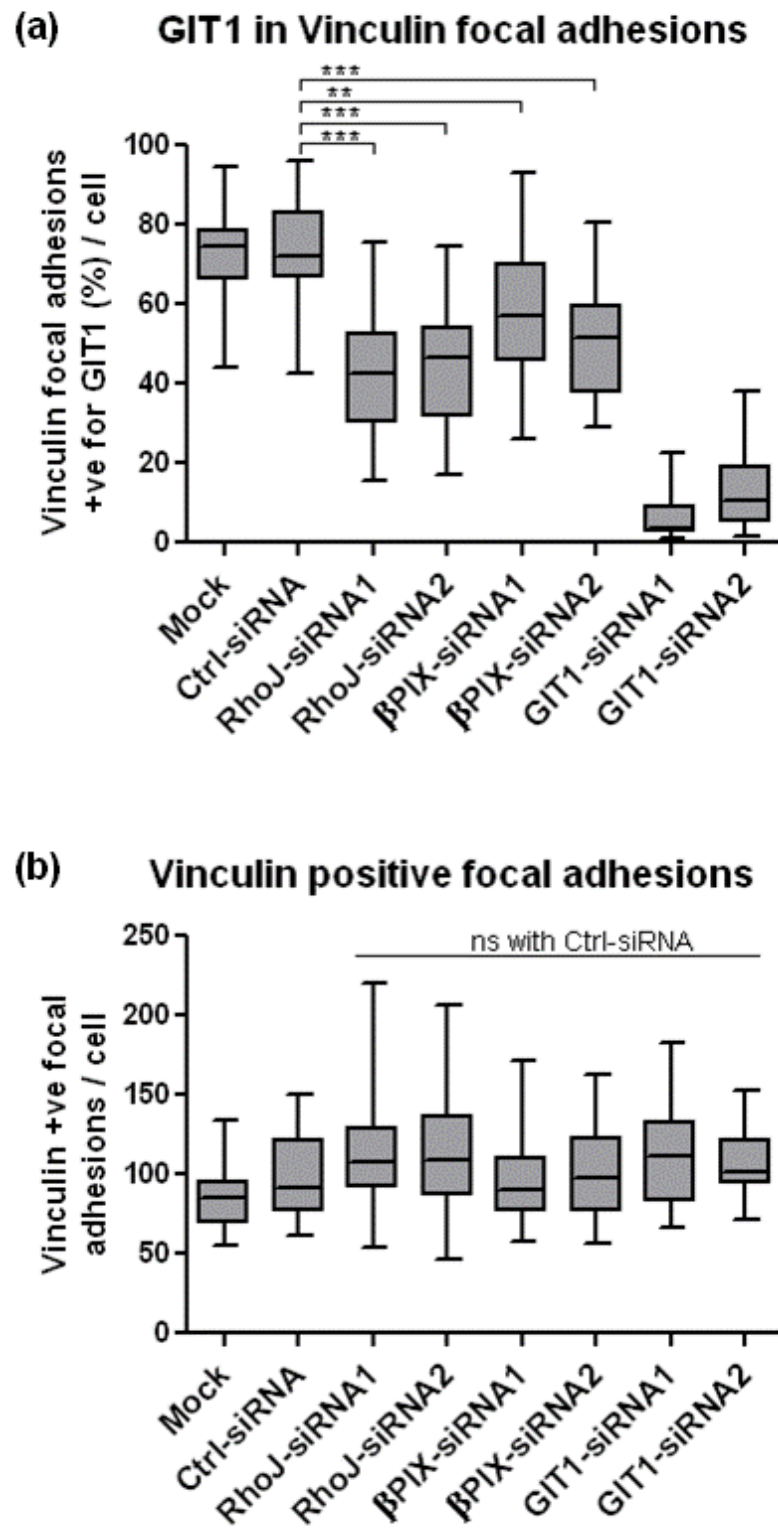
Fig. 4.11 The influence of RhoJ or βPIX siRNA silencing on the localisation of GIT1 to focal adhesions (continued).

RhoJ- or GIT1-siRNA silenced HUVECs (Fig.4.10). The localisation of GIT1 to vinculin-positive FAs was also decreased after either RhoJ or βPIX knock-down (Fig. 4.11). All results from the studies on localisation of RhoJ, βPIX and GIT1 to FAs are summarised in Table 4.3.

In summary, these findings suggested that RhoJ interacts with the GIT1/βPIX complex in HUVECs. Firstly, RhoJ co-localised with GIT1 and βPIX in FAs. Secondly, a presence of βPIX was required for localisation of RhoJ to FAs. Thirdly, overexpression of activated RhoJ caused an increase of GIT1 and βPIX in FAs and raised the total levels of the βPIX protein in HUVECs.

Tab. 4.3 Summary of the effect of RhoJ, βPIX or GIT1 knock-down and overexpression of daRhoJ on recruitment of these proteins to FAs. The table summarises results presented in the figures 4.5-4.11. In the first three panels arrows indicate an increase (↑) or a decrease (↓) in the number of focal adhesions positive (+ve) for the indicated proteins in HUVECs treated with RhoJ-, βPIX- or GIT1-specific siRNA. The bottom panel shows the influence of daRhoJ on the number of total FAs and amount of βPIX or GIT1 in these FAs.

	Vinculin +ve FAs (total FAs)	RhoJ +ve FAs (%)	GIT1 +ve FAs (%)	βPIX +ve FAs (%)
RhoJ-siRNA	↑		↓↓	↓
GIT1-siRNA	↑/=	↓↓		↓
βPIX-siRNA	↑/=	↓↓↓	↓	
	Vinculin +ve FAs (total FAs)		**Amount of GIT1 in FAs**	**Amount of βPIX in FAs**
daRhoJ	↓		↑↑↑	↑↑↑

4.5. Discussion

Rho GTPases are known to regulate cytoskeletal rearrangements and FA formation, processes very important for cell migration (Raftopoulou and Hall 2004). Our group showed that RhoJ is a small Rho GTPase expressed predominantly in ECs (Herbert, Stekel et al. 2008; Kaur, Leszczynska et al. 2011) and studies described in the previous chapter revealed that RhoJ localises to FAs, regulates their numbers and facilitates EC motility. In turn, data presented in this chapter for the first time identified the RhoJ-binding proteins in ECs and these are known to play important role in the regulation of FA turnover and cell motility.

Firstly RhoJ-binding candidates were pulled-down from the cellular lysates using RhoJ mutants locked either in active or inactive states as fusion proteins with GST. It was expected that the constitutively active GTP-bound RhoJ mutant should bind GAPs or effector proteins, while the dominant negative mutant, which was locked in the nucleotide-free form, should sequester GEFs (Garcia-Mata, Wennerberg et al. 2006). Indeed, mass spectrometry analysis of pull-down samples revealed that RhoJ bound to many proteins including GAPs, GEFs and potential effectors such as those containing CRIB domains or involved in the regulation of cell movement, cytoskeletal rearrangements and regulation of FAs. The most interesting RhoJ-binding candidates included MRCKA, MRCKB, IQGAP1, αPIX, βPIX, GIT1 and scribble (described briefly in the Table 4.2). Among these, of particular interest were GIT1 and PIX proteins since they form a complex which localises to FAs and regulates their disassembly (Zhao, Manser et al. 2000). This complex is targeted to FAs via the c-terminal domain of GIT1, which binds to paxillin (Turner, Brown et al. 1999). α- and βPIX on the other hand are GEFs for Rac1 and Cdc42. Thus RhoJ may be targeted to FAs via its interaction with the GIT1/PIX complex. At first glance it was surprising that α- and βPIX GEFs were pulled-down by the dominant active but not the dominant negative RhoJ mutant.

However, Baird *et al.* demonstrated that dimeric αPIX can bind to activated forms of some Rho GTPases (Baird, Feng et al. 2005). They showed that binding to Cdc42-GTP enhanced the GEF activity of αPIX towards Rac1. On the other hand binding of activated Rac1 to αPIX dimers strongly inhibited their GEF activity towards Rac1 and thus provided a negative feedback loop.

The interactions between RhoJ and its shortlisted binding partners were validated in a Y2H assay which showed that only MRCKA and GIT1 bound directly to the dominant active and wild type RhoJ. However, since both GIT1 and βPIX proteins were detected in the GST-daRhoJ pull-down samples by western blotting, it was concluded that βPIX most likely was precipitated via its binding to GIT1. However, a direct interaction of RhoJ with βPIX while not observed in the Y2H assay may still occur in ECs.

 Based on the Y2H results, attempts were made to map the domain of GIT1 which binds to RhoJ. Firstly, Francesca Edelmann in our laboratory made the c-terminal truncation mutants of GIT1 and she determined that the SHD domain of GIT1 was required for the GIT1-RhoJ interaction (unpublished data). Subsequently, the studies performed here suggested that the SHD domain on its own was not sufficient to bind to RhoJ, indicating that other domains may be necessary for the GIT1-RhoJ interaction. The region located N terminal to the SHD domain contains the Arf GAP domain, a minor paxillin binding site and ankyrin repeats (showed in the Figure 4.4 B). Both the GAP domain and the ankyrin repeats are involved in the localisation of GIT1 to endosomes and other intracellular vesicles (Di Cesare, Paris et al. 2000; Manabe, Kovalenko et al. 2002; Paris, Za et al. 2002), and it was shown that the paxillin/GIT1/PIX/PAK complex localised to intracellular vesicles after FA disassembly (Rosenberger and Kutsche 2006). Since it was demonstrated in the previous chapter that RhoJ localised both to the intracellular vesicles and to FAs in ECs, it might be possible that RhoJ

could traffick with this complex. However, further studies are required to test this hypothesis and to precisely map the domains of GIT1 which bind RhoJ.

In order to investigate the interaction of RhoJ with the GIT1/βPIX complex in ECs immunofluorescence was performed and showed that GFP-RhoJ (both its wild type and dominant active forms) co-localised with endogenous GIT1 and βPIX in FA-like regions. Interestingly, studies by Loo and colleagues showed that both GIT1 and βPIX co-localised with paxillin-positive FAs in an asymmetrical manner, while paxillin and vinculin showed complete co-localisation (Loo, Ng et al. 2004). They suggested that proteins which interact directly with the GIT1/βPIX complex would show a similarly asymmetrical co-localisation with major FA markers. Indeed, this asymmetrical co-localisation pattern was seen for RhoJ co-stained with vinculin-, talin- and pFAK-specific antibodies in HUVECs (Fig. 3.4 and 3.5) thus supporting the hypothesis that RhoJ interacts with the GIT1/βPIX complex.

It was previously reported that in fibroblasts and HeLa cells dominant active mutants of Cdc42 and Rac1 were driving localisation of one of their effector proteins PAK to FAs, and active PAK was then causing a loss of SFs and disassembly of FAs (Manser, Huang et al. 1997). The subsequent studies by Manser *et al.* discovered that βPIX was required for localisation of PAK to these FAs and dominant active Cdc42 mutant was potentiating the amount of βPIX in these structures leading to the Rac1-dependent activation of PAK (Manser, Loo et al. 1998). Experiments described in this chapter revealed that overexpression of active RhoJ similarly increased the amount βPIX and GIT1 in FAs (Fig. 4.5 and 4.6, respectively) and it was previously shown that dominant active RhoJ reduced the number of FAs and SFs in migrating ECs (Fig. 3.12). Thus it is possible that signals which activate RhoJ may potentiate the recruitment of the βPIX/GIT1 complex to FAs and lead to their disassembly by activation of the βPIX/Rac1/PAK pathway. On the other hand the interaction of GIT1 with paxillin can

also promote FA disassembly and it was shown that overexpression of GIT1 increased cell migration (Zhao, Manser et al. 2000; Manabe, Kovalenko et al. 2002; Feng, Baird et al. 2010). Thus an alternative hypothesis is that active RhoJ facilitates EC migration by increasing the amount of the βPIX/GIT1 complex in FAs. Then increased interactions between the βPIX/GIT1 complex and paxillin may promote the FA disassembly.

However, the exact mechanism of RhoJ recruitment to FAs remains unclear. The Y2H experiments indicated that RhoJ binds directly to GIT1. On the other hand, the siRNA knock-down of GIT1 in HUVECs only partially reduced the number of RhoJ-positive FAs, while silencing of βPIX very strongly inhibited localisation of RhoJ to these structures. Interestingly, the overexpression of dominant active RhoJ not only potentiated the amount of βPIX and GIT1 in FAs, but it also increased the total levels of the βPIX protein in HUVECs, suggesting that active RhoJ may stabilise βPIX or positively regulate its expression. Thus it seems evident that RhoJ is linked to the GIT1/βPIX complex when it localises to FAs and the presence of βPIX is crucial to preserve this localisation of RhoJ, but the mechanism for that remains unresolved.

MRCKA and -B are CRIB domain-containing kinases which promote cytoskeletal reorganisation and formation of peripheral focal complexes downstream of Cdc42 (Leung, Chen et al. 1998). RhoJ belongs to the Cdc42-like subfamily of Rho GTPases and when activated it can bind effector proteins containing the CRIB domain (Vignal, De Toledo et al. 2000; Aspenstrom, Fransson et al. 2004). MRCKA and -B were among the strongest RhoJ binding candidates identified here by mass spectrometry and the interaction of MRCKA with RhoJ was later confirmed in the Y2H assay. Interestingly, in the pull-down/mass spectrometry assay RhoJ bound to MRCK but not to the other CRIB domain-containing proteins such as PAK, WASP, or N-WASP which are also present in ECs (Derry, Ochs et al. 1994; Galan

Moya, Le Guelte et al. 2009; Sheldon, Andre et al. 2009; Kang, Wang et al. 2010). Perhaps MRCK is a more specific effector of Cdc42-like Rho GTPases since previous data showed that MRCK strongly bound to active Cdc42 but less so to active Rac1 (Leung, Chen et al. 1998). It is necessary to determine if RhoJ and MRCK interact in ECs and if so, then it will be critical to define physiological relevance of these interactions.

In summary, the GST-RhoJ pull-down/mass spectrometry assay resulted in the identification of potential RhoJ-binding partners in ECs. Among these, the βPIX/GIT1 complex was shown to be important for the localisation of RhoJ to FAs while dominant active RhoJ potentiated the amount of βPIX and GIT1 proteins in these structures. Thus, data presented in this chapter provided the link between RhoJ and proteins which facilitate the FA turnover and cell motility.

5. RHOJ ACTIVATION IN ENDOTHELIAL CELLS

5.1. RhoJ activation

RhoJ is a typical Rho GTPase which cycles between active GTP-bound and inactive GDP-bound states (Vignal, De Toledo et al. 2000). The presence of either a GTP or GDP nucleotide in Rho GTPases determines the difference in the conformation of their so-called Switch I and Switch II regions (Paduch, Jelen et al. 2001). The activation of Rho GTPases is regulated by proteins from the GEF and GAP families, which respond to upstream signals and switch on and off these small G proteins, respectively (Schmidt and Hall 2002; Moon and Zheng 2003). Effector proteins can then recognise only activated Rho GTPases and propagate signals downstream in the cell (Bishop and Hall 2000).

Assays that allow the measurement of various activated Rho GTPases in cellular extracts have been established as summarised by Pellegrin and Mellor (2008). These assays use GST fused with the domains of effector proteins that are known to selectively bind the activated forms of Rho GTPases. The GST-fused effector domain can be loaded onto the glutathione agarose beads and when incubated with cellular extracts should pull-down only active Rho GTPases. Vignal *et al.* showed that active RhoJ can be pulled-down by a CRIB domain from PAK or WASP (Vignal, De Toledo et al. 2000). The CRIB domain was also used by other groups to detect the active levels of Rac1, Rac2, Cdc42, TC10 and TC10β (Sander, van Delft et al. 1998; Benard, Bohl et al. 1999; Haddad, Zugaza et al. 2001; Benard and Bokoch 2002; Chiang, Hou et al. 2002; Aspenstrom, Fransson et al. 2004; Tong, Liss et al. 2007). Since the same effector domain can bind various GTP-bound Rho GTPases, it is crucial that specific antibodies are used to detect the active levels of particular small G proteins (Pellegrin and Mellor 2008).

A range of upstream signals had been found to lead to the activation of Rho GTPases; these include cell surface receptors for various cytokines, growth factors, adhesion molecules or GPCRs (Schwartz 2004). Chiang *et al.* showed that mouse RhoJ (TC10β and TC10βLong), when overexpressed in adipocytes, was activated upon insulin stimulation (Chiang, Hou et al. 2002).

As shown by members of our laboratory, RhoJ is endogenously expressed in ECs (Kaur, Leszczynska et al. 2011), and work described in chapter 3 demonstrated that dominant active RhoJ promotes EC migration and tubule formation – processes which are very important during angiogenesis. Therefore, it was hypothesised that RhoJ might be activated by pro-angiogenic signals.

VEGFA is the most potent ligand of VEGFR2 in promoting angiogenesis and its signalling regulates processes such as cell survival, migration, proliferation, vascular permeability, actin remodelling or FA turnover (Olsson, Dimberg et al. 2006). Another important stimulus, FGF-2, is present in the ECM of blood vessels (Presta, Dell'Era et al. 2005). When various factors activate angiogenesis, the basement membrane is degraded by matrix metallo-proteinases. Then the growth factors trapped in the basement membrane (including FGF-2) are secreted to stimulate the development of new blood vessels (Adams and Alitalo 2007).

The layer of ECs that lines blood vessels is a semi-permeable barrier that allows the exchange of liquid and plasma proteins between the blood and neighbouring tissue (Vandenbroucke, Mehta et al. 2008). The level of permeability of blood vessels can be controlled by various factors including thrombin, TNF-α or lipopolysaccharide (Vandenbroucke, Mehta et al. 2008). It was shown that the presence of thrombin, which is an agonist of GPCRs, is crucial in the regulation of endothelial barrier function and thrombin-induced signalling was shown to

mediate the activity of various Rho GTPases (Beckers, van Hinsbergh et al. 2010; Spindler, Schlegel et al. 2010).

The work presented in this chapter aimed to examine the activation of RhoJ in ECs by pro-angiogenic factors. Firstly, an assay was optimised to detect active RhoJ in ECs and it was subsequently used to measure the levels of active RhoJ in ECs treated with VEGFA, FGF-2 and thrombin. This allowed testing RhoJ activation downstream of two classes of cell-surface receptors: RTKs and GPCRs.

5.2. Optimisation of an assay for the pull-down of active RhoJ in ECs

An assay was optimised to determine levels of active RhoJ in cellular extracts of ECs. A method was adapted from one used for testing the activation of Cdc42 or Rac1 (Erasmus and Braga 2006). This used GST tagged CRIB domains from WASP and PAK proteins, which previously were shown to bind only active RhoJ (Vignal, De Toledo et al. 2000).

To test if this assay would work for pulling-down active RhoJ in ECs, an initial experiment was performed where HUVEC lysate containing endogenous RhoJ was incubated with GTPγS (a stable analogue of GTP) or with GDP, and then RhoJ binding to GST-CRIB was examined. The loading of nucleotides onto Rho GTPases *in vitro* occurs readily in the absence of Mg^{2+}. However, to stop this exchange process, a magnesium ion is required, which coordinates binding of the nucleotide to the appropriate amino acids in the protein (Paduch, Jelen et al. 2001). The amount of magnesium present at the beginning and at the end of nucleotide loading process is thus critical, and this was shown in the following experiments. Initially, GTP/GDP loading was performed in the presence of EDTA, which chelates the positively charged metal ions and therefore reduces the magnesium concentration. However, if these conditions were used during the whole experiment, the nucleotides did not remain
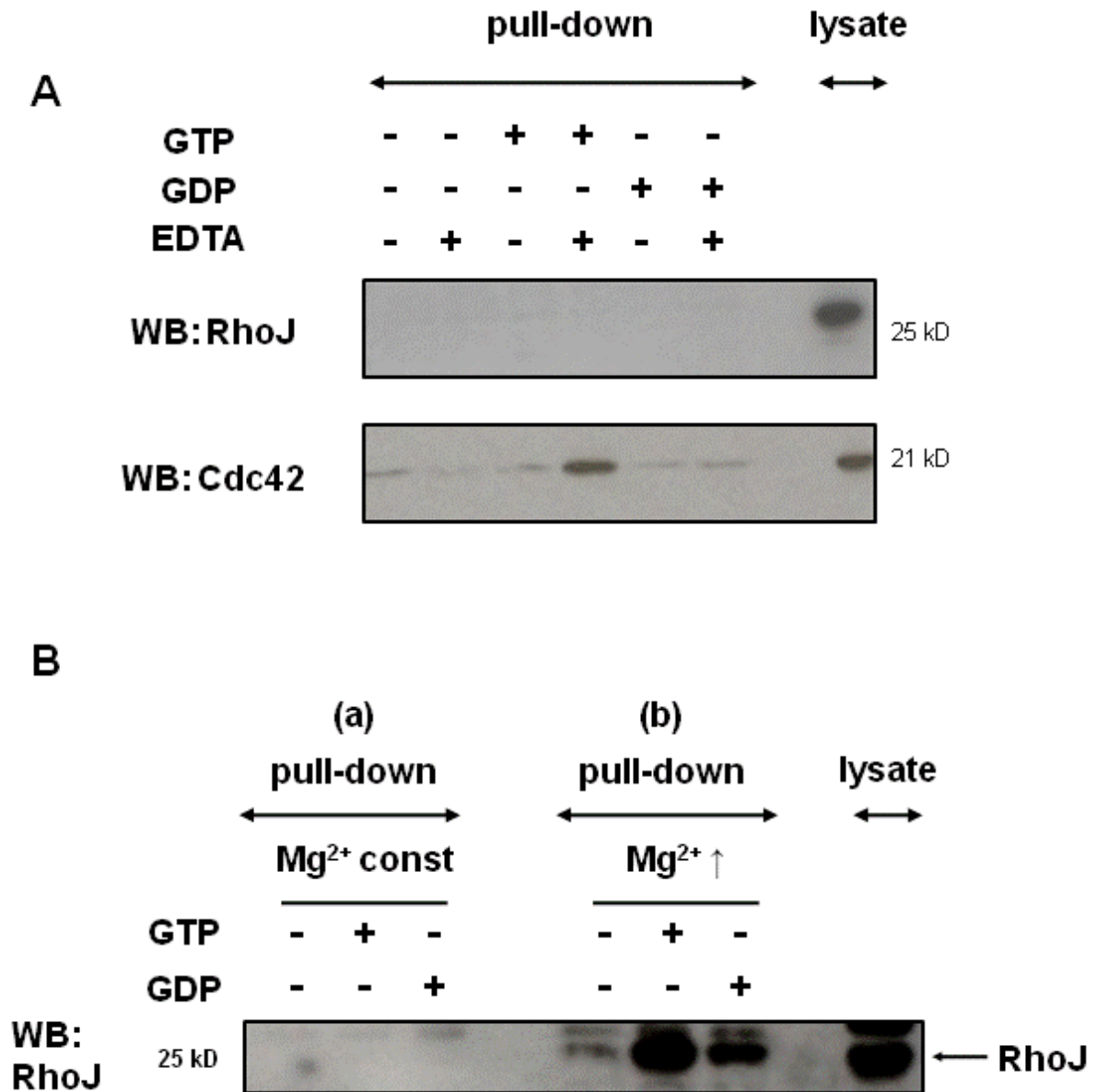
Fig. 5.1 Optimisation of GTP/GDP loading on RhoJ.
A, HUVEC lysates were incubated with GTPγS (GTP) or GDP for 30 min at 30°C in the presence or absence of EDTA, as indicated. Then GST-CRIB (from PAK) bound to glutathione agarose beads was added and the pull-down performed for 1 h at 4 °C. The beads were then washed and resuspended in 2x SDS sample-loading buffer. Samples were subjected to SDS-PAGE and western blotting with RhoJ- and Cdc42-specific antibodies. **B**, Comparison of GTP/GDP locking on RhoJ in the presence of low or high magnesium concentrations. HUVECs lysates were incubated with GTPγS (GTP) or GDP in the presence of EDTA for 30 min at 30 °C (a) or for 10 min at room temperature (b). Then in samples from (b) the concentration of magnesium ions was increased to 30 mM. Active RhoJ was then pulled-down with GST-CRIB (from WASP) bound to glutathione agarose beads for 1 h at 4 °C (for a and b). The beads were then washed and resuspended in 2x SDS sample-loading buffer. Samples were subjected to SDS-PAGE and western blotting with RhoJ-specific antibodies.
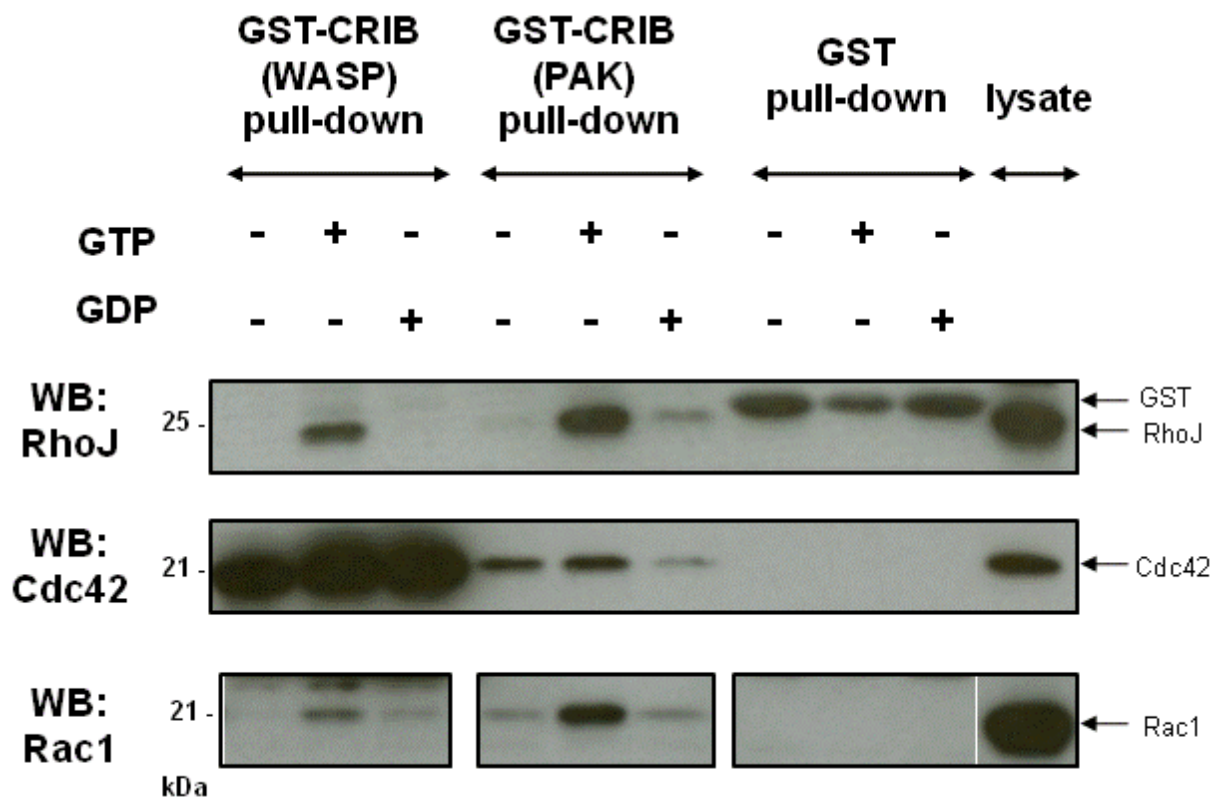
Fig. 5.2 Comparison of pull-down of GTP-loaded RhoJ, Cdc42 and Rac1 from HUVEC lysates by CRIB domains from WASP and PAK.
HUVEC lysates were incubated with GTPγS (GTP) or GDP in the presence of EDTA for 10 min at room temperature. Then the concentration of magnesium ions was increased to 30 mM and pull-downs of active Rho GTPases were performed with GST-CRIB (from WASP or PAK, as indicated) or GST bound to glutathione agarose beads at 4 ºC for 1 h. The beads were then washed and resuspended in 2x SDS sample-loading buffer. Samples were subjected to SDS-PAGE and western blotting with RhoJ, Cdc42 and Rac1- specific antibodies, as indicated.

Fig. 5.3 GTP/GDP loading on endogenous RhoJ in HMEC-1 and on HA-RhoJ expressed in HEK 293Ts.
A, HMEC-1 lysates were incubated with GTPγS (GTP) or GDP in the presence of EDTA for 10 min at room temperature. Then the concentration of magnesium ions was increased to 30 mM and the pull-down of active RhoJ was performed with GST-CRIB (from WASP) bound to glutathione agarose beads at 4 ℃ for 1 h. The beads were then washed and resuspended in 2x SDS sample-loading buffer. Samples were subjected to SDS-PAGE and western blotting with RhoJ- specific antibodies. **B**, HEK 293Ts were transf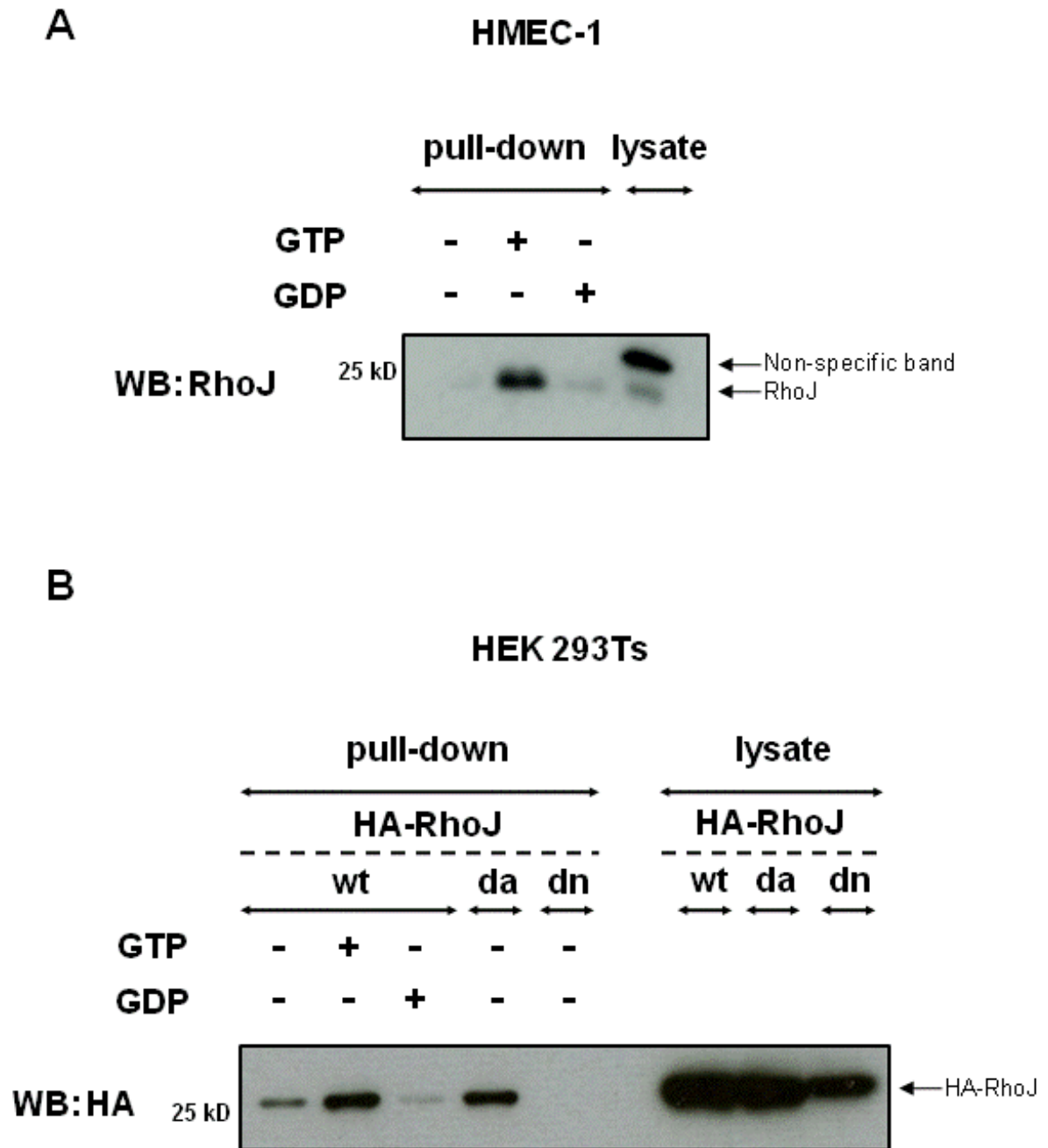ected with plasmids encoding HA-wtRhoJ, HA-daRhoJ or HA-dnRhoJ. Their lysates were subjected to GTP/GDP loading as indicated and GST-CRIB pull-downs using the same conditions as in A. Western blotting was performed with HA-specific antibodies.

bound to RhoJ, and therefore RhoJ was not pulled-down by GST-CRIB (Fig. 5.1 A). In contrast, this low level of Mg^{2+} was enough to keep GTP locked in Cdc42 (Fig. 5.1 A). This is likely to be due to the differences in the magnesium ion coordinating regions of various small G proteins (Paduch, Jelen et al. 2001). However, when the levels of Mg^{2+} were raised to 30 mM after nucleotide loading, this appeared to be sufficient to lock the GTP or GDP in RhoJ and was confirmed by pull-down with GST-CRIB (Fig. 5.1 B).

These conditions of loading GTP or GDP on RhoJ, Cdc42 and Rac1 in HUVEC lysate were confirmed by pull-down with two different fusion proteins containing CRIB domains (from PAK and WASP) (Fig. 5.2). The pull-down of Cdc42 with GST-CRIB from WASP was not specific for the active form of Cdc42 for these conditions, therefore in further studies GST-CRIB from PAK was used, which specifically pulled-down active RhoJ, Cdc42 and Rac1. This assay was also validated for detecting endogenous GTP-loaded RhoJ in HMEC-1 or for HA-RhoJ and flag-RhoJ ectopically expressed in HEK 293Ts (Fig. 5.3, for flag-RhoJ data not shown).

In the following experiments, which aimed to determine the active levels of RhoJ, cell lysis buffer was used, in which the concentration of Mg^{2+} was 30 mM.

5.3. RhoJ activation by pro-angiogenic stimuli

Having established conditions to pull-down active RhoJ, this assay has been used to measure the level of active RhoJ in ECs. The first experiment was to determine whether resting cells, by removing serum and growth factors, would reduce the basal levels of active RhoJ in unstimulated cells. HUVECs were starved for different time periods in medium which lacked growth factors and serum, then cells were harvested and active Rho GTPases were pulled-down by GST-CRIB. The amount of active RhoJ and Cdc42 did not change significantly after
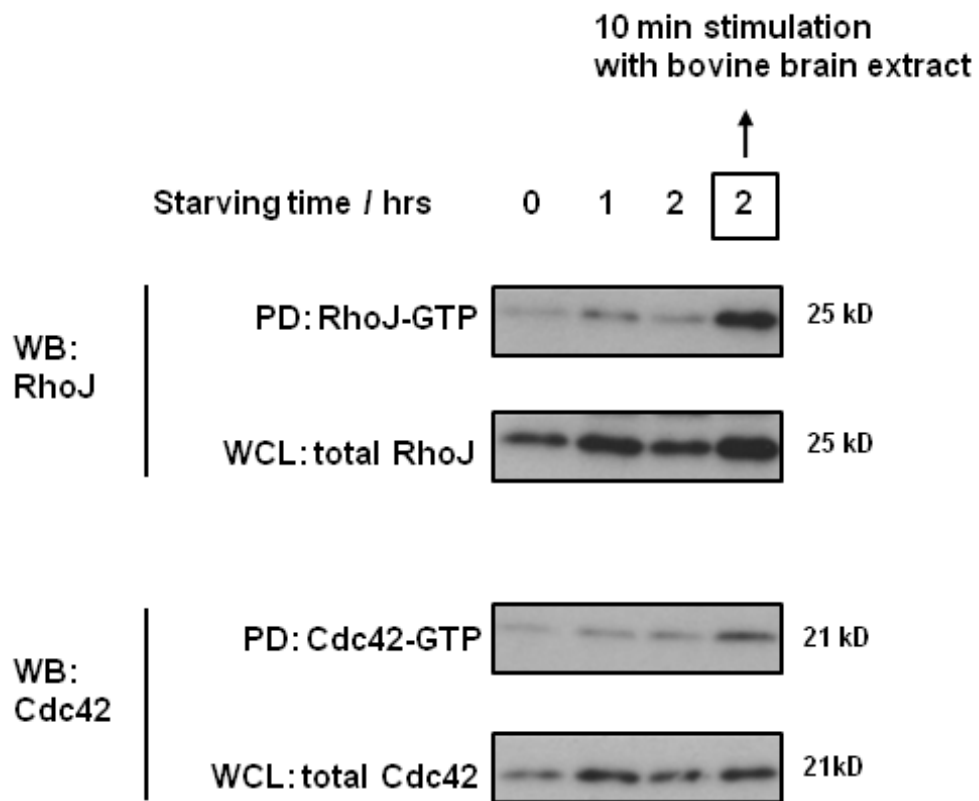
Fig. 5.4 Testing the levels of basal active RhoJ and Cdc42 in HUVECs.
HUVECs were starved by incubation in M199 medium supplemented only with glutamine for different time periods, as indicated. One group of cells starved for 2 h was additionally stimulated for 10 min with 5x bovine brain extract (indicated by arrow). Cells were then lysed and pull-downs of active Rho GTPases were performed with GST-CRIB bound to glutathione agarose beads. Western blotting was performed on pull-down (PD) and whole cell lysate (WCL) samples with anti-RhoJ or anti-Cdc42 antibodies, as indicated. Densitometry was performed and levels of activated Rho GTPases were calculated as PD values relative to WCL values (indicated under western blot images for RhoJ and Cdc42). This experiment was performed only once.

1 and 2 hours of starving in comparison to non-starved cells (Fig. 5.4). Not much was known at this stage about RhoJ "activators", but as a potential positive control, one group of the cells was starved for 2 h and then stimulated with bovine brain extract which contains large amounts of FGF-2 and supports the growth of ECs (Maciag, Cerundolo et al. 1979). In this experiment bovine brain extract was used at a 5-fold higher concentration than that used for HUVECs culture, and this resulted in increased levels of both active RhoJ and Cdc42. Although starving cells for 1 or 2 h did not change the basal levels of active RhoJ and Cdc42, it was shown that these Rho GTPases were clearly activated by bovine brain extract after starvation. Thus in the subsequent experiments cells were rested in the serum- and growth factor-free medium for 1 h prior to stimulation with various factors.

A series of pull-down assays were then performed to test the activation of RhoJ upon stimulation with VEGFA, FGF-2 and thrombin. VEGFA and FGF-2 are very important factors which regulate growth, survival and migration of ECs (Presta, Dell'Era et al. 2005; Olsson, Dimberg et al. 2006). Thrombin, on the other hand, stimulates vascular permeability by inducing reversible loss of adhesion between cell-cell junctions (Vandenbroucke, Mehta et al. 2008).

Stimulation of HUVECs by VEGFA activated both RhoJ and Cdc42, however the kinetics for the activation of these Rho GTPases were different (Fig. 5.5). The activation of Cdc42 was higher than that seen for RhoJ and peaked at 15 min; this was consistent with another report in the literature (Garrett, Van Buul et al. 2007). The activation of RhoJ was more delayed and prolonged, starting at 15 min, peaking at 30 min and then slowly declining (it was still noticeable at around 60 min after VEGF treatment). Stimulation with VEGF was performed 5 times and statistical significance for RhoJ activation was seen at 15 min and for Cdc42 at all time points when compared to 0 min.
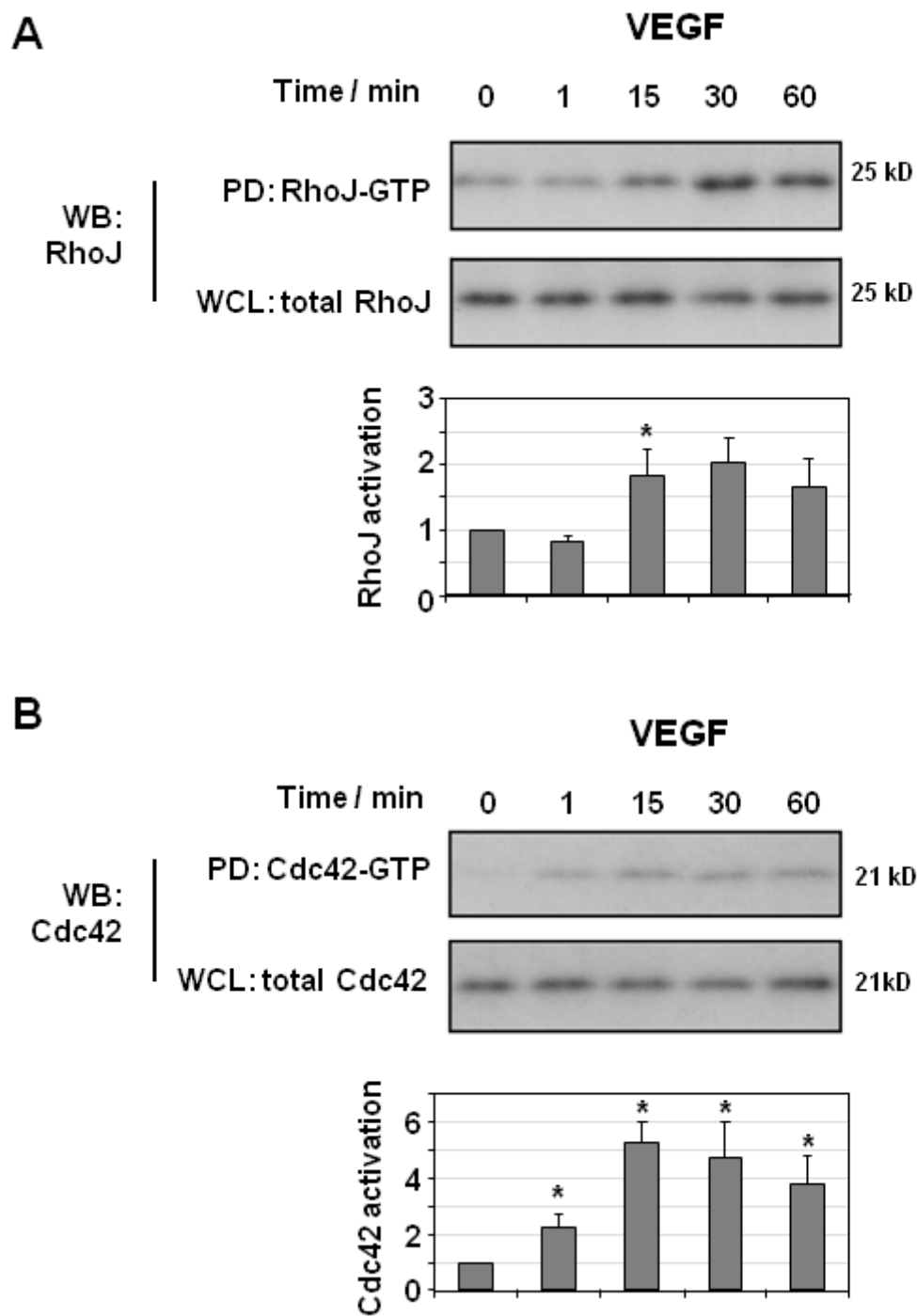
Fig. 5.5 Activation of RhoJ and Cdc42 by VEGF-A in HUVECs.
HUVECs were stimulated with VEGF-A (10 ng/ml) for the times indicated. Active RhoJ (RhoJ-GTP) or Cdc42 (Cdc42-GTP) were pulled-down with GST-CRIB (from PAK). Western blotting was performed on pull-down (PD) and whole cell lysate (WCL) samples with anti-RhoJ (**A**) or anti-Cdc42 (**B**) antibodies, as indicated. Densitometry was performed to determine RhoJ and Cdc42 activation. This was plotted as pulled-down values relative to WCL, where 0 min was normalised to 1; graphs include mean and standard errors derived from 5 independent experiments. The Wilcoxon signed-rank test was used to determine statistical significance of RhoJ or Cdc42 activation for different time points compared with 1 at zero min (* for p<0.05).
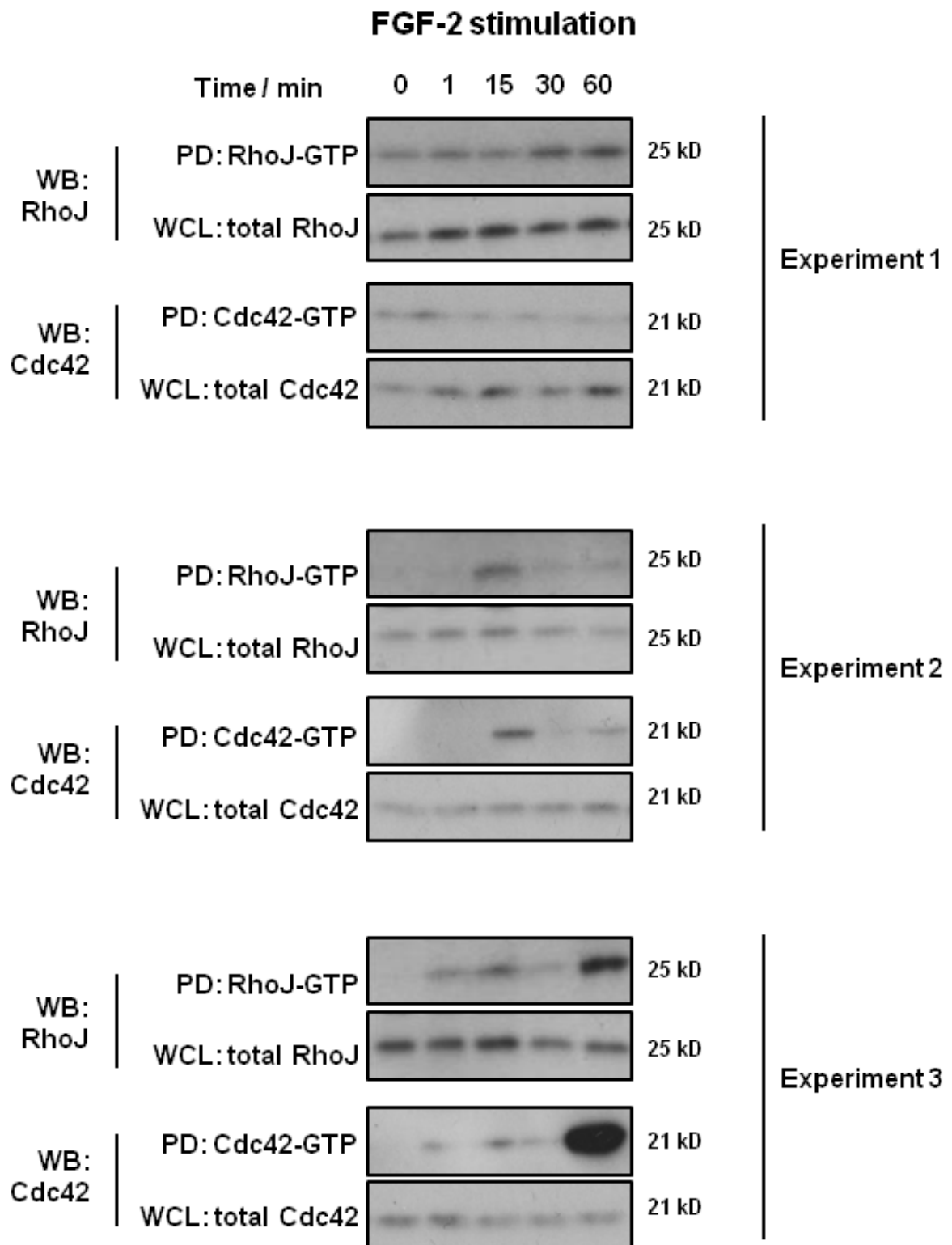
Fig. 5.6 Activation of RhoJ and Cdc42 by FGF-2 in HUVECs.
HUVECs were stimulated with FGF-2 (10 ng/ml) supplemented with 10 µg/ml of heparin for the times indicated. Active RhoJ (RhoJ-GTP) or Cdc42 (Cdc42-GTP) were pulled-down with GST-CRIB (from PAK). Western blotting was performed on pull-down (PD) and whole cell lysate (WCL) samples with RhoJ-specific and Cdc42-specific antibodies, as indicated. The figure shows activation of RhoJ and Cdc42 by FGF-2 in 3 different HUVEC isolates.
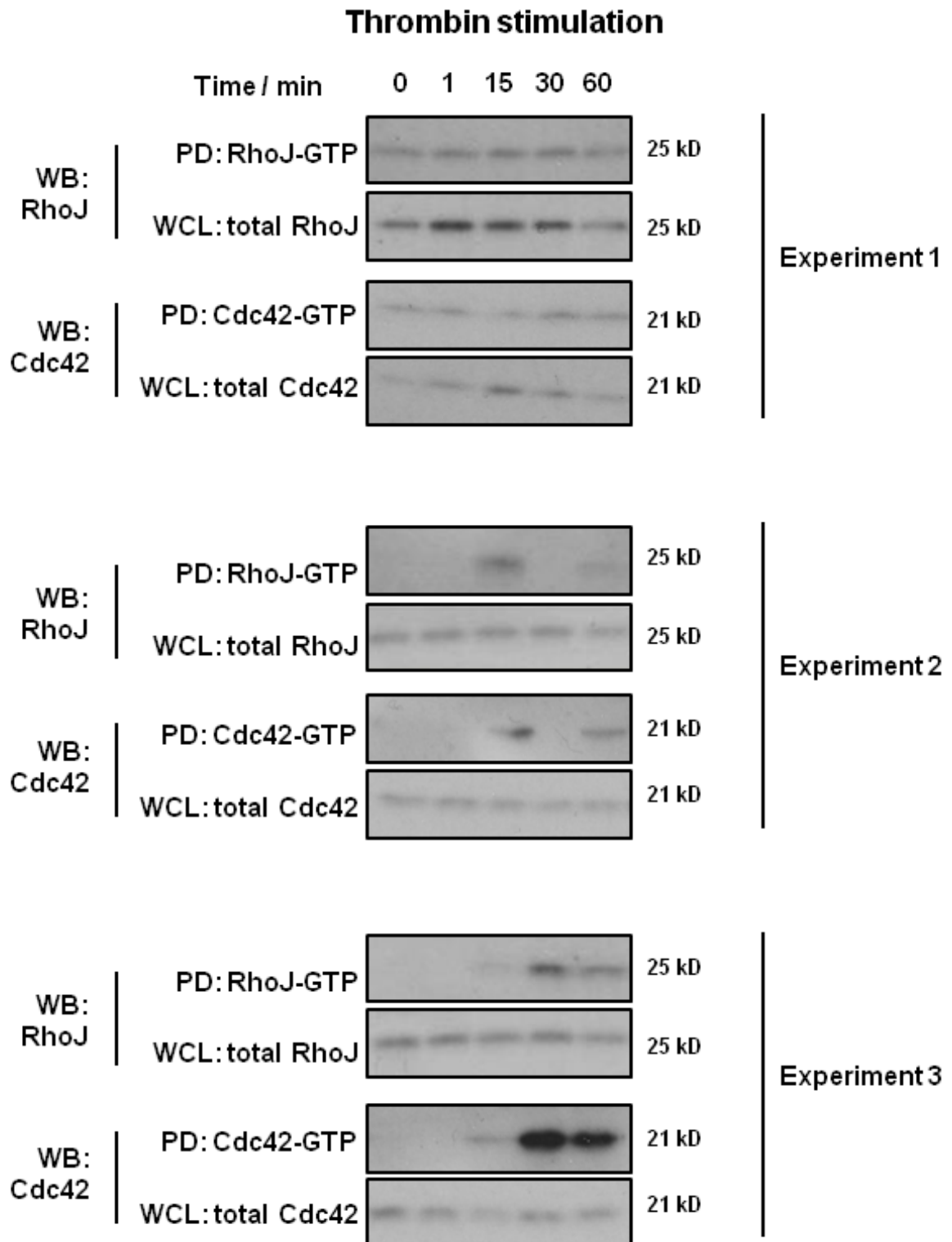
Fig. 5.7 Activation of RhoJ and Cdc42 by thrombin in HUVECs.
HUVECs were stimulated with thrombin (2.5 U/ml) for the times indicated. Active RhoJ (RhoJ-GTP) or Cdc42 (Cdc42-GTP) were pulled-down with GST-CRIB (from PAK). Western blotting was performed on pull-down (PD) and whole cell lysate (WCL) samples with RhoJ-specific and Cdc42-specific antibodies, as indicated. The figure shows activation of RhoJ and Cdc42 by thrombin in 3 different HUVEC isolates.

176

Stimulation by FGF-2 and thrombin was performed in 3 different HUVEC isolates (Fig. 5.6 and 5.7, respectively). FGF-2 activated RhoJ in all three experiments, while the activation of Cdc42 was clear only in experiments 2 and 3 (Fig. 5.6). On the other hand, stimulation with thrombin activated both RhoJ and Cdc42 only in experiments 2 and 3 (Fig. 5.7). The kinetics of RhoJ and Cdc42 activation by FGF-2 and thrombin were not consistent between different HUVEC isolates. However, the activation kinetics for RhoJ stimulated with FGF-2 and thrombin seemed to mirror each other in particular HUVEC donors. Thus it would be important to determine whether these stimuli activate RhoJ through the same signalling pathway. Moreover, the experiments presented here would need to be repeated several times to determine the most commonly observed activation kinetics for RhoJ in HUVECs. The results presented in Fig. 5.6 and 5.7 show evidence that FGF-2 and thrombin are likely to act upstream of RhoJ-mediated signalling pathways in ECs.

5.4. Discussion

It was shown previously that dominant active RhoJ mutant promoted EC migration and *in vitro* tube formation (Fig. 3.11 and 3.10, respectively), and both these processes are very important during angiogenesis which occurs *in vivo* (Adams and Alitalo 2007). Work which is described in this chapter established that RhoJ is activated in ECs by the pro-angiogenic factor VEGFA. In addition, preliminary experiments indicated that FGF-2 and thrombin are also likely to activate RhoJ in these cells.

Some active Rho GTPases can be pulled-down from cellular lysates and therefore their activation by various stimuli can be examined. Here, an assay was optimised to detect levels of active RhoJ in ECs using the CRIB motifs from proteins such as WASP and PAK, which were shown before to bind to active RhoJ (Vignal, De Toledo et al. 2000). Magnesium ions are crucial for maintaining the interaction between Rho GTPases and the guanine nucleotides.

The concentration required for this may vary for different family members (Paduch, Jelen et al. 2001), thus it was important to determine the level of magnesium in the lysis buffer that would preserve the nucleotide-bound RhoJ in cell lysates. It was found that RhoJ requires a higher Mg^{2+} concentration to lock GTPγS or GDP within the protein than Cdc42. This is likely to be due to differences in the amino acid sequences between these two Rho GTPases, which are responsible for nucleotide binding and magnesium ion coordination (Paduch, Jelen et al. 2001).

Once this assay was optimised it was used to investigate the activation of RhoJ in ECs by pro-angiogenic factors such as VEGFA, FGF-2 and thrombin. All of these stimuli activated RhoJ, however only treatment with VEGFA was repeated enough times to obtain statistical significance of this activation. It had been previously reported that VEGFA, which is a potent activator of angiogenesis, activates RhoA, Rac1 and Cdc42 in ECs and the kinetics of these activations vary (Lamalice, Houle et al. 2004; Garrett, Van Buul et al. 2007; Beckers, van Hinsbergh et al. 2010). The activation of Cdc42 and RhoA by VEGFA peaks at around 15 minutes and declines thereafter. On the other hand, Rac1 activation peaks twice, first at around 5 minutes and again at around 30 minutes after VEGFA stimulation. The experiments performed here showed that RhoJ activation by VEGFA occurs with the second peak of Rac1 activation as it is maximal at around 30 min and slowly declines thereafter.

Interestingly, some studies showed that VEGFA activates Rac1 through its GEF, Vav2, and both Vav2 and Rac1 are required for VEGFA-induced EC migration (Soga, Connolly et al. 2001; Garrett, Van Buul et al. 2007). Although it is not clear through which signalling pathway VEGFA activates RhoJ, it was shown that endothelial tubulogenesis is dependent on the presence of RhoJ in an organotypic assay (Kaur, Leszczynska et al. 2011), and in this assay this process strongly depends on the presence of VEGF and FGF-2 (Bishop, Bell et al.

1999). Thus it is possible that endogenous RhoJ is activated by VEGF or by FGF-2 to mediate EC migration and tubulogenesis.

The preliminary experiments indicated that RhoJ can be activated not only downstream of RTKs such as VEGFR or FGF receptor but also by thrombin. This agonist binds to GPCRs such as PAR-1 and leads to their cleavage. This results in the activation of coupled heterotrimeric G-proteins and induction of their down-stream signalling (McLaughlin, Shen et al. 2005). It is known that thrombin initially inactivates Rac1 and induces RhoA activity, which results in increased cell contractility and permeability of the endothelial wall. However, prolonged stimulation with thrombin inhibits RhoA activity and increases levels of active Rac1 and Cdc42, which then signal to restore cellular junctions and endothelial barrier function (Vandenbroucke, Mehta et al. 2008). Since it was shown that RhoJ negatively regulates cell contractility (Kaur, Leszczynska et al. 2011), it is possible that RhoJ might be involved in thrombin-mediated recovery of the EC barrier. However, more experiments need to be performed, firstly to establish the kinetics of RhoJ activation by thrombin, and secondly to determine the physiological relevance of this activation.

In summary, the data presented in this chapter demonstrated that pro-angiogenic factors such as VEGF, FGF-2 and thrombin activate RhoJ in ECs. Thus RhoJ may act downstream of pro-angiogenic factors to regulate angiogenesis *in vivo.*

6. GENERAL DISCUSSION

ECs are critical for the formation of new blood vessels, a process known as angiogenesis (Adams and Alitalo 2007). RhoJ was indicated by our group as a highly endothelial expressed Rho GTPase and has been implicated in EC movement, growth and tube formation, all processes crucial for angiogenesis (Herbert, Stekel et al. 2008; Kaur, Leszczynska et al. 2011). Little was then known about the pathways and proteins that interact with RhoJ in ECs. Thus, the work presented in this thesis aimed to better understand the role of RhoJ in ECs by studying its intracellular localisation and function, determining its binding partners and testing the activation of RhoJ by pro-angiogenic stimuli.

These studies for the first time characterised the localisation of endogenous RhoJ and showed that in ECs it is present in FAs. Previously, members of our laboratory had shown that RhoJ knock-down by siRNA impaired EC migration, tubulogenesis and increased actomyosin contractility and FA numbers (Kaur, Leszczynska et al. 2011). Here, overexpression of the dominant active RhoJ mutant resulted in the converse phenotype to that seen with RhoJ knock-down, thus reinforcing these roles of RhoJ in EC biology. In addition, it was demonstrated that VEGFA, FGF-2 and thrombin activate RhoJ in ECs, suggesting that RhoJ signals downstream of various cell surface receptors including RTKs or GPCRs. GIT1 and PIX proteins, which are known to regulate cell motility and FA turnover, were identified here as RhoJ-binding partners, thus providing a link between the localisation and function of RhoJ in ECs. This work focused on studying the relationship between RhoJ, βPIX and GIT1, however RhoJ could potentially interact with other members of GIT and PIX protein families and this should be taken into consideration in future experiments. The model presented in Fig. 6.1 places RhoJ among the components of FAs and summarises the current understanding of its role in ECs.
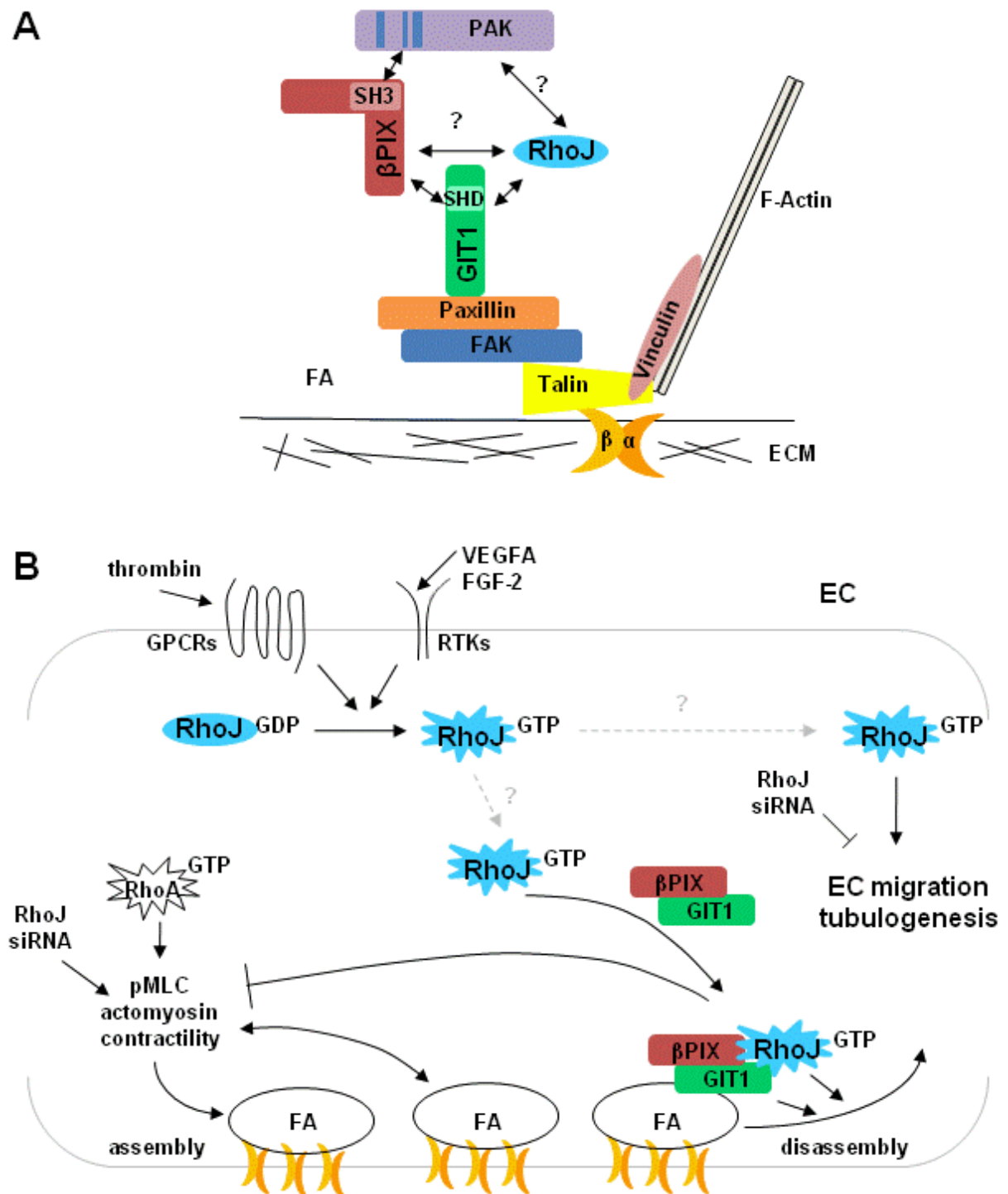
Fig. 6.1 Localisation and function of RhoJ in ECs.
A, The localisation of RhoJ to FAs largely depends on the presence of βPIX and partially on GIT1. RhoJ may interact with βPIX directly or through the interaction with GIT1 or another protein, e.g. PAK. **B**, The role of RhoJ has been studied via its siRNA knock-down (Sukhbir Kaur) or via overexpression of daRhoJ mutant. The loss of RhoJ in ECs caused an increase in actomyosin contractility and formation of FAs and SFs. This resulted in inhibited cell migration and tubulogenesis. On the other hand, overexpression of daRhoJ resulted in the converse phenotype. The proposed mechanism is via recruitment of the GIT1/βPIX complex to FAs, where it promotes FA disassembly and cell migration. This, in turn, is likely to negatively regulate actomyosin contractility.

The processes of SF formation and FA turnover are closely linked during cell migration. SF formation can increase the number and maturation of FAs and, conversely, disassembly of the latter can diminish actomyosin contractility. Reciprocal regulation of these two processes is crucial during directional cell migration (Parsons, Horwitz et al. 2010), and active RhoJ was shown to negatively regulate both FA and SF numbers in migrating ECs. However, the precise mechanism of this RhoJ function is not yet fully understood. Localisation to FAs and the binding partners, FA proteins GIT1 and βPIX, identified in this study lead to the hypothesis that RhoJ is a part of the machinery which regulates the dynamics of FAs, and this in turn would affect actomyosin contractility (Fig. 6.1 B).

GIT1 and βPIX are known to form a tight complex which localises to FAs and promotes FA disassembly and cell migration (Manser, Huang et al. 1997; Manser, Loo et al. 1998; Zhao, Manser et al. 2000; Manabe, Kovalenko et al. 2002; Loo, Ng et al. 2004; Feng, Baird et al. 2010). Although the exact mechanism of the interaction between RhoJ and this complex remains unresolved, it was demonstrated that RhoJ co-localises with these proteins in ECs and the presence of βPIX promotes the localisation of endogenous RhoJ to FAs. In addition, the role of RhoJ in the recruitment of GIT1 and βPIX to FAs has been demonstrated, as overexpression of daRhoJ increased the amount of these proteins in FAs. Thus, as a next step, it will be critical to establish whether the function of RhoJ in ECs is mediated via its interaction with the GIT1/βPIX complex. To address this question, ECs expressing daRhoJ could be treated with either βPIX- or GIT1-specific siRNAs. If daRhoJ promotes EC migration and decreases FA/SF numbers via interaction with the GIT1/βPIX complex, then knocking-down either βPIX or GIT1 in these cells should abrogate the effects of daRhoJ. It would be also crucial to prove that RhoJ binds directly to GIT1 or βPIX in ECs. This could be achieved using a fluorescence resonance energy transfer (FRET) technique, which allows the

detection of interactions between two molecules which are in the proximity of up to 10 nm (Ciruela 2008).

Providing that the functions of the GIT1/βPIX complex and RhoJ are interdependent in ECs, it would be important to dissect in detail the mechanism and direct consequence of their interaction. Some studies indicated that binding of GIT1 to paxillin promotes FA disassembly and increases the rate of cell migration (Zhao, Manser et al. 2000; Manabe, Kovalenko et al. 2002; Feng, Baird et al. 2010), and it was demonstrated here that daRhoJ also decreases FA numbers and promotes EC migration. The Y2H experiment showed that RhoJ can physically bind to GIT1 and it was hoped that mapping the GIT1 domain which binds RhoJ would help to elucidate the context of these interactions. This would also allow the design of a peptide or a dominant negative GIT1 mutant, which when introduced to ECs could disrupt the interaction between endogenous RhoJ and GIT1. However, the interaction between these proteins seems to be more complex in ECs. siRNA studies showed that although GIT1 plays some role in RhoJ localisation to FAs, its presence was not critical for this process, as GIT1 knock-down only partially reduced the localisation of RhoJ to these structures. On the other hand, the knock-down of βPIX nearly abolished RhoJ localisation to FAs suggesting that, although not seen in a Y2H system, the interaction between RhoJ and βPIX may still occur in ECs.

PIX proteins are known GEFs for Cdc42 and Rac1 (Rosenberger and Kutsche 2006), and since the interplay between RhoJ and βPIX was demonstrated in ECs, it is possible that βPIX acts as a GEF for RhoJ. A pilot experiment which tested the basal level of active RhoJ in ECs after βPIX knock-down was performed, but no decrease in steady state RhoJ activation was observed (data not shown). The GEF activity of βPIX can be enhanced by Src-mediated

phosphorylation (Feng, Baird et al. 2006), and it would be useful to determine if βPIX participates as a GEF in VEGF-, FGF-2- or thrombin-mediated activation of RhoJ.

The GIT1/βPIX complex acts as a scaffold, which brings various proteins into close proximity (Frank and Hansen 2008). GIT1 is recruited to FAs via its c-terminal domain which directly binds to paxillin (Turner, Brown et al. 1999; Manabe, Kovalenko et al. 2002). βPIX, being a GEF, binds to Cdc42 and Rac1, as well as to their effector, PAK, which is known to promote EC motility (Galan Moya, Le Guelte et al. 2009). The interaction between RhoJ and PAK has not been investigated in these studies. Nevertheless, evidence suggests that the function of both proteins may overlap in ECs and others have demonstrated binding of daRhoJ to PAK in a Y2H assay (Vignal, De Toledo et al. 2000; Aspenstrom, Fransson et al. 2004). It was shown that the dominant active Cdc42 mutant increases the amount of βPIX in FAs, which then recruits PAK and leads to Rac1-dependent activation of PAK and subsequent loss of SFs and FAs (Manser, Huang et al. 1997; Manser, Loo et al. 1998). Since daRhoJ similarly potentiates the amount of βPIX in FAs, increased migration seen in ECs overexpressing daRhoJ may be caused by increased activity of PAK.

Given that RhoJ was indicated as a component of FA complexes, it may be regulated by general signals which modulate the dynamics of these structures. Various factors, including integrin clustering or stimulation by growth factors, were shown to activate FAK and Src (Rodriguez-Fernandez 1999), and these kinases are crucial for cell migration and FA disassembly (Tomar and Schlaepfer 2009). Some studies showed that GIT1 can directly bind to FAK (Zhao, Manser et al. 2000), and when phosphorylated in a FAK and Src dependent manner GIT1 facilitates FA disassembly (van Nieuw Amerongen, Natarajan et al. 2004). In addition, FAK recruits and participates in activation of various GAPs and GEFs, which in turn control the activity of RhoA and Rac1, and therefore regulate cell migration (Tomar and

Schlaepfer 2009). If GIT1 or PIX bring RhoJ to the close proximity of FAK, conceivably RhoJ could be a substrate of FAK-recruited GAPs and GEFs. Thus, it would be important to explore a potential interaction of RhoJ with FA components other than βPIX and GIT1.

The overexpression of RhoJ clearly drives its localisation not only to FAs, but also to the plasma membrane and endosomal, lysosomal and other intracellular vesicles. Furthermore, the involvement of endogenous RhoJ in Tf recycling to the plasma membrane and its release in ECs has been demonstrated, thus indicating that RhoJ might play a role in endocytic pathways in ECs. Various studies showed that components of disassembling FAs such as paxillin, βPIX, GIT1 and PAK are firstly internalised, and then recycled to the plasma membrane, where they eventually join the newly forming FAs (Di Cesare, Paris et al. 2000; Matafora, Paris et al. 2001; Manabe, Kovalenko et al. 2002). In some cases, these complexes traffick through endosomes (Di Cesare, Paris et al. 2000; Matafora, Paris et al. 2001), while in other cases they are recycled through undefined cytoplasmic punctate structures (Manabe, Kovalenko et al. 2002). Although the staining of endogenous RhoJ indicated its localisation to FAs it cannot be excluded that under certain conditions this protein may also be found in intracellular vesicles. It is possible that RhoJ may co-localise with GIT1/βPIX containing cytoplasmic complexes and further detailed analyses are required to test this hypothesis.

Although GIT1 expression is not specific to ECs, some studies indicated its importance in the vasculature. The knock-out of this gene in mice caused severe malformation of pulmonary vasculature, observed as a pronounced reduction of pulmonary blood vessel numbers and an increase of alveolar spaces (Pang, Hoefen et al. 2009). It would be interesting to examine whether ECs isolated from GIT1$^{-/-}$ mice would migrate at normal speed and whether overexpression of daRhoJ would affect migration and FA/SF dynamics in these cells. This would additionally test interdependence between RhoJ and GIT1 function.

186

Another study by Wang and colleagues showed that GIT1 mediates VEGF-induced formation of podosomes in ECs (Wang, Taba et al. 2009). These actin-rich structures are a distinct type of adhesions, important in highly motile cells (Albiges-Rizo, Destaing et al. 2009). Interestingly, Billottet *et al.* tested the influence of activated Rho GTPases on podosome formation in ECs and found that overexpression of the daRhoJ mutant induced development of these adhesion structures (Billottet, Rottiers et al. 2008). Since VEGF was shown to activate RhoJ in ECs it would be important to verify if RhoJ participates in VEGF/GIT1 mediated podosome formation. Wang *et al.* (2009) also demonstrated that GIT1 knock-down strongly inhibited EC migration in a scratch wound assay, and a similar effect was seen with RhoJ knock-down (Kaur, Leszczynska et al. 2011). This supports the hypothesis that RhoJ and GIT1 may be involved in the same signalling pathway in ECs.

RhoJ knock-down and overexpression of daRhoJ indicated that this Rho GTPase negatively regulates EC contractility (Kaur, Leszczynska et al. 2011). As mentioned before, this might be a consequence of reduced FA numbers. Alternatively, RhoJ may directly regulate a signalling pathway which controls actomyosin contractile forces. Nishizuka and colleagues (2003) screened for genes which were up-regulated in NIH-3T3 mouse fibroblasts stably overexpressing RhoJ. They found that overexpression of RhoJ increased the level of another Rho GTPase, RhoE, and RhoE is known to negatively regulate SFs and cell contractility by activating p190RhoGAP, which inactivates RhoA (Wennerberg, Forget et al. 2003) or by directly binding to and inhibiting the RhoA effector ROCK I (Riento, Guasch et al. 2003). If, similarly, RhoJ up-regulates RhoE expression in ECs, then it may negatively regulate actomyosin contractility and therefore facilitate EC migration via RhoE. Nonetheless, RhoJ may reduce cell contractility through various signalling pathways and its exact role in this mechanism needs to be determined.

So far, the importance of RhoJ function was elucidated in ECs *in vitro*, however its role *in vivo* remains uncertain. It has been demonstrated that daRhoJ enhanced EC sprouting in an organotypic assay (Kaur, Leszczynska et al. 2011). Furthermore, active RhoJ down-regulated the number of SFs and FAs particularly in highly motile ECs situated at the leading edge of a scratch. These observations suggest that RhoJ may play a particular role in the tip cells of sprouting capillaries. Generation of RhoJ knock-out mouse model would help to identify *in vivo* function of RhoJ.

RhoJ is also expressed in ECs of already established blood vessels, as shown by *in situ* hybridisation on human tissue sections (Kaur, Leszczynska et al. 2011). Quiescent ECs lining the wall of blood vessel, provide a semi-permeable barrier which allows the exchange of various metabolites or trespassing of other cells to the adjacent tissues (Bogatcheva and Verin 2008). The integrity of the endothelial wall is maintained by the cortical actin, which forms a ring of filaments connecting cell-cell adhesions and FAs. The induction of cell permeability causes RhoA-mediated formation of SFs and temporary disorganisation of cortical actin and cell-cell junctions (Bogatcheva and Verin 2008). It was shown that GIT1 is recruited to FAs and reverses thrombin-induced and RhoA-dependent contractility of ECs, suggesting that it plays a role in the recovery of the endothelial barrier function (van Nieuw Amerongen, Natarajan et al. 2004). It was demonstrated here that thrombin can activate RhoJ in ECs and that the daRhoJ mutant both enhances the localisation of GIT1 to FAs and negatively regulates EC contractility. Thus, it might be possible that these proteins act together to regulate the permeability of established blood vessels, but the link between RhoJ and GIT1 in this process needs to be examined.

In summary, the work presented in this thesis provides information on endogenous localisation, function, and binding partners of RhoJ in ECs. These data support the hypothesis

that RhoJ is an important player in ECs. They demonstrate its activation by pro-angiogenic stimuli. They also demonstrate FA localisation, a role in FA turnover and actomyosin contractility and interaction with the FA proteins GIT1 and βPIX, proteins also involved in FA turnover. These findings form the basis for a potential mechanism of RhoJ action in EC migration. They contribute to our fundamental understanding of EC behaviour and biology and form the basis for future studies which will more precisely determine the mechanism of RhoJ function.

LIST OF REFERENCES

Abecassis, I., B. Olofsson, et al. (2003). "RhoA induces MMP-9 expression at CD44 lamellipodial focal complexes and promotes HMEC-1 cell invasion." Exp Cell Res **291**(2): 363-76.

Abraham, S., M. Yeo, et al. (2009). "VE-Cadherin-mediated cell-cell interaction suppresses sprouting via signaling to MLC2 phosphorylation." Curr Biol **19**(8): 668-74.

Adachi, H. and M. Tsujimoto (2006). "Endothelial scavenger receptors." Prog Lipid Res **45**(5): 379-404.

Adams, R. H. and K. Alitalo (2007). "Molecular regulation of angiogenesis and lymphangiogenesis." Nat Rev Mol Cell Biol **8**(6): 464-78.

Ades, E. W., F. J. Candal, et al. (1992). "HMEC-1: establishment of an immortalized human microvascular endothelial cell line." J Invest Dermatol **99**(6): 683-90.

Adini, I., I. Rabinovitz, et al. (2003). "RhoB controls Akt trafficking and stage-specific survival of endothelial cells during vascular development." Genes Dev **17**(21): 2721-32.

Adra, C. N., A. R. Iyengar, et al. (1998). "Human ARHGDIG, a GDP-dissociation inhibitor for Rho proteins: genomic structure, sequence, expression analysis, and mapping to chromosome 16p13.3." Genomics **53**(1): 104-9.

Albiges-Rizo, C., O. Destaing, et al. (2009). "Actin machinery and mechanosensitivity in invadopodia, podosomes and focal adhesions." J Cell Sci **122**(Pt 17): 3037-49.

Alitalo, K., T. Tammela, et al. (2005). "Lymphangiogenesis in development and human disease." Nature **438**(7070): 946-53.

Amano, M., K. Chihara, et al. (1997). "Formation of actin stress fibers and focal adhesions enhanced by Rho-kinase." Science **275**(5304): 1308-11.

Aronheim, A., Y. C. Broder, et al. (1998). "Chp, a homologue of the GTPase Cdc42Hs, activates the JNK pathway and is implicated in reorganizing the actin cytoskeleton." Curr Biol **8**(20): 1125-8.

Arthur, W. T. and K. Burridge (2001). "RhoA inactivation by p190RhoGAP regulates cell spreading and migration by promoting membrane protrusion and polarity." Mol Biol Cell **12**(9): 2711-20.

Arthur, W. T., S. M. Ellerbroek, et al. (2002). "XPLN, a guanine nucleotide exchange factor for RhoA and RhoB, but not RhoC." J Biol Chem **277**(45): 42964-72.

Aspenstrom, P., A. Fransson, et al. (2004). "Rho GTPases have diverse effects on the organization of the actin filament system." Biochem J **377**(Pt 2): 327-37.

Aspenstrom, P., A. Ruusala, et al. (2007). "Taking Rho GTPases to the next level: the cellular functions of atypical Rho GTPases." Exp Cell Res **313**(17): 3673-9.

Audebert, S., C. Navarro, et al. (2004). "Mammalian Scribble forms a tight complex with the betaPIX exchange factor." Curr Biol **14**(11): 987-95.

Bagrodia, S., D. Bailey, et al. (1999). "A tyrosine-phosphorylated protein that binds to an important regulatory region on the cool family of p21-activated kinase-binding proteins." J Biol Chem **274**(32): 22393-400.

Bagrodia, S., S. J. Taylor, et al. (1998). "A novel regulator of p21-activated kinases." J Biol Chem **273**(37): 23633-6.

Baird, D., Q. Feng, et al. (2005). "The Cool-2/alpha-Pix protein mediates a Cdc42-Rac signaling cascade." Curr Biol **15**(1): 1-10.

Bamburg, J. R. (1999). "Proteins of the ADF/cofilin family: essential regulators of actin dynamics." Annu Rev Cell Dev Biol **15**: 185-230.

Bartel, P., C. T. Chien, et al. (1993). "Elimination of false positives that arise in using the two-hybrid system." Biotechniques **14**(6): 920-4.

Bayless, K. J. and G. E. Davis (2002). "The Cdc42 and Rac1 GTPases are required for capillary lumen formation in three-dimensional extracellular matrices." J Cell Sci **115**(Pt 6): 1123-36.

Bazzoni, G. and E. Dejana (2004). "Endothelial cell-to-cell junctions: molecular organization and role in vascular homeostasis." Physiol Rev **84**(3): 869-901.

Beckers, C. M., V. W. van Hinsbergh, et al. (2010). "Driving Rho GTPase activity in endothelial cells regulates barrier integrity." Thromb Haemost **103**(1): 40-55.

Bellovin, D. I., K. J. Simpson, et al. (2006). "Reciprocal regulation of RhoA and RhoC characterizes the EMT and identifies RhoC as a prognostic marker of colon carcinoma." Oncogene **25**(52): 6959-67.

Benard, V., B. P. Bohl, et al. (1999). "Characterization of rac and cdc42 activation in chemoattractant-stimulated human neutrophils using a novel assay for active GTPases." J Biol Chem **274**(19): 13198-204.

Benard, V. and G. M. Bokoch (2002). "Assay of Cdc42, Rac, and Rho GTPase activation by affinity methods." Methods Enzymol **345**: 349-59.

Benitah, S. A., M. Frye, et al. (2005). "Stem cell depletion through epidermal deletion of Rac1." Science 309(5736): 933-5.

Benninger, Y., T. Thurnherr, et al. (2007). "Essential and distinct roles for cdc42 and rac1 in the regulation of Schwann cell biology during peripheral nervous system development." J Cell Biol 177(6): 1051-61.

Berthold, J., K. Schenkova, et al. (2008). "Rho GTPases of the RhoBTB subfamily and tumorigenesis." Acta Pharmacol Sin 29(3): 285-95.

Billottet, C., P. Rottiers, et al. (2008). "Regulatory signals for endothelial podosome formation." Eur J Cell Biol 87(8-9): 543-54.

Birukova, A. A., D. Adyshev, et al. (2006). "GEF-H1 is involved in agonist-induced human pulmonary endothelial barrier dysfunction." Am J Physiol Lung Cell Mol Physiol 290(3): L540-8.

Bishop, A. L. and A. Hall (2000). "Rho GTPases and their effector proteins." Biochem J 348 Pt 2: 241-55.

Bishop, E. T., G. T. Bell, et al. (1999). "An in vitro model of angiogenesis: basic features." Angiogenesis 3(4): 335-44.

Bogatcheva, N. V. and A. D. Verin (2008). "The role of cytoskeleton in the regulation of vascular endothelial barrier function." Microvasc Res 76(3): 202-7.

Bosco, E. E., J. C. Mulloy, et al. (2009). "Rac1 GTPase: a "Rac" of all trades." Cell Mol Life Sci 66(3): 370-4.

Boureux, A., E. Vignal, et al. (2007). "Evolution of the Rho family of ras-like GTPases in eukaryotes." Mol Biol Evol 24(1): 203-16.

Brady, D. C., J. K. Alan, et al. (2009). "The transforming Rho family GTPase Wrch-1 disrupts epithelial cell tight junctions and epithelial morphogenesis." Mol Cell Biol 29(4): 1035-49.

Brown, M. D. and D. B. Sacks (2006). "IQGAP1 in cellular signaling: bridging the GAP." Trends Cell Biol 16(5): 242-9.

Brunet, N., A. Morin, et al. (2002). "RhoGDI-3 regulates RhoG and targets this protein to the Golgi complex through its unique N-terminal domain." Traffic 3(5): 342-57.

Bryan, B. A. and P. A. D'Amore (2007). "What tangled webs they weave: Rho-GTPase control of angiogenesis." Cell Mol Life Sci 64(16): 2053-65.

Bryan, B. A., E. Dennstedt, et al. (2010). "RhoA/ROCK signaling is essential for multiple aspects of VEGF-mediated angiogenesis." Faseb J 24(9): 3186-95.

Campellone, K. G. and M. D. Welch (2010). "A nucleator arms race: cellular control of actin assembly." Nat Rev Mol Cell Biol 11(4): 237-51.

Cappello, S., A. Attardo, et al. (2006). "The Rho-GTPase cdc42 regulates neural progenitor fate at the apical surface." Nat Neurosci 9(9): 1099-107.

Carmeliet, P. (2003). "Angiogenesis in health and disease." Nat Med 9(6): 653-60.

Carmeliet, P., F. De Smet, et al. (2009). "Branching morphogenesis and antiangiogenesis candidates: tip cells lead the way." Nat Rev Clin Oncol 6(6): 315-26.

Cascone, I., E. Giraudo, et al. (2003). "Temporal and spatial modulation of Rho GTPases during in vitro formation of capillary vascular network. Adherens junctions and myosin light chain as targets of Rac1 and RhoA." J Biol Chem 278(50): 50702-13.

Caswell, P. T., S. Vadrevu, et al. (2009). "Integrins: masters and slaves of endocytic transport." Nat Rev Mol Cell Biol 10(12): 843-53.

Chardin, P. (2006). "Function and regulation of Rnd proteins." Nat Rev Mol Cell Biol 7(1): 54-62.

Chen, F., L. Ma, et al. (2000). "Cdc42 is required for PIP(2)-induced actin polymerization and early development but not for cell viability." Curr Biol 10(13): 758-65.

Chen, L., G. Liao, et al. (2007). "Rac1 controls the formation of midline commissures and the competency of tangential migration in ventral telencephalic neurons." J Neurosci 27(14): 3884-93.

Chen, L., G. Liao, et al. (2006). "Cdc42 deficiency causes Sonic hedgehog-independent holoprosencephaly." Proc Natl Acad Sci U S A 103(44): 16520-5.

Chen, R. H., S. Corbalan-Garcia, et al. (1997). "The role of the PH domain in the signal-dependent membrane targeting of Sos." Embo J 16(6): 1351-9.

Chenette, E. J., N. Y. Mitin, et al. (2006). "Multiple sequence elements facilitate Chp Rho GTPase subcellular location, membrane association, and transforming activity." Mol Biol Cell 17(7): 3108-21.

Chenna, R., H. Sugawara, et al. (2003). "Multiple sequence alignment with the Clustal series of programs." Nucleic Acids Res 31(13): 3497-500.

Cherfils, J. and P. Chardin (1999). "GEFs: structural basis for their activation of small GTP-binding proteins." Trends Biochem Sci 24(8): 306-11.

Chesarone, M. A., A. G. DuPage, et al. (2010). "Unleashing formins to remodel the actin and microtubule cytoskeletons." Nat Rev Mol Cell Biol 11(1): 62-74.

191

Chiang, S. H., C. A. Baumann, et al. (2001). "Insulin-stimulated GLUT4 translocation requires the CAP-dependent activation of TC10." Nature **410**(6831): 944-8.

Chiang, S. H., J. C. Hou, et al. (2002). "Cloning and functional characterization of related TC10 isoforms, a subfamily of Rho proteins involved in insulin-stimulated glucose transport." J Biol Chem **277**(15): 13067-73.

Cho, Y. J., B. Zhang, et al. (2005). "Generation of rac3 null mutant mice: role of Rac3 in Bcr/Abl-caused lymphoblastic leukemia." Mol Cell Biol **25**(13): 5777-85.

Chrostek, A., X. Wu, et al. (2006). "Rac1 is crucial for hair follicle integrity but is not essential for maintenance of the epidermis." Mol Cell Biol **26**(18): 6957-70.

Chuang, Y. Y., A. Valster, et al. (2007). "The atypical Rho family GTPase Wrch-1 regulates focal adhesion formation and cell migration." J Cell Sci **120**(Pt 11): 1927-34.

Ciruela, F. (2008). "Fluorescence-based methods in the study of protein-protein interactions in living cells." Curr Opin Biotechnol **19**(4): 338-43.

Claing, A., S. J. Perry, et al. (2000). "Multiple endocytic pathways of G protein-coupled receptors delineated by GIT1 sensitivity." Proc Natl Acad Sci U S A **97**(3): 1119-24.

Clark, E. A., T. R. Golub, et al. (2000). "Genomic analysis of metastasis reveals an essential role for RhoC." Nature **406**(6795): 532-5.

Clemens, M. J. (2005). "Translational control in virus-infected cells: models for cellular stress responses." Semin Cell Dev Biol **16**(1): 13-20.

Coisy-Quivy, M., O. Touzet, et al. (2009). "TC10 controls human myofibril organization and is activated by the sarcomeric RhoGEF obscurin." J Cell Sci **122**(Pt 7): 947-56.

Connolly, J. O., N. Simpson, et al. (2002). "Rac regulates endothelial morphogenesis and capillary assembly." Mol Biol Cell **13**(7): 2474-85.

Corbetta, S., S. Gualdoni, et al. (2005). "Generation and characterization of Rac3 knockout mice." Mol Cell Biol **25**(13): 5763-76.

Cote, J. F. and K. Vuori (2002). "Identification of an evolutionarily conserved superfamily of DOCK180-related proteins with guanine nucleotide exchange activity." J Cell Sci **115**(Pt 24): 4901-13.

Davis, G. E., W. Koh, et al. (2007). "Mechanisms controlling human endothelial lumen formation and tube assembly in three-dimensional extracellular matrices." Birth Defects Res C Embryo Today **81**(4): 270-85.

Dayanir, V., R. D. Meyer, et al. (2001). "Identification of tyrosine residues in vascular endothelial growth factor receptor-2/FLK-1 involved in activation of phosphatidylinositol 3-kinase and cell proliferation." J Biol Chem **276**(21): 17686-92.

De Smet, F., I. Segura, et al. (2009). "Mechanisms of vessel branching: filopodia on endothelial tip cells lead the way." Arterioscler Thromb Vasc Biol **29**(5): 639-49.

de Toledo, M., F. Senic-Matuglia, et al. (2003). "The GTP/GDP cycling of rho GTPase TCL is an essential regulator of the early endocytic pathway." Mol Biol Cell **14**(12): 4846-56.

del Rio, A., R. Perez-Jimenez, et al. (2009). "Stretching single talin rod molecules activates vinculin binding." Science **323**(5914): 638-41.

Del Toro, R., C. Prahst, et al. (2010). "Identification and functional analysis of endothelial tip cell-enriched genes." Blood **116**(19): 4025-33.

Del Valle-Perez, B., V. G. Martinez, et al. (2010). "Filamin B plays a key role in vascular endothelial growth factor-induced endothelial cell motility through its interaction with Rac-1 and Vav-2." J Biol Chem **285**(14): 10748-60.

Derry, J. M., H. D. Ochs, et al. (1994). "Isolation of a novel gene mutated in Wiskott-Aldrich syndrome." Cell **79**(5): following 922.

Dharmawardhane, S., A. Schurmann, et al. (2000). "Regulation of macropinocytosis by p21-activated kinase-1." Mol Biol Cell **11**(10): 3341-52.

Di Cesare, A., S. Paris, et al. (2000). "p95-APP1 links membrane transport to Rac-mediated reorganization of actin." Nat Cell Biol **2**(8): 521-30.

Doherty, G. J. and H. T. McMahon (2009). "Mechanisms of endocytosis." Annu Rev Biochem **78**: 857-902.

Donovan, D., N. J. Brown, et al. (2001). "Comparison of three in vitro human 'angiogenesis' assays with capillaries formed in vivo." Angiogenesis **4**(2): 113-21.

Dorn, T., U. Kuhn, et al. (2007). "RhoH is important for positive thymocyte selection and T-cell receptor signaling." Blood **109**(6): 2346-55.

Dow, L. E., J. S. Kauffman, et al. (2007). "The tumour-suppressor Scribble dictates cell polarity during directed epithelial migration: regulation of Rho GTPase recruitment to the leading edge." Oncogene **26**(16): 2272-82.

192

Dransart, E., B. Olofsson, et al. (2005). "RhoGDIs revisited: novel roles in Rho regulation." Traffic **6**(11): 957-66.

Dubash, A. D., M. M. Menold, et al. (2009). "Chapter 1. Focal adhesions: new angles on an old structure." Int Rev Cell Mol Biol **277**: 1-65.

Ellis, S. and H. Mellor (2000). "The novel Rho-family GTPase rif regulates coordinated actin-based membrane rearrangements." Curr Biol **10**(21): 1387-90.

Ellis, S. and H. Mellor (2000). "Regulation of endocytic traffic by rho family GTPases." Trends Cell Biol **10**(3): 85-8.

Enciso, J. M., C. M. Konecny, et al. (2010). "Endothelial cell migration during murine yolk sac vascular remodeling occurs by means of a Rac1 and FAK activation pathway in vivo." Dev Dyn **239**(10): 2570-83.

Eng, J. K., L. McCormack, et al. (1994). "An Approach to Correlate Tandem Mass Spectral Data of Peptides with Amino Acid Sequences in a Protein Database " J Am Soc Mass Spectrom **5**: 976-989

Erasmus, J. C. and V. M. Braga (2006). "Rho GTPase activation by cell-cell adhesion." Methods Enzymol **406**: 402-15.

Espert, L., C. Rey, et al. (2004). "The exonuclease ISG20 is directly induced by synthetic dsRNA via NF-kappaB and IRF1 activation." Oncogene **23**(26): 4636-40.

Etienne-Manneville, S. (2009). "Scribble at the crossroads." J Biol **8**(12): 104.

Etienne-Manneville, S. and A. Hall (2002). "Rho GTPases in cell biology." Nature **420**(6916): 629-35.

Ewan, L. C., H. M. Jopling, et al. (2006). "Intrinsic tyrosine kinase activity is required for vascular endothelial growth factor receptor 2 ubiquitination, sorting and degradation in endothelial cells." Traffic **7**(9): 1270-82.

Ezratty, E. J., M. A. Partridge, et al. (2005). "Microtubule-induced focal adhesion disassembly is mediated by dynamin and focal adhesion kinase." Nat Cell Biol **7**(6): 581-90.

Falcone, S., E. Cocucci, et al. (2006). "Macropinocytosis: regulated coordination of endocytic and exocytic membrane traffic events." J Cell Sci **119**(Pt 22): 4758-69.

Feng, Q., J. G. Albeck, et al. (2002). "Regulation of the Cool/Pix proteins: key binding partners of the Cdc42/Rac targets, the p21-activated kinases." J Biol Chem **277**(7): 5644-50.

Feng, Q., D. Baird, et al. (2004). "Novel regulatory mechanisms for the Dbl family guanine nucleotide exchange factor Cool-2/alpha-Pix." Embo J **23**(17): 3492-504.

Feng, Q., D. Baird, et al. (2006). "Cool-1 functions as an essential regulatory node for EGF receptor- and Src-mediated cell growth." Nat Cell Biol **8**(9): 945-56.

Feng, Q., D. Baird, et al. (2010). "Phosphorylation of the cool-1/beta-Pix protein serves as a regulatory signal for the migration and invasive activity of Src-transformed cells." J Biol Chem **285**(24): 18806-16.

Filipenko, N. R., S. Attwell, et al. (2005). "Integrin-linked kinase activity regulates Rac- and Cdc42-mediated actin cytoskeleton reorganization via alpha-PIX." Oncogene **24**(38): 5837-49.

Flamme, I., T. Frolich, et al. (1997). "Molecular mechanisms of vasculogenesis and embryonic angiogenesis." J Cell Physiol **173**(2): 206-10.

Flanders, J. A., Q. Feng, et al. (2003). "The Cbl proteins are binding partners for the Cool/Pix family of p21-activated kinase-binding proteins." FEBS Lett **550**(1-3): 119-23.

Foster, R., K. Q. Hu, et al. (1996). "Identification of a novel human Rho protein with unusual properties: GTPase deficiency and in vivo farnesylation." Mol Cell Biol **16**(6): 2689-99.

Franco, S. J. and A. Huttenlocher (2005). "Regulating cell migration: calpains make the cut." J Cell Sci **118**(Pt 17): 3829-38.

Frank, S. R. and S. H. Hansen (2008). "The PIX-GIT complex: a G protein signaling cassette in control of cell shape." Semin Cell Dev Biol **19**(3): 234-44.

Fryer, B. H. and J. Field (2005). "Rho, Rac, Pak and angiogenesis: old roles and newly identified responsibilities in endothelial cells." Cancer Lett **229**(1): 13-23.

Fujio, Y. and K. Walsh (1999). "Akt mediates cytoprotection of endothelial cells by vascular endothelial growth factor in an anchorage-dependent manner." J Biol Chem **274**(23): 16349-54.

Fukumoto, Y., K. Kaibuchi, et al. (1990). "Molecular cloning and characterization of a novel type of regulatory protein (GDI) for the rho proteins, ras p21-like small GTP-binding proteins." Oncogene **5**(9): 1321-8.

Galan Moya, E. M., A. Le Guelte, et al. (2009). "PAKing up to the endothelium." Cell Signal **21**(12): 1727-37.

Gampel, A. and H. Mellor (2002). "Small interfering RNAs as a tool to assign Rho GTPase exchange-factor function in vivo." Biochem J **366**(Pt 2): 393-8.

Gampel, A., L. Moss, et al. (2006). "VEGF regulates the mobilization of VEGFR2/KDR from an intracellular endothelial storage compartment." Blood **108**(8): 2624-31.

Gampel, A., P. J. Parker, et al. (1999). "Regulation of epidermal growth factor receptor traffic by the small GTPase rhoB." Curr Biol **9**(17): 955-8.

Garcia-Mata, R. and K. Burridge (2007). "Catching a GEF by its tail." Trends Cell Biol **17**(1): 36-43.

Garcia-Mata, R., K. Wennerberg, et al. (2006). "Analysis of activated GAPs and GEFs in cell lysates." Methods Enzymol **406**: 425-37.

Garrett, T. A., J. D. Van Buul, et al. (2007). "VEGF-induced Rac1 activation in endothelial cells is regulated by the guanine nucleotide exchange factor Vav2." Exp Cell Res **313**(15): 3285-97.

Garvalov, B. K., K. C. Flynn, et al. (2007). "Cdc42 regulates cofilin during the establishment of neuronal polarity." J Neurosci **27**(48): 13117-29.

Gasman, S., Y. Kalaidzidis, et al. (2003). "RhoD regulates endosome dynamics through Diaphanous-related Formin and Src tyrosine kinase." Nat Cell Biol **5**(3): 195-204.

Gavard, J. and J. S. Gutkind (2006). "VEGF controls endothelial-cell permeability by promoting the beta-arrestin-dependent endocytosis of VE-cadherin." Nat Cell Biol **8**(11): 1223-34.

Gerhardt, H. (2008). "VEGF and endothelial guidance in angiogenic sprouting." Organogenesis **4**(4): 241-6.

Gerhardt, H., M. Golding, et al. (2003). "VEGF guides angiogenic sprouting utilizing endothelial tip cell filopodia." J Cell Biol **161**(6): 1163-77.

Gietz, R. D. and R. A. Woods (2002). "Transformation of yeast by lithium acetate/single-stranded carrier DNA/polyethylene glycol method." Methods Enzymol **350**: 87-96.

Glading, A., D. A. Lauffenburger, et al. (2002). "Cutting to the chase: calpain proteases in cell motility." Trends Cell Biol **12**(1): 46-54.

Glogauer, M., C. C. Marchal, et al. (2003). "Rac1 deletion in mouse neutrophils has selective effects on neutrophil functions." J Immunol **170**(11): 5652-7.

Gomes, E. R., S. Jani, et al. (2005). "Nuclear movement regulated by Cdc42, MRCK, myosin, and actin flow establishes MTOC polarization in migrating cells." Cell **121**(3): 451-63.

Gorvel, J. P., T. C. Chang, et al. (1998). "Differential properties of D4/LyGDI versus RhoGDI: phosphorylation and rho GTPase selectivity." FEBS Lett **422**(2): 269-73.

Gould, G. W. and J. Lippincott-Schwartz (2009). "New roles for endosomes: from vesicular carriers to multi-purpose platforms." Nat Rev Mol Cell Biol **10**(4): 287-92.

Grant, B. D. and J. G. Donaldson (2009). "Pathways and mechanisms of endocytic recycling." Nat Rev Mol Cell Biol **10**(9): 597-608.

Greenberg, S. and S. Grinstein (2002). "Phagocytosis and innate immunity." Curr Opin Immunol **14**(1): 136-45.

Groeger, G. and C. D. Nobes (2007). "Co-operative Cdc42 and Rho signalling mediates ephrinB-triggered endothelial cell retraction." Biochem J **404**(1): 23-9.

Gu, Y., H. D. Chae, et al. (2006). "RhoH GTPase recruits and activates Zap70 required for T cell receptor signaling and thymocyte development." Nat Immunol **7**(11): 1182-90.

Gu, Y., M. D. Filippi, et al. (2003). "Hematopoietic cell regulation by Rac1 and Rac2 guanosine triphosphatases." Science **302**(5644): 445-9.

Guasch, R. M., P. Scambler, et al. (1998). "RhoE regulates actin cytoskeleton organization and cell migration." Mol Cell Biol **18**(8): 4761-71.

Haddad, E., J. L. Zugaza, et al. (2001). "The interaction between Cdc42 and WASP is required for SDF-1-induced T-lymphocyte chemotaxis." Blood **97**(1): 33-8.

Haendeler, J., G. Yin, et al. (2003). "GIT1 mediates Src-dependent activation of phospholipase Cgamma by angiotensin II and epidermal growth factor." J Biol Chem **278**(50): 49936-44.

Hakem, A., O. Sanchez-Sweatman, et al. (2005). "RhoC is dispensable for embryogenesis and tumor initiation but essential for metastasis." Genes Dev **19**(17): 1974-9.

Hall, A. (1998). "Rho GTPases and the actin cytoskeleton." Science **279**(5350): 509-14.

Haque, S. J. and B. R. Williams (1998). "Signal transduction in the interferon system." Semin Oncol **25**(1 Suppl 1): 14-22.

Heasman, S. J. and A. J. Ridley (2008). "Mammalian Rho GTPases: new insights into their functions from in vivo studies." Nat Rev Mol Cell Biol **9**(9): 690-701.

Heath, V. L., S. L. Shaw, et al. (2004). "Hph1p and Hph2p, novel components of calcineurin-mediated stress responses in Saccharomyces cerevisiae." Eukaryot Cell **3**(3): 695-704.

Hellstrom, M., L. K. Phng, et al. (2007b). "VEGF and Notch signaling: the yin and yang of angiogenic sprouting." Cell Adh Migr **1**(3): 133-6.

Hellstrom, M., L. K. Phng, et al. (2007a). "Dll4 signalling through Notch1 regulates formation of tip cells during angiogenesis." Nature **445**(7129): 776-80.

Herbert, J. M., D. Stekel, et al. (2008). "A novel method of differential gene expression analysis using multiple cDNA libraries applied to the identification of tumour endothelial genes." BMC Genomics **9**: 153.

Higgins, M. K. and H. T. McMahon (2002). "Snap-shots of clathrin-mediated endocytosis." Trends Biochem Sci 27(5): 257-63.

Hippenstiel, S., B. Schmeck, et al. (2002). "Rho protein inactivation induced apoptosis of cultured human endothelial cells." Am J Physiol Lung Cell Mol Physiol 283(4): L830-8.

Hoefen, R. J. and B. C. Berk (2006). "The multifunctional GIT family of proteins." J Cell Sci 119(Pt 8): 1469-75.

Holinstat, M., N. Knezevic, et al. (2006). "Suppression of RhoA activity by focal adhesion kinase-induced activation of p190RhoGAP: role in regulation of endothelial permeability." J Biol Chem 281(4): 2296-305.

Holinstat, M., D. Mehta, et al. (2003). "Protein kinase Calpha-induced p115RhoGEF phosphorylation signals endothelial cytoskeletal rearrangement." J Biol Chem 278(31): 28793-8.

Hotulainen, P. and P. Lappalainen (2006). "Stress fibers are generated by two distinct actin assembly mechanisms in motile cells." J Cell Biol 173(3): 383-94.

Hu, K. Q. and J. Settleman (1997). "Tandem SH2 binding sites mediate the RasGAP-RhoGAP interaction: a conformational mechanism for SH3 domain regulation." Embo J 16(3): 473-83.

Huang, M., J. B. Duhadaway, et al. (2007). "RhoB regulates PDGFR-beta trafficking and signaling in vascular smooth muscle cells." Arterioscler Thromb Vasc Biol 27(12): 2597-605.

Huang, M. and G. C. Prendergast (2006). "RhoB in cancer suppression." Histol Histopathol 21(2): 213-8.

Humphries, J. D., P. Wang, et al. (2007). "Vinculin controls focal adhesion formation by direct interactions with talin and actin." J Cell Biol 179(5): 1043-57.

Iden, S. and J. G. Collard (2008). "Crosstalk between small GTPases and polarity proteins in cell polarization." Nat Rev Mol Cell Biol 9(11): 846-59.

Ilic, D., Y. Furuta, et al. (1995). "Reduced cell motility and enhanced focal adhesion contact formation in cells from FAK-deficient mice." Nature 377(6549): 539-44.

Ispanovic, E., D. Serio, et al. (2008). "Cdc42 and RhoA have opposing roles in regulating membrane type 1-matrix metalloproteinase localization and matrix metalloproteinase-2 activation." Am J Physiol Cell Physiol 295(3): C600-10.

Jack, E. R., J. Madine, et al. (2008). "Membrane interactions of peptides representing the polybasic regions of three Rho GTPases are sensitive to the distribution of arginine and lysine residues." Mol Membr Biol 25(1): 14-22.

Jaffe, A. B. and A. Hall (2005). "Rho GTPases: biochemistry and biology." Annu Rev Cell Dev Biol 21: 247-69.

Jain, R. K. (2003). "Molecular regulation of vessel maturation." Nat Med 9(6): 685-93.

Jakobsson, L., C. A. Franco, et al. (2010). "Endothelial cells dynamically compete for the tip cell position during angiogenic sprouting." Nat Cell Biol 12(10): 943-53.

JeBailey, L., A. Rudich, et al. (2004). "Skeletal muscle cells and adipocytes differ in their reliance on TC10 and Rac for insulin-induced actin remodeling." Mol Endocrinol 18(2): 359-72.

Johnson, D. I. (1999). "Cdc42: An essential Rho-type GTPase controlling eukaryotic cell polarity." Microbiol Mol Biol Rev 63(1): 54-105.

Johnson, M., M. Sharma, et al. (2009). "IQGAP1 regulation and roles in cancer." Cell Signal 21(10): 1471-8.

Jones, N. P. and M. Katan (2007). "Role of phospholipase Cgamma1 in cell spreading requires association with a beta-Pix/GIT1-containing complex, leading to activation of Cdc42 and Rac1." Mol Cell Biol 27(16): 5790-805.

Kamei, M., W. B. Saunders, et al. (2006). "Endothelial tubes assemble from intracellular vacuoles in vivo." Nature 442(7101): 453-6.

Kang, H., J. Wang, et al. (2010). "Relative actin nucleation promotion efficiency by WASP and WAVE proteins in endothelial cells." Biochem Biophys Res Commun 400(4): 661-6.

Katsumi, A., J. Milanini, et al. (2002). "Effects of cell tension on the small GTPase Rac." J Cell Biol 158(1): 153-64.

Kaur, S., K. Leszczynska, et al. (2011). "RhoJ/TCL regulates endothelial motility and tube formation and modulates actomyosin contractility and focal adhesion numbers." Arterioscler Thromb Vasc Biol 31(3): 657-64.

Kawachi, H., A. Fujikawa, et al. (2001). "Identification of GIT1/Cat-1 as a substrate molecule of protein tyrosine phosphatase zeta /beta by the yeast substrate-trapping system." Proc Natl Acad Sci U S A 98(12): 6593-8.

Kawaji, A., M. Nishizuka, et al. (2010). "TC10-like/TC10betaLong regulates adipogenesis by controlling mitotic clonal expansion." Biol Pharm Bull 33(3): 404-9.

Kim, S., J. Ko, et al. (2003). "The GIT family of proteins forms multimers and associates with the presynaptic cytomatrix protein Piccolo." J Biol Chem 278(8): 6291-300.

Kim, S., S. H. Lee, et al. (2001). "Leucine zipper-mediated homodimerization of the p21-activated kinase-interacting factor, beta Pix. Implication for a role in cytoskeletal reorganization." J Biol Chem **276**(14): 10581-4.

Kiosses, W. B., R. H. Daniels, et al. (1999). "A role for p21-activated kinase in endothelial cell migration." J Cell Biol **147**(4): 831-44.

Kjoller, L. and A. Hall (1999). "Signaling to Rho GTPases." Exp Cell Res **253**(1): 166-79.

Ko, J., S. Kim, et al. (2003). "Interaction between liprin-alpha and GIT1 is required for AMPA receptor targeting." J Neurosci **23**(5): 1667-77.

Koh, C. G., E. Manser, et al. (2001). "Beta1PIX, the PAK-interacting exchange factor, requires localization via a coiled-coil region to promote microvillus-like structures and membrane ruffles." J Cell Sci **114**(Pt 23): 4239-51.

Koh, C. G., E. J. Tan, et al. (2002). "The p21-activated kinase PAK is negatively regulated by POPX1 and POPX2, a pair of serine/threonine phosphatases of the PP2C family." Curr Biol **12**(4): 317-21.

Kubota, Y., H. K. Kleinman, et al. (1988). "Role of laminin and basement membrane in the morphological differentiation of human endothelial cells into capillary-like structures." J Cell Biol **107**(4): 1589-98.

Kurokawa, K. and M. Matsuda (2005). "Localized RhoA activation as a requirement for the induction of membrane ruffling." Mol Biol Cell **16**(9): 4294-303.

Lamalice, L., F. Houle, et al. (2004). "Phosphorylation of tyrosine 1214 on VEGFR2 is required for VEGF-induced activation of Cdc42 upstream of SAPK2/p38." Oncogene **23**(2): 434-45.

Lamarche, N. and A. Hall (1994). "GAPs for rho-related GTPases." Trends Genet **10**(12): 436-40.

Lamaze, C., T. H. Chuang, et al. (1996). "Regulation of receptor-mediated endocytosis by Rho and Rac." Nature **382**(6587): 177-9.

Lamaze, C., A. Dujeancourt, et al. (2001). "Interleukin 2 receptors and detergent-resistant membrane domains define a clathrin-independent endocytic pathway." Mol Cell **7**(3): 661-71.

Lauffenburger, D. A. and A. F. Horwitz (1996). "Cell migration: a physically integrated molecular process." Cell **84**(3): 359-69.

Lee, J. G. and E. P. Kay (2006). "FGF-2-induced wound healing in corneal endothelial cells requires Cdc42 activation and Rho inactivation through the phosphatidylinositol 3-kinase pathway." Invest Ophthalmol Vis Sci **47**(4): 1376-86.

Lee, S. H. and R. Dominguez (2010). "Regulation of actin cytoskeleton dynamics in cells." Mol Cells **29**(4): 311-25.

Lei, M., W. Lu, et al. (2000). "Structure of PAK1 in an autoinhibited conformation reveals a multistage activation switch." Cell **102**(3): 387-97.

Lelias, J. M., C. N. Adra, et al. (1993). "cDNA cloning of a human mRNA preferentially expressed in hematopoietic cells and with homology to a GDP-dissociation inhibitor for the rho GTP-binding proteins." Proc Natl Acad Sci U S A **90**(4): 1479-83.

Leonard, D., M. J. Hart, et al. (1992). "The identification and characterization of a GDP-dissociation inhibitor (GDI) for the CDC42Hs protein." J Biol Chem **267**(32): 22860-8.

Leung, T., X. Q. Chen, et al. (1998). "Myotonic dystrophy kinase-related Cdc42-binding kinase acts as a Cdc42 effector in promoting cytoskeletal reorganization." Mol Cell Biol **18**(1): 130-40.

Li, R., B. Zhang, et al. (1997). "Structural determinants required for the interaction between Rho GTPase and the GTPase-activating domain of p190." J Biol Chem **272**(52): 32830-5.

Li, S., N. F. Huang, et al. (2005). "Mechanotransduction in endothelial cell migration." J Cell Biochem **96**(6): 1110-26.

Li, X., X. Bu, et al. (2002). "The hematopoiesis-specific GTP-binding protein RhoH is GTPase deficient and modulates activities of other Rho GTPases by an inhibitory function." Mol Cell Biol **22**(4): 1158-71.

Li, X., L. Liu, et al. (2002). "Inhibition of protein geranylgeranylation and RhoA/RhoA kinase pathway induces apoptosis in human endothelial cells." J Biol Chem **277**(18): 15309-16.

Liang, P. H., T. P. Ko, et al. (2002). "Structure, mechanism and function of prenyltransferases." Eur J Biochem **269**(14): 3339-54.

Liebl, J., S. B. Weitensteiner, et al. (2010). "Cyclin-dependent Kinase 5 Regulates Endothelial Cell Migration and Angiogenesis." J Biol Chem **285**(46): 35932-43.

Liu, A. X., N. Rane, et al. (2001). "RhoB is dispensable for mouse development, but it modifies susceptibility to tumor formation as well as cell adhesion and growth factor signaling in transformed cells." Mol Cell Biol **21**(20): 6906-12.

Liu, N., G. Zhang, et al. (2007). "RhoC is essential for the metastasis of gastric cancer." J Mol Med **85**(10): 1149-56.

Liu, X., H. Wang, et al. (1998). "NMR structure and mutagenesis of the N-terminal Dbl homology domain of the nucleotide exchange factor Trio." Cell **95**(2): 269-77.

Loo, T. H., Y. W. Ng, et al. (2004). "GIT1 activates p21-activated kinase through a mechanism independent of p21 binding." Mol Cell Biol **24**(9): 3849-59.

Luna, A., O. B. Matas, et al. (2002). "Regulation of protein transport from the Golgi complex to the endoplasmic reticulum by CDC42 and N-WASP." Mol Biol Cell **13**(3): 866-79.

Luzio, J. P., B. A. Rous, et al. (2000). "Lysosome-endosome fusion and lysosome biogenesis." J Cell Sci **113 (Pt 9)**: 1515-24.

Macedo, M. F. and M. de Sousa (2008). "Transferrin and the transferrin receptor: of magic bullets and other concerns." Inflamm Allergy Drug Targets **7**(1): 41-52.

Machacek, M., L. Hodgson, et al. (2009). "Coordination of Rho GTPase activities during cell protrusion." Nature **461**(7260): 99-103.

Maciag, T., J. Cerundolo, et al. (1979). "An endothelial cell growth factor from bovine hypothalamus: identification and partial characterization." Proc Natl Acad Sci U S A **76**(11): 5674-8.

Madaule, P. and R. Axel (1985). "A novel ras-related gene family." Cell **41**(1): 31-40.

Manabe, R., M. Kovalenko, et al. (2002). "GIT1 functions in a motile, multi-molecular signaling complex that regulates protrusive activity and cell migration." J Cell Sci **115**(Pt 7): 1497-510.

Manser, E., H. Y. Huang, et al. (1997). "Expression of constitutively active alpha-PAK reveals effects of the kinase on actin and focal complexes." Mol Cell Biol **17**(3): 1129-43.

Manser, E., T. H. Loo, et al. (1998). "PAK kinases are directly coupled to the PIX family of nucleotide exchange factors." Mol Cell **1**(2): 183-92.

Matafora, V., S. Paris, et al. (2001). "Molecular mechanisms regulating the subcellular localization of p95-APP1 between the endosomal recycling compartment and sites of actin organization at the cell surface." J Cell Sci **114**(Pt 24): 4509-20.

Mavria, G., Y. Vercoulen, et al. (2006). "ERK-MAPK signaling opposes Rho-kinase to promote endothelial cell survival and sprouting during angiogenesis." Cancer Cell **9**(1): 33-44.

McLaughlin, J. N., L. Shen, et al. (2005). "Functional selectivity of G protein signaling by agonist peptides and thrombin for the protease-activated receptor-1." J Biol Chem **280**(26): 25048-59.

Mehta, D. and A. B. Malik (2006). "Signaling mechanisms regulating endothelial permeability." Physiol Rev **86**(1): 279-367.

Mehta, D., A. Rahman, et al. (2001). "Protein kinase C-alpha signals rho-guanine nucleotide dissociation inhibitor phosphorylation and rho activation and regulates the endothelial cell barrier function." J Biol Chem **276**(25): 22614-20.

Meller, N., S. Merlot, et al. (2005). "CZH proteins: a new family of Rho-GEFs." J Cell Sci **118**(Pt 21): 4937-46.

Michiels, F., J. C. Stam, et al. (1997). "Regulated membrane localization of Tiam1, mediated by the NH2-terminal pleckstrin homology domain, is required for Rac-dependent membrane ruffling and C-Jun NH2-terminal kinase activation." J Cell Biol **137**(2): 387-98.

Milkiewicz, M., E. Ispanovic, et al. (2006). "Regulators of angiogenesis and strategies for their therapeutic manipulation." Int J Biochem Cell Biol **38**(3): 333-57.

Moon, S. Y. and Y. Zheng (2003). "Rho GTPase-activating proteins in cell regulation." Trends Cell Biol **13**(1): 13-22.

Murphy, C., R. Saffrich, et al. (1996). "Endosome dynamics regulated by a Rho protein." Nature **384**(6608): 427-32.

Murphy, C., R. Saffrich, et al. (2001). "Dual function of rhoD in vesicular movement and cell motility." Eur J Cell Biol **80**(6): 391-8.

Murphy, G. A., P. A. Solski, et al. (1999). "Cellular functions of TC10, a Rho family GTPase: regulation of morphology, signal transduction and cell growth." Oncogene **18**(26): 3831-45.

Nakamura, T., M. Komiya, et al. (2002). "Grit, a GTPase-activating protein for the Rho family, regulates neurite extension through association with the TrkA receptor and N-Shc and CrkL/Crk adapter molecules." Mol Cell Biol **22**(24): 8721-34.

Nassar, N., G. R. Hoffman, et al. (1998). "Structures of Cdc42 bound to the active and catalytically compromised forms of Cdc42GAP." Nat Struct Biol **5**(12): 1047-52.

Nayal, A., D. J. Webb, et al. (2006). "Paxillin phosphorylation at Ser273 localizes a GIT1-PIX-PAK complex and regulates adhesion and protrusion dynamics." J Cell Biol **173**(4): 587-9.

Nicholson-Dykstra, S., H. N. Higgs, et al. (2005). "Actin dynamics: growth from dendritic branches." Curr Biol **15**(9): R346-57.

Nie, Z., D. S. Hirsch, et al. (2003). "Arf and its many interactors." Curr Opin Cell Biol **15**(4): 396-404.

Nimnual, A. S., L. J. Taylor, et al. (2003). "Redox-dependent downregulation of Rho by Rac." Nat Cell Biol **5**(3): 236-41.

Nishiya, N., W. B. Kiosses, et al. (2005). "An alpha4 integrin-paxillin-Arf-GAP complex restricts Rac activation to the leading edge of migrating cells." Nat Cell Biol **7**(4): 343-52.

Nishizuka, M., E. Arimoto, et al. (2003). "Crucial role of TCL/TC10beta L, a subfamily of Rho GTPase, in adipocyte differentiation." J Biol Chem **278**(17): 15279-84.

Nobes, C. and A. Hall (1994). "Regulation and function of the Rho subfamily of small GTPases." Curr Opin Genet Dev **4**(1): 77-81.

Nobes, C. D. and A. Hall (1995). "Rho, rac, and cdc42 GTPases regulate the assembly of multimolecular focal complexes associated with actin stress fibers, lamellipodia, and filopodia." Cell **81**(1): 53-62.

Nobes, C. D., I. Lauritzen, et al. (1998). "A new member of the Rho family, Rnd1, promotes disassembly of actin filament structures and loss of cell adhesion." J Cell Biol **141**(1): 187-97.

Nodari, A., D. Zambroni, et al. (2007). "Beta1 integrin activates Rac1 in Schwann cells to generate radial lamellae during axonal sorting and myelination." J Cell Biol **177**(6): 1063-75.

Nola, S., M. Sebbagh, et al. (2008). "Scrib regulates PAK activity during the cell migration process." Hum Mol Genet **17**(22): 3552-65.

Obermeier, A., S. Ahmed, et al. (1998). "PAK promotes morphological changes by acting upstream of Rac." Embo J **17**(15): 4328-39.

Okamoto, H., Y. Yatomi, et al. (2000). "Sphingosine 1-phosphate stimulates G(i)- and Rho-mediated vascular endothelial cell spreading and migration." Thromb Res **99**(3): 259-65.

Olofsson, B. (1999). "Rho guanine dissociation inhibitors: pivotal molecules in cellular signalling." Cell Signal **11**(8): 545-54.

Olsson, A. K., A. Dimberg, et al. (2006). "VEGF receptor signalling - in control of vascular function." Nat Rev Mol Cell Biol **7**(5): 359-71.

Osmani, N., N. Vitale, et al. (2006). "Scrib controls Cdc42 localization and activity to promote cell polarization during astrocyte migration." Curr Biol **16**(24): 2395-405.

Oviedo, P. J., A. Sobrino, et al. (2010). "Estradiol induces endothelial cell migration and proliferation through estrogen receptor-enhanced RhoA/ROCK pathway." Mol Cell Endocrinol.

Paduch, M., F. Jelen, et al. (2001). "Structure of small G proteins and their regulators." Acta Biochim Pol **48**(4): 829-50.

Pages, G., J. Milanini, et al. (2000). "Signaling angiogenesis via p42/p44 MAP kinase cascade." Ann N Y Acad Sci **902**: 187-200.

Paik, J. H., S. Chae, et al. (2001). "Sphingosine 1-phosphate-induced endothelial cell migration requires the expression of EDG-1 and EDG-3 receptors and Rho-dependent activation of alpha vbeta3- and beta1-containing integrins." J Biol Chem **276**(15): 11830-7.

Palamidessi, A., E. Frittoli, et al. (2008). "Endocytic trafficking of Rac is required for the spatial restriction of signaling in cell migration." Cell **134**(1): 135-47.

Pang, J., R. Hoefen, et al. (2009). "G-protein-coupled receptor kinase interacting protein-1 is required for pulmonary vascular development." Circulation **119**(11): 1524-32.

Paris, S., R. Longhi, et al. (2003). "Leucine-zipper-mediated homo- and hetero-dimerization of GIT family p95-ARF GTPase-activating protein, PIX-, paxillin-interacting proteins 1 and 2." Biochem J **372**(Pt 2): 391-8.

Paris, S., L. Za, et al. (2002). "Analysis of the subcellular distribution of avian p95-APP2, an ARF-GAP orthologous to mammalian paxillin kinase linker." Int J Biochem Cell Biol **34**(7): 826-37.

Park, E., M. Na, et al. (2003). "The Shank family of postsynaptic density proteins interacts with and promotes synaptic accumulation of the beta PIX guanine nucleotide exchange factor for Rac1 and Cdc42." J Biol Chem **278**(21): 19220-9.

Parsons, J. T., A. R. Horwitz, et al. (2010). "Cell adhesion: integrating cytoskeletal dynamics and cellular tension." Nat Rev Mol Cell Biol **11**(9): 633-43.

Parton, R. G. and K. Simons (2007). "The multiple faces of caveolae." Nat Rev Mol Cell Biol **8**(3): 185-94.

Passaniti, A., R. M. Taylor, et al. (1992). "A simple, quantitative method for assessing angiogenesis and antiangiogenic agents using reconstituted basement membrane, heparin, and fibroblast growth factor." Lab Invest **67**(4): 519-28.

Patan, S. (2004). "Vasculogenesis and angiogenesis." Cancer Treat Res **117**: 3-32.

Pellegrin, S. and H. Mellor (2007). "Actin stress fibres." J Cell Sci **120**(Pt 20): 3491-9.

Pellegrin, S. and H. Mellor (2008). "Rho GTPase activation assays." Curr Protoc Cell Biol **Chapter 14**: Unit 14 8.

Pertz, O., L. Hodgson, et al. (2006). "Spatiotemporal dynamics of RhoA activity in migrating cells." Nature **440**(7087): 1069-72.

Petrache, I., M. T. Crow, et al. (2003). "Central involvement of Rho family GTPases in TNF-alpha-mediated bovine pulmonary endothelial cell apoptosis." Biochem Biophys Res Commun **306**(1): 244-9.

Phee, H., R. T. Abraham, et al. (2005). "Dynamic recruitment of PAK1 to the immunological synapse is mediated by PIX independently of SLP-76 and Vav1." Nat Immunol **6**(6): 608-17.

Pollard, T. D. and G. G. Borisy (2003). "Cellular motility driven by assembly and disassembly of actin filaments." Cell **112**(4): 453-65.

Premont, R. T., A. Claing, et al. (1998). "beta2-Adrenergic receptor regulation by GIT1, a G protein-coupled receptor kinase-associated ADP ribosylation factor GTPase-activating protein." Proc Natl Acad Sci U S A **95**(24): 14082-7.

Premont, R. T., S. J. Perry, et al. (2004). "The GIT/PIX complex: an oligomeric assembly of GIT family ARF GTPase-activating proteins and PIX family Rac1/Cdc42 guanine nucleotide exchange factors." Cell Signal **16**(9): 1001-11.

Presta, M., P. Dell'Era, et al. (2005). "Fibroblast growth factor/fibroblast growth factor receptor system in angiogenesis." Cytokine Growth Factor Rev **16**(2): 159-78.

Qian, X., T. N. Wang, et al. (1997). "Thrombospondin-1 modulates angiogenesis in vitro by up-regulation of matrix metalloproteinase-9 in endothelial cells." Exp Cell Res **235**(2): 403-12.

Qualmann, B. and H. Mellor (2003). "Regulation of endocytic traffic by Rho GTPases." Biochem J **371**(Pt 2): 233-41.

Raftopoulou, M. and A. Hall (2004). "Cell migration: Rho GTPases lead the way." Dev Biol **265**(1): 23-32.

Ren, X. D., W. B. Kiosses, et al. (1999). "Regulation of the small GTP-binding protein Rho by cell adhesion and the cytoskeleton." Embo J **18**(3): 578-85.

Ren, X. D. and M. A. Schwartz (2000). "Determination of GTP loading on Rho." Methods Enzymol **325**: 264-72.

Ridley, A. J. (2001). "Rho proteins: linking signaling with membrane trafficking." Traffic **2**(5): 303-10.

Ridley, A. J. (2006). "Rho GTPases and actin dynamics in membrane protrusions and vesicle trafficking." Trends Cell Biol **16**(10): 522-9.

Ridley, A. J., M. A. Schwartz, et al. (2003). "Cell migration: integrating signals from front to back." Science **302**(5651): 1704-9.

Riento, K., R. M. Guasch, et al. (2003). "RhoE binds to ROCK I and inhibits downstream signaling." Mol Cell Biol **23**(12): 4219-29.

Roberts, A. W., C. Kim, et al. (1999). "Deficiency of the hematopoietic cell-specific Rho family GTPase Rac2 is characterized by abnormalities in neutrophil function and host defense." Immunity **10**(2): 183-96.

Rodriguez-Fernandez, J. L. (1999). "Why do so many stimuli induce tyrosine phosphorylation of FAK?" Bioessays **21**(12): 1069-75.

Roof, R. W., M. D. Haskell, et al. (1998). "Phosphotyrosine (p-Tyr)-dependent and -independent mechanisms of p190 RhoGAP-p120 RasGAP interaction: Tyr 1105 of p190, a substrate for c-Src, is the sole p-Tyr mediator of complex formation." Mol Cell Biol **18**(12): 7052-63.

Rosenberger, G., A. Gal, et al. (2005). "AlphaPIX associates with calpain 4, the small subunit of calpain, and has a dual role in integrin-mediated cell spreading." J Biol Chem **280**(8): 6879-89.

Rosenberger, G. and K. Kutsche (2006). "AlphaPIX and betaPIX and their role in focal adhesion formation." Eur J Cell Biol **85**(3-4): 265-74.

Rossman, K. L. and S. L. Campbell (2000). "Bacterial expressed DH and DH/PH domains." Methods Enzymol **325**: 25-38.

Rossman, K. L., C. J. Der, et al. (2005). "GEF means go: turning on RHO GTPases with guanine nucleotide-exchange factors." Nat Rev Mol Cell Biol **6**(2): 167-80.

Sambrook, J. and D. Russel (2001). SDS-Polyacrylamide Gel Electrophoresis of Proteins. Molecular Cloning. J. Sambrook and D. Russel. New York, Cold Sprong Harbor Laboratory Press. **3:** A8.40-A8.45.

Sander, E. E., S. van Delft, et al. (1998). "Matrix-dependent Tiam1/Rac signaling in epithelial cells promotes either cell-cell adhesion or cell migration and is regulated by phosphatidylinositol 3-kinase." J Cell Biol **143**(5): 1385-98.

Sanz-Moreno, V., G. Gadea, et al. (2008). "Rac activation and inactivation control plasticity of tumor cell movement." Cell **135**(3): 510-23.

Satoh, M., H. Ogita, et al. (2006). "Requirement of Rac1 in the development of cardiac hypertrophy." Proc Natl Acad Sci U S A **103**(19): 7432-7.

Schmidt, A. and A. Hall (2002). "Guanine nucleotide exchange factors for Rho GTPases: turning on the switch." Genes Dev **16**(13): 1587-609.

Schwartz, M. (2004). "Rho signalling at a glance." J Cell Sci **117**(Pt 23): 5457-8.

Scott, A. and H. Mellor (2009). "VEGF receptor trafficking in angiogenesis." Biochem Soc Trans **37**(Pt 6): 1184-8.

Seebach, J., H. J. Madler, et al. (2005). "Tyrosine phosphorylation and the small GTPase rac cross-talk in regulation of endothelial barrier function." Thromb Haemost **94**(3): 620-9.

Shattil, S. J., C. Kim, et al. (2010). "The final steps of integrin activation: the end game." Nat Rev Mol Cell Biol **11**(4): 288-300.

Sheldon, H., M. Andre, et al. (2009). "Active involvement of Robo1 and Robo4 in filopodia formation and endothelial cell motility mediated via WASP and other actin nucleation-promoting factors." Faseb J **23**(2): 513-22.

Shikata, Y., K. G. Birukov, et al. (2003b). "Involvement of site-specific FAK phosphorylation in sphingosine-1 phosphate- and thrombin-induced focal adhesion remodeling: role of Src and GIT." Faseb J **17**(15): 2240-9.

Shikata, Y., K. G. Birukov, et al. (2003a). "S1P induces FA remodeling in human pulmonary endothelial cells: role of Rac, GIT1, FAK, and paxillin." J Appl Physiol **94**(3): 1193-203.

Sieg, D. J., C. R. Hauck, et al. (1999). "Required role of focal adhesion kinase (FAK) for integrin-stimulated cell migration." J Cell Sci **112 (Pt 16)**: 2677-91.

Simpson, K. J., A. S. Dugan, et al. (2004). "Functional analysis of the contribution of RhoA and RhoC GTPases to invasive breast carcinoma." Cancer Res **64**(23): 8694-701.

Slevin, M., A. B. Elasbali, et al. (2006). "Identification of differential protein expression associated with development of unstable human carotid plaques." Am J Pathol **168**(3): 1004-21.

Small, J. V., T. Stradal, et al. (2002). "The lamellipodium: where motility begins." Trends Cell Biol **12**(3): 112-20.

Snyder, J. T., K. L. Rossman, et al. (2001). "Quantitative analysis of the effect of phosphoinositide interactions on the function of Dbl family proteins." J Biol Chem **276**(49): 45868-75.

Soga, N., J. O. Connolly, et al. (2001). "Rac regulates vascular endothelial growth factor stimulated motility." Cell Commun Adhes **8**(1): 1-13.

Sorkin, A. and M. von Zastrow (2009). "Endocytosis and signalling: intertwining molecular networks." Nat Rev Mol Cell Biol **10**(9): 609-22.

Spiering, D. and L. Hodgson (2011). "Dynamics of the Rho-family small GTPases in actin regulation and motility." Cell Adh Migr **5**(2).

Spindler, V., N. Schlegel, et al. (2010). "Role of GTPases in control of microvascular permeability." Cardiovasc Res **87**(2): 243-53.

Stam, J. C., E. E. Sander, et al. (1997). "Targeting of Tiam1 to the plasma membrane requires the cooperative function of the N-terminal pleckstrin homology domain and an adjacent protein interaction domain." J Biol Chem **272**(45): 28447-54.

Stockton, R., J. Reutershan, et al. (2007). "Induction of vascular permeability: beta PIX and GIT1 scaffold the activation of extracellular signal-regulated kinase by PAK." Mol Biol Cell **18**(6): 2346-55.

Su, Z. J., C. N. Hahn, et al. (2004). "A vascular cell-restricted RhoGAP, p73RhoGAP, is a key regulator of angiogenesis." Proc Natl Acad Sci U S A **101**(33): 12212-7.

Sugihara, K., N. Nakatsuji, et al. (1998). "Rac1 is required for the formation of three germ layers during gastrulation." Oncogene **17**(26): 3427-33.

Symons, M. and N. Rusk (2003). "Control of vesicular trafficking by Rho GTPases." Curr Biol **13**(10): R409-18.

Takahashi, T., S. Yamaguchi, et al. (2001). "A single autophosphorylation site on KDR/Flk-1 is essential for VEGF-A-dependent activation of PLC-gamma and DNA synthesis in vascular endothelial cells." Embo J **20**(11): 2768-78.

Tan, I., J. Yong, et al. (2008). "A tripartite complex containing MRCK modulates lamellar actomyosin retrograde flow." Cell **135**(1): 123-36.

Tan, W., T. R. Palmby, et al. (2008). "An essential role for Rac1 in endothelial cell function and vascular development." Faseb J **22**(6): 1829-38.

Tao, W., D. Pennica, et al. (2001). "Wrch-1, a novel member of the Rho gene family that is regulated by Wnt-1." Genes Dev **15**(14): 1796-807.

Tcherkezian, J. and N. Lamarche-Vane (2007). "Current knowledge of the large RhoGAP family of proteins." Biol Cell **99**(2): 67-86.

ten Klooster, J. P., Z. M. Jaffer, et al. (2006). "Targeting and activation of Rac1 are mediated by the exchange factor beta-Pix." J Cell Biol **172**(5): 759-69.

Tomar, A. and D. D. Schlaepfer (2009). "Focal adhesion kinase: switching between GAPs and GEFs in the regulation of cell motility." Curr Opin Cell Biol **21**(5): 676-83.

Tong, S., A. S. Liss, et al. (2007). "The activation of TC10, a Rho small GTPase, contributes to v-Rel-mediated transformation." Oncogene **26**(16): 2318-29.

Totaro, A., S. Paris, et al. (2007). "Identification of an intramolecular interaction important for the regulation of GIT1 functions." Mol Biol Cell **18**(12): 5124-38.

Turner, C. E., M. C. Brown, et al. (1999). "Paxillin LD4 motif binds PAK and PIX through a novel 95-kD ankyrin repeat, ARF-GAP protein: A role in cytoskeletal remodeling." J Cell Biol **145**(4): 851-63.

Ungewickell, E. J. and L. Hinrichsen (2007). "Endocytosis: clathrin-mediated membrane budding." Curr Opin Cell Biol **19**(4): 417-25.

Vallon, M., F. Rohde, et al. (2010). "Tumor endothelial marker 5 expression in endothelial cells during capillary morphogenesis is induced by the small GTPase Rac and mediates contact inhibition of cell proliferation." Exp Cell Res **316**(3): 412-21.

van Hengel, J., P. D'Hooge, et al. (2008). "Continuous cell injury promotes hepatic tumorigenesis in cdc42-deficient mouse liver." Gastroenterology **134**(3): 781-92.

van Nieuw Amerongen, G. P., K. Natarajan, et al. (2004). "GIT1 mediates thrombin signaling in endothelial cells: role in turnover of RhoA-type focal adhesions." Circ Res **94**(8): 1041-9.

Vandenbroucke, E., D. Mehta, et al. (2008). "Regulation of endothelial junctional permeability." Ann N Y Acad Sci **1123**: 134-45.

Vega, F. M. and A. J. Ridley (2008). "Rho GTPases in cancer cell biology." FEBS Lett **582**(14): 2093-2101.

Vicente-Manzanares, M., M. A. Koach, et al. (2008). "Segregation and activation of myosin IIB creates a rear in migrating cells." J Cell Biol **183**(3): 543-54.

Vicente-Manzanares, M., X. Ma, et al. (2009). "Non-muscle myosin II takes centre stage in cell adhesion and migration." Nat Rev Mol Cell Biol **10**(11): 778-90.

Vidali, L., F. Chen, et al. (2006). "Rac1-null mouse embryonic fibroblasts are motile and respond to platelet-derived growth factor." Mol Biol Cell **17**(5): 2377-90.

Vignal, E., A. Blangy, et al. (2001). "Kinectin is a key effector of RhoG microtubule-dependent cellular activity." Mol Cell Biol **21**(23): 8022-34.

Vignal, E., M. De Toledo, et al. (2000). "Characterization of TCL, a new GTPase of the rho family related to TC10 andCcdc42." J Biol Chem **275**(46): 36457-64.

Vigorito, E., S. Bell, et al. (2004). "Immunological function in mice lacking the Rac-related GTPase RhoG." Mol Cell Biol **24**(2): 719-29.

Vincent, S., P. Jeanteur, et al. (1992). "Growth-regulated expression of rhoG, a new member of the ras homolog gene family." Mol Cell Biol **12**(7): 3138-48.

Vitale, N., W. A. Patton, et al. (2000). "GIT proteins, A novel family of phosphatidylinositol 3,4, 5-trisphosphate-stimulated GTPase-activating proteins for ARF6." J Biol Chem **275**(18): 13901-6.

Voyta, J. C., D. P. Via, et al. (1984). "Identification and isolation of endothelial cells based on their increased uptake of acetylated-low density lipoprotein." J Cell Biol **99**(6): 2034-40.

Walmsley, M. J., S. K. Ooi, et al. (2003). "Critical roles for Rac1 and Rac2 GTPases in B cell development and signaling." Science **302**(5644): 459-62.

Wang, J., Y. Taba, et al. (2009). "GIT1 mediates VEGF-induced podosome formation in endothelial cells: critical role for PLCgamma." Arterioscler Thromb Vasc Biol **29**(2): 202-8.

Wang, W., R. Eddy, et al. (2007). "The cofilin pathway in breast cancer invasion and metastasis." Nat Rev Cancer **7**(6): 429-40.

Waschke, J., W. Baumgartner, et al. (2004). "Requirement of Rac activity for maintenance of capillary endothelial barrier properties." Am J Physiol Heart Circ Physiol **286**(1): H394-401.

Waschke, J., S. Burger, et al. (2006). "Activation of Rac-1 and Cdc42 stabilizes the microvascular endothelial barrier." Histochem Cell Biol **125**(4): 397-406.

Webb, D. J., K. Donais, et al. (2004). "FAK-Src signalling through paxillin, ERK and MLCK regulates adhesion disassembly." Nat Cell Biol **6**(2): 154-61.

Webb, D. J., M. W. Mayhew, et al. (2006). "Identification of phosphorylation sites in GIT1." J Cell Sci **119**(Pt 14): 2847-50.

Webb, D. J., J. T. Parsons, et al. (2002). "Adhesion assembly, disassembly and turnover in migrating cells -- over and over and over again." Nat Cell Biol **4**(4): E97-100.

Weisz Hubsman, M., N. Volinsky, et al. (2007). "Autophosphorylation-dependent degradation of Pak1, triggered by the Rho-family GTPase, Chp." Biochem J **404**(3): 487-97.

Wennerberg, K. and C. J. Der (2004). "Rho-family GTPases: it's not only Rac and Rho (and I like it)." J Cell Sci **117**(Pt 8): 1301-12.

Wennerberg, K., M. A. Forget, et al. (2003). "Rnd proteins function as RhoA antagonists by activating p190 RhoGAP." Curr Biol **13**(13): 1106-15.

West, K. A., H. Zhang, et al. (2001). "The LD4 motif of paxillin regulates cell spreading and motility through an interaction with paxillin kinase linker (PKL)." J Cell Biol **154**(1): 161-76.

Wheeler, A. P. and A. J. Ridley (2004). "Why three Rho proteins? RhoA, RhoB, RhoC, and cell motility." Exp Cell Res **301**(1): 43-9.

Wilkins, A., Q. Ping, et al. (2004). "RhoBTB2 is a substrate of the mammalian Cul3 ubiquitin ligase complex." Genes Dev **18**(8): 856-61.

Wu, M., Z. F. Wu, et al. (2004). "RhoC induces differential expression of genes involved in invasion and metastasis in MCF10A breast cells." Breast Cancer Res Treat **84**(1): 3-12.

Yang, L., L. Wang, et al. (2007). "Rho GTPase Cdc42 coordinates hematopoietic stem cell quiescence and niche interaction in the bone marrow." Proc Natl Acad Sci U S A **104**(12): 5091-6.

Yang, N., O. Higuchi, et al. (1998). "Cofilin phosphorylation by LIM-kinase 1 and its role in Rac-mediated actin reorganization." Nature **393**(6687): 809-12.

Yao, H., E. J. Dashner, et al. (2006). "RhoC GTPase is required for PC-3 prostate cancer cell invasion but not motility." Oncogene **25**(16): 2285-96.

Yin, G., J. Haendeler, et al. (2004). "GIT1 functions as a scaffold for MEK1-extracellular signal-regulated kinase 1 and 2 activation by angiotensin II and epidermal growth factor." Mol Cell Biol **24**(2): 875-85.

Zalcman, G., V. Closson, et al. (1996). "RhoGDI-3 is a new GDP dissociation inhibitor (GDI). Identification of a non-cytosolic GDI protein interacting with the small GTP-binding proteins RhoB and RhoG." J Biol Chem **271**(48): 30366-74.

Zhang, H., D. J. Webb, et al. (2003). "Synapse formation is regulated by the signaling adaptor GIT1." J Cell Biol **161**(1): 131-42.

Zhao, Z. S. and E. Manser (2005). "PAK and other Rho-associated kinases--effectors with surprisingly diverse mechanisms of regulation." Biochem J **386**(Pt 2): 201-14.

Zhao, Z. S., E. Manser, et al. (1998). "A conserved negative regulatory region in alphaPAK: inhibition of PAK kinases reveals their morphological roles downstream of Cdc42 and Rac1." Mol Cell Biol **18**(4): 2153-63.

Zhao, Z. S., E. Manser, et al. (2000). "Coupling of PAK-interacting exchange factor PIX to GIT1 promotes focal complex disassembly." Mol Cell Biol **20**(17): 6354-63.

APPENDIX: RE-PRINT OF THE THESIS-RELATED

PUBLICATION

Kaur, S.*, <u>K. Leszczynska*</u>, S. Abraham, M. Scarcia, S. Hiltbrunner, C. J. Marshall, G. Mavria, R. Bicknell and V. L. Heath (2011). "RhoJ/TCL Regulates Endothelial Motility and Tube Formation and Modulates Actomyosin Contractility and Focal Adhesion Numbers." (*Arterioscler Thromb Vasc Biol*. 2011;31:657-664.)

* Authors contributed equally to this work